2016-03-01

In Vitro Molecular Modification of Human Cultured and Primary Cells Using Lance Array Nanoinjection

John W. Sessions
Brigham Young University - Provo

In Vitro Molecular Modification of Human Cultured and Primary Cells

Using Lance Array Nanoinjection

John W. Sessions

A dissertation submitted to the faculty of
Brigham Young University
in partial fulfillment of the requirements for the degree of

Doctor of Philosophy

Brian D. Jensen, Chair
Sandra Hope
Larry L. Howell
Anton E. Bowden
Brian D. Iverson

Department of Mechanical Engineering

Brigham Young University

March 2016

ABSTRACT

In Vitro Molecular Modification of Human Cultured and Primary Cells
Using Lance Array Nanoinjection

John W. Sessions
Department of Mechanical Engineering, BYU
Doctor of Philosophy

Fundamentally altering cellular function at a genetic level is a major area of interest in the biologic sciences and the medical community. By engineering transfectable constructs that can be inserted to dysfunctional cellular systems, scientists can mitigate aberrant genetic behavior to produce proper molecular function. While viral vectors have been a mainstay in the past, there are many limitations, particularly related to safety, that have changed the focus of genome editing to incorporate alternative methods for gene delivery.

Lance Array Nanoinjection (LAN), a second-generation microfabricated transfection biotechnology, is one of these alternative technologies. LAN works by utilizing both simultaneous electrostatic interaction with molecular loads and physical lancing of hundreds of thousands of target cell membranes. The purpose of this work is to demonstrate LAN in the context of *in vitro* transfection of immortalized culture cells and primary cells. As part of that exploration, three distinct areas of investigation are considered, which include: characterizing environmental factors that impact LAN transfection, demonstrating LAN genetic modification of immortalized HeLa 229 culture cells using an indicator marker, and lastly, investigating the effects of LAN on human primary, neonatal fibroblasts.

Keywords: Lance Array Nanoinjection, saline solution, lance geometry, carbon coating, transient low temperature, injection speed, serial injection, propidium iodide, CRISPR-Cas9, primary fibroblast, PDGFR-β, wound healing

ACKNOWLEDGMENTS

It is an impossible task to recognize all of the people that have been a guide for me through this educational journey. With that said though, a proper acknowledgement of some of the key players must be named. First and foremost, my wife, Allyson, has prominently been an endless source of encouragement and support, making this experience one of the many made possible for me because of her great sacrifices. Also, I give great credit to my parents, Gary and Annette, for their support, selflessness, and teaching me the value of waiting for promptings of the Spirit and working hard in the meantime. Additionally, I thank my wife's parents, David and Susan, for their example of resilence and charity in the face of challenge.

Additionally, I must also highlight my project team. Dr. Brian Jensen has been a great source of gentle wisdom through the many projects. Dr. Sandra Hope not only added the essential ingredients of molecular biology but also timely infusions of contagious laughter. A special thank you also belongs to Dr. Larry Howell, Dr. Anton Bowden, and Dr. Brian Iverson for their being a part of my committee and providing direction along the way. Also, I would also mention Dr. Jonathan Alder for his assistance with developing CRISPR-Cas9 constructs used in experimentation.

Furthermore, I would also like to thank the National Science Foundation for facilitating this research. This material is based upon work supported in part by the National Science Foundation under Grant No. ECCS-1055916. Any opinions, findings, and conclusions or recommendations expressed in this material are those of the author(s) and do not necessarily reflect the views of the National Science Foundation.

Lastly and most importantly, I would like to express my gratitude to my Heavenly Father for orchestrating this adventure. Moses wrote following a vision, "Now... I know that man is nothing." (Moses 1:10) Indeed, I can say the same. God is Our Director in all things, from our lives' smallest details to the largest mountains in our present view.

TABLE OF CONTENTS

LIST OF TABLES

LIST OF FIGURES

NOMENCLATURE

ABS	Acrylonitrile Butadiene Styrene
$ANGPT2$	Angiopoietin 2
$CRISPR$	Clustered Regularly Interspaced Short Palindromic Repeats
DNA	Deoxyribonucleic Acid
$DRIE$	Deep Reactive Ion Etch
EGF	Epidermal Growth Factor
$eGFP$	Enhanced Green Fluorescent Protein
$EGFR$	Epidermal Growth Factor Receptor
FGF	Fibroblast Growth Factor
GFP	Green Fluorescing Protein
$gRNA$	guide Ribonucleic Acid
$HBSS$	Hanks Balanced Salt Solution
hGH	Human Growth Hormone
$HIF-1\alpha$	Hypoxia-Inducible Factor-1α
$IGF-1$	Insulin-Like Growth Factor-1
$IL-8$	Interleukin-8
$iNOS$	Inducible Nitric Oxide Synthase
$KGF-1$	Keratinocyte Growth Factor-1
LAN	Lance Array Nanoinjection
NTC	Non-Treated Sample
$NHEJ$	Non-Homologous End Joining
PBS	Phosphate Buffered Saline
$PDGF-A$	Platelet-Derived Growth Factor A
$PDGF-B$	Platelet-Derived Growth Factor B
$PDGFR-\beta$	Platelet-Derived Growth Factor Receptor β
PI	Propidium Iodide
PLA	Polylactic Acid
$PLFGF$	Placental Growth Factor
$SDF-1\alpha$	Stromal-Derived Growth Factor-1α
$TGF-1$	Transforming Growth Factor-1
$VEGF$	Vascular Endothelial Growth Factor

CHAPTER 1. INTRODUCTION TO GENE THERAPY AND GENE MEDICINE

1.1 Motivation

Gene therapy and gene medicine approaches to correcting disease represent a major paradigm shift in how clinicians are able to help patients, moving from a framework of reactionary treatment of disease manifestations to fundamental, proactive prevention of disease when genetic alterations are causative [1–3]. While still in a relatively early stage of development, medical approaches designed to engineer genetic outcomes have had promising results in terms of both monogenic [4–11] and polygenic [12–17] disease corrections.

Unfortunately, the actual method for transmission of the genetic loads to target cells remains a challenge [18–21]. Many biotechnologies have been created to help address this issue (with mixed results) [22]. The primary goal of all of these methods is to site-direct genetic loads into cells without harming the host systemically or the target cell locally [18]. Key features frequently noted as critical design requirements for these biotechnologies include:

- High transfection efficiency
- Effective in a wide range of cell types
- Flexible pay load capacity
- No immunologic response
- No insertional mutagenesis

1.2 Problem Statement/Hypothesis

One non-viral transfection biotechnology, known as Lance Array Nanoinjection (LAN), has been created with these design requirements in mind. LAN works by using a combination of

physical penetration of target cell membranes and electrical delivery of molecular loads using a microfabricated silicon etched array of lances [23, 24]. Lance arrays contain 10 μm length lances spaced 10 μm from center to center in a grid pattern, ultimately forming 4 million lances on a 2 cm by 2 cm chip.

Procedurally, nanoinjection works in a series of four major steps which include: staging the lance in the solution containing the desired molecular load, electrical attraction of the molecular load onto the lance, physical penetration of the cell membrane of target cells and electrical repulsion of the molecular load into the cytoplasmic space, and finally removal of the lance [25–27].

There are several attractive features of LAN relative to other transfection methods. First, it does not rely on delivery agents that can cross-react with the immune system (such is the case with several viruses [28–32]), nor does it create cytotoxic effects in target cells (such is the case with many chemical based methods [22, 28]). Second, because the lances are 1-2.5 μm in diameter, the resulting pores created during the injection event are relatively large, making it possible for large molecules to transiently pass into the cell. Even though the pores are relatively large, the trauma induced during the process is relatively minimal, as evidenced by high cell viability rates (78% to 91%) previously noted [24]. This latter feature of cell viability is an issue in some instrumentation based transfection methods, such as electroporation [33] and microinjection [25].

The research here presents the results of *in vitro* molecular modification of culture and primary cells by Lance Array Nanoinjection (LAN). Formally stated, the hypothesis of this research is:

It is hypothesized that using an array of silicon etched lances in a process known as nanoinjection, molecular loads, such as propidium iodide and DNA, can be placed into the intracellular space of both cultured and primary cell types via electrical interaction. Furthermore, it is also hypothesized that these modifications will be both non-threatening to target cells viability as well as efficient in terms of expression.

In an effort to explore this hypothesis, three major objectives have been created which include:

1. Characterize environmental factors that impact transfection efficiency
2. Demonstrate LAN genetic modification of immortalized HeLa culture cells using an indicator marker

3. Investigate the effects of LAN genetic modification of human primary, neonatal fibroblasts

This chapter provides background information on transfection technologies and also gives a brief overview of the approaches used to support these research objectives and the contributions made in the form of publications.

1.3 Background

1.3.1 LAN in the Context of Transfection Technologies

Traditionally, viruses have been the benchmark for which transfection efficiency is measured. However, they fall short of meeting critical design requirements for robust transfection (as detailed above), particularly in preparation for clinical application. Adenoviruses, Adeno-associated viruses, and lentiviruses are all considered to have high transfection rates in a wide range of cell types [30, 34–42]. Unfortunately, adenoviruses are immunologically inflammatory which can be life-threatening [29, 43], adeno-associated viruses can cause insertional mutagenesis which can be cytotoxic [35, 36], and lentiviruses cause immunologic responses and insertional mutagenesis [30–32, 44]. While retroviruses are useful in CNS (central nervous system) targets [37, 45], the risk of insertional mutagenesis is quite high [37, 46]. Furthermore, viruses in general are limited in their effectiveness because of the limited payload capacity ($\leq$ 10 kilo base pairs (kbp)) [37].

In contrast, LAN is able to by-pass many of these short-comings. First, LAN does not utilize protein vehicles which could cross-react with the immune system, thereby removing immunologic response issues. Second, LAN creates relatively large pores in target cells (1-2 μm diameter), allowing for large molecular loads to enter, thus reducing the concern of not having sufficient payload capacity. Third, LAN is compatible with gene editing tools such as CRISPR-Cas9 that mitigate concerns regarding insertional mutagenesis. While the same can be said of viruses if re-programmed to remove self-insertional mechanisms, LAN does not have the same rigor of testing to go through prior to use as viral delivery because insertional mutagenesis in the context of LAN is only an element directly related to the molecular load type, not LAN as a delivery method.

1.3.2 Previous Nanoinjection Works

In order to place context to the proposed LAN based research for culture and primary cells, a brief overview of previous foundational works is presented.

Single Lance Nanoinjection

Initial development of the Nanoinjection concept began at Brigham Young University in 2007 where researchers developed a method for exogenous DNA delivery to mouse embryonic cells via a solid, microfabricated lance. This process became known as 'nanoinjection' and is described as electrical attraction of molecular elements such as DNA onto a micron-sized needle structure, inserting the needle through the target cell membrane, and then electrically repelling the molecular load into the pronucleus to be integrated during pro-nuclei disintegration and nuclear formation events [25, 47]. Subsequent work showed effects of voltage pulsing while the lance is inserted in the embryo, allowing for a phenomena known as intracellular electroporetic nanoinjection, which is a localized transient pore formation event in the pronucleus allowing molecular loads to enter [27].

Lance Array Nanoinjection

More recently, researchers have modified the single lance nanoinjector to be an array of 10 micron-length lances capable of nanoinjecting hundreds of thousands of cells simultaneously [24, 25, 48]. The biologic application for the design change reflects the fact that these lance arrays can molecularly modify somatic, adherent cell types–a critical distinction from the embryonic target cells used previously.

Electrical Modelling

Previous research involving the Single Lance Nanoinjector helped to characterize and model the electrostatic attraction and repulsion of DNA to the device [26, 49, 50] and an extension of this work has been conducted for LAN [51, 52]. The rationale behind this effort deals with the need to model molecular load delivery based on electrical pulse levels. Based on conclusions derived

from these works, it has been theorized that much lower voltages (i.e. 1.5V) are required to provide molecular delivery than traditional electroporation transfection protocols (typical kV), which suffer from low cell viability rates as a result of high voltage exposure.

Early Biologic Testing

Mechanistic evaluation of LAN has also been performed, with initial testing with propidium iodide (PI), a dye normally impermeable to the cell membrane [24, 53]. In these experiments, it has been shown that following LAN that HeLa target cells have elevated levels of propidium iodide, manifested by increase fluorescence during flow cytometry.

Current Status of LAN

As mentioned previously, LAN development hinges upon *in vitro* transfection of target cells. While previous work has provided key foundational elements to this end, full investigation of *in vitro* modification of both immortalized culture cells and primary cells is the focus of this work.

1.4 Research Approach/Literature Contributions

The sequential approach to establishing LAN in culture and primary cells can be compartmentalized broadly into the three major objectives outlined in this chapter. Discussed briefly here are supporting research topics that explore these objectives.

1.4.1 Objective 1: Characterize environmental factors that impact molecular load delivery

Chapter 2 investigates the effects of three different saline solutions on propidium iodide uptake in nanoinjected HeLa cells. The body of this chapter comes from a conference paper presented at the 2014 International Design Engineering Technical Conference in Buffalo, NY.

Chapter 3 investigates the effect of lance geometry and carbon coating of silicon lances on propidium iodide uptake in Lance Array Nanoinjection of HeLa 229 cells. The body of this

chapter comes from a journal article accepted for publication in the *Journal of Micromechanics and Microengineering*.

Chapter 4 investigates the effects of transient low temperature on propidium iodide uptake in Lance Array Nanoinjected HeLa cells. The body of this chapter comes from a journal article submitted to the *Journal of Nanotechnology in Engineering and Medicine*.

Chapter 5 investigates the effect of injection speed and serial injection on propidium iodide entry into cultured HeLa and primary neonatal fibroblast cells using Lance Array Nanoinjection. The body of this chapter comes from a journal article submitted to *SpringerPlus*.

1.4.2 Objective 2: Demonstrate LAN genetic modification of immortalized HeLa culture cells using an indicator marker

Chapter 6 investigates the effect of a CRISPR-Cas9 plasmid designed to knock-out constitutively expressed GFP in HeLa cells using Lance Array Nanoinjection. The body of this chapter comes from a journal article submitted to *SpringerPlus*.

1.4.3 Objective 3: Investigate the effects of LAN genetic modification of human primary, neonatal fibroblasts

Chapter 7 comprises a combination of two review journal articles that is included to provide a context to chronic wound healing, particularly in regards to the platelet derived growth factor receptor β (PDGFR-β) and genetic engineering. The first portion of the chapter was derived from a paper published in the *Journal of Diabetes Science and Technology*. The second portion of the chapter was derived from a paper submitted to *Experimental Dermatology*.

Chapter 8 investigates the ability of LAN to deliver a CRISPR-Cas9 plasmid to primary, neonatal fibroblasts using Lance Array Nanoinjection. This plasmid is designed to up-regulate PDGFR-β in the fibroblasts. This work is designed as a proof-of-concept work that demonstrates a clinically relevant application of LAN in conjunction with chronic wound healing. The body of this chapter comes from a journal article submitted to *PLoS ONE*.

1.5 Summary of Presented Research

The final chapter, Chapter 9, provides a brief survey of salient results of the research presented. As part of this chapter, a short discussion will be devoted to highlighting why these findings are important as well as provide a context for potential future work.

CHAPTER 2. SALINE SOLUTION EFFECTS ON PROPIDIUM IODIDE UPTAKE

The following chapter was constructed from a conference paper that was presented at the 2014 International Design Engineering Technical Conference (Buffalo, NY) and is entitled "Saline Solution Effects on Propidium Iodide Uptake in Nanoinjected HeLa Cells" [54]. As a result, there may be some material that is contained elsewhere in this dissertation but is presented here as a representation of this original conference article.

2.1 Introduction

Genetic engineering of various mammalian target cells has become a new frontier in medicine. Researchers are actively investigating the efficacy of modifying disease states that include but are not limited to: joint erosive arthritis [55], intervertebral disc degeneration [55], aseptic orthopedic implant loosening [55–57], osteoporosis [55], soft tissue repair (cartilage, tendon, ligament) [55], bone healing [55, 58–60], ventricular arrhythmia [61], congestive heart failure [62], chronic diabetic wounds [63–68], incisional scar formation [69, 70], psoriatic skin disorders [71], hereditary blood disorders [72], etc. Because genetic engineering aims to control aberrant function or improve existing function at the fundamental cellular level, there is potential to significantly impact patient healthcare by improving genetic engineering technologies.

However, the process of introducing exogenous genetic material into a mammalian cell is not trivial but rather multi-step and highly complex [73,74]. One of the initial barriers to exogenous molecular load delivery is introducing molecular loads into the cytoplasm without compromising the structural and functional integrity of the cell.

Traditionally, genetic reprogramming techniques have sought to penetrate and integrate molecular loads into target cells using one of two major methods: viral [75, 76] and non-viral [71, 77, 78]. Viral methodologies generally consist of using a viral vector programmed with a

specific genetic sequence. Once engineered, these viral particles are allowed to infect targeted tissues.

Unfortunately, viral gene therapy techniques have several challenges that limit clinical use. These limitations to viral gene therapy include issues related to immunologic safety, virus containment to targeted tissues, vector production costs, limits to the amount of genetic load capacity of the virus, and production containment and safety [59]. Furthermore, within the medical culture, major barriers exist for viral method acceptance (despite their benchmark efficiencies) because of a tainted safety history. For example, French clinical trials in treating X-linked Severe Combined Immunodeficiency with a murine viral vector initially proved successful in creating functional immune systems in nine of ten treated patients. However, 3 of the ten developed leukemia and one died [79].

Because of these limitations with viral based genetic engineering, researchers have put considerable effort into generating alternate, non-viral methods for gene delivery. Currently, there are several combinations of physical delivery applications practiced. Characteristically, physical methods of exogenous genetic delivery use either physical or chemical approaches for delivery. Two of those most common approaches include lipofection [77] and some form of electroporation [74, 78, 80]. Lipofection, in short, consists of lipophilic molecules that encapsulate a molecular load, such as DNA, in the extra-cellular space and transport the load to the intracellular space because of the cell membrane's permeability to lipophilic molecules. Electroporation operates by applying an external electrical field to the cell and consequently causing formation of transient pores that allows for extracellular molecules to pass into the cell. Both techniques have intrinsic limitations that can be tied to the fact that they can cause significant compromise to the cell and consequently produce lower cell viability, an undesired outcome for clinical use.

Recently, researchers have demonstrated an alternative, non-viral technique for molecular load delivery called nanoinjection [26]. Nanoinjection is a process described as electrical attraction of a molecular loads onto a micron-sized needle structure, inserting the needle through the cell membrane, and then electrically repulsing the molecular load into the cytoplasm. This process, using a single lance nanoinjector, has been used successfully in transgenic mice generation [25].

More recent modifications to the nanoinjection process include modifying the single lance injector to be an array of 10 μm-length nanoinjector needles capable of nanoinjecting thousands

of cells simultaneously [81]. HeLa cell studies have illustrated that nanoinjection can effectively deliver propidium iodide into target cells without compromising cell viability [24].

The present research seeks to extend previous work related to nanoinjection by examining two environmental factors, namely saline injection solution type and peak pulse amplitude, that contribute to propidium iodide delivery into HeLa cells. Previous examination by other researchers [82] have demonstrated in electroporation studies, that solutions with increasing potassium (K^+) require higher electrical field strengths to induce electroporation, a transient biological response where pores form in the cell membrane. The rationale for this finding is that when a cell, which has a transmembrane potential (V_m), is exposed to an electrical field, the anodic side of the cell membrane is first to reach a $V_m = 0$, at which point pores can begin to form. If the extracellular environment contains increasing amounts of K^+, then the voltage magnitudes at which this behavior can initiate are greater. Since cell viability decreases with higher voltage application in electroporation, it is desirable to know in the context of nanoinjection if at lower voltages comparable PI uptake can occur by simply using a different injection solution.

2.2 Methods

2.2.1 Lance Array Fabrication and Injection Device

Silicon lance arrays were photolithographically defined and etched using DRIE (deep reactive ion etching). Following etching, the silicon was coated in a 0.5 μm thick layer of carbon using chemical vapor deposition (CVD). Lances measure 1-1.5 μm in diameter and 8-10 μm in length and are spaced at 10 μm. The silicon wafer is then cut into 2 cm by 2 cm square chips, each containing roughly 4 million lances [81] (see Figure 2.1).

The injection device consists of an orthoplanar spring [83, 84], fabricated with acrylonitrile butadiene styrene (ABS) plastic using rapid prototyping, that has attached at its base with double sided carbon tape the carbon coated silicon chip described above. Two electrical components are housed within the orthoplanar device: gold contacts located at the interface between the orthoplanar spring and the carbon coated silicon chip, and the stainless steel wire extending from the gold contacts to the outer surface of the injection device (see Figure 2.2).

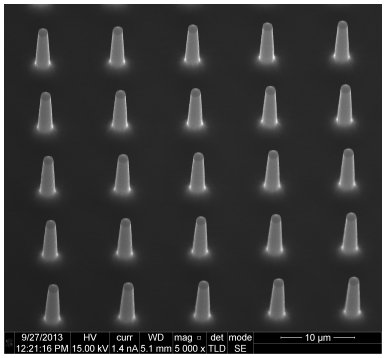

Figure 2.1: SEM image of lance array. Lances measure 1-1.5 μm in diameter and 8-10 μm in length and are spaced at 10 μm in a grid pattern. Contained on a 2 cm by 2 cm lance array chip are approximately 4 million lances, making it possible for each HeLa cell to be injected approximately 2-3 times in one injection event

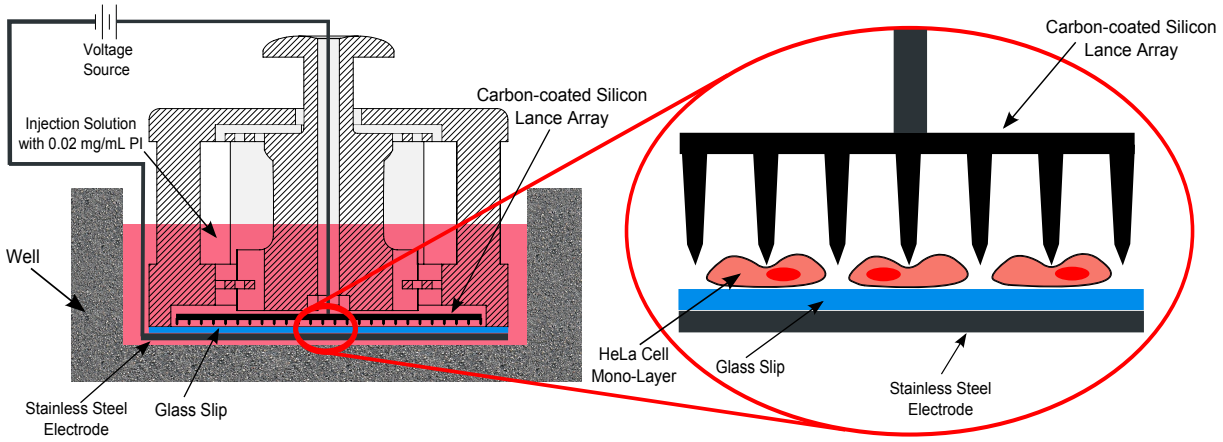

Figure 2.2: Illustrates a cross-sectional view of the manual injection device (left) and a zoomed in view of the lance array interacting with the HeLa cell culture adhered to the glass slip (right). During the injection process, the cell culture and the bottom portion of the injection device is submerged in HBSS containing PI

2.2.2 Propidium Iodide

In treatment samples, propidium iodide (PI) was used as an indicator of delivery efficacy. PI is a positively charged (2+) molecule that cannot penetrate the cell membrane of living cells [85–87]. Traditionally used to label dead cells that have had their cell membranes compromised, PI operates as a red fluorescing dye that intercalates between base pairs of both RNA and DNA. This association with genetic material increases the fluorescent nature of PI 20 to 30 times, making

the appropriately exposed cell identifiable with flow cytometry [88]. Because nanoinjection is supposed to create transient pores via lancing action, the PI identified in living cells is characterized as a good indication that PI indeed entered the cell and that the cell survived.

2.2.3 Nanoinjection Technique

The mechanics of nanoinjection can be separated into two major components, the second being used for samples treated with pulsed voltage protocols. The first component includes the physical lancing of the cell membrane by pressing downward on the injection device. This consequently causes the carbon coated silicon chip attached to the lower side of the injection device to lance/penetrate the cell membrane of the target cell. The second component includes using electrical attraction of particles, such as PI, to the lance and then electrically repulsing the particle (with a reversal of voltage) once the lance has penetrated the cell membrane. Shown is Figure 2.3 is a step-wise process of how these two components operate during the injection process.

2.2.4 Testing Methods

Testing Plate Preparation

HeLa 229 cancer cells were cultured in Dulbeccos Modified Eagles Medium (DMEM) with 10% Fetal Bovine Serum (FBS) and Gentamicin and then, incubated at 37C with 5% carbon dioxide. Once cells had matured, six well plates were prepared with roughly 10^6 cells per well, which were allowed to adhere to a 22 mm by 22 mm glass slide over a 24 hr period, creating a confluent mono-layer. For experiments to be performed with voltage application, a stainless steel electrode plate was added to each well beneath the glass slide.

After allowing the cells to adhere to the glass slide for 24 hr in the incubator, the six well plates had the DMEM removed and then each well was rinsed with Hanks Balanced Salt Solution (HBSS). Then, depending on the particular saline being tested, the wells were supplied with 2 mL of either Hanks Balanced Salt Solution (HBSS), Phosphate Buffered Solution with K^+ (PBS+K^+), or Phosphate Buffered Solution without K^+ (PBS-K^+). These salines represent the injection saline

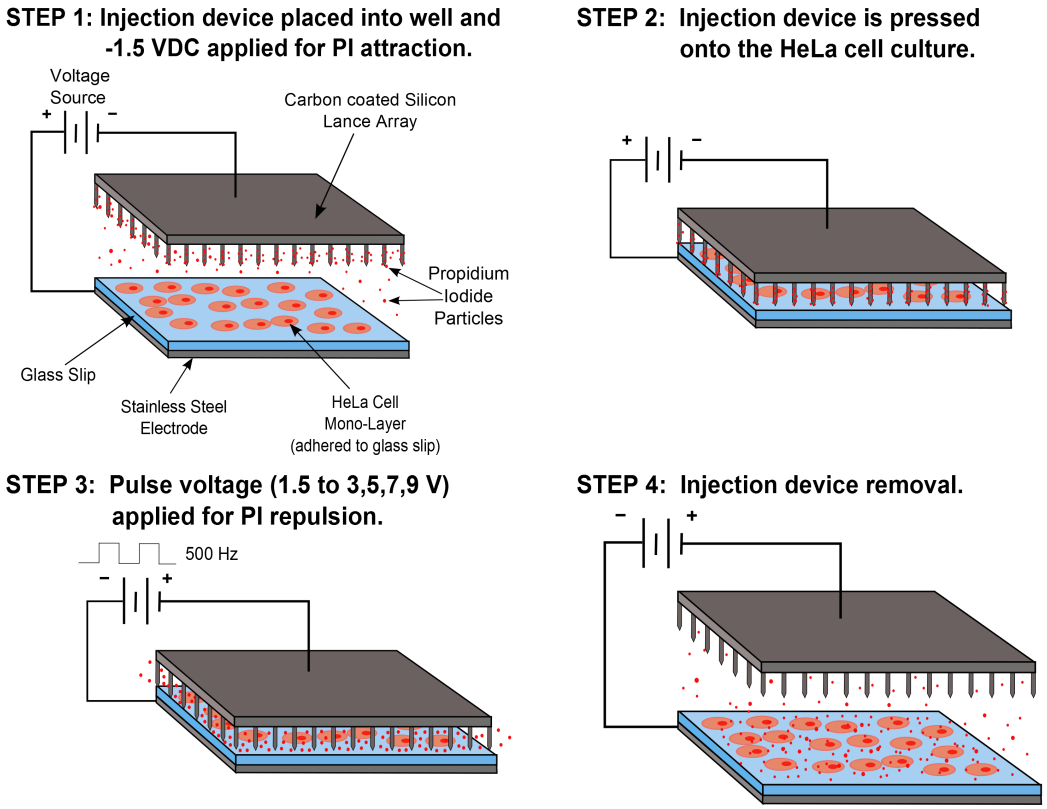

Figure 2.3: The nanoinjection process consists of four major steps. Step 1 (Top Left) involves placing the injection device into the test well on the 6-well plate and applying -1.5VDC. Step 2 (Top Right) involves pressing the lance array downward into the HeLa cell culture. Step 3 (Bottom Left) involves application of a series of square wave pulses. Step 4 (Bottome Right) involves removal of the lance array from the cell culture

solution. Following the placement of the injection saline, PI was added to the well bringing the concentration of PI in the well to 0.02 mg of PI/mL of injection saline solution.

The injection process, which can be seen in Figure 2.3, consisted of lowering the injection device with carbon coated silicon chip attached into a treatment well. The well, now containing the specific injection saline (either HBSS, PBS+K^+, or PBS-K^+), completely covers the carbon coated silicon chip, glass slip with HeLa cells attached, and the stainless steel electrode.

At this point, one of eight treatment protocols was followed for each saline type and includes:

1. **Negative Control** - No applied voltage, No Lancing, and No PI

2. **Positive Control** - No applied voltage, No Lancing, and +PI (0.02 mg/mL solution)

3. **Treatment Protocol: Lancing Only** - No applied voltage or PI, +Lancing

4. **Treatment Protocol: Lancing and PI** - Lance assisted Diffusion: No applied voltage, +Lancing, and +PI (0.02 mg/mL solution)

5. **Treatment Protocol: Pulsed 3V** - 20 s application of -1.5VDC for PI attraction followed by 5 s square wave voltage repulsion pulse of 1.5V to 3V with a 2ms period; +Lancing, and +PI (0.02 mg/mL solution)

6. **Treatment Protocol: Pulsed 5V** - 20 s application of -1.5VDC for PI attraction followed by 5 s square wave voltage repulsion pulse of 1.5V to 5V with a 2ms period; +Lancing, and +PI (0.02 mg/mL solution)

7. **Treatment Protocol: Pulsed 7V** - 20 s application of -1.5VDC for PI attraction followed by 5 s square wave voltage repulsion pulse of 1.5V to 7V with a 2ms period; +Lancing, and +PI (0.02 mg/mL solution)

8. **Treatment Protocol: Pulsed 9V** - 20 s application of -1.5VDC for PI attraction followed by 5 s square wave voltage repulsion pulse of 1.5V to 9V with a 2ms period; +Lancing, and +PI (0.02 mg/mL solution)

Post Testing Flow Cytometry Preparation

All samples, following specific testing protocols, were treated with 0.5 mL of 5x Trypsin (Sigma) and incubated for 5 min to remove adherent HeLa cells from the glass slip. Following incubation, wells were treated with 1 mL of DMEM to de-activate the trypsin and then transferred to FACS tubes (BD Biosciences) for centrifugation for 10 min at 2000 rpm. Supernatants were removed following centrifugation and re-suspended in 0.25 mL in HBSS for flow cytometry (BD Biosciences).

2.2.5 Flow Cytometry and Statistical Analysis

Following post testing preparation, samples were analyzed using flow cytometry to quantify cell viability and PI uptake in living and dead cells. For each sample examined, 10,000 events were captured and characterized. Analysis software (BD FACSDiva, Dako Summit) allowed for visualization of these data sets using forward and side scatter.

Statistical analysis was then employed to determine cell survival and PI uptake for each data set. For cell survival, samples were normalized against the negative controls. This normalization was performed in two steps. The first step consisted of representing the total number of living cells in the sample divided by the total number of living and dead cells in the sample. That numerical result was then divided by the ratio of the number of living cells in the control well divided by the number of living and dead cells in the negative control particular to that six well plate.

$$\mathrm{a} = \frac{\text{Living Cells in Test Sample}}{\text{Total Living and Dead Cells in Test Sample}}$$

$$\mathrm{b} = \frac{\text{Living Cells in Negative Control}}{\text{Total Living and Dead Cells in Negative Control}}$$

$$\textit{Cell Survival} = \frac{a}{b}$$

For PI uptake, samples were normalized against the positive controls and represented in a similar manner as previously described. The total number of living, PI positive cells in a sample were divided by the total number of living cells in a sample. That numerical result was then divided by the total number of living, PI positive cells in the positive control divided by the total number of living cells in the positive control particular to that six well plate.

$$\mathrm{c} = \frac{\text{Living and PI}^{+}\text{ Cells in Test Sample}}{\text{Total Living Cells in Test Sample}}$$

$$\mathrm{d} = \frac{\text{Living and PI}^{+}\text{ Cells in Positive Control}}{\text{Total Living Cells in Positive Control}}$$

Table 2.1: Normalized PI Uptake Efficiency P-Values

Comparisons	Lance	Lance+PI	1.5-3 V	1.5-5 V	1.5-7 V	1.5-9 V
HBSS vs PBS+K^+	0.0125	0.0163	0.0352	0.0095	0.0184	0.1536
HBSS vs PBS-K^+	0.0005	0.4804	0.1014	0.0415	0.4625	0.3861
PBS+K^+ vs PBS-K^+	0.0125	0.1017	0.0010	0.0000	0.0159	0.1027

Table 2.2: Normalized Cell Survival P-Values

Comparisons	Lance	Lance+PI	1.5-3 V	1.5-5 V	1.5-7 V	1.5-9 V
HBSS vs PBS+K^+	0.3892	0.0652	0.0630	0.2614	0.0155	0.0919
HBSS vs PBS-K^+	0.0074	0.0270	0.1995	0.0016	0.0038	0.2895
PBS+K^+ vs PBS-K^+	0.0244	0.0029	0.3986	0.0257	0.2068	0.0448

$$PI\,Uptake = \frac{c}{d}$$

Following normalization, sample populations were examined for outliers using a modified Thompson Tau test and then statistically evaluated using a students t-test for statistical significance between populations, with p-values less than 0.05 considered statistically significant.

2.3 Results and Discussion

2.3.1 PI Uptake Efficiency

Figure 2.4 shows the relative efficiency of PI uptake in living HeLa cells for the three different salines (HBSS, PBS+K^+, and PBS-K^+) at two different non-voltage protocols and four different voltage pulsing protocols. Table 2.1 shows relative p-values (significance measured as $p<0.05$) for comparisons between the different sample groups.

The overall behavior of the PI uptake can be categorized into three major findings. First and most notable is that PBS+K^+ sample groups are significantly better than the other two salines at PI delivery at all voltages, except at the 9V pulsed voltage. While not significantly higher at 9V, PBS+K^+ samples appear to be modestly higher than the other salines. Peak efficiency for PBS+K^+ occurs at 7V pulsed voltage, reaching a ratio of 3.352.

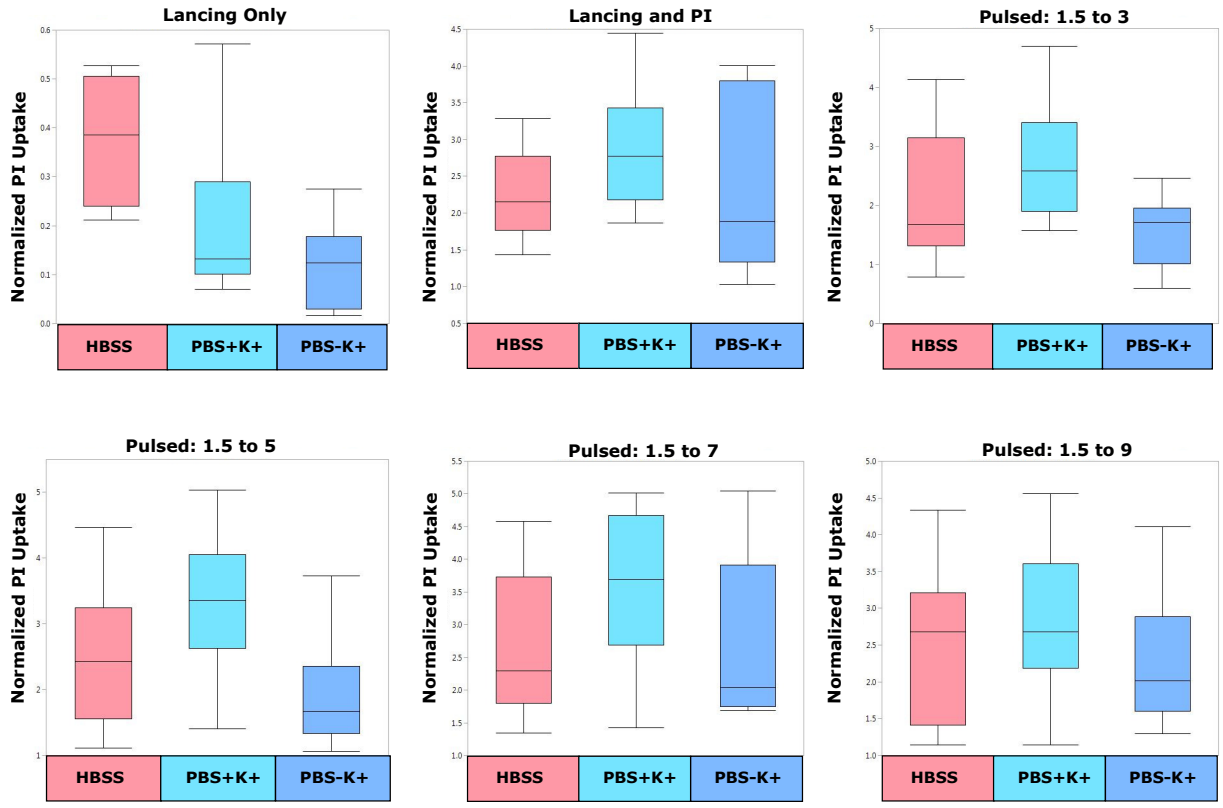

Figure 2.4: Relative efficiency of PI uptake in living HeLa cells for different salines and LAN injection protocols.

A second finding illustrated in the PI Uptake efficiency is seen by comparing the Lance/PI group and the four different voltage groups. It is noted that there is only a significant increase in PI uptake in PBS+K^+ at 5V (p=0.0422) and 7V (p=0.0148) pulsed voltages. The other two saline groups exhibit no significant increase in PI uptake when voltage applied and in fact, PBS-K^+ actually experiences a reduction in PI uptake at 3V and 5V pulsed voltage compared to Lance/PI group. For 9V pulsed voltages, none of the salines types exhibited significance increases over the Lance-PI treatment group.

A third finding can be seen in context of comparing the saline types to themselves at the four pulsed voltages. In comparing 3V against 5V, only PBS+K^+ is significantly higher (p=0.0220) among the three salines. At 5V to 7V, only PBS-K^+ is significantly higher (p=0.0159). At 7V to 9V, only +K^+ is significantly lower (p=0.011).

2.3.2 Cell Survival

Figure 2.5 shows the relative cell survival of HeLa cells as a result of nanoinjection for the three different salines (HBSS, PBS with potassium, and PBS without potassium) at two different non-voltage protocols and four different voltage pulsing protocols. Table 2.2 shows relative p-values (significance measured as $p<0.05$) for comparison between the different sample groups.

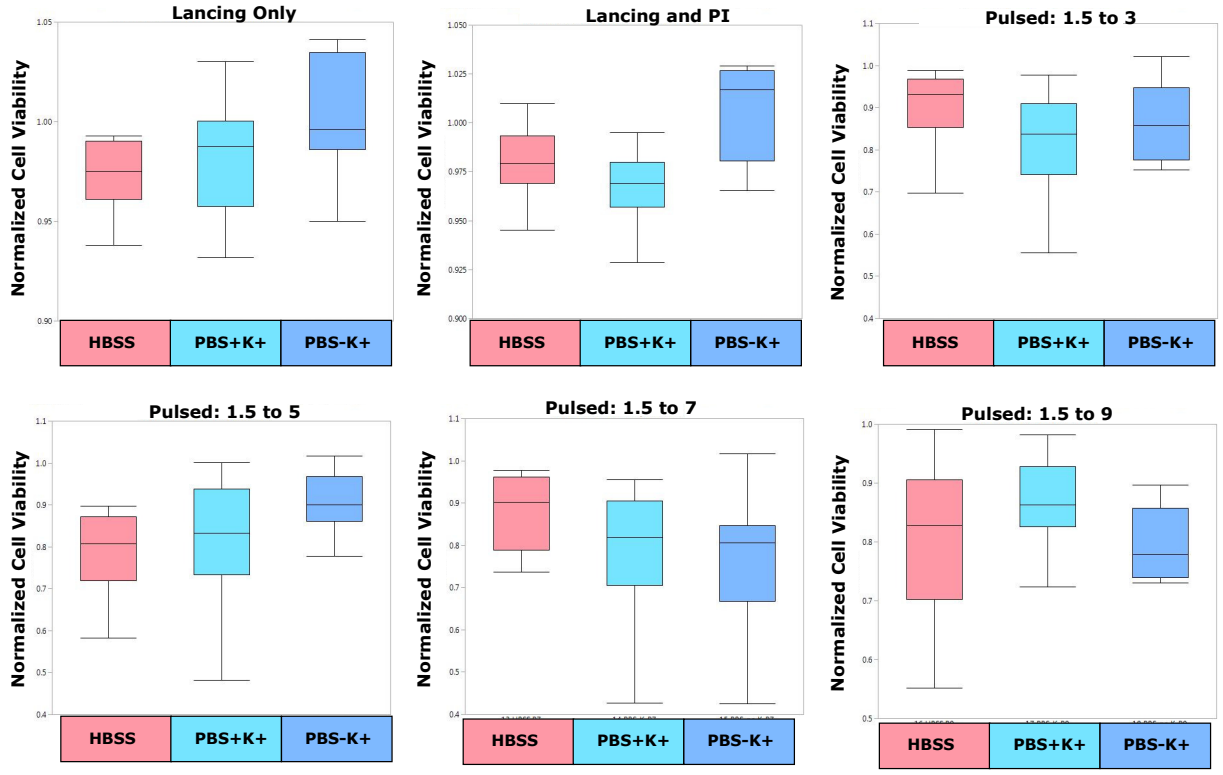

Figure 2.5: Relative cell survival of HeLa cells for different salines and LAN injection protocols.

Of particular note is the relative behavior exhibited between the Lance/PI group and the 3V pulsed voltage group. While there is no significant difference between the PI uptake when comparing Lance/PI to 3V pulsed voltage, there is a dramatic difference in cell survival between these two groups ($p = 0.0025, 0.0000, 0.0182$ for HBSS, PBS+K^+, PBS-K^+ respectively). Embedded in this relationship though, is the fact that PI uptake efficiency is based upon cells that are both living and PI positive. While it is true that there are comparable PI uptake efficiencies between the Lance/PI

and 3V pulsed voltage groups, the 3V pulsed voltage group actually have more cells labeled with PI initially but don't survive the process and thereby reduces the PI uptake efficiency.

A second finding that is worth noting is that when comparing the cell survival of the Lance sample group to the Lance/PI group, that in both cases PBS-K^+ is significantly better than the other two salines. While modest in degree, it appears that PBS-K^+ offers approximately 3% increase in cell survival. This finding suggests that potassium, which is present in HBSS and PBS+K^+, may destabilize the cell enough to prevent cellular recovery post-nanoinjection. This finding is not as clearly defined when voltage protocols are used suggesting that the role of potassium is complicated by voltage.

2.3.3 Potassium Effects

As mentioned previously, prior research indicates that the threshold voltage required for electroporation of a cell membrane is reduced in low potassium extracellular solutions. Based on the data represented in the context of nanoinjection, this finding in regard to potassium is not supported. This suggests two possibilities that require further investigation. The first is that nanoinjection with the voltage protocols outlined above may not actually induce electroporation of the cell membrane because it is not sufficiently large enough, despite the close proximity of the electrode to the cell membrane. Another possibility is that because the cell membrane is physically lanced, the relative behavior of the cell in the potassium environments may react differently. Because there are micron-sized pores created by the lancing process, the cell membrane has no need to create transient electroporation pores to re-establish homeostatic transmembrane potential.

2.4 Conclusion

In order to improve genetic engineering, researchers will need technologies that can facilitate molecular load delivery to the intracellular space without compromising cell survival. Nanoinjection is one such technology that appears to be a viable option.

In this study, PI uptake efficiency and cell survival are investigated in the context of using different injection salines, non-voltage lancing protocols, and pulse voltage protocols. Shown here is that PBS+K^+ experiences higher overall PI uptake efficiencies than HBSS and PBS-K^+. Also,

cell survival is variable in degree for voltage treated samples, ranging primarily between 75% and 87%.

CHAPTER 3. THE EFFECT OF LANCE GEOMETRY AND CARBON COATING OF SILICON LANCES

The following chapter was constructed from a journal article that has been accepted for publication by the *Journal of Micromechanics and Microengineering* and is entitled "The Effect of Lance Geometry and Carbon Coating of Silicon Lances on Propidium Iodide Uptake in Lance Array Nanoinjection of HeLa 229 Cells". As a result, there may be some material that is contained elsewhere in this dissertation but is presented here as a representation of this original journal article.

3.1 Introduction

Correcting disease at a fundamental cellular level has been and continues to be a promising medical research area [56, 89, 90]. Because of advancements in both creation and manipulation of relevant target cells, such as induced pluripotent stem cells [91–94], as well as enhancements in site-directed gene modification tools, such as CRISPR/Cas9 [95–97], there is an intensified need to develop methods for combining these tool types into meaningful biotechnologies [98–100]. Unfortunately, placing gene editing constructs into useful target cells types is complicated by the delivery process, both in terms of effectively getting genetic pay-loads to the intracellular space of target cells and maintaining cell viability following treatment.

Many methods have been developed to help address the need to facilitate molecular load delivery and can categorically be separated into four areas, which include viral [101–103], particle-based [104–106], reagent-based [77, 107], or instrumentation-based methods [74, 107, 108]. Engineered viruses are the most common biologic carrier method for molecular delivery largely because of the self-promotional features associated with the viral life-cycle [109, 110]. Once reprogrammed with the desired genetic pay-load, viruses can infect specific surface marker carrying cells [111–114] and manufacture the desired effect, using the viruses' own re-purposed machinery if necessary [115].

Unfortunately, even though viral transfection methods often exhibit benchmark efficiencies for molecular delivery, there are clinically-limiting drawbacks to using viral transfection, which include: immunologic safety, viral containment to target tissues, limits to genetic load capacity, and insertional mutagenesis [116]. Essentially, these "procedural limitations" of viral vectors have caused researchers to investigate alternative non-viral methods, particularly particle-based and instrumentation-based, for transfection [117].

In terms of instrumentation-based biotechnologies, several researchers have created high throughput nanowire biomolecule delivery and sensing systems which have demonstrated utility in terms of transfection applications [118–122]. This work contributes to this group of work by focusing on a non-viral, instrumentation-based transfection technology, known as nanoinjection, that uses nanowire-like silicon lance structures to electrically interact and deliver biomolecules to target cells [25].

The first generation nanoinjection device was originally designed as a six-bar microelectromechanical device designed to modify single mouse embryos with foreign transgenes [25–27]. Since that time, the scope of nanoinjection has been extended to be used for simultaneous modification of hundreds of thousands of somatic cells using an array of silicon etched lances, a process known as Lance Array Nanoinjection (LAN) [23, 24, 54].

Procedurally, LAN works in four major steps which combine physical penetration of the cell membrane and electrical delivery of molecular loads. Figure 3.1 shows these four steps which include the following: staging–electrical attraction of molecular loads, injection–physical penetration of target cell membranes, delivery–electrical repulsion of molecular loads, and finally, removal–withdrawal of the lances from the target cells' intracellular space [24].

This work presents two major fabrication alterations to the silicon lance array typically used for LAN, which include: lance geometry (lance tip shape and shaft diameter), and presence of a carbon coating. The purpose of lance geometry testing is to evaluate how cells respond to cell membrane damage when injections are performed by different lance geometries. Because cellular trauma is a concern in regards to preserving cell viability, lance geometry is an important investigative factor in terms of LAN. The purpose for the lance coating test is to evaluate how carbon coating presence can impact the electrical events that occur during LAN, a parameter important for molecular load delivery in both in terms of the attraction and repulsion of molecular loads [26].

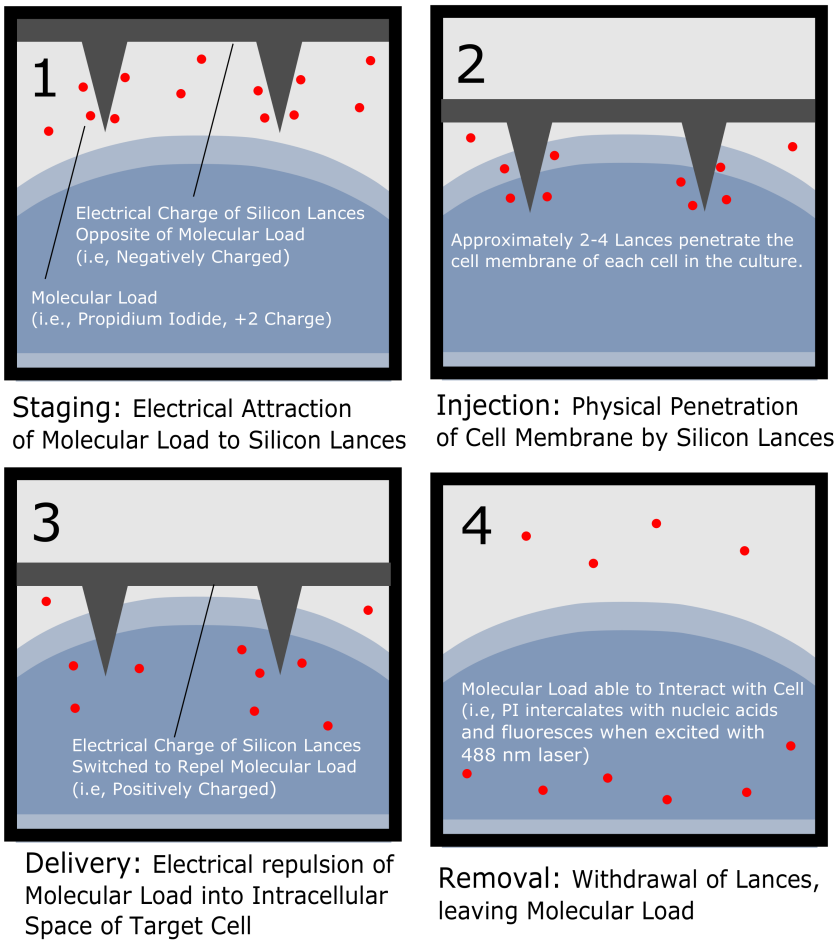

Figure 3.1: Illustrates the general process of Lance Array Nanoinjection with notes specific to the delivery of Propidium Iodide molecular load used for the biological testing portion of the presented work.

In an effort to create a lance array that both conducts electricity easily and thereby allows for a low applied voltage for LAN, silicon lances were constructed with a thin ($<$100 nm thick) carbon coating. To help evaluate the effects of these alterations, biologic testing results are presented, which explore the performance with which propidium iodide (PI), a cell membrane impermeable dye, can be delivered to HeLa 229 cells via LAN.

3.2 Materials and Methods

3.2.1 Lance Array Fabrication

Microfabrication of the silicon lance arrays have been previously described in the literature [23] and is noted briefly here only for convenience in regards to the alternations or additions made for the lances tested in this work. Silicon lance array construction consists of photolithographic definition of positive photoresist (AZ330F) in an array of circular features spaced at 10 μm followed by deep reactive ion etching (DRIE). In order to create pointed lances, a sulfur hexafluoride (SF6) isotropic plasma etch undercuts the photoresist features, resulting in a conical shape that supports the photoresist dot. This etch is typically in the range of 30 to 60 seconds, depending on the desired undercut depth. Following SF6 etching, the photoresist dots are stripped using acetone and then exposed for 2 minutes in an oxygen plasma etch. The final lance array consists of a 2 cm by 2 cm chip etched with an array of 10 μm length solid lances which are spaced every 10 μm in both planar directions (see Figure 3.2).

Lance Geometry Fabrication

Silicon lance arrays construction for lance geometry testing can be categorized into three different groups and include: Flat, Narrow (FN, 1 μm diameter); Flat, Wide (FW, 2-2.5 μm diameter); and Pointed (P, 1 μm diameter) (see Figure 3.2). The lance microfabrication used the same process as what is described in Lance Array Fabrication with two alterations. First, only the P lances underwent the sulfur hexafluoride etch to create a pointed tip. Second, the relative diameter of the lance was controlled by altering the length of photoresist exposure – the shorter exposure times yielded a larger diameter dot, which resulted in larger diameter lances.

Lance Carbon Coating Fabrication

Silicon lance array construction for carbon coated testing followed the same process as what is described in Lance Array Fabrication with one additional step. Following the oxygen plasma etch, the lances were coated in a $<$100 nm thick layer of carbon using chemical vapor deposition (ethylene at 230 sccm, hydrogen at 218-220 sccm, at 900C for 5 min) (see Figure 3.3)

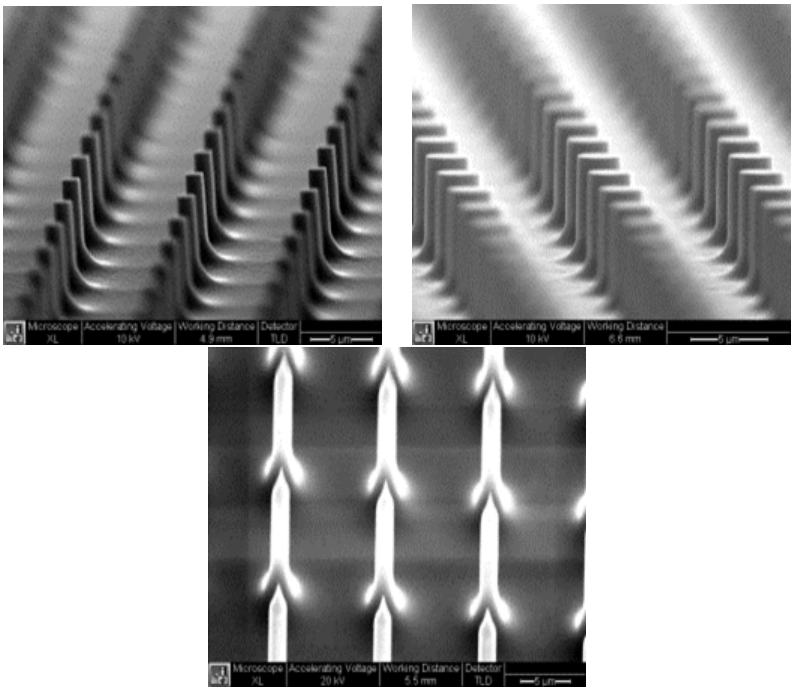

Figure 3.2: SEM images of the three different shaped silicon lance arrays. (Top) Shows rows of Flat, Narrow (FN) lance tips, measuring 1 μm in diameter. (Middle) Shows rows of Flat, Wide (FW) lance tips, measuring 2 to 2.5 μm in diameter. (Bottom) Shows rows of Pointed (P) lance tips, measuring 1 μm in diameter.

Though the angle of the lances in Figure 3.3 makes them look flat, these lances were fabricated using the pointed protocol.

As mentioned previously, coating the silicon lances in a thin layer of carbon is hypothesized to alter the performance of PI delivery during LAN. Experimental investigation of the electrical performance of the two lance array types (Si and CC) demonstrate that non-coated silicon lance arrays (Si) have a resistance of 1364 Ω and the carbon coated silicon lance arrays (CC) have a resistance of 395 Ω.

3.2.2 Nanoinjection Device

Figure 3.4 provides a side-view schematic of the LAN device seated in a six well plate filled with an injection solution containing the molecular load to be injected. Noted are three major elements making up the LAN device, which includes: the orthoplanar spring (with electrical connection), the silicon lance array, and the glass slide/counter electrode. The orthoplanar spring

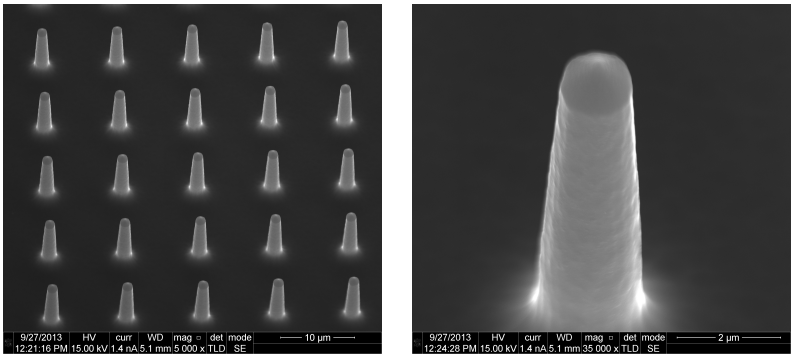

Figure 3.3: SEM images of carbon coated silicon lance array. (Left) Shows arrangement of lances post-carbon coating treatment. (Right) Close up image of a single carbon coated lance.

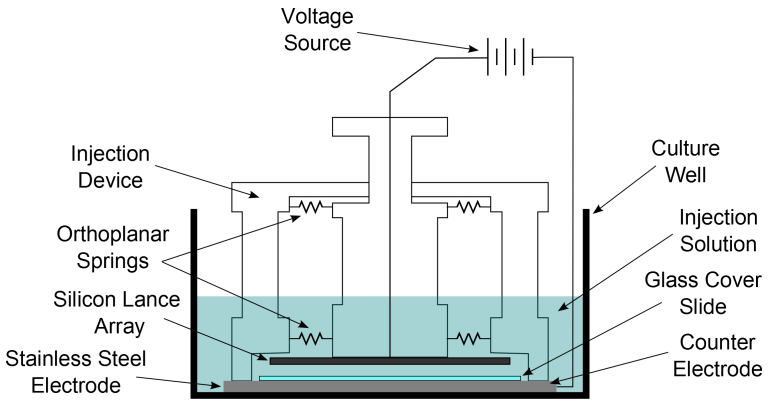

Figure 3.4: Nanoinjector device used for both Lance Geometry testing and Carbon Coating testing.

design has been described previously in the literature [23,84] and contains compliant flexural members that inhibit transverse and rotational motions during vertical actuation. The silicon lance array adheres to the inferior portion of the orthoplanar spring using double-sided carbon tape, thereby electrically connecting the lance array to a switch box that provides the appropriate electrical inputs according to the treatment sample type. Shown below the lance array is a glass slide sitting atop a stainless steel counter-electrode (serves as ground). The glass slide contains the cell culture.

Operation of the nanoinjection device occurs as manual force is applied to the superior surface of the orthoplanar spring, allowing the attached lance array (with lances oriented downward) to move in a vertical direction towards the cell culture atop the glass slide. Manual force is applied until the lance array contacts the glass slide substrate, thereby ensuring target cells have been injected.

3.2.3 Biologic Testing

Testing Preparation

HeLa 229 culture cells were incubated on glass slides contained in six well plates (Sarstedt) at 37C and 5% carbon dioxide cultured in Dulbeccos Modified Eagles Medium (DMEM, Gibco) with 10% Fetal Bovine Serum (FBS, Denville Scientific) and Gentamicin (Sigma-Aldrich). Cells were allowed to adhere to a glass slide over a 24 hour period prior to testing. At the time of testing, the cell cultures had formed a mono-layer of approximately 70% confluency or cell density across a 1 cm diameter area centrally located on the glass slide

Following the 24 hr incubation test prep period, the six well plates containing the cultured cells were removed from the incubator and had DMEM/FBS growth media removed and then cells were rinsed in 1 mL per well of Hanks Balance Saline Solution (HBSS, Gibco). The respective treatment protocols detail specific treatments applied to the wells from this point forward.

Lance Geometry Experimental Design

The following describes the various well types:

- **Non-Treated Control (NTC):** Following the addition of HBSS, no treatment was performed on this well.

- **Background PI Control (BC):** Received 80 μL of PI solution (concentration: 500 μg of PI powder per mL PBS) per 1 mL of HBSS in injection well, no lancing, and no further treatment.

- **Treatment Protocol Lancing (FN, FW, or P):** Received 80 μL of PI solution (concentration: 500 μg of PI powder per mL PBS) per 1 mL of HBSS in injection well, lanced using a either a Flat, Narrow (FN); Flat, Wide (FW); or Pointed (P) lance array using the injection device described above. The injection device was inserted into each well and manual force was applied for five seconds to depress the lance array into the cell culture. Following

the lancing, the injection device was removed from the well. No voltage was used, so that random diffusion was responsible for transporting PI through the opened pores into the cells.

Lance Coating Experimental Design

As noted in the Test Preparation, HeLa 229 cells were cultured on a glass slide 24 hrs before testing. Additionally, these glass samples were placed on top of a stainless steel flat plate during this incubation process. This plate serves as the counter-electrode during testing. Each six well plate had one non-treated control well, a background PI control well, and four treatment wells.

Directly following incubation, media was removed from the wells, each well was washed with HBSS solution, and 2 mL HBSS solution was added to each well as an injection medium preparatory to LAN.

The following describes the various well types. Note that each treatment protocol was performed on both carbon coated lance arrays (CC) and non-coated silicon lance arrays (Si).

- **Non-Treated Control (NTC):** Received no PI in injection solution, no lancing, and no voltage.

- **Background PI Control (BC):** Received 40 μL of PI solution (concentration: 500 μg of PI powder per mL PBS) per 1 mL of HBSS in injection well, no lancing, and no voltage.

- **Treatment Protocol (CC/0V or Si/0V):** Received 40 μL of PI solution (concentration: 500 μg of PI powder per mL PBS) per 1 mL of HBSS in injection well, lanced for 5 seconds, and no voltage applied. These treatment samples were used to evaluate the diffusion rate of PI through the patent cell membrane.

- **Treatment Protocol: $+1.5$V DC (CC/1.5V DC or Si/1.5V DC)** Received 40 μL of PI solution (concentration: 500 μg of PI powder per mL PBS) per 1 mL of HBSS in injection well. Injection process occured as: lances lowered into six-well plate with -1.5V applied for 20 seconds to attract PI to lances, physical lancing of cell membranes, $+1.5$V applied for 5 seconds to repulse PI from the lances, and then removal of lances from cell.

- **Treatment Protocol: +5V Pulsed (CC/5V Pul or Si/5V Pul)** Received 40 μL of PI solution (concentration: 500 μg of PI powder per mL PBS) per 1 mL of HBSS in injection well. Injection process occured as: lances lowered into six-well plate with -1.5V applied for 20 seconds to attract PI to lances, physical lancing of cell membranes, followed by ten pulses between $+1.5$V and $+5$V applied within 20 ms, $+1.5$V DC applied for 5 seconds to repulse PI from the lances, and then removed from cells.

3.2.4 Propidium Iodide

In designated treatment wells, propidium iodide (PI, Sigma-Aldrich), a dye that is both impermeable to an intact cell membrane and fluoresces 20 to 30 times greater when intercalating with nucleic acid base pairs, was used as an indicator for nanoinjection efficacy. Because the nanoinjection process induces a physical pore to form as a result of being lanced, PI positive, living cells are qualified as successful transfection events. Quantification of test wells using PI (as well as control samples) is handled using flow cytometry.

For both experiments, a PI solution was prepared at a concentration of 500 μg of propidium iodide powder per 1 mL of PBS. Because large differences in PI+ uptake were desired for the Lance Geometry experimentation, because PI+ uptake is dependent only on diffusion, 80 μL of PI solution was placed in each 1 mL of HBSS prior to injection. For Lance Coating experimentation, an equivalent of 40 μL of PI solution was placed in each 1 mL of HBSS prior to injection, half the concentration used in the Lance Geometry experiment because other factors are believed to contribute to PI+ uptake.

3.2.5 Post Testing Flow Cytometry Preparation

After specific testing protocols were run, all samples were treated with 0.5 mL of 5X Trypsin (Gibco) and incubated for 5 min to remove the cells from the glass slide after which each well was treated with 1 mL of DMEM/FBS media to deactivate the trypsin. The samples were then transferred to FACS tubes (BD BioSciences) for centrifugation for 10 min at 2000 rpm. Following centrifugation, supernatants were removed and remaining cells were re-suspended in 0.25 mL of PBS for final preparation prior to flow cytometry.

3.2.6 Flow Cytometry

Following flow cytometry preparation, the samples were qualified using flow cytometry (BDCanto) to determine the cell viability (living vs dead cells) and PI uptake (fluorescing vs non-fluorescing cells). Each sample examined had approximately 10,000 events counted and characterized. Post flow processing occurred in respective analysis softwares (BD FACS Diva-Dako Summit) to visualize samples.

3.2.7 Statistical Analysis

Data gathered from the post flow analysis in Summit was used to calculate the percentage and cell count of living cells contained in the total cell population, also referred to as cell viability, as well as the percentage and cell count of the PI+ cells contained in the living cell population, also referred to as PI+ uptake.

Following this post processing, data sets were compared statistically initially using ANOVA testing to characterize presence of statistically significant relationships [123] followed by two-sided student t-tests ($\alpha = 0.05$) using JMP (SAS).

3.3 Results and Discussion

3.3.1 Lance Geometry Experimentation

Figure 3.5 shows a box-and-whisker plot of the percent of living cells in the total cell populations, or cell viability, for the Lance Geometry experiment. Accompanying this figure is Table 3.1, which provides statistically significant p-values for the comparision of the associated sample types. Among treatment groups, FN had a significantly higher cell viability than FW and P groups, albeit the difference in mean viabilities is $<3\%$ (see Table 3.2). For all comparisons involving the treatment groups vs. both NTC and BC controls, statistically significant differences are noted.

Figure 3.6 shows a plot of the percent of PI+ cells found in the living cell populations, or PI+ uptake, for the Lance Geometry experiment. Table 3.1 also shows the associated p-values. For treatment group comparisons, the FN group was significantly lower than both FW and P groups,

Table 3.1: Lance Geometry Experimentation: P-values for comparing percentage of living cells in total cell population and PI+ cells in living cell population

Comparisons	% Total Cell Pop. that is Living	% Living Cell Pop. that is PI+
NTC vs BC	0.8682	<0.0000
NTC vs FN	<0.0000	<0.0000
NTC vs FW	<0.0000	<0.0000
NTC vs P	<0.0000	<0.0000
BC vs FN	<0.0000	<0.0000
BC vs FW	<0.0000	<0.0000
BC vs P	<0.0000	<0.0000
FN vs P	<0.0000	<0.0000
FN vs FW	0.0087	<0.0000
FW vs P	0.3422	0.5441

having a difference in mean PI+ uptake between P group of nearly 15% (see Table 3.2). Similar to cell viability for Lance Geometry experimentation, the PI+ uptake for all treatment groups vs both NTC and BC controls are stastically significant.

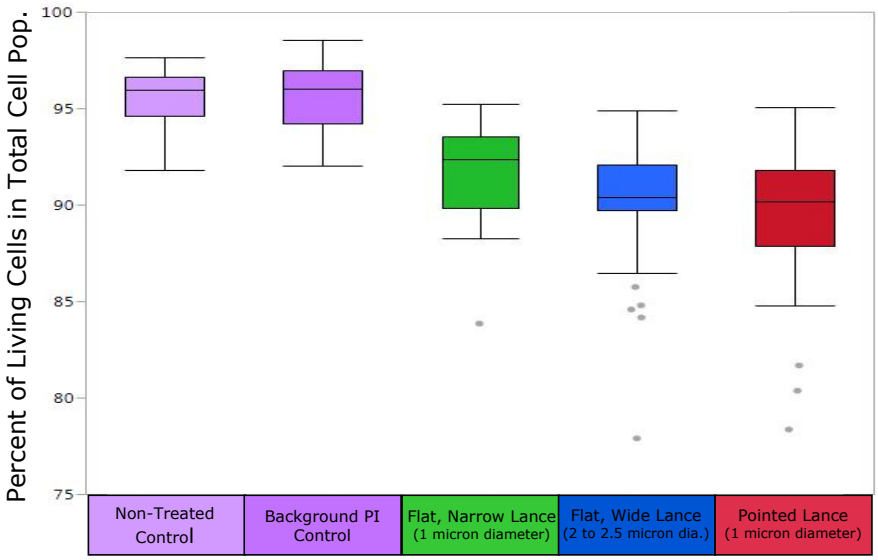

Figure 3.5: Cell Viability results for Lance Geometry Experimentation are represented as the percent of living cells in the total cell population for respective sample types. Table 3.1 shows statistically significant relationships for comparison between sample types.

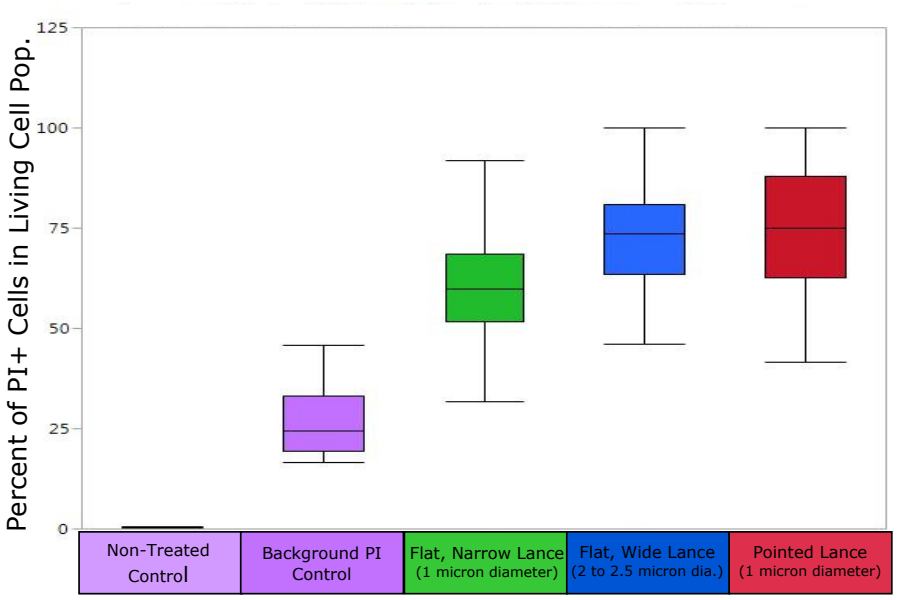

Figure 3.6: PI Uptake results for Lance Geometry Experimentation are represented as the percent of PI positive cells in the living cell population for respective sample types. Table 3.1 shows statistically significant relationships for comparison between sample types.

Table 3.2: Lance Geometry Experimentation: Sample Size and Mean Value Summary

Sample Type	n	% Cell Viability (CV)	CV Cell Count	% PI Uptake (PI)	PI Cell Count
NTC	15	95.52%	167,166	0.33%	583
BC	17	95.69%	167,452	26.71%	46,735
FN	40	91.73%	160,529	60.11%	105,195
FW	40	90.08%	157,640	73.50%	129,213
P	80	89.57%	156,745	75.08%	131,996

The Lance Geometry findings in regards to cell viability are suggestive of how the cell membrane reacts to surface defects. In reference [124], it was shown that a blunt tip AFM probe measuring 800 nm in diameter required more than three times less force to penetrate human epidermal melanocytes as opposed to a probe with the same diameter but with a pointed tip (Penetration Force for Blunt tip: 0.67 nN, Penetration Force for Pointed tip: 1.90 nN). Furthermore, it was shown that an AFM tip measuring 200 nm in diameter with a blunt tip required a penetration force of 0.65 nN, suggesting that penetration force is less dependent upon diameter of probe and more dependent upon the tip being blunt or pointed. By comparison, we have previously shown [125]

using lance array nanoinjection that an average of 2.3 μN per lance is required to puncture HeLa cell membranes using pointed lances. In our study, we quantified the force per lance required to maximize PI delivery into the cells, which may be different than the force required for a single lance to pierce the cell membrane

Given this basis, it was anticipated that with FW and FN lance types a lower amount of cellular disruption would occur because less force would be required to penetrate, resulting in higher cell viability rates. However, in this experiment, cell viability rates were only significantly higher for the FN vs FW and P cases. Even so, the cell viability differences for FN and FW were $<$3% different than P samples.

A possible explanation for the difference between reference [124] and this work deals with the fact that the AFM experimental results were force controlled. The LAN process used in this study was not force-controlled (particularly on the order of nN), and therefore membrane penetration mechanics and cell viability may be irrelevant in regards to geometry when there is such a difference in force magnitude application.

In terms of PI+ uptake, the findings demonstrate that PI uptake is greatest in P treatment samples (75.08%), followed closely by FW treatment samples (73.50%). The rationale for this outcome is not clear. It was anticipated that the FW samples would have a larger PI+ uptake rate than both the FN and P samples because the effective surface defect area created from FW lances would be between 4 to 6.25 times greater. However, despite this fact, the comparison between FW and P is not significant.

It is possible, in terms of the PI+ uptake for FW and P lances, that even though the P shaft is smaller than the FW, that perhaps the way the cell membrane and underlying structures are disrupted following injection with the pointed lance tip makes it more difficult for the cell to heal the surface defect allowing more diffusion of PI across the membrane.

3.3.2 Lance Coating Experimentation

Figure 3.7 shows a plot of cell viability for the Lance Coating experiment and is further summarized in Table 3.3 and Table 3.5 for statistical comparison. Noted in this comparison study between the non-coated and the carbon-coated silicon lances is the lack of statistically significant difference between the lance type groups when comparing similar testing conditions. One

Table 3.3: Lance Coating Experimentation: P-values for comparing different sample types in terms of Percentage of Living Cells in Total Cell Population

Sample Type	NTC	BC	CC/0V	Si/0V	CC/1.5V DC	Si/1.5V DC	CC/5 V Pul
BC	0.6436						
CC/0V	0.0308	0.0613					
Si/0V	0.0201	0.0399	0.8644				
CC/1.5V DC	<0.0000	<0.0000	<0.0000	<0.0000			
Si/1.5V DC	<0.0000	<0.0000	<0.0000	<0.0000	0.2006		
CC/5V Pul	<0.0000	<0.0000	<0.0000	<0.0000	0.0806	0.7116	
Si/5V Pul	<0.0000	<0.0000	<0.0000	<0.0000	0.0358	0.4487	0.0077

exception to this observation is the comparison of CC/5V Pul to Si/5V Pul, where CC/5V Pul is significantly higher by 5%. It is not clear why the CC/5V Pul has a higher cell viability rate in this situation. It is possible that the difference is a function of the electrical exposure, and requires further investigation. Also seen in these results is the gradual decrease in cell viability as the amount of electrical exposure increases when referenced by NTC and BC controls, regardless of lance type.

Figure 3.8, Table 3.3, and Table 3.5 present the PI+ uptake for the two lance coating types. Notably, there are no statistically significant relationships between the CC and Si lance array types when similar testing conditions exist, suggesting no advantage is gained by carbon coating the lance array.

Although not the focus of the lance coating experimentation, also shown in these results is that electrical application can increase significantly PI+ uptake (ie. see comparison of CC/0V:CC/1.5V DC and Si/0V:Si/1.5V DC) as well as cause a decrease in PI+ uptake (ie. see comparison of CC/1.5V DC:CC/5V Pul and Si/1.5V DC:Si/5V Pul). The later comparison suggests that perhaps electrically pulsing the lances once inserted into the cell has an adverse effect either in terms of PI+ release directly and/or cell viability, which in turn reduces the number of PI+ living cells.

3.4 Conclusion

Improving the delivery of molecular loads to target cells is a critical part of integrating meaningful biologic discovery with clinical and benchtop application. The primary goal for LAN

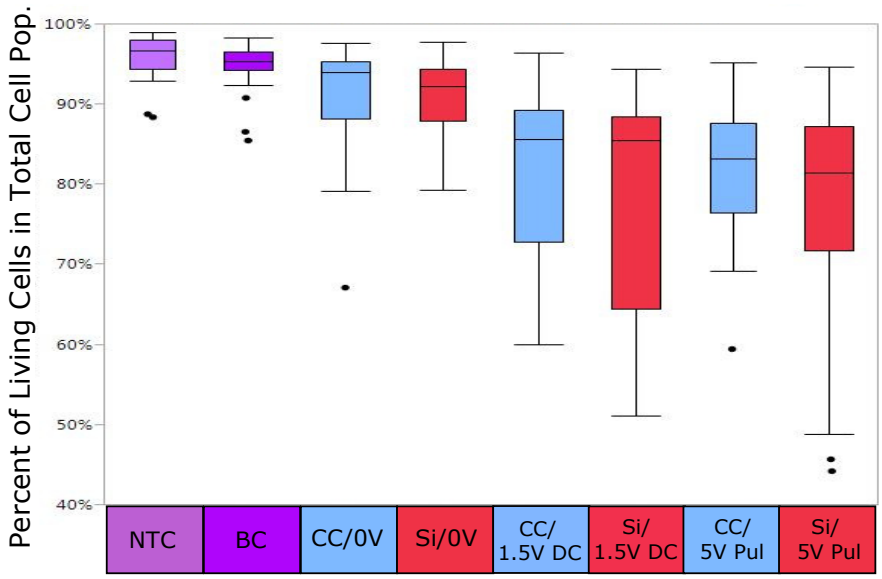

Figure 3.7: Cell Viability results for Lance Coating Experimentation are represented as the percent of living cells in the total cell population for respective sample types. Table 3.3 shows statistically significant relationships for comparison between sample types.

Table 3.4: Lance Coating Experimentation: P-values for comparing different sample types in terms of Percentage of PI+ Cells in Living Cell Population

Sample Type	NTC	BC	CC/0V	Si/0V	CC/1.5V DC	Si/1.5V DC	CC/5 V Pul
BC	<0.0000						
CC/0V	<0.0000	0.0186					
Si/0V	<0.0000	0.0242	0.8980				
CC/1.5V DC	<0.0000	<0.0000	<0.0000	<0.0000			
Si/1.5V DC	<0.0000	<0.0000	<0.0000	<0.0000	0.8613		
CC/5V Pul	<0.0000	<0.0000	<0.0000	<0.0000	0.0060	0.0112	
Si/5V Pul	<0.0000	<0.0000	<0.0000	<0.0000	0.1716	0.2399	0.1619

as a transfection technology is to effectively deliver molecular loads without compromising cell viability. Since LAN relies both on physical and electrical interactions with target cells, structural design and function of the microfabricated silicon lances are closely wrapped together.

Investigated in this work are two parameters, lance geometry (tip shape and shaft diameter) and coating, believed to impact the ability of a non-viral transfection technology, known as Lance Array Nanoinjection, to deliver propidium iodide to the intracellular space of HeLa 229 cells.

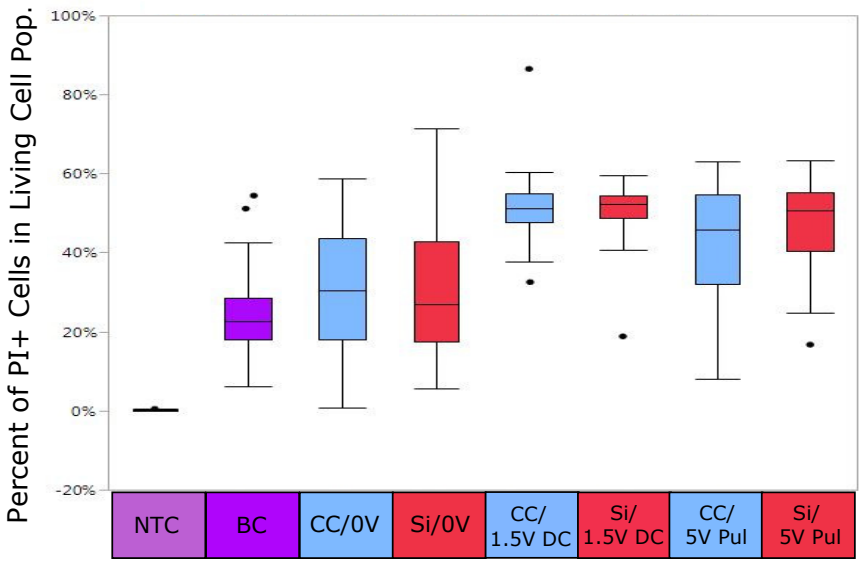

Figure 3.8: PI Uptake results for Lance Coating Experimentation are represented as the percent of PI positive cells in the living cell population for respective sample types. Table 3.4 shows statistically significant relationships for comparison between sample types.

Table 3.5: Lance Coating Experimentation: Sample Size and Mean Value Summary

Sample Type	n	% Cell Viability (CV)	CV Cell Count	% PI Uptake	PI Uptake Cell Count
NTC	28	95.84%	167,726	0.17%	295
BC	40	94.85%	165,985	24.84%	43,466
CC/0V	52	91.29%	158,836	31.24%	77,886
Si/0V	48	90.98%	158,400	30.91%	81,329
CC/1.5V DC	35	81.15%	147,297	51.29%	64,581
Si/1.5V DC	33	78.42%	143,154	50.75%	65,668
CC/5V Pul	48	81.87%	144,076	43.57%	88,583
Si/5V Pul	43	76.86%	136,697	47.31%	87,540

Findings indicate two major items in terms of lance geometry. First, FN lances produce a slightly higher cell viability rate (91.73%) than the other two lance geometries (FW: 90.08%, P: 89.57%). Second, P lances produce the highest PI uptake rate of 75.08%.

Lastly, findings related to the carbon coating of the silicon lances (CC) demonstrate that neither cell viability or PI uptake rates are increased when comparing to non-coated lances (Si) during both non-voltage and voltage injection events.

Given the fact that cell viability rates of all lance geometries are nearly 90% and that greater PI uptake was seen with P lances, it appears that using P shaped lances would be the recommended geometry for future nanoinjection experiments. Noted earlier was the fact that lance shape does not necessarily translate to degree of cellular trauma detectable in post-injection flow cytometry analysis. Future histological investigation of cellular structures post-injection may be warranted in the context of lance geometry to determine if lance shapes influence cellular damage and/or cell viability.

While the electrical effects of the carbon coating on the silicon lances proved to be inconsequential, it is still of interest to characterize other microfabricated lances in terms of the effects of electrical behavior during LAN. Future investigation in this area may include similar testing protocols with alternative materials used for lance arrays, such as carbon nanotubes.

CHAPTER 4. TRANSIENT LOW TEMPERATURE

The following chapter has been submitted as a journal article to the *Journal of Nanotechnology in Engineering and Medicine* and is currently in review. The title of this journal article is "Transient Low Temperature Effects on Propidium Iodide Uptake in Lance Array Nanoinjected HeLa Cells". As a result, there may be some material that is contained elsewhere in this dissertation but is presented here as a representation of this original journal article.

4.1 Introduction

Biologic engineering applications utilizing specific cell lines and/or entire organisms have been accelerated by the use of programmable endonucleases such as zinc-fingers (ZFNs) [126], transcription activator-like effector nucleases (TALENs), and clustered interspaced short palindromic repeats and associated cas9 (CRISPR-Cas9) [127–129]. These tools present researchers with a large degree of freedom in designing site-specific modifications to the genome. The ability to directly insert [130, 131], activate [132–134], repress [132, 135], and/or knock-out [97] genes at multiple sites, even in a single transfection event [136–138], is now possible.

Further fueling excitement in regards to genetic engineering is the ability to direct these and related technologies towards mitigating and controlling disease processes. Specifically, therapies are being directed at treating both human monogenic diseases such as lipoprotein lipase deficiency (LPLD) [4], leber cogenital amaurosis (LCA) [5–9], and hemophilia B [10, 11] as well as more genetically complex diseases such as heart failure [12–15], B-cell malignancies [16], and neurodegenerative diseases [17] using exogenously deliverd genetic material to alter aberrent cellular behaviors.

While the ability to modify target cells has dramatically improved, the ability to physically deliver these effector molecules to target cells is still constrained in many ways. What makes it challenging for transfection methods to achieve successful transformation is that there are barriers

that inhibit molecular delivery and can be described as barriers related either to physical or physiological elements of cellular targets. In the context of physical barriers, molecular loads must cross both the cell membrane and cell nucleus before genomic modification can be achieved.

In the past, engineered viruses have been an attractive option for overcoming genetic delivery to target cells because viruses have cell adhesion proteins that help transport the virus across the cell membrane [111–114]. When coupled with the tropic ability of viruses to target specific cell types within a mixed population such as blood, researchers have been able to achieve benchmark transfection rates.

Despite these strengths, viral transfection methods have limitations that make widespread application difficult, especially in the clinical setting. Weaknesses in regards to viral transfection include: immunologic safety, viral containment to target tissues, limits to genetic load capacity, and potential insertional mutagenesis [116]. Because of these drawbacks researchers have sought alternative, non-viral modalities for molecular delivery [117].

4.1.1 Nanoinjection

One of these non-viral transfection technologies has been described in the literature as a process called nanoinjection [25, 26]. Originally designed to facilitate transgenic mouse embyro modification, a second generation of nanoinjection technology has been developed that is designed to modify hundreds of thousands of somatic cells simultaneously [24]. This second generation nanoinjection process is called lance array nanoinjection (LAN) because it utilizes an array of microfabricated silicon lances measuring 10 microns in length, spaced every 10 microns to facilitate both the physical piercing and electrical manipulations required for LAN (see Figure 4.1).

Procedurally, LAN occurs in four major steps, which include: staging the lance array in an injection solution containing the molecular load of choice, electrical attraction of the molecular load onto the lance structure, physically lancing of the cell culture–effectively placing the molecular load attached to the lance in the cells' cytoplasm and electrically repulsing the molecular load into the intracellular space of the cell, and retraction of lances from cell culture [24].

Prior nanoinjection research has focussed on intrinsic variables specific to nanoinjection in terms of both modelling and experimentation of electrical parameters effecting delivery of molec-

ular loads, particularly DNA [50, 139, 140]. This work seeks to expand that perspective by investigating the thermal environmental effects on target cells undergoing LAN.

4.1.2 Cell Membrane in Response to Transient Low Temperature

Because LAN, like all other non-viral transfection methods, relies on cell membrane mechanics for molecular transport into the cell's cytoplasm, it is critical that factors related to the cell membrane behavior be well understood. One particularly important environmental stressor that alters membrane function is sub-physiologic temperature (i.e., $<37^{\circ}$C) [141–154].

4.1.3 Cell Membrane Stiffening at Low Temperature

In general terms, the mammalian cell membrane is constructed of a phospholipid bilayer containing protein aggregates and carbohydrates with regions of cholesterol rich domains, which play an important part in membrane transport as it relates to temperature [142, 143]. Al-Fageeh et al. [141] notes that with *in vitro* reduction in temperature, rigidity of the membrane increases as internal hydrophobic portions of the phospholipids begin to pack more closely, increasing the stiffness of the membrane structure [143].

In order to mitigate this effect, many cellular systems will attempt to maintain a constant degree of membrane fluidity in the face of reduced temperature, an idea known as homeoviscous adaptation. In order to facilitate this goal during cold stress, the cell initiates activity of fatty acid desaturase and dehydrases to convert saturated fatty acids to poly-unsaturated fatty acids, effectively reducing the length of the chain and increasing fluidity of the membrane [141, 144–148]. Although these measures do attempt to mitigate the stiffening of the cell membrane, it does not altogether prevent stiffening when exposed to reduced temperature [143].

4.1.4 Diminished Cytoskeleton at Low Temperature

While the cell membrane itself is structurally stiffer with reduced temperature, atomic force microscopy studies indicate that the overall integrity of the cell decreases in stiffness as temperature decreases [149–151]. This behavior is caused by the disassembly of the underlying cytoskeleton which serves as a structural scaffold that runs throughout the intracellular space of the cell.

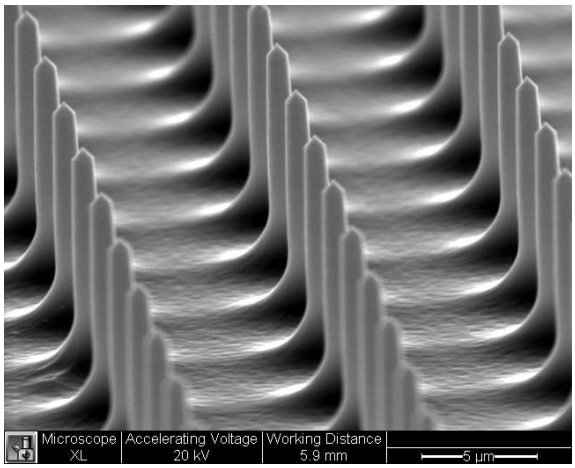

Figure 4.1: SEM image of Lance Array Silicon chip. Lances measure 10 microns in height, 1-2.5 microns in diameter, with a 10 micron spacing

This fact becomes relevant in terms of LAN because the cytoskeleton plays a critical role in cell membrane wound healing. When surface damage occurs to the cell membrane, the cytoskeleton facilitates actinomyosin contraction and recruiting of repair machinery to the damaged site [152–154], a function that is hypothesized to be impaired at low temperature because of reduced cytoskeleton presence.

The purpose of this work is to characterize the behavior of HeLa 229 cells in response to transient low temperature (3°C) relative to warmer samples (23°C) following lance array nanoinjection (LAN). It is hypothesized that because the cell membrane is stiffer and the cytoskeleton is compromised (and thereby functionally impaired) at low temperature, that pores created by LAN will remain patent longer for samples treated at 3°C than samples treated at 23°C. To help characterize this hypothesized thermal-dependent pore formation event, propidium iodide (PI, Sigma-Aldrich), a dye impermeable to the cell membrane that fluoresces when interacting with nucleic acids, will be added to injected cell cultures at various intervals post-injection. When the cells have pores still present at the time of PI introduction into the sample solution, PI should pass through the cell membranes of living HeLa cells, interact with nucleic acids, and fluoresce during flow cytometry. Figure 4.2 illustrates this process, which is a variant to nanoinjection processes used in the past [24].

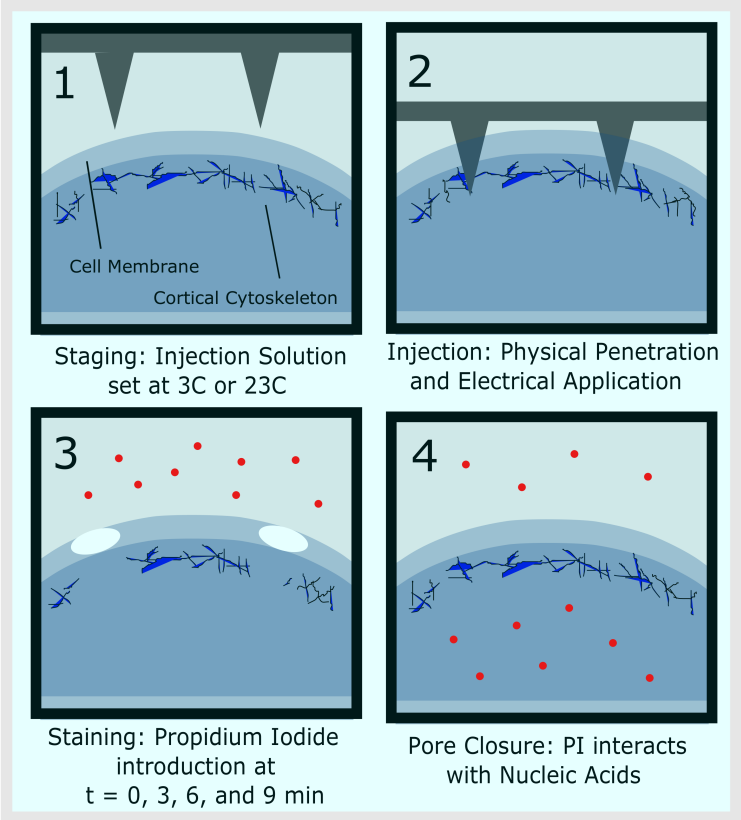

Figure 4.2: Lance Array Nanoinjection Stepwise Process. 1: Staging lance array into injection solution maintained at either 3°C or 23°C. 2: Injection of cell culture, consisting of both physical penetration of the cell membrane and electrical treatment. 3: Staining of cell culture by introduction of PI into the extracellular solution at 0, 3, 6, and 9 minutes post-injection. 4: Induced pores from injection event eventually close and PI molecules in the intracellular space of injected cells interact with nucleic acids, increasing PI fluorescence.

4.2 Methods

4.2.1 Lance Array Fabrication

Microfabrication of the silicon lance array consists of four major steps, which include patterning with positive photoresist (AZ330F), deep reactive ion etching (DRIE), a sulfur hexafluoride (SF6) isotropic plasma etch, and a final cleaning step. More details of the microfabrication are contained in prior work [23].

4.2.2 Injection Set-Up

Nanoinjection Device and Electrical Switch Box

The nanoinjection device consists of six major elements which include: stepper motor, orthoplanar spring, coiled spring, lance array holder, lance array, and electrical connection. The rapid-prototyped, ABS (acrylonitrile butadiene styrene) orthoplanar spring has a stepper motor attached superiorly that presses against a coiled spring that acts to move the orthoplanar spring upward and downward. Attached to the orthoplanar spring apparatus at the inferior end is a lance array holder that allows for the insertion and removal of the silicon-etched lance array. Gold contacts were used to electrically connect the lance array to an electrical switch box (see Figure 4.3).

The electrical switch box, which is connected to the injection device, operates by receiving 2 input signals and switching between these at specific times. Treatment samples receiving electrical treatment experience an initial -1.5V for 20 seconds, followed by insertion of the lances into the cells, followed by a 20 ms interval of positive pulsed voltage (2 ms period, 50 percent duty cycle), followed lastly by a 5 second interval of $+1.5$V.

During injection events typically performed using LAN, the initial negative voltage attracts the molecular load to the lances and the positive pulses repel the PI into the cells [24]. For this study the PI was added into solution after injection to help elucidate molecular mechanisms in response to LAN. The electrical treatment was kept the same as what has been reported in the past to allow for comparison [24].

Cell Culture Platform

The 3D printed Cell Culture Platform (MakerBot Replicator 2) consists of three parts—the PLA (polylactic acid) base, glass slide, and the PLA top clip. The glass slide was used to provide a flat, uniform culturing surface for the HeLa cells. This glass slide snap-fitted into the PLA base. Once snapped into place, the top PLA clip was placed on the assembly to provide a uniform base for the Nanoinjection Device described above to rest on during nanoinjection. In addition to allowing for the glass slide to attach, the base also contains an exposed wire coil that serves as an electrical ground. The addition of the 3D printed Platform was to help facilitate better alignment of individual components that proved to be of value in preliminary testing (see Figure 4.4).

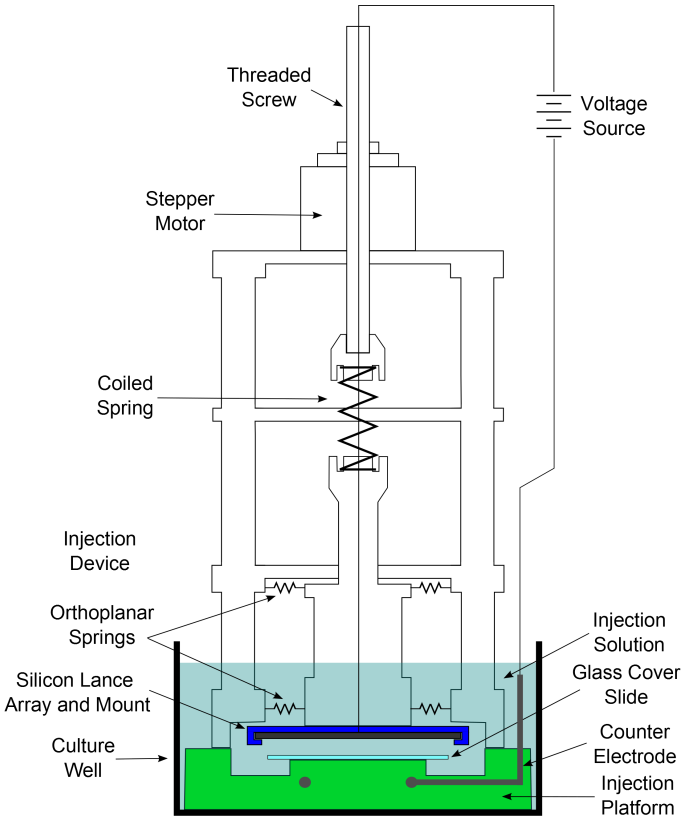

Figure 4.3: Diagram of Nanoinjection Device. Components shown (top to bottom) include: Stepper motor mounted to ABS orthoplanar spring, threaded screw acting to actuate silicon lance array mounted above 3D printed Cell Culture Platform, and associated electrical connections (ground connected to Cell Culture Platform).

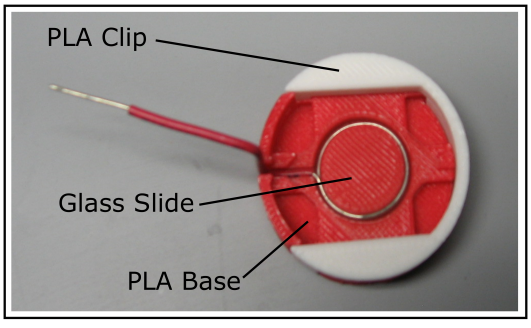

Figure 4.4: Cell Culture Platform assembly. Glass slide containing cell culture secured between the bottom PLA base and top PLA clip to provide proper alignment during injection.

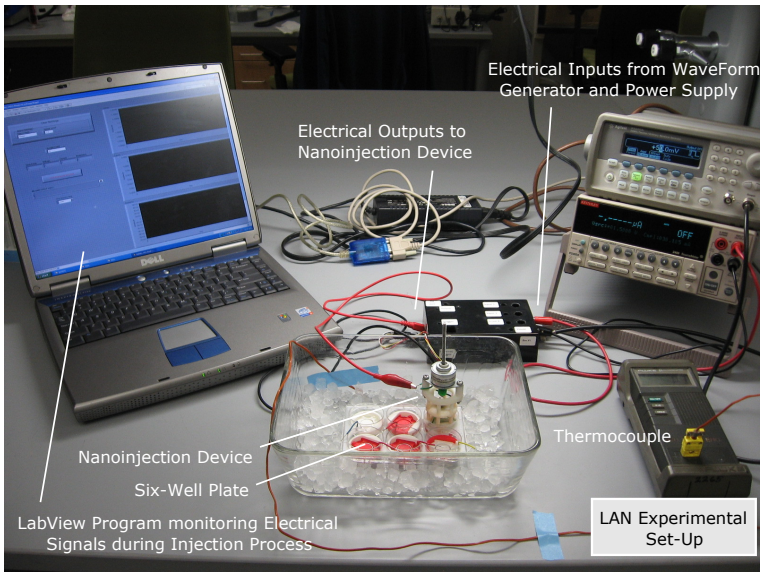

Figure 4.5: Experimental set-up illustrating injections performed for 3°C treatment samples. A thermocouple was used to verify surrounding fluid temperature of ice/water bath of 3°C prior to treatment. LabView program was used to verify proper electrical signals delivered to Nanoinjection Device. Six well plate containing Cell Culture Platforms and associated cell cultures were aligned to Nanoinjection Device.

4.2.3 Propidium Iodide

In designated treatment wells, propidium iodide (PI, Sigma-Aldrich), a dye that is both impermeable to an intact cell membrane and fluoresces 20 to 30 times greater when associated with genetic material, was used as an indicator for nanoinjection efficacy. Because the nanoinjection process induces a physical pore to form as a result of being lanced, PI positive, living cells are qualified as successful modification events. Quantification of test wells using PI (as well as control samples) is handled using flow cytometry.

4.2.4 Testing Preparation

HeLa 229 culture cells were incubated at 37C and 5% carbon dioxide cultured in Dulbeccos Modified Eagles Medium (DMEM, Gibco) with 10% Fetal Bovine Serum (FBS, Denville Scientific) and streptomycin/penicillin (Gibco). Six well plates were seeded with cell cultures and allowed to adhere to a glass slide in conjunction with the 3D printed Cell Culture Platform over a 24 hour period, producing an approximately 70% confluent mono-layer of cells.

Following the 24 hr incubation, the six well plates containing the cultured cells were removed from the incubator and had growth media removed and then cells were rinsed in 1 mL per well of phosphate buffered solution (PBS). The respective treatment protocols detail specific treatments applied to the wells from this point forward.

As noted previously, cultured samples were prepared in the 3D printed PLA platform and top clip components. Typical six well plates were organized to have a non-treatment control (no voltage, no lancing, no PI), a backgroung PI control (only PI added), and the remaining wells for treatments at two different test temperatures, room (23°C) and ice (3°C), at two different voltage protocols.

In order to ensure the exposure of the cells to the different temperatures, six well plates were given 20 min to come to temperature. For test samples exposed to ice temperatures, the six well plates were placed in ice baths. This time frame was selected for the cold exposure because it was determined that was the amount of time required to get the sample to 3°C and longer-term exposure to cold temperatures has been shown to induce cell cycle arrest, reduced energy production, and activation of apoptosis [151, 155–157].

Figure 4.5 shows the experimental set-up used for injections. Equipment include a thermocouple (Fluke 51 K/J Thermometer) used for verifying amibent temperature of the injection fluid, a waverform generator (Agilent 33220A) and power supply (Keithley 2400 Sourcemeter) for providing electrical input signals, an electrical switch box for controlling electrical signal delivery to the nanoinjection device, a LabView VI (National Instruments) program used to monitor electrical signal inputs, and the nanoinjection device with the associated six-well plate (Sarstedt) and cell culture platforms.

Treatment Protocols

The following describes the various well types:

- **Non-Treatment Control (NTC):** Received no lancing, no applied voltage, and no PI. Non-treated controls were generated for each temperature (23°C and 3°C).

- **Background Control for PI (BC):** Received no lancing, no applied voltage. Received 0.02 mg/mL PI. Background PI controls were generated for each temperature (23°C and 3°C).

- **Treatment Protocol +5V Pulsed:** Lanced, and received applied voltage which consisted of: 20 second application of −1.5 DC voltage, followed by 10 squarewaves pulsed between +1.5V to +5V with a 2 ms period, followed by 5 seconds of a +1.5 DC voltage. These treatment samples were generated for each temperature (23°C and 3°C). PI was finally added at four different time intervals (0, 3, 6, and 9 min) measured from the time the when lances were removed from the cells.

- **Treatment Protocol +7V Pulsed:** Lanced, and received applied voltage which consisted of: 20 second application of −1.5 DC voltage, followed by 10 squarewaves pulsed between +1.5V to +7V with a 2 ms period, followed by 5 seconds of a +1.5 DC voltage. These treatment samples were generated for each temperature (23°C and 3°C). PI was finally added at four different time intervals (0, 3, 6, and 9 min) measured from the time the when lances were removed from the cells.

For convenience, specific treatment sample types will be referred to by temperature of injection solution, pulsed voltage protocol used, and if requisite, the time interval at which PI was introduced. For example, 3°C/7V/T3 means a treatment sample that was injected in a solution at 3°C using a 7V pulsed voltage protocol and the specific time PI was added was 3 minutes post-injection.

4.2.5 Post Testing Flow Cytometry Preparation

After specific testing protocols were run, all samples were treated with 0.5 mL of 5X Trypsin (Gibco) and incubated for 5 minutes for removal of cells from the glass slide. Once the HeLa cells were removed, each well was treated with 1 mL of DMEM/FBS media to deactivate the trypsin. The samples were then transferred to FACS tubes (BD BioSciences) for centrifugation for 10 min at 2000 rpm. Following centrifugation, supernatants were removed and remaining cells were re-suspended in 0.25 mL of PBS for final preparation prior to flow cytometry.

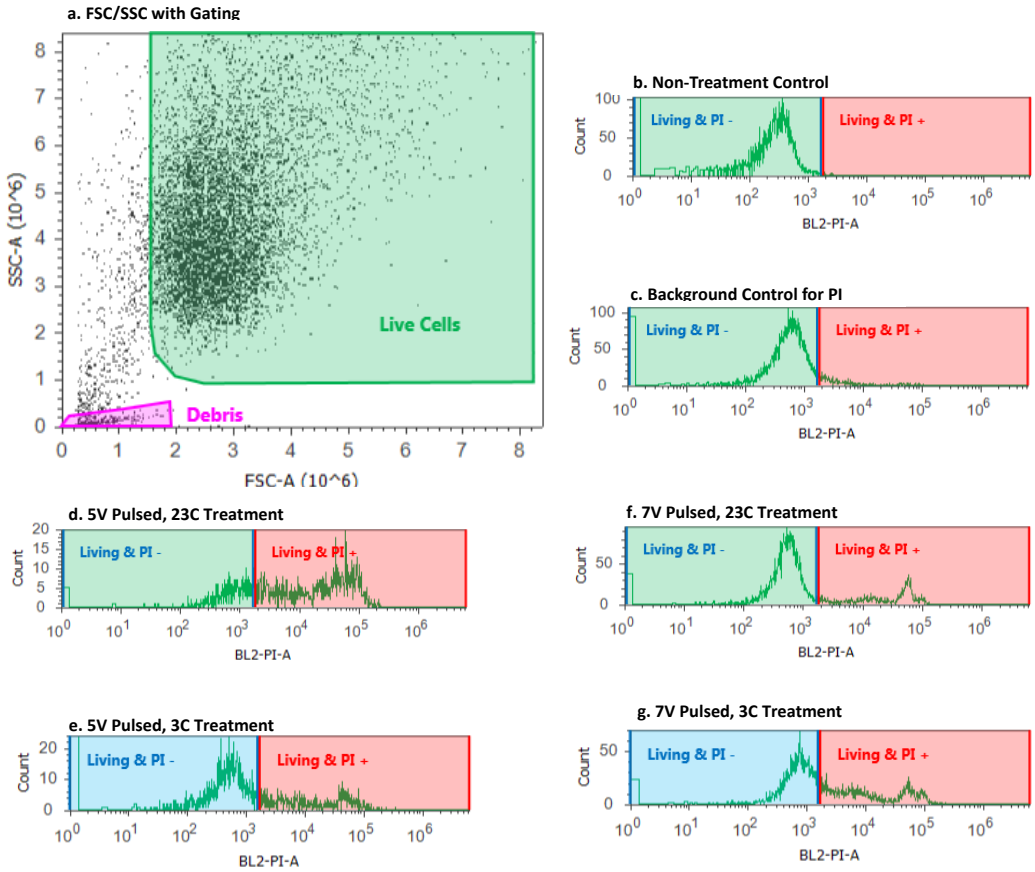

Figure 4.6: Flow cytometry examples of six different sample types explored in this experiment. a) Demonstrates how cells were gated for Living Cells from forward and side-scatter signals. b-g) Represents gating of living cells based on signal intensity of samples from blue-laser 2 sensor (BL-2). Note: The threshold for PI+ signals was determined from non-treated control samples and is used globally to determine PI+ cells in treatment samples.

4.2.6 Flow Cytometry

Following flow cytometry preparation, the samples were qualified using flow cytometry (Attune Acoustic Focusing Flow Cytometer, Life Technologies) to determine the cell viability and PI uptake. Each sample examined had approximately 10,000 events counted and characterized. Post flow analysis occurred in Attune Cytometric 2.1 (Applied Biosystems, Life Technologies) to visualize, gate desired cell populations, and develop primary level data for each sample. Figure 4.6 helps to demonstrate how these cell populations were gated and quantified.

4.2.7 Statistical Analysis

Data gathered from the post flow analysis in Attune was statistically analyzed in JMP (SAS). Prior to analyses, treatment samples were normalized relative to both non-treated control and background PI control samples at room temperature. Specifically, normalized cell viability and propidium iodide (PI) uptake was calculated according to:

$$a = \frac{\text{Living Cells in Test Sample}}{\text{Total Living and Dead Cells in Test Sample}}$$

$$b = \frac{\text{Living Cells in Non} - \text{Treated Control}}{\text{Total Living and Dead Cells in Non} - \text{Treated Control}}$$

$$\text{Normalized Cell Survival} = \frac{a}{b}$$

$$c = \frac{\text{Living and PI}^{+}\text{ Cells in Test Sample}}{\text{Total Living Cells in Test Sample}}$$

$$d = \frac{\text{Living and PI}^{+}\text{ Cells in Backgroun PI Control}}{\text{Total Living Cells in Backgroun PI Control}}$$

$$\text{Normalized PI Uptake} = \frac{c}{d}$$

This normalization step was used to help control for confounding variables particular to individual six-well plates.

Following both PI Uptake and Cell Viability Normalizations, data sets were compared statistically using ANOVA and student t-tests. Further analysis was conducted to evaluate statistical significance using the more conservative methods by using the permutation testing in JMP (1000 iterations, two-sided p-value) [158]. Additionally, linear combinations statistical methods were used to examine whether 3°C samples as a whole were statistically different from 23°C samples. Using the same criteria, sample sets were also contrasted using linear combinations for examining whether 5V samples as a whole were statistically different from 7V samples.

4.3 Results and Discussion

4.3.1 Normalized PI Uptake

Figure 4.7 shows a collection of box-plots showing the respective data for each sample set and relative statistically significant relationships following permutation analysis. Analysis of the 3°C/7V Pulsed samples shows a statistically significant difference (two-sided p-value) with both 23°C/5V Pulsed and 23°C/7V Pulsed samples at all times, with the exception of the 6 min comparison between 3°C/7V Pulsed and the 23°C/5V Pulsed. Furthermore, in both the 3 and 9 minute comparisons, 3°C/7V sample sets are significantly different from 3°C/5V Pulsed samples. Shown in the Table 4.1 and Table 4.2 are corresponding values for the two-sided p-values attached to the comparison of samples at each time interval for both PI uptake and cell viability. (See Figure 4.7)

Shown in Figure 4.8 are sample population means for each sample type relative to the time post-injection when the samples had PI added. Figure 4.8 illustrates three key findings. First, all treatent samples demonstrate an increase in normalized PI uptake for samples from 0 minutes to 3 minutes followed by a decrease from 3 minutes to 6 minutes. With the exception of the 3°C/5V Pulsed samples, all samples measured a more minor secondary increase in normalized PI uptake from 6 minutes to 9 minutes.

Second, both colder samples have higher degrees of normalized PI uptake than the 23°C sample types, with the 3°C/7V Pulsed samples having the highest overall magnitude of PI uptake

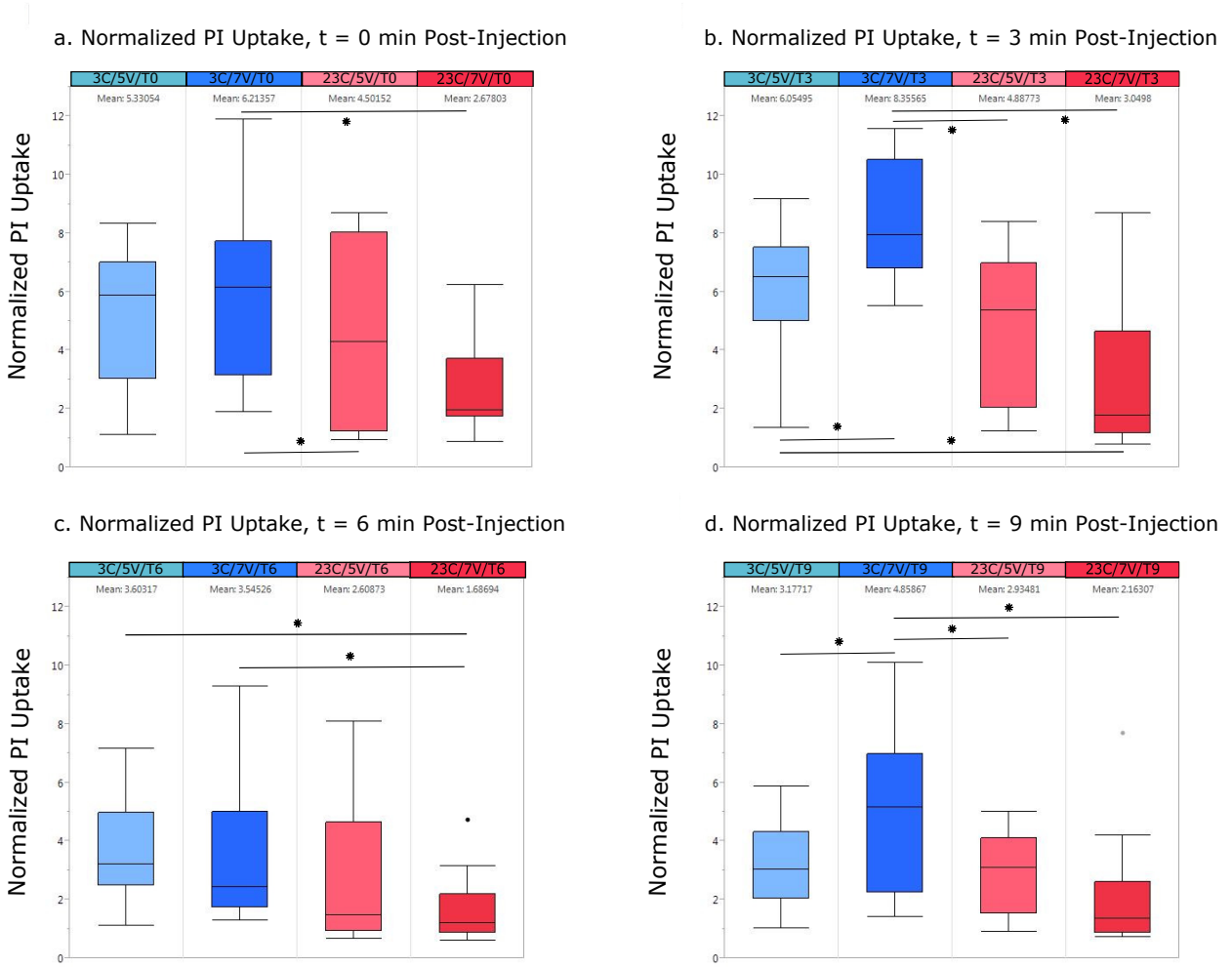

Figure 4.7: Box Plots of Normalized Propidium Iodide Uptake for all sample types, grouped according to post-injection time when PI was added. Statistically significant relationships based on the permutation testing are indicated with a star.

with the exception of the nearly comparable value it shares with the 3°C/5V Pulsed samples at 6 minutes.

Lastly, the ordering of the sample types by degree of PI uptake indicates that the 3°C/7V Pulsed samples had the greatest PI delivery efficiency, while the 23°C/7V Pulsed samples had the lowest PI delivery efficiency.(See Figure 4.8)

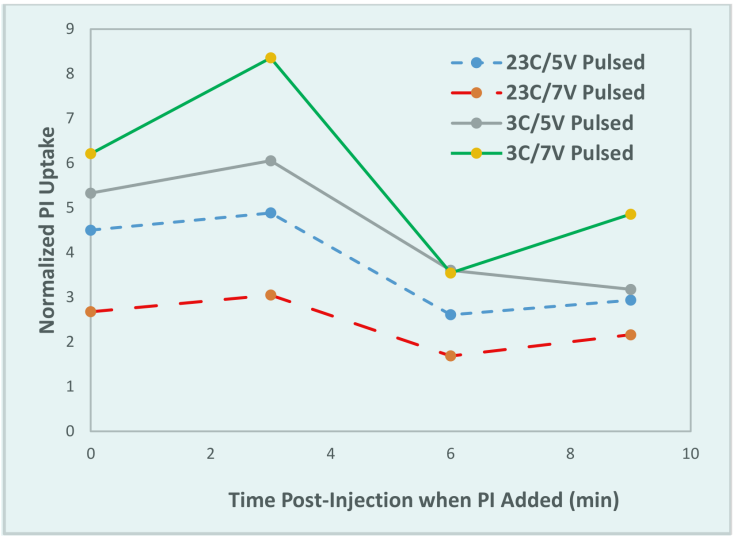

Figure 4.8: Mean Normalized PI Uptake for all sample types through time.

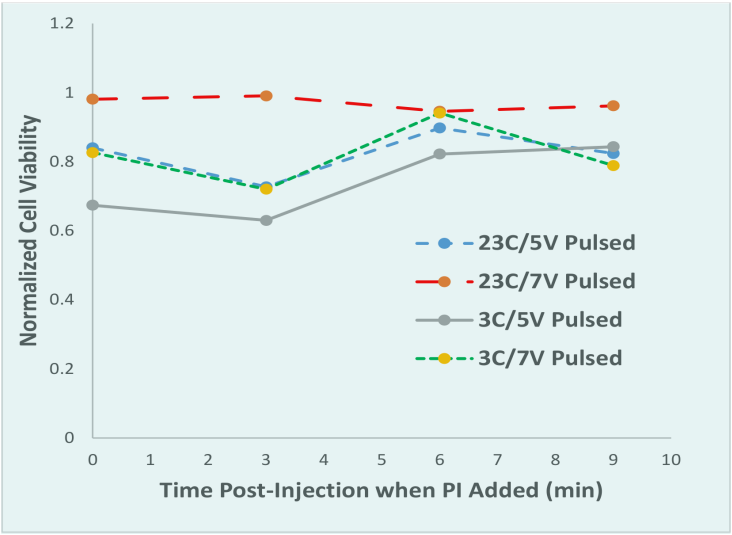

Figure 4.9: Mean Normalized Cell Viability for all sample types through time.

Table 4.1: Normalized PI Uptake Efficiency P-Values for Thermal Testing

Comparisons	0 Min Delay	3 Min Delay	6 Min Delay	9 Min Delay
23°C/5V vs 23°C/7V	0.109	0.145	0.235	0.321
23°C/5V vs 3°C/5V	0.512	0.168	0.192	0.648
23°C/5V vs 3°C/7V	0.207	0.001	0.297	0.031
23°C/7V vs 3°C/5V	0.003	0.006	0.005	0.123
23°C/7V vs 3°C/7V	0.001	0.000	0.014	0.005
3°C/5V vs 3°C/7V	0.402	0.005	0.932	0.026

Table 4.2: Normalized Cell Viability Efficiency P-Values for Thermal Testing

Comparisons	0 Min Delay	3 Min Delay	6 Min Delay	9 Min Delay
23°C/5V vs 23°C/7V	0.087	0.000	0.599	0.173
23°C/5V vs 3°C/5V	0.055	0.086	0.397	0.859
23°C/5V vs 3°C/7V	0.868	0.923	0.655	0.739
23°C/7V vs 3°C/5V	0.000	0.000	0.037	0.048
23°C/7V vs 3°C/7V	0.012	0.000	0.941	0.011
3°C/5V vs 3°C/7V	0.025	0.084	0.099	0.467

4.3.2 Normalized Cell Viability

Figure 4.9 are sample population means for the normalized cell viability for each sample type at the different times post-injection. This graph demonstrates an effective range of cell viability of 63% (3°C/5V Pulsed at t = 3 min) to 99% (23°C/7V Pulsed at t = 3 min). With the exception of 23°C/7V Pulsed samples, it appears that cell viability decreases from 0 to 3 minutes post-injection, followed by an increase during 3 to 6 minutes.

4.3.3 Temperature and Pulsed Voltage Contrasts

Table 4.3 illustrates p-values related to the linear combinations of temperature contrast. First, in the context of temperature contrast between 23°C and 3°C samples, it appears that cell viability is significantly different during the first two sample intervals (T0 and T3), favoring samples exposed to warmer conditions. The PI uptake for this same comparison also indicates that the colder samples had significantly higher levels for all time intervals investigated.

Table 4.3: Linear Combination P-Values for Temperature Contrast

Comparisons	0 Min Delay	3 Min Delay	6 Min Delay	9 Min Delay
Cell Viability: 23°C vs 3°C	0.002	0.000	0.462	0.198
PI Uptake: 23°C vs 3°C	0.003	0.000	0.005	0.004

Table 4.4: Linear Combination P-Values for Voltage Contrast

Comparisons	0 Min Delay	3 Min Delay	6 Min Delay	9 Min Delay
Cell Viability: 5V vs 7V	0.002	0.000	0.066	0.241
PI Uptake: 5V vs 7V	0.730	0.357	0.819	0.199

Table 4.4 shows pulsed voltage comparison using the same method. It appears that there is a significant difference for the first two time intervals (T0 and T3) in terms of cell viability, favoring the samples that experienced higher pulse voltages. PI uptake is not significantly different for the voltage comparison criteria at all time intervals investigated.

The results suggest several cellular response mechanics in regards to concomitant thermal stress and surface structural dysruption. Discussed earlier were the effects that lower physiological temperature has on target cells in regards to the cell membrane/material stiffening as well as diminished cytoskeletal support leading to reduced surface defect healing.

4.3.4 Surface Defect Healing

In the context of surface defect healing, Figure 4.8 shows a decrease in PI uptake between 3 and 6 minutes post-injection for all treatment sample types. This suggests that large numbers of induced pores are closing in some degree during this time period. Notably, because the lance arrays are designed to create approximately the same number of pores in each injected well, it is suggested by the larger decrease in PI uptake for the 3°C samples over this interval that surface defect healing rate is greater during cold stress. However, it also suggests that while the magnitude of induced pore closure rate may be greater in the 3°C samples during 3 to 6 minutes post-injection, that the 23°C samples have a lower number of pores still patent after this event. In the initial hypothesis, it was believed that colder samples would have stiffer membrane material properties and therefore

have a greater number of pores patent for a longer period of time. Statistically, this relative behavior between temperatures can be viewed in Table 4.3.

To help corroborate the conclusion that the major pore closing event occurs between 3 to 6 minutes post-injection, Figure 4.9 illustrates that over the same time period, cell viability levels increase, with the exception of the 23°C/7V Pulsed sample which experiences a modest decrease in cell viability (approximately 5%). A likely explanation is that as induced pores begin to close, manifested in terms of reduced PI uptake, the transmembrane ion gradients that were dysrupted by the injection event begin to stabilize and thereby improve cell survival.

Returning to Figure 4.8 and the suggested pore-closure events occurring in all sample types between 3 to 6 minutes post-injection, it is worth noting these findings in terms of the original hypothesis regarding cytoskeletal function in surface defect healing. It was originally hypothesized that at the reduced temperature, cytoskeletal integrity would be diminished and thereby the functional ability of the cell to repair surface defects would be reduced. However, that behavior is not seen in Figure 4.8 in terms of a lag time in pore closure with the 3°C samples. A possible reason that behavior is not found may deal with the fact that reduced temperature exposure to treatment samples was transient enough to not adversely diminish cytoskeletal structure/function.

4.3.5 Temperature-Dependent Ion Re-Balancing

One particular behavior that is also suggested in Figure 4.8 is a temperature-dependent re-balancing of ion gradients during the post-injection period. Early in the experimentation of this work, it was anticipated that the cell would experience a temperature-dependent re-balancing due to the decreased production of ATP at lower temperature, a behavior noted in other mammalian cell types at approximately 3°C [159]. The propidium iodide molecular load used post-injection was thought to be actively removed via membrane bound ATP-driven pumps [160]. When PI is added to the post-injected solution, while the target cells are still re-establishing ion gradients due to the multiple (2-4 pores per cell) 1-2.5 micron-sized pores, it is believed that the PI and transiently mis-placed ions would be removed from the intracellular space via ATP-pumps. Demonstrated in Figure 4.8 is that the 3°C samples at all time periods post-injection, had greater levels of PI still present in the intracellular space, suggesting that ATP production is reduced with lower temperature, therefore reducing PI removal from the cell as well.

In context of the two voltage protocols used during the LAN event, there appears to be no clear pattern as far as PI uptake is concerned as noted in Table 4.4. In terms of the injection process, this finding is not surprising since because PI was not yet added to the solution until after the injection process.

4.3.6 Minor PI Uptake Rebound

Figure 4.8 shows during 6 to 9 minutes post-injection, that all samples (except 3°C/5V Pulsed samples) experience a rebound in the degree of PI uptake. Treatment sample 3°C/7V Pulsed experience the greatest rebound in PI while 23°C/5V and 23°C/7V Pulsed samples experience a more comparable level of PI uptake rebound. The timing and degree for this behavior is not clear.

4.3.7 Cell Survival with Large Surface Defect

To the authors' knowledge, this is the first time pores formed with such a large diameter (approximately 2.5 microns in diameter, 2-4 per cell) in the presence of the thermal stress has been conducted in context of cell survival. Remarkedly, even in the presence of such relatively large compromises to the cell structure, these cell cultures still maintain an average cell viability of 78.08% for 3°C samples and 89.61% for 23°C samples.

4.4 Conclusion

Characterizing cell culture environmental factors and the role they play in alterations to structural and functional behavior of target cells is a critical foundational research topic for enhancing non-viral transfection technologies. Presented here is a non-viral transfection technology known as Lance Array Nanoinjection (LAN), a method that relies on both physical penetration of the cell membrane and electrical delivery of charged molecular loads. Experimentally, it was shown that LAN in the presence of thermal variation delivers greater amounts of propidium iodide to target cells when samples are cooled to 3°C rather than maintained at 23°C. Furthermore, it is suggested in this work that HeLa cells respond uniquely in regards to pore closure 3 to 6 minutes post-injection and that despite the surface damage from the injection, they maintain average cell viability rates between 78.08% and 89.61% for 3°C and 23°C treated samples, respectively.

CHAPTER 5. INJECTION SPEED AND SERIAL INJECTION

The following chapter has been submitted as a journal article to *SpringerPlus* and is currently in review. The title of this journal article is "The Effect of Injection Speed and Serial Injection on Propidium Iodide entry into Cultured HeLa and Primary Neonatal Fibroblast Cells using Lance Array Nanoinjection". As a result, there may be some material that is contained elsewhere in this dissertation but is presented here as a representation of this original journal article.

5.1 Introduction

Gene therapy and gene medicine approaches to correcting disease represent a major paradigm shift in how clinicians are able to help patients, moving from a framework of reactionary treatment of disease manifestations to fundamental, proactive prevention of genetic alterations causing the disease [1–3]. While still in a relatively early stage of development, medical approaches designed to engineer genetic outcomes have had promising results in terms of both monogenic [4–11] and polygenic [12–17] disease corrections.

Unfortunately, the actual method for transmission of the genetic loads to target cells remains a challenge [18–21]. Many biotechnologies have been created to help address this issue (with mixed results) [22, 161–165]. The primary goal of all of these methods is to site-direct genetic loads into cells without harming the host systemically or the target cell locally [18]. Key features frequently noted as critical design requirements for these biotechnologies include:

- High transfection efficiency
- Effective in a wide range of cell types
- Flexible pay load capacity
- No immunologic response

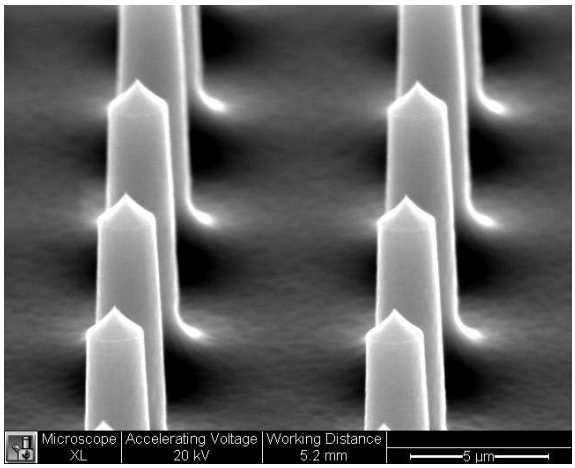

Figure 5.1: SEM image of two rows of lances contained on the Lance Array Silicon chip. Lances measure 10 μm in length, 1-2.5 microns in diameter, and spaced 10 μm from center to center

- No insertional mutagenesis

One non-viral transfection biotechnology, known as Lance Array Nanoinjection (LAN), has been created with these design requirements in mind. LAN works by using a combination of physical penetration of target cell membranes and electrical delivery of molecular loads using a microfabricated silicon etched array of lances [23, 24]. Figure 5.1 shows an SEM image of a lance array which contains 10 μm length lances spaced 10 μm from center to center in a grid pattern, ultimately forming 4 million lances on a 2 cm by 2 cm chip.

Procedurally, nanoinjection works in a series of four major steps which include: staging the lance in the solution containing the desired molecular load, electrical attraction of the molecular load onto the lance, physical penetration of the cell membrane of target cells and electrical repulsion of the molecular load into the cytoplasmic space, and finally removal of the lance [25–27] (See Figure 5.2 for illustration of LAN process).

There are several attractive features of LAN relative to other transfection methods. First, it does not rely on delivery agents that can cross-react with the immune system (such is the case with several viruses [28–32]), nor does it create cytotoxic effects in target cells (such is the case with many chemical based methods [22, 28]). Second, because the lances are 1-2.5 μm in diameter, the resulting pores created during the injection event are relatively large, making it possible for large molecules to transiently pass into the cell. Even though the pores are relatively large, the trauma

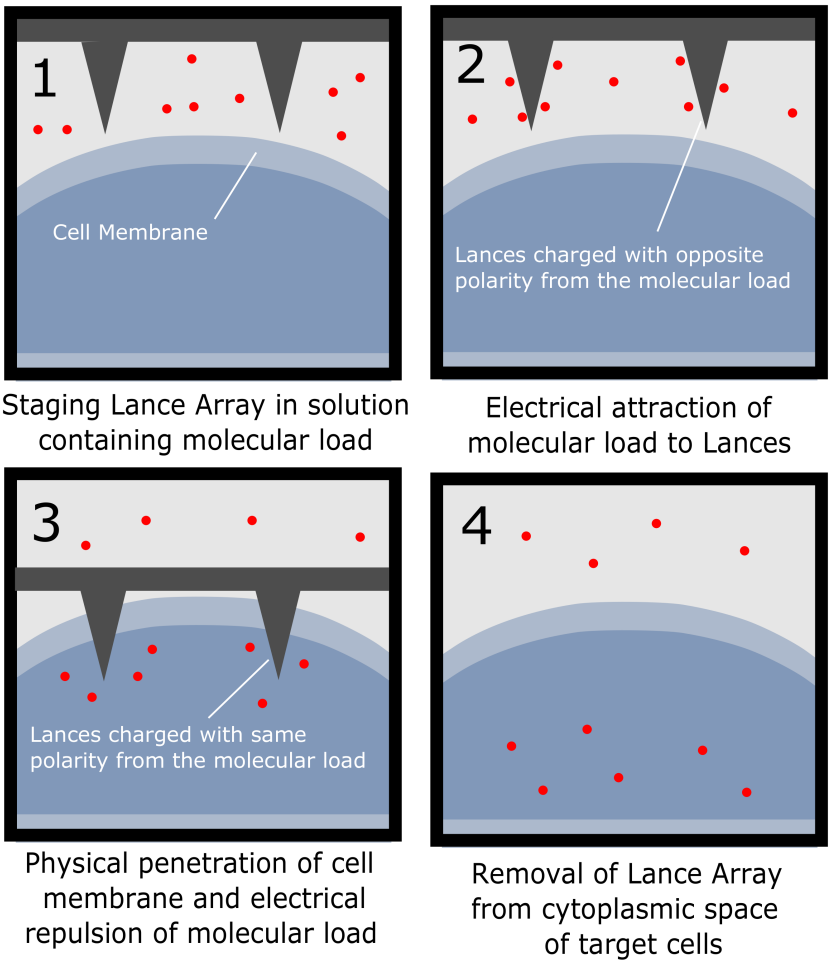

Figure 5.2: Lance Array Nanoinjection Stepwise Process. 1: Staging the lance array in the solution containing the desired molecular load. 2: Electrical attraction of the molecular load onto the lances. 3: Physically penetrating the cell membrane of target cells and electrical repulsion of the molecular load into the cytoplasmic space. 4: Removal of the lance array, leaving the molecular load in the intracellular space of target cells

induced during the process is relatively minimal, as evidenced by high cell viability rates (78% to 91%) previously noted [24]. This latter feature of cell viability is an issue in some instrumentation based transfection methods, such as electroporation [33] and microinjection [25].

Despite these attractive features of LAN, one short-coming that LAN as well as all non-viral transfection technologies encounter is that transfection rates are lower than what can be achieved with viral modalities [28]. This work seeks to directly address this challenge related to efficient molecular delivery by considering two intertwined procedural variables unique to LAN

which include: the speed of injection and serial injection of the same sample. In prior testing, it has been noted that following a single injection event, many cells do not stay adherent to the glass slide used for staging the injection process. The purpose of investigating the effect of speed of injection is to determine the extent that cell removal can be minimized such that serial injection protocols can be investigated.

Indeed, it is shown in this work that by slowing the speed of the injection process that target cells are able to remain adherent to the glass slide using for staging the injection. Because the cells remain post-injection, it is possible to inject multiple times and thereby increase the amount of molecular load delivered to the cell.

To help establish the robustness of this procedural investigation, as part of the serial injection testing, two different cell types, immortalized HeLa culture and primary neonatal fibroblast cells, were used to determine how the different cell types respond. To demonstrate molecular load delivery, propidium iodide (PI), a dye typically impermeable to the cell membrane, was used in conjunction with flow cytometry to quantify the injection-dose response.

Because the speed of injection experimentation led to serial injection experimentation, the following will be compartmentalized to consider the speed of injection work first, followed immediately by the serial injection work.

5.2 General Methods

This work consists of two major experiments – the speed of injection and serial injection experiments. The speed of injection work, which is presented first, is a precursor experiment that led to further exploration that makes up the serial injection experiment. Both used common experimental elements which are detailed in this general methods section. For experimental elements unique to the specific experiment, separate descriptions are provided.

5.2.1 Lance Array Fabrication

Reference [23] provides a complete description of the microfabrication process used for creating the silicon lance array and is presented here simply for convenience. The lance array microfabrication process consisted of using positive photoresist (AZ330F) to pattern a grid of

circles that became pillar-like structures following deep reactive ion etching (DRIE). These pillars were then treated with a sulfur hexafluoride (SF6) isotropic plasma etch, which serves to form a pointed tip on the pillars, resulting in lances (see Figure 5.1).

5.2.2 Injection Set-Up

Figure 5.3 shows a schematic, cross-sectional view of the injection device and contains eight major components which include: stepper motor, threaded rod, coiled spring, orthoplanar spring, electrical connections, silicon lance array, glass slide for the cell culture, and cell culture platform. The stepper motor and electrical connections receive input signals from the electrical control box (see Figure 5.4). During the injection process, the stepper motor causes the threaded rod to vertically displace the coiled and orthoplanar springs. The lance array is attached to the inferior surface of the orthoplanar spring and interacts with the cell culture contained on the glass slide according the process outlined in Figure 5.2. The cell culture platform serves to facilitate alignment with the orthoplanar spring and also helps fix the glass slide, preventing it from adhering to the silicon lance array.

5.2.3 Electrical Control Box

The electrical control box, which provides electrical input to the injection device, operates by receiving three inputs from three separate power supplies (2400 SourceMeter, Keithley) (see Figure 5.4). Figure 5.5 is a full electrical schematic of the electrical control box where it illustrates electrical inputs from the power supplies running through two relays arranged in series. The first relay was used to allow either Input 1 or 2 to pass, while the second relay was used to allow the input from the previous relay or Input 3 to pass. This allowed one input at a time to pass using two digital pins (one to control each relay, using 5V or GND).

The output signals from the electrical control box used for the serial injection testing can be described as the following: Output 1, current controlled of either 1.5 or 3.0 mA for 20 seconds; Output 2, 10 intermittent pulsing events between 0V and +7V for 20 ms (2 ms period); Output 3, 5 second interval of +1.5V. In addition to these actions, the electrical control box also operates the

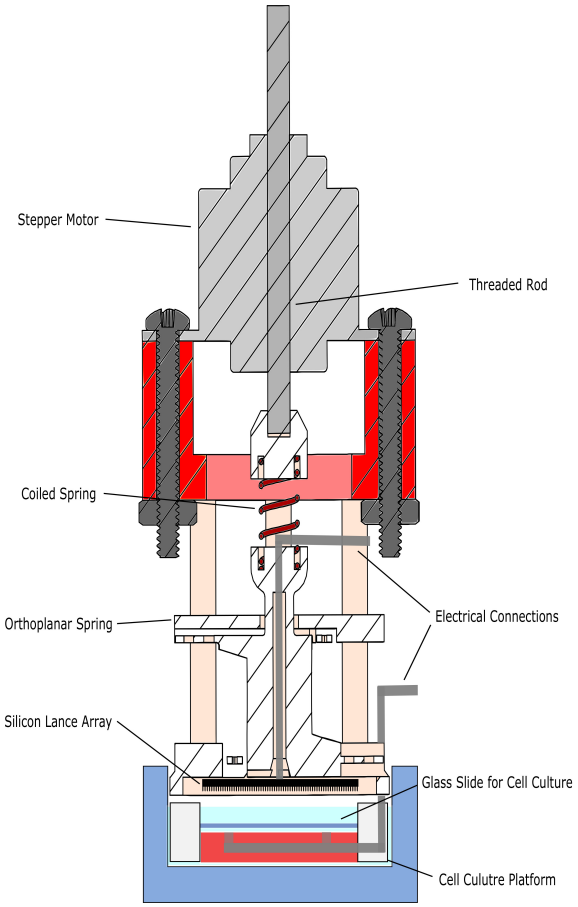

Figure 5.3: Cross-sectional schematic of LAN injection device relative to cell culture platform. Components include (top to bottom): stepper motor, threaded rod, coiled and orthoplanar springs, electrical connections, silicon lance array, glass slide for cell culture, and cell culture platform

stepper motor attached to the superior end of the injection device. It should be noted, Outputs 2 and 3 occur when the lances are inserted into the cells.

5.3 Methods: Speed of Injection Experimentation

5.3.1 Stepper Motors

Two separate stepper motors (28BYJ-48-5V, Rohs; TSFNA25-150-17-023-LW4, Anaheim Automation (AA)) were used to for the speed of injection testing in order to achieve the speeds needed and still ensure that the stepper motors would not skip steps by being driven too quickly. Five different speeds were used for this experiment, which include 0.08, 0.16, 0.60, 1.80, 3.00

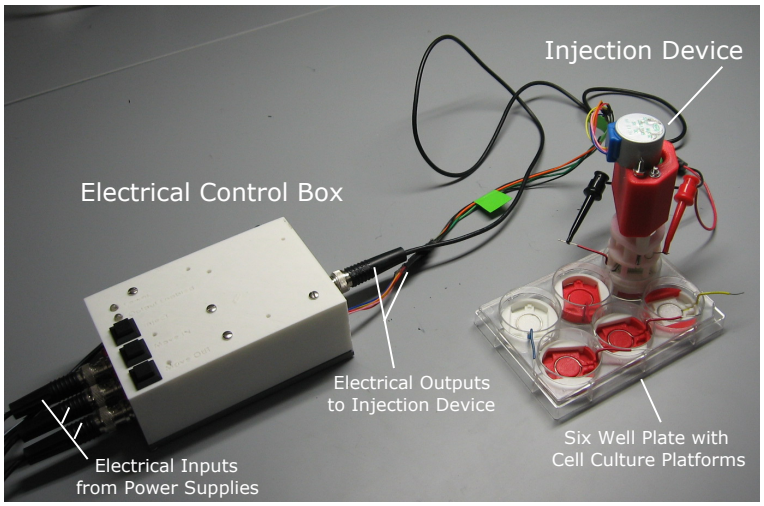

Figure 5.4: Experimental set-up showing the electrical control box receiving three separate input signals coming from three power supplies (not shown) and outputing appropriately timed output signals to the injection device mounted above the prepared six-well plate. Cell culture platforms with the prepared cell cultures are seen as white and red circular components resting in the wells of the six-well plate

mm/sec. For the slower speeds of 0.08 and 0.16 mm/sec, the Rohs stepper motor was used and for 0.60, 1.80, and 3.00 mm/sec speeds, the AA stepper motor was used. The injection device was the same for all sets of injection tests, with the exception of the stepper motor being changed to match speed conditions.

5.3.2 Cell Culture Preparation

HeLa 229 cells were plated on glass slides within six-well plates (Sarstedt) and incubated at 37C and 5% carbon dioxide. Culture media contained Dulbeccos Modified Eagles Medium (DMEM, Gibco) with 10% Fetal Bovine Serum (FBS, Denville Scientific) and streptomycin/penicillin (Gibco). Cell cultures were allowed to incubate for 24 hrs following the plating process to ensure adequate adherence to the glass slide. Following the 24 hrs, a mono-layer of HeLa cells, which were approximately 70% confluent, had their growth media removed and were re-supplied with 2 mL of phosphate buffered solution (PBS, Gibco) in final preparation for injection.

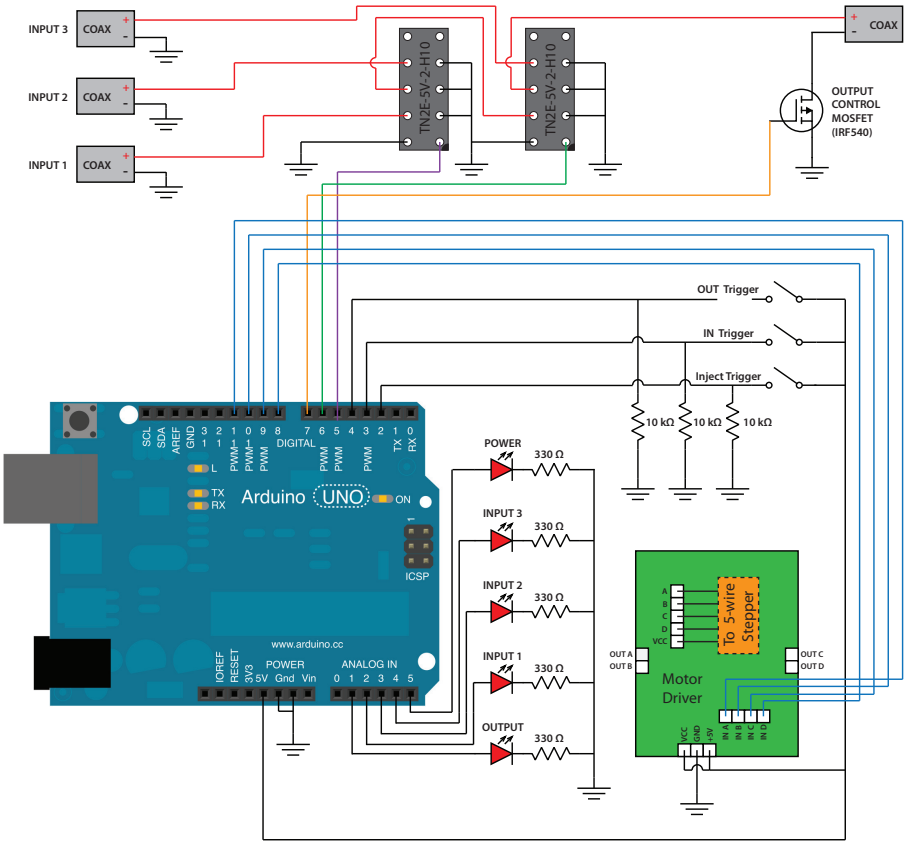

Figure 5.5: Electrical schematic for the current control box. An Arduino was used to control two relays and a stepper motor driver for the injection process. Five LEDs are used as indicators for power, output, and which input being passed through the box

5.3.3 Treatment Protocols

The following describes the various sample types used in the speed of injection testing:

- **Non-Treatment Control (NTC):** Received no lancing.

- **Treatment Protocol for Different Speeds:** Samples were lanced a single time and received no applied voltage during the injection process. Five different injection speeds were applied during the injection event and include: 0.08, 0.16, 0.60, 1.80, 3.00 mm/sec.

As a convention, specific treatment sample types will be designated by the speed of injection. For example, HeLa/0.08 refers to a treatment sample that was lanced a single time at 0.08 mm/sec.

5.3.4 Post-Treatment Analysis

After the injections were completed, all samples were given 0.5 mL of 5X trypsin (Gibco) and incubated 5 minutes at 37C to facilitate removal of the cells from the glass slides. After the 5 minutes, samples were treated with 1.5 mL of DMEM/FBS media to deactivate the trypsin and then centrifuged at 2000 rpm for 10 minutes. The supernatant was then removed, 0.25 mL of PBS was added to each sample, and each sample was then vortexed to prepare them for hemocytometry. Quantification of the number of cells were performed according to standard hemocytometry methods using trypan blue [166].

5.3.5 Statistical Analysis

After cell counts were obtained using hemocytometry, data for treatment samples were normalized relative to the Non-Treatment Controls according to the following formula.

$$\frac{\text{Cell Count in Treatment Sample}}{\text{Cell Count in Non} - \text{Treated Control}}$$

This normalized data was then statistically analyzed in JMP (SAS), using initially an ANOVA test to screen for statistically significant relationships (F-Ratio: 16.5426) followed by individual student t-tests ($\alpha = 0.05$).

5.4 Results and Discussion: Speed of Injection Experimentation

Figure 5.6 shows a set of box plot results for the data generated for the five different injection speeds. The left-most two box plots were obtained by using the slower stepper motor (Rohs), while the other three box plots were obtained from the slightly faster stepper motor (AA). It can be seen that statistically significant relationships exist in all cases between the slower and faster stepper motors (<0.0001) (see Table 5.1).

Table 5.2 provides a summary of the results showing that for both the 0.08 and 0.16 mm/sec speeds, that the mean normalized cell count is more than double the highest normalized mean obtained with the faster stepper motor.

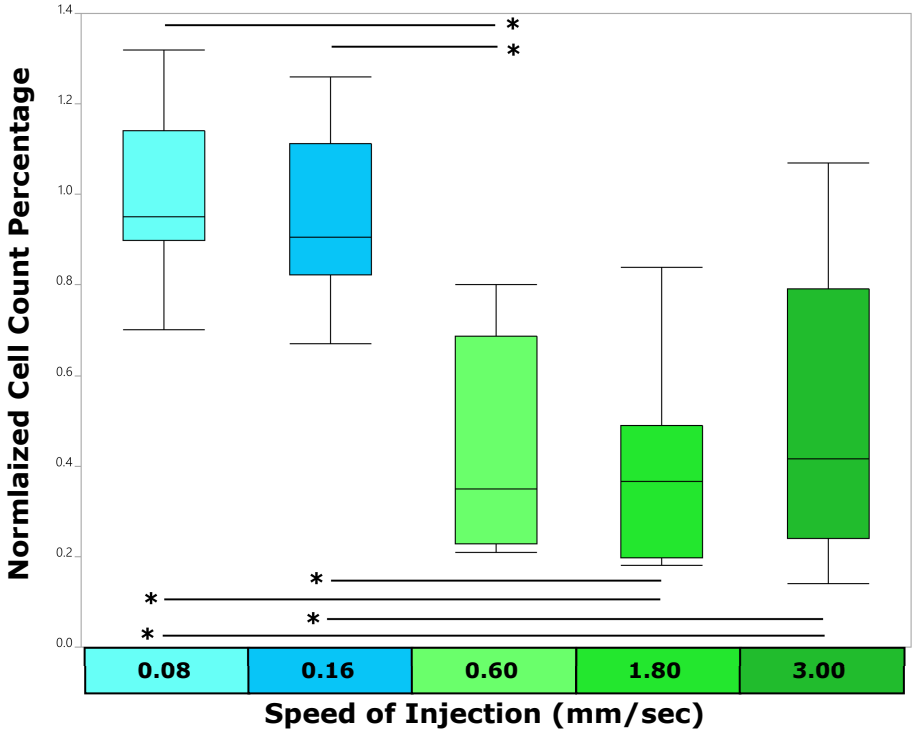

Figure 5.6: Injection Speed Box Plot. The two left-most box plots were the result of the slower stepper motor (Rohs) whereas the three right-most box plots were the result of the faster stepper motor (AA). Statistically significant relationships are noted with an asterisk

Table 5.1: P-Values for Speed of Injection Experiment

Comparison	P-Value	Comparison	P-Value
HeLa/0.08 vs HeLa/0.16	0.6466	HeLa/0.16 vs HeLa/1.80	<0.0001
HeLa/0.08 vs HeLa/0.60	<0.0001	HeLa/0.16 vs HeLa/3.00	<0.0001
HeLa/0.08 vs HeLa/1.80	<0.0001	HeLa/0.60 vs HeLa/1.80	0.7180
HeLa/0.08 vs HeLa/3.00	<0.0001	HeLa/0.60 vs HeLa/3.00	0.4362
HeLa/0.16 vs HeLa/0.60	<0.0001	HeLa/1.80 vs HeLa/3.00	0.2566

Table 5.2: Statistical Summary for Injection Speed Experiment

Injection Speed (mm/sec)	Sample Size (n)	Mean Normalized Cell Count
HeLa/0.08	10	0.993
HeLa/0.16	10	0.946
HeLa/0.60	10	0.427
HeLa/1.80	10	0.390
HeLa/3.00	10	0.507

Suggested in these results is that the cultured cells are able to adhere better to the glass surface used for staging the injection when using injection speeds of 0.08 to 0.16 mm/sec. These findings are consistent with atomic force microscopy (AFM)-based single-cell force spectroscopy (SCFS) studies [167–173]. Friedrichs *et al* [174] demonstrated with a single cell adhered to an AFM probe by cell adhesion molecules (CAMs), that when placed in contact with a substrate surface, the speed with which the AFM probe was removed was directly related to the viscous forces created between the substrate surface and the cell. If sufficiently strong viscous forces were generated by removing the AFM probe (with the attached cell) fast enough, the cell would experience a series of five major events which include:

1. Shrinking of the surface area contact between the cell and substrate surface.
2. Cell body removal from the substrate with only membrane nanotubes linking the cell and substrate.
3. Stressing of the CAM linkages between the cell and AFM probe – reaching a non-linear maximum level as cytoskeletal structures are strained in the direction of motion.
4. Peripheral rupture of the CAM structures leading to a rapid decrease in adhesion force between the cell and the AFM probe.
5. Cell removal from the AFM probe as the viscous effects from the substrate-cell interface overcome the cellular adhesion to the AFM probe.

Returning to the context of LAN, it is suggested that for the majority of cells present on the glass slides that experience injection speeds of $\leq$0.16 mm/sec, that the viscous forces created by the removal of the silicon lance array does not exceed the strength with which the cells are adhered to the glass slide. For treatment samples experiencing greater speeds of lance array removal, it appears that fewer cells are able to withstand these removal forces and are pulled away from the glass.

5.5 Methods: Serial Injection Experimentation

Using the fact that slowing the injection process results in an increase in cell number remaining on the glass slide substrate used for staging the injection process, it was proposed to

investigate whether or not target cells could be injected multiple times and exhibit an increase in molecular load delivery. Furthermore, it was also proposed to determine whether a difference exists in molecular delivery when using different cell types. To explore this latter item, two cell types were selected which include HeLa 229 cells (commonly used in basic research) and primary, human neonatal fibroblasts (BJ(ATCC® CRL-2522™)) (used in wound healing applications).

For convenience, the injection speed of 0.16 mm/sec was used for the serial injection testing because it was twice as fast as the 0.08 mm/sec speed setting and still had a high mean number of cells still adherent to the glass slide following injection (i.e. 94.6%).

5.5.1 Cell Culture Preparation

For both cell types, test preparation began with seeding glass slides contained within six-well plates with 2 mL of a growth media, which consisted of: Dulbeccos Modified Eagles Medium (DMEM, Gibco), 10% Fetal Bovine Serum (FBS, Denville Scientific), and streptomycin/penicillin (Gibco). Cells were incubated overnight prior to injection at standard conditions of 37C and 5% carbon dioxide.

Following this process, glass slides were transferred to new six-well plates and snapped into 3D printed cell culture platforms (used to help align the injection device). Cells, now staged for the injection process, were given 2 mL of phosphate buffered solution (PBS, Gibco) per well. At this point, both cell types had formed a mono-layer of approximately 70% confluency.

5.5.2 Propidium Iodide

Propidium iodide (Sigma-Aldrich) was used as a molecular marker in this experiment because it is typically impermeable to the cell membrane. Because the lances used in LAN penetrate target cells and then deliver PI to the intracellular space of these target cells, it is an indicator of successful delivery. Once in the cell, PI can intercalate will nucleic acids, which results in fluorescent activity 20 to 30 times greater than normal, thereby providing a detectable means of transfection rates during flow cytometry.

5.5.3 Treatment Protocols

Treatment samples were generated using the following protocols for both HeLa and Fibroblast cells which include:

- **Non-Treatment Control (NTC):** Received no lancing, no applied voltage, and no PI.

- **Background Control for PI (BC):** Received no lancing, no applied voltage. Received 0.02 mg/mL PI.

- **Treatment Protocol 1.5 or 3.0 mA, injected 1, 2, or 3 times:** Lanced, receive 0.02 mg/mL PI, and received current control which consisted of: 20 second application of either 1.5 or 3.0 mA, followed by 10 intermittent pulsing events between 0V and +7V for 20 ms (2 ms period), followed by 5 seconds of a +1.5 DC voltage.

  Those treatment samples that were injected more than once were incubated for one hour before the sample was injected again. This refractory period has been shown in previous testing to prevent excessive stress to target cells.

As a convention, specific treatment sample types will be designated by cell type, current control setting used during injection, and the number of times the sample was injected. For instance, Fibro 1.5 mA, x2 refers to a fibroblast treatment sample that was injected with 1.5 mA (used for Input 1), two times.

5.5.4 Post Testing Flow Cytometry Preparation

Following injections, all samples were incubated for 2 hrs prior to being treated with 0.5 mL of 5X Trypsin (Gibco) and incubated for 5 minutes for removal of cells from the glass slide. Following treatment with trypsin, samples were given 1.5 mL of DMEM/FBS to deactivate the trypsin. After transferring individual samples to FACS tubes, the samples were centrifuged for 10 min at 2000 rpm. Final preparation for flow cytometry of the samples include decanting supernatants and re-suspending cell pellets in 0.5 mL of PBS.

5.5.5 Flow Cytometry

Quantification of samples was performed using flow cytometry (Attune Acoustic Focusing Flow Cytometer, Life Technologies). Approximately 20,000 events were captured and characterized for each sample. Data extraction was performed using Attune Cytometric 2.1 software (Applied Biosystems, Life Technologies) by facilitating visualization of events, gating of appropriate cell populations, and developing primary level data usable for JMP (SAS) statistical analysis.

5.5.6 Statistical Analysis

Primary level data generated from post-flow analysis in Attune Cytometric software was evaluated in a two part process. First, the percentage of living, PI positive cells in each sample were calculated according to the following formula:

$$\frac{\text{Number of Living PI Positive Cells in Sample}}{\text{Number of Living Cells in Sample}}$$

Second, data was then screened in JMP for statistical signficance using ANOVA test (F-Ratio for HeLa study: 21.0098; F-Ratio for Fibroblast study: 49.1873) followed by individual student t-tests ($\alpha = 0.05$).

5.6 Results and Discussion: Serial Injection Experimentation

Figure 5.7 shows box plot results of the HeLa cell serial injection experiment. Three findings can be seen in these plots and quantitatively represented in Table 5.3 and Table 5.4. First, the samples receiving 3.0 mA during Input 1 had a higher mean number of modified cells than samples receiving 1.5 mA. The relative maximum for the 3.0 mA samples reached a mean value of 60.47%, which is nearly four times greater than the relative maximum achieved for the 1.5 mA group. Second, within groups receiving the same current control during Input 1 of the injection process, samples that were injected twice had a higher mean number of modified cells than those samples injected one or three times. Third, within the current control groups, both groups receiving

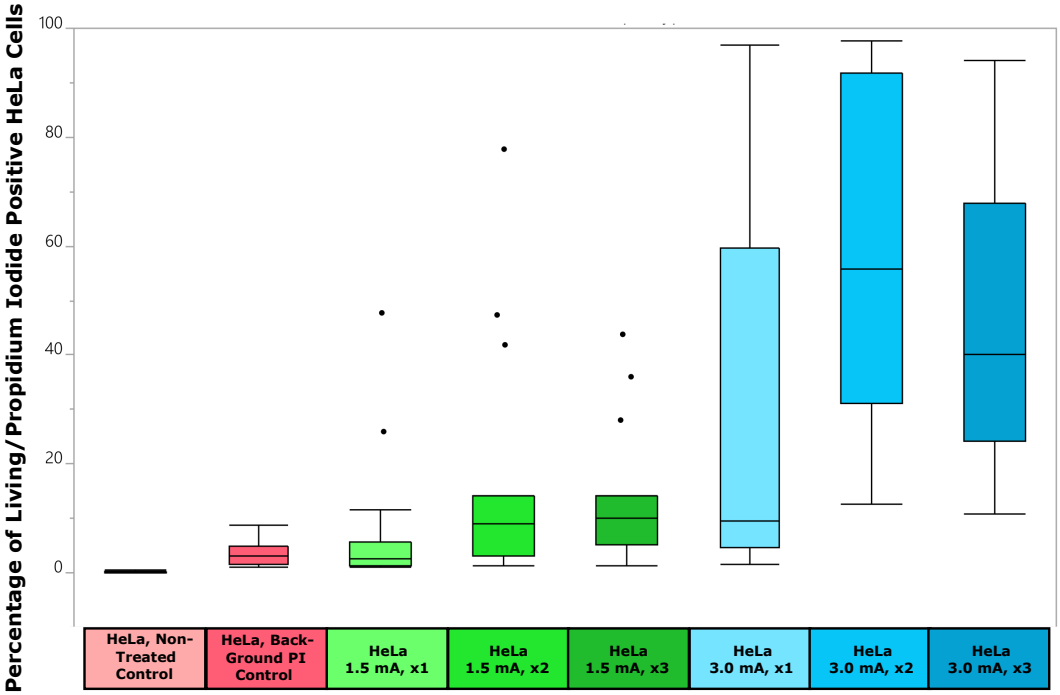

Figure 5.7: Mean Percentage of Living/Propidium Iodide Positive HeLa Cells for all sample types. Because of the number of statistical relationships that were derived, statistically significant relationships are not noted on the box plot figure. For statistical significant relationships, reference Table 5.3

three injections had mean values for PI uptake that were intermediate levels for the current control group.

Figure 5.8 shows the box plot results for the serial injection of primary, fibroblasts using the two different current control settings. Two main features are observed in the results. First, the Fibro 3.0 mA, x2 sample group had the highest mean percent of modified cells for all samples (i.e. 20.97%), being more than three times greater than the best mean percent in the 1.5 mA group. Second, similar to the behavior seen in the HeLa samples for serial injection, the fibroblasts treated with 3.0 mA also had a relative maximum mean value for the two times injected group.

Table 5.5 and Table 5.6 provide both statistically significant relationship and summaries for the experiment. Of note, the fibroblasts exhibit lower mean values for the PI delivery than analogous HeLa samples. Also of note, the HeLa samples that were treated with 3.0 mA had a

Table 5.3: P-Values for HeLa Serial Injection Experiment

Comparison	P-Value	Comparison	P-Value
NTC vs BC	0.5813	1.5mA,x1 vs 1.5mA,x3	0.3578
NTC vs 1.5mA,x1	0.2629	1.5mA,x1 vs 3.0mA,x1	0.0009
NTC vs 1.5mA,x2	0.0114	1.5mA,x1 vs 3.0mA,x2	<0.0001
NTC vs 1.5mA,x3	0.0346	1.5mA,x1 vs 3.0mA,x3	<0.0001
NTC vs 3.0mA,x1	<0.0001	1.5mA,x2 vs 1.5mA,x3	0.6946
NTC vs 3.0mA,x2	<0.0001	1.5mA,x2 vs 3.0mA,x1	0.0381
NTC vs 3.0mA,x3	<0.0001	1.5mA,x2 vs 3.0mA,x2	<0.0001
BC vs 1.5mA,x1	0.5299	1.5mA,x2 vs 3.0mA,x3	<0.0001
BC vs 1.5mA,x2	0.0402	1.5mA,x3 vs 3.0mA,x1	0.0141
BC vs 1.5mA,x3	0.1032	1.5mA,x3 vs 3.0mA,x2	<0.0001
BC vs 3.0mA,x1	<0.0001	1.5mA,x3 vs 3.0mA,x3	<0.0001
BC vs 3.0mA,x2	<0.0001	3.0mA,x1 vs 3.0mA,x2	<0.0001
BC vs 3.0mA,x3	<0.0001	3.0mA,x1 vs 3.0mA,x3	0.0274
1.5mA,x1 vs 1.5mA,x2	0.1903	3.0mA,x2 vs 3.0mA,x3	0.0574

Table 5.4: Statistical Summary for HeLa Cell Serial Injection Experiment

Comparisons	Sample Size (n)	Mean (%)
HeLa, NTC	24	0.1996
HeLa, BC	24	3.3325
HeLa 1.5mA, x1	16	7.3231
HeLa 1.5mA, x2	16	16.4594
HeLa 1.5mA, x3	16	13.7281
HeLa 3.0mA, x1	16	30.9944
HeLa 3.0mA, x2	15	60.4720
HeLa 3.0mA, x3	15	46.7300

much larger variability in the grouping of data points when compared to the fibroblast 3.0 mA treatment groups.

Key elements shown in the results of both HeLa and fibroblast cells is that the cells respond to the series of injections by having an increase in PI introduction, with the exception of the samples injected 3 times. Two possibilities to explain the decrease in PI observed in three times injected samples are related to physiologic responses to LAN. One possibility is that the 1 hr rest period given to the cells following injection is not long enough for cellular structures to recover from the injection event. Even though LAN has been shown to be mild in terms of cell viability after a single injection event [24], it is possible that after three injections, that a longer rest period is

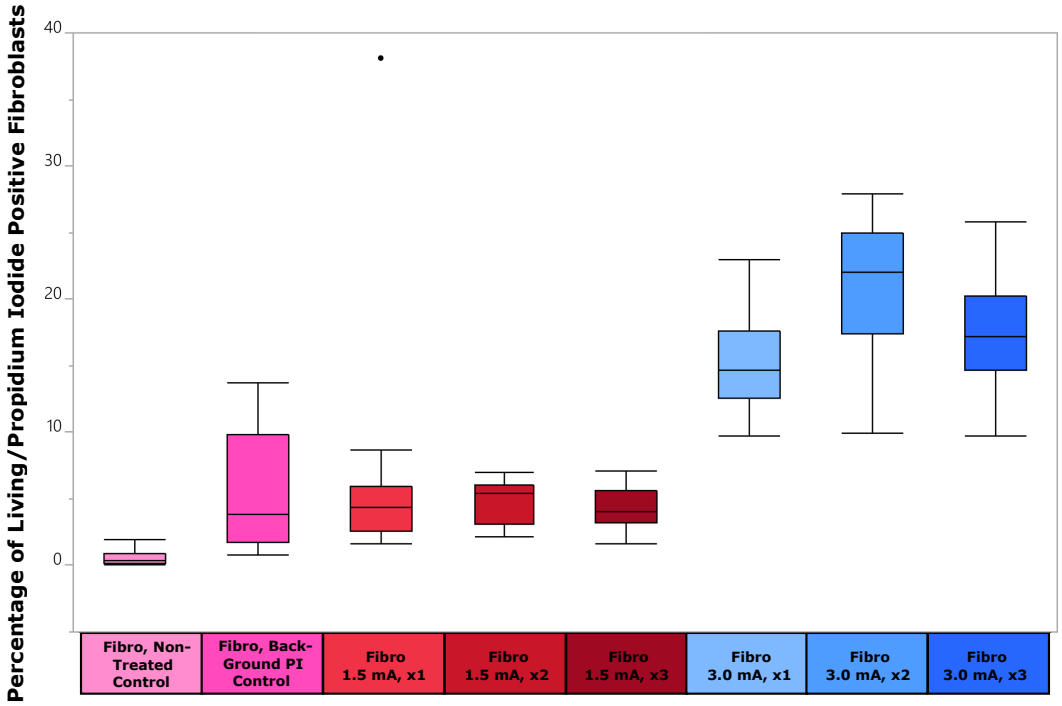

Figure 5.8: Mean Percentage of Living/Propidium Iodide Positive Fibroblast Cells for all sample types. Because of the number of statistical relationships that were derived, statistically significant relationships are not noted on the box plot figure. For statistical significant relationships, reference Table 5.3

Table 5.5: P-Values for Fibroblast Serial Injection Experiment

Comparison	P-Value	Comparison	P-Value
NTC vs BC	<0.0001	1.5mA,x1 vs 1.5mA,x3	0.1745
NTC vs 1.5mA,x1	<0.0001	1.5mA,x1 vs 3.0mA,x1	<0.0001
NTC vs 1.5mA,x2	0.0028	1.5mA,x1 vs 3.0mA,x2	<0.0001
NTC vs 1.5mA,x3	0.0095	1.5mA,x1 vs 3.0mA,x3	<0.0001
NTC vs 3.0mA,x1	<0.0001	1.5mA,x2 vs 1.5mA,x3	0.6654
NTC vs 3.0mA,x2	<0.0001	1.5mA,x2 vs 3.0mA,x1	<0.0001
NTC vs 3.0mA,x3	<0.0001	1.5mA,x2 vs 3.0mA,x2	<0.0001
BC vs 1.5mA,x1	0.6775	1.5mA,x2 vs 3.0mA,x3	<0.0001
BC vs 1.5mA,x2	0.5598	1.5mA,x3 vs 3.0mA,x1	<0.0001
BC vs 1.5mA,x3	0.2826	1.5mA,x3 vs 3.0mA,x2	<0.0001
BC vs 3.0mA,x1	<0.0001	1.5mA,x3 vs 3.0mA,x3	<0.0001
BC vs 3.0mA,x2	<0.0001	3.0mA,x1 vs 3.0mA,x2	0.0002
BC vs 3.0mA,x3	<0.0001	3.0mA,x1 vs 3.0mA,x3	0.1438
1.5mA,x1 vs 1.5mA,x2	0.3646	3.0mA,x2 vs 3.0mA,x3	0.0286

Table 5.6: Statistical Summary for Fibroblasts Cell Serial Injection Experiment

Comparisons	Sample Size (n)	Mean (%)
Fibro, NTC	23	0.5383
Fibro, BC	24	5.7713
Fibro 1.5mA, x1	16	6.3556
Fibro 1.5mA, x2	15	4.9353
Fibro 1.5mA, x3	16	4.2588
Fibro 3.0mA, x1	16	15.1175
Fibro 3.0mA, x2	16	20.9738
Fibro 3.0mA, x3	14	17.4550

required in order to reduce cellular stress and increase cell survival rates. A second possibility is related to the effects on the cellular adhesion to the glass slide following injection. Perhaps even though cells are able to maintain adhesion to the glass slide at high rates (as shown in the first portion of this work), that residual strain collects in the CAM structures and after three times of injection, the CAM can no longer adhere to the glass, resulting in a decreased observed number of PI in the sample. Suggested here is further investigation into what effects the rest period duration has on the ability of cultured cells to withstand multiple injection events.

Despite the decreases seen in the samples injected three times, the samples are still exhibiting relatively high levels of PI modification. For instance, the fact that the primary fibroblasts had a lower number of cells modified than the HeLa cells is not unexpected, particularly given the fact that BJ(ATCC® CRL-2522™) fibroblasts are difficult to modify [175–177]. Even so, non-optimized delivery of PI still reached levels of 20.97%. Furthermore, it is clear that the magnitude of the current control used in Input 1 has a dramatic impact on PI delivery and warrants further exploration.

5.7 General Discussion

The combination of results obtained for the speed of injection and the serial injection testing represent three major findings. First, cell cultures are able to adhere to the glass slide used for staging the injection process much better (i.e. $>$94.6%) when the speed of injection is reduced below 0.16 mm/sec. Second, during serial injection testing, samples treated with 3.0 mA during Input 1 and injected twice appear to have the greatest mean percent of living, PI positive cells.

Third, the cell type appears to have an effect on how well cells are modified by PI during the injection process, with HeLa cells performing better than primary, neonatal fibroblasts.

All three of these findings are viewed as particularly important milestones in regards to LAN because of how influential they are in establishing higher transfection rates. As noted earlier, there are several biotechnologies that have attempted to address the challenge of molecular delivery by non-viral means but are still plagued with transfection efficiency issues, which varying widely because of intrinsic weaknesses that are part of the technology or because of the cell type being transfected [28].

Traditionally, viruses have been the benchmark for which transfection efficiency is measured. However, they fall short of meeting critical design requirements for robust transfection, particularly in preparation for clinical application. Adenoviruses, Adeno-associated viruses, and lentiviruses are all considered to have high transfection rates in a wide range of cell types [30, 34–42]. Unfortunately, adenoviruses are immunologically inflammatory which can be life-threatening [29, 43], adeno-associated viruses can cause insertional mutagenesis which can be cytotoxic [35, 36], and lentiviruses cause immunologic responses and insertational mutagenesis [30–32, 44]. While retroviruses are useful in CNS (central nervous system) targets [37, 45], the risk of insertional mutagenesis is quite high [37, 46]. Furthermore, viruses in general are limited in their effectiveness because of the limited pay load capacity ($\leq$ 10 kbp) [37] (see Table 5.7).

In contrast, Lance Array Nanoinjection is able to by-pass many of these short-comings. First, LAN does not utilize protein vehicles which could cross-react with the immune system, thereby removing immunologic response issues. Second, LAN creates relatively large pores in target cells (1-2 μm diameter), allowing for large molecular loads to enter, thus reducing the concern of not having sufficient pay load capacity. Third, LAN is compatible with gene editing tools such as CRISPR-Cas9 that mitigate concerns regarding insertional mutagenesis. While the same can be said of viruses if re-programmed to remove self-insertional mechanisms, LAN does not have the same rigor of testing to go through prior to use as viral delivery because insertional mutangenesis in the context of LAN is only an element directly related to the molecular load type, not LAN as a delivery method.

Table 5.7: Benchmark Comparison of Viral Transfection Technologies

Viral Vector	Load Capacity (kbp)	Transduction Rate	Wide Cell Types Use	Immune Reaction	Insertational Mutagenesis
Adenovirus	8.5 [37]	[34]	[37, 38]	[29]	N/A [38]
Adeno-Associated	4-5 [37]	[35, 36]	[39]	[37]	[35, 36]
Retrovirus	10 [37]	[178]	[37, 45]	[43]	[37, 46]
Lentivirus	10 [37]	[30]	[30, 40–42]	[30–32]	[30, 44]
Key	High Degree	Medium Degree	Low Degree		

5.8 Conclusion

Effectively placing molecular loads into target cells without threatening the cell's survival is the overall goal of transfection biotechnologies. One non-viral method presented in this work is known as Lance Array Nanoinjection, a MEMS based device that relies on physical interaction with target cells and electrical direction of molecular loads. Shown in two sequential experiments is the effect that the speed of injection and the ability to inject cells repeatedly have on target cells. In the speed of injection investigation, it was shown that slower injection speeds improve the number of cells still adherent following injection, reaching a peak mean of 99.3% at 0.08 mm/sec injection speed. Using these results, serial injection testing with HeLa 229 cells and BJ(ATCC® CRL-2522™) cells (neonatal, primary fibroblasts) were conducted by injecting samples multiple times (1, 2, and 3 times) at two different current control settings (1.5 and 3.0 mA). Results show that HeLa cells treated with 3.0 mA and injected twice (x2) had the greatest mean PI uptake of 60.47% and that neonatal fibroblasts treated with the same protocol reached mean PI uptake rates of 20.97%. Together these findings help to establish LAN as a method that can obtain modification rates comparable to other transfection technologies.

CHAPTER 6. CRISPR-CAS9 DIRECTED KNOCK-OUT OF CONSTITUTIVELY EXPRESSED GFP IN HELA CELLS

The following chapter has been sumitted as a journal article to *SpringerPlus* and is currently in review. The title of this article is "CRISPR-Cas9 Directed Knock-Out of Constitutively Expressed GFP in HeLa Cells using Lance Array Nanoinjection".[1] As a result, there may be some material that is contained elsewhere in this dissertation but is presented here as a representation of this original journal article.

6.1 Introduction

The creativity and scale with which researchers are utilizing clustered regularly interspaced short palindromic repeat (CRISPR) sequences and Cas9 (CRISPR-associated) proteins for genomic editing has led to an explosion of possibilities in both transgenic research and gene therapy applications [127–129, 179–182]. Three major elements fueling this movement include the target versatility and ease with which researchers can generate CRISPR-Cas plasmids [183], the ability to modify multiple genomic locations in a single step [137, 138], and the ability to do so at rates difficult to obtain using other editing methods such as transcription activator-like effector nucleases (TALEN) [184, 185].

Despite the great potential CRISPR/Cas9 plasmids offer, there are limitations that make delivering such molecular loads to target cells challenging for widespread application. Commonly used viruses, such as adenoviruses, adeno-associated viruses, and lentiviruses, are known for having high transfection rates [30,35]. However, adenoviruses cause excessive immune reactions [29], adeno-associated viruses can cause insertional mutagenesis [35], and lentiviruses can cause both immune reactions and insertional mutagenesis [30–32, 186]. While CRISPR-Cas provides an ele-

[1]This work was also presented at a poster presentation at the 2015 NanoEngineering for Medicine and Biology (NEMB) annual meeting (St. Paul, MN) and has been accepted as part of an oral presentation at the 2016 International Society for Transgenic Technologies (ISTT) annual meeting (Prague, Czech Republic).

gant method to by-pass many of the concerns related to insertional mutagenesis [187], viruses are still constrained by pay load capacity, which can limit utility [37].

In an effort to address concerns raised with viral transduction, researchers have put emphasis on developing chemical, physical, and/or electrical transfection technologies aimed at producing a robust delivery method in terms of effective delivery and expression without compromising cell viability [188–190]. Unfortunately, the trade-off for using non-viral approaches has resulted in lower transfection rates [28] and additional challenges, such as genetic load transfer and preservation across both the cell and nuclear membranes [191–195]. Commonly used chemical methods (such as cationic lipids and polymers) can be effective in transfection [196–198] (although not as effective as viral modalities) [199–206] but are also potentially toxic to cells because of dosage requirements, usually require optimization experimentation for each cell type, and do not work in all cell lines [22,28]. Physical methods like microinjection and electrical methods like electroporation can be effective [207] but often are traumatic to the target cells, reducing cell viability [25, 28].

Recently, a new non-viral transfection technology, known as Lance Array Nanoinjection (LAN) was introduced which was designed with many of these challenges in mind. LAN uses a microfabricated silicon etched array of lances to physically penetrate hundreds of thousands of cells simultaneously and electrically deliver attached molecular loads [23,24,208] (see Figure 6.1). Built upon a first generation technology used to create transgenic mice [25–27], LAN interacts directly with the molecular load via electrical interactions, thereby eliminating viral-induced immune responses and carrier-vehicle cytotoxicity issues. Furthermore, LAN creates transient pores between 1-2.5 μm in diameter (making it possible to deliver large loads) and it has cell survival rates of 78% to 91% post-injection [24].

In this report, we extend previous work by combining LAN with CRISPR-Cas9 technology. To do this, a CRISPR-Cas9 plasmid was designed to knock-out (KO) constitutive green fluorescent protein (GFP) expression in HeLa cells via Non-Homologous End-Joining (NHEJ) repair. Two major variables explored in this work included: the current-control setting used during the initial attraction of DNA to the silicon lances prior to cell membrane penetration (1.5, 4.5, and 6.0 mA) and the number of times samples were injected (one time, x1; three times, x3). We report that cells injected x3 had a significantly higher number of cells with GFP knocked-out when compared to samples x1 injected samples and that the injection-dose response was non-linear. Also, it

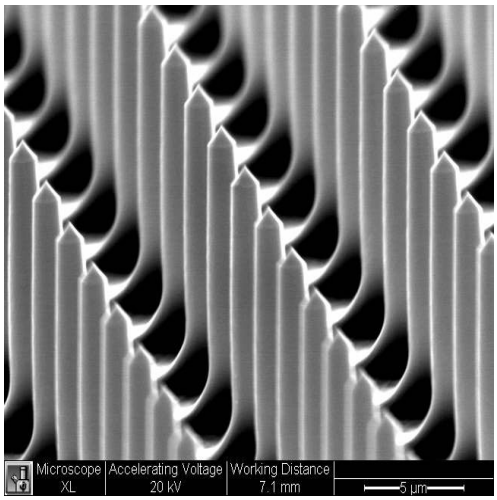

Figure 6.1: Isometric projection of silicon etched lance array taken by scanning electron microscope. Lances measure 8 to 10 μm in length and 1 to 2.5 μm in diameter. Spacing of lances from center-to-center measure 10 μm in both planar directions in a grid of 2000 by 2000 lances per chip

was observed that an intermediate current control setting (4.5 mA) used during the LAN process produced the greatest percentage of living, GFP negative HeLa cells.

6.2 Materials and Methods

6.2.1 GFP+/FRT HeLa Cell Line

We generated an isogenic cell line containing a single copy of EGFP (enhanced green fluorescent protein) by cloning the code sequence of EGFP into pCDNA5/FRT and introducing this plasmid into HeLa/FRT cells in the presence of Flip recombinase (Flp-In System, Life Technologies, Carlsbad, CA). Hygromycin selected HeLa cells expressed 99% GFP and were grown in Dulbeccos Modified Eagles Medium (DMEM, Life Technologies, Carlsbad, CA) with 10% Fetal Bovine Serum (FBS, Denville Scientific, Holliston, MA) and streptomyocin/penicillin (Gibco, Waltham, MA) and incubated at 37C and 5% carbon dioxide.

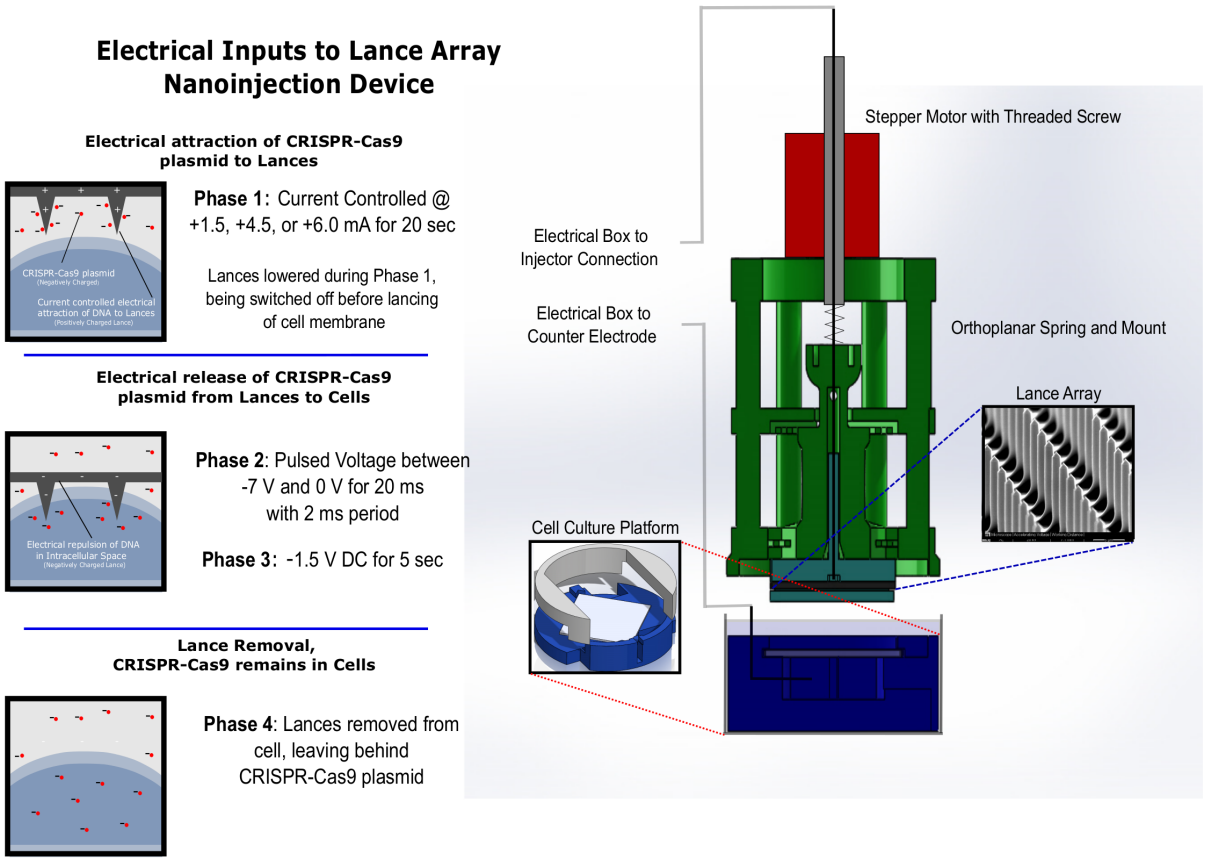

Figure 6.2: Diagram of the LAN set-up. (Left) Describes the four Phases of the LAN process in terms of electrical parameters and physical events. (Right) Illustrates the connection of the stepper motor to the orthoplanar spring to the silicon lance array. With the lance array pointed downward, during the injection process, the lances are inserted into cultured cells secured on the cell culture platform

6.2.2 CRISPR Plasmid

In order to facilitate GFP knock-out in the GFP+/FRT HeLa cell line, a CRISPR-Cas9 plasmid was constructed using sgRNA primers directed towards the N-terminus of EGFP, which would disrupt GFP production via NHEJ repair inaccuracies [183, 209].

The CRISPR-Cas9 GFP knock-out plasmid was created by preparing and ligating sgRNA GFP oligos to a pSpCas9(BB)-2A-Puro (PX459) plasmid, a gift from Feng Zhang (Addgene plasmid 48139) [183]. The top and bottom oligos were prepared to be inserted into the pSpCas9(BB)-2A-Puro plasmid using protocol previously described in the literature [183]. Plasmids were then

transformed into competent top10 cells using a standard transformation protocol. DNA was amplified and extracted from the top10 cells following the protocols of Qiagen Maxi and Mega prep kits (Qiagen, Valencia, CA).

6.2.3 Injection Set-Up

The LAN device used for injections is comprised of five major components which include: silicon-etched lance array, orthoplanar spring and mount, cell culture platform, stepper motor and threaded screw, and electrical switch box. Figure 6.2 illustrates the interactions of these components and provides a context to the LAN process.

6.2.4 Silicon-Etched Lance, Orthoplanar Spring and Mount

The LAN device contains of a microfabricated silicon wafer containing the etched lances (Figure 6.1) attached to an orthoplanar spring which has the stepper motor mounted on top (Figure 6.2). The lance array serves to physically penetrate cell membranes and also to electrically interact with DNA. The orthoplanar spring has an attachment on its bottom surface for the silicon lance chip to be inserted, thereby providing vertical motion required for injection as well as the electrical connections. Construction of both the lance array and the orthoplanar spring are discussed in prior literature [23, 84].

6.2.5 Cell Culture Platform

The cell culture platform consists of three individual pieces: two PLA 3D printed platform pieces (MakerBot Replicator 2, MakerBot, Brooklyn, NY) (snap-fit together) and the glass slide (contains adhered cells). The system is designed such that the glass slide can be assembled into the cell culture platform during injection, which helps with alignment of the orthoplanar spring/lance array attachment. Following injection, the glass slide can be easily removed from the assembly for incubation.

6.2.6 Stepper Motor and Threaded Screw

The stepper motor is shown in Figure 6.2 as a component attached to the top surface of the orthoplanar spring and serves as an actuator of the spring in orchestration with the electrical input signals delivered to the silicon lances. The stepper motor is controlled by an Arduino Uno (Small Projects, Somerville, MA) and has been calibrated to vertically operate the threaded screw insert at 160 m/sec.

6.2.7 Electrical Box

The electrical box is designed to take electrical input signals from three different power sources (Keithley 2400, Cleveland, OH) and to output them to the two electrical leads; one lead passing through the upper portions of the injection device to supply charge to the lance array, and another lead passing through the cell culture platform to act as a counter-electrode beneath the cell culture. Figure 6.2 describes the electrical conditions supplied by the electrical box during the four phases of the injection process. The timing of the electrical signal delivery to the nanoinjection device is controlled by an Arduino Uno.

6.2.8 Testing Preparation

GFP Positive/FRT HeLa cells were prepared approximately 24 hrs in advance on 18 mm by 18 mm glass slides contained in six well plates. Cells were incubated during this period at 37C, 5% carbon dioxide, and supplied with 2 mL of DMEM with 10% FBS and streptomyocin/penicillin. Cells cultures on the glass slides were approximately 70% confluent.

Following this 24 hr incubation, the HeLa cells were snapped into the 3D-printed cell culture platforms. Following transfer to the platforms, cells were supplied with 2 mL of fresh DMEM and 4 μL of 25 mM chloroquine and then incubated for an additional 15 minutes. After being pretreated with chloroquine, DMEM was removed and 2 mL of phosphate buffered solution (PBS, Gibco, Waltham, MA) was added. Incubation for an addition 15 minutes followed. Immediately prior to injection, treatment samples were supplied with the CRISPR-Cas9 plasmid at a concentration of 750 ng of DNA/mL of PBS injection solution.

6.2.9 Post Testing Flow Cytometry Preparation

Following injection, all samples had their glass slides removed from 3D-printed cell culture platforms and placed into six-well plates with 2 mL of DMEM. All treatment samples were then incubated for a period of seven days to allow the existing GFP to be lost from cells. After seven days of incubation, all samples were trypsinized with 0.5 mL of 5x trypsin (Sigma Aldrich, St. Louis, MO) per well and incubated for 5 min. Trypsin was then deactivated with 1.5 mL of DMEM per well and then transferred to FACS tubes for centrifugation for 10 min at 2000 rpm. Following centrifugation, samples' supernatant were removed and cells were re-suspended in 0.5 mL of PBS with 80 L of propidium iodide (PI, 500 μg/mL; Sigma Aldrich, St. Louis, MO). The PI served as a viability stain for selecting living cells from dead cells in post flow cytometry analysis.

6.2.10 Flow Cytometry

All samples were quantified using flow cytometry (Attune Acoustic Focusing Flow Cytometer, Life Technologies, Carlsbad, CA). Prior to flow, appropriate single color samples were generated for GFP and PI in order to compensate for signal cross-over. Each sample was then run and had approximately 20,000 events counted and characterized.

Using Attune's post-processing software, samples were gated based on PI signals for living vs dead cells. Using only the living cell populations, samples were then gated based on the GFP signal in order to characterize the efficacy of the CRISPR-Cas9/LAN knock-out of GFP. Figure 6.3 illustrates example flow cytometry results based on the gating procedure described.

6.2.11 Statistical Analysis

Data gathered from flow cytometry was analyzed statistically in JMP (SAS, Cary, NC) using an ANOVA test (F-ratio = 48.0318) and Student t-tests (α = 0.05). The efficiency statistic reported in the Results section is based on number of living GFP Negative cells in each sample. Of note, based on the hypotheses that the samples injected three times will be greater than or equal to the samples injected once, t-tests involving the comparison of the controls to treatment groups or treatment groups against one another, a one-tailed p-value is reported. Because samples are allowed to incubate for seven days post-injection, relative viability rates are not available. For

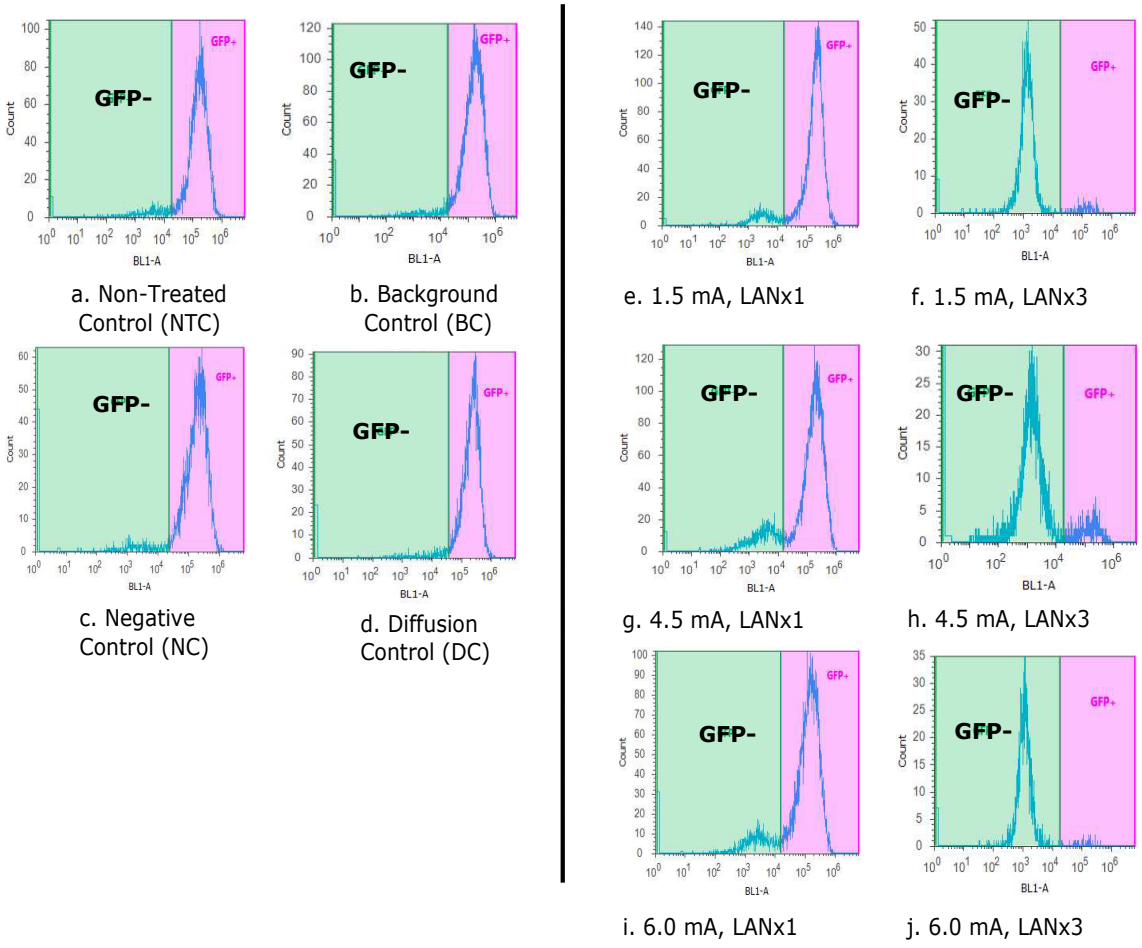

Figure 6.3: Representative flow cytometry results from the ten different samples types. (Left Cluster) Illustrate controls from the experiment (a-d), which contain largely GFP positive populations. (Right Cluster) Illustrate treatment samples that have been injected one time (e, g, i) and comparably treated samples that have been injected three times (f, h, j), with 1 hr rest periods between injection events

context of viability rates following LAN, other works have reported viability rates post-injection between approximately 75% to 90% [208].

6.3 Results

Ten groups of samples were created in order to characterize the effects that the number of injection events and the current control settings used during LAN would have on GFP knock-out in the GFP Positive/FRT HeLa cells. Four of these sample types were controls, which consisted of: Non-Treated Controls (NTC) – received no injection, no applied current/voltage, and no DNA;

Background Controls for nanoinjection (BC) – received DNA, but no applied electrical protocols or physical injection; Negative Controls for electrical exposure (NC) – received physical injection, but with no applied electrical protocols or DNA; and lastly Diffusion Controls (DC) received physical injection and DNA, but no applied electrical protocol.

Treated samples make up the other six sample types. Single Injection (x1) samples were physically injected only one time under the following conditions:

- Phase 1: 20 second application of 1.5 mA, 4.5 mA, or 6.0 mA across lance array (performed with lances external to cell) for the purpose of DNA collection on the lance.
- Phase 2: Lance array inserted into cell culture and pulsed with 10 square-wave pulses of amplitude between 0 to -7V for 20 ms.
- Phase 3: Directly following pulsing, a 5 second period of -1.5V DC is applied
- Phase 4: Lance array is removed from the cells.

Multiple Injection (x3) samples were Injected under the same conditions as described for Single Injections (x1) with the exception that following the first injection, cell cultures were placed back into the incubator for 1 hr before injecting again. This process was repeated for a total of 3 injection events into the same cell culture.

For convenience with treatment sample nomenclature, specific treatment sample types will be referred to by the current control setting used during Phase 1 and the number of times the sample was injected. For instance, 1.5 mA, x1 means that the sample received 1.5 mA during Phase 1 and the samples were nanoinjected only once.

6.3.1 Multiple LAN injections are more effective at GFP Knock-Out

The construction of the HeLa cell line was noted earlier, and consisted of a pFRT/laczeo HeLa cell line (Flp-In System, Life Technologies) which was purchased and transfected with a pcDNA5/FRT expression vector containing both the gene of interest and means to facilitate its production, which include: a green fluorescent protein (GFP) gene, a CMV promoter, and a FRT site. The FRT site is situated right before the compliment ATG sequence for the hygromycin gene

Table 6.1: LAN Statistical summary of the sample types and associated GFP KO rates

Sample Type	Sample Size (n)	Mean GFP KO Percent	Median GFP KO Percent
NTC	21	5.27%	5.37%
NC	26	3.92%	3.62%
BC	18	5.96%	5.37%
DC	23	4.04%	3.82%
1.5 mA,x1	16	6.92%	6.11%
4.5 mA,x1	8	21.63%	17.37%
6.0 mA,x1	16	22.65%	8.45%
1.5 mA,x3	20	66.79%	72.78%
4.5 mA,x3	27	79.56%	93.77%
6.0 mA,x3	20	70.01%	70.32%

found in the Flp-In host HeLa cell line. Co-transfection with the pOG44 vector expresses the flip recombinase machinery that allows the pcDNA5/FRT to flip into the pFRT/laczeo HeLa cell line, thereby making the hygromycin gene in the HeLa cells functionally complete. Once both transfection events were accomplished, HeLa cells that successfully had flipped-in the GFP gene at the FRT site could be selected by hygromycin.

The construction of the CRISPR-Cas9 plasmid was noted earlier, and consisted of a pSpCas9(BB)-2A-Puro (PX459) plasmid, a gift from Feng Zhang (Addgene plasmid 48139) [183] that was modified with oligos that code for sgRNA that directs Cas9 to the FRT site to disrupt GFP production via NHEJ. If the CRISPR-Cas9 GFP knock-out plasmid is successful in disrupting the GFP gene at the targeted FRT site, the HeLa cells will become GFP negative because these HeLa cells only have a single GFP gene.

Table 6.1 shows the statistical summary of the flow cytometry results of the respective sample groups demonstrating the disruption of the GFP gene. Two key findings were noted in regards to the number of injections and transfection rates. First, the transfection rates for the x3 injected samples are significantly higher than the x1 injected samples, with the 4.5 mA, x3 treatment samples achieving a median GFP knock-out efficiency of 93.77% (see Table 2). The box plots in Figure 6.4 and Figure 6.5 box plots show that the collection of data points representing the 4.5 mA, x3 treatment group is relatively closely grouped, with 75% of observations having greater than 65% transfection rates.

Table 6.2: One-Sided T-test Results from Comparisons of Multiple (x3) vs Single (x1) Injected Samples

Multiple Injections (1) vs Single Injections (2)	P-Value	Difference in Mean GFP KO (1-2)
1.5 mA,x3 vs 1.5 mA,x1	<0.0001	59.87%
4.5 mA,x3 vs 4.5 mA,x1	<0.0001	57.93%
6.0 mA,x3 vs 6.0 mA,x1	<0.0001	47.36%

Data collected from flow cytometry and analyzed in JMP represents mean and median GFP KO rates for the respective sample types. Percentage of cells successfully transfected is calculated as the number of living and GFP negative cells divided by the number of living cells in each sample.

Second, Table 6.2 demonstrates that a large difference was observed between mean values for all treatment group comparisons when examining the effect of number of injections. The largest difference was observed in the 1.5 mA samples, exhibiting a change of 59.87% when comparing x1 to x3 injected samples. When viewed in context of Table 6.1, it is noted that the injection-dose response of all treatment samples is non-linear, meaning the rate of GFP knock-out did not follow a linear scale with the number of times cells were injected. In the case of the 1.5 mA current controlled samples, the single injection mean transfection rate is 6.11%. On a linear scale, the predicted value for samples injected three times should be roughly 18.33%. Instead, for 1.5 mA, x3 treatment samples the transfection rate is 72.78%, nearly 4 times greater than the linear predicted value. Similar but less pronounced observations were made in the case of the 4.5 mA and 6.0 mA samples, resulting in differences in linear predictions and observed mean transfection rates of 14.67% and 2.06%, respectively.

Represented data was initially screened in JMP using ANOVA test to determine presence of statistically significance relationships followed by one-sided t-test ($\alpha = 0.05$) evaluation of specific comparisons. Default minimum p-value reported is 0.0001. Note: All represented relationships are statistically different.

6.3.2 Mid-range current control most effective at GFP Knock-Out

Table 6.3 shows the results from statistical comparisons between sample types, grouped according to the number of times the samples were injected. While it is of note that there were no

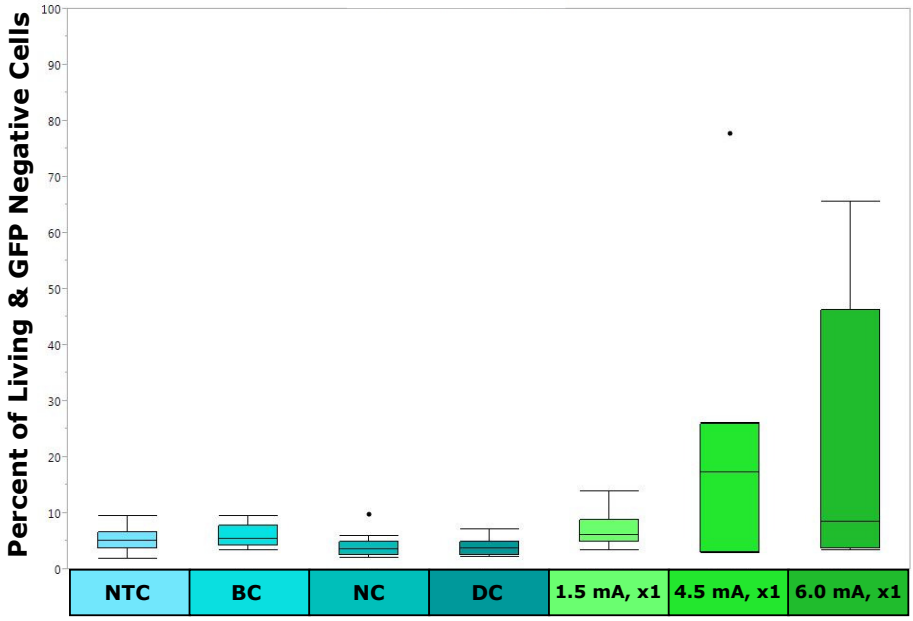

Figure 6.4: Combined box plot results for controls and single injection (x1) treatment samples. Statistically significant relationships are noted Table 6.2 and Table 6.3

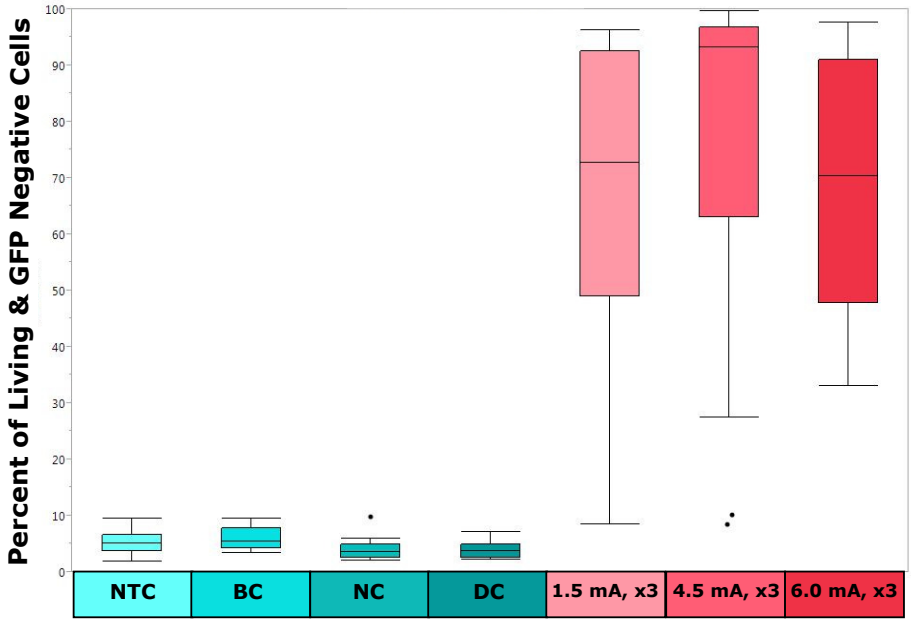

Figure 6.5: Combined box plot results for controls and multiple injection (x3) treatment samples. Statistically significant relationships are noted Table 6.2 and Table 6.3

Table 6.3: One-sided T-test Results from Intra-Group Comparisons
(by Number of Times Injected)

Single (x1) Injected Comparisons	P-Value	Multiple (x3) Injected Comparisons	P-Values
1.5 mA,x1 vs 4.5 mA,x1	0.0684	1.5 mA,x3 vs 4.5 mA,x3	0.0985
1.5 mA,x1 vs 6.0 mA,x1	0.0093	1.5 mA,x3 vs 6.0 mA,x3	0.3454
4.5 mA,x1 vs 6.0 mA,x1	0.4621	4.5 mA,x3 vs 6.0 mA,x3	0.8895

intra-group comparisons that were statistically significant in regards to current control effects on GFP knock-out (with the exception of 1.5 mA, x1 vs 6.0 mA, x1 injections), it should be observed that the relative position of the median values for both the single and multiple injection groups appears to follow a pattern, favoring the 4.5 mA treated samples (see Fig. 4 and Fig. 5). The data suggests that using an intermediate current control setting of 4.5 mA during Phase 1 that may improve transfection efficiency. This observed behavior is shown numerically in Table 6.1 and graphically in Figure 6.4 and Figure 6.5. Notably, 4.5 mA, x1 out performs the other single injection sample groups in terms of the median KO percent by at least 8% and the 4.5 mA, x3 behaves the same by exceeding the other x3 injected sample groups by at least 20%.

Represented data was initially screened in JMP using ANOVA test to determine presence of statistically significance relationships followed by one-sided t-test ($\alpha = 0.05$) evaluation of specific comparisons. Default minimum p-value reported is 0.0001. Note: Only one statistically significant relationship was identified between the 1.5 mA, x1 and 6.0 mA, x1.

6.4 Discussion

Much like other transfection methods, the designed intent of LAN is to direct genetic loads into target cells without threatening their survival. Noted earlier, viruses have been a mainstay in transfection protocols because of the higher transfection rates that can be achieved relative to non-viral modalities [28]. LAN is a non-viral method designed to address this short-coming by generically delivering any electrically charged molecular load by electrostatic attraction and release into the intracellular space of target cells via small micron-sized lance structures.

This process of electrical interaction with molecular loads and physical penetration of the cell membrane was originally created for mouse embryonic transgenic research using a microelec-

tromechanical system (MEMS)-based single silicon lance [210]. Using this device, it was shown that nanoinjection had comparable transfection rates to microinjection but increased embryo survival rates [25]. This delivery system was particularly useful because genetic delivery merely needed to be cytoplasmic due to the localized electroporative effect the lance had on the pronuclei an event termed intracellular electroporetic nanoinjection (IEN) [27].

Later, nanoinjection was extended to somatic cell targets by utilizing an array of silicon etched lances, a design used in this work. Electrostatic principles used to initially determine DNA behavior with the single lance injector [26, 140] have been also applied in LAN, both structurally [23, 84] and procedurally [24, 208].

Initial experimentation with LAN was designed to show the effectiveness with which small molecular loads (such as propidium iodide, PI) could be delivered to cultured cells and what impact that would have on survival. Results showed a voltage-dependent relationship for PI delivery, while maintaining viability rates between 78% to 91% [24]. Similar results were obtained using LAN in experimentation designed to assess the effects of different saline solution types used during injection [208].

This current work marks the first LAN proof-of-concept results regarding the use of CRIPSR-Cas9 plasmids to knock-out gene function. Table 1 indicates that the maximum median GFP KO efficiencies of 70.32% to 93.77% can be achieved using LAN after injecting HeLa cells three times.

Contextually, these LAN efficiencies are encouraging because high-throughput screening of the human genome using CRISPR-Cas9 plasmids designed to knock-out (KO) gene function have proven to be critical to understanding gene function [187]. Maggio et al. [211] recently demonstrated the KO behavior of CRISPR-Cas9 using adenoviral vector delivery of gRNA and Cas9 in two separate vectors. Designed to target the AAVS1 safe harbor locus in a panel of human cells types which include: cervix carcinoma HeLa cells, osteosarcoma U2OS cells, hMSCs, and myoblasts, this team showed relative gene KO when increasing amounts of the two vectors were applied. In the case of HeLa cell experimentation, Maggio et al. achieved maximum gene KO of 31% when 100 TU/cell of both vectors, an efficiency rate less than a third of the maximum efficiency reported here using LAN in the same cell type. While it can be said that this study targeted a different locus and therefore had altered efficiency rates, there is no clear indication that this experiments gene target was easier to alter.

In addition to exhibiting high knock-out efficiency rates, this work also shows in Figure 6.4 and Figure 6.5 the non-linear difference between the x1 and x3 injected samples, a behavior not previously noted in LAN. For example, 1.5 mA, x1 samples had a median KO rate of 6.11%, while 1.5 mA, x3 samples had a median KO rate of 72.78%, a rate nearly 12 times higher. While the magnitudes are not as high for the other sample comparisons, the non-linear trend is still present.

One possible explanation for this behavior is related to cellular response to cell membrane defects, such as defects created by lance induced pores. When a surface defect occurs in a cell membrane, the cell responds by attempting to mobilize and remodel structural elements such as actinomyosin, microtubules, and the cell membrane by contracting around the wound and allowing repair machinery to close membrane gaps [153, 154]. In LAN samples that experience multiple injections, one possible explanation for increased GFP KO is that repair mechanisms may be delayed because of prior insults still being repaired. If true, saturation of repair mechanisms would permit longer periods of time for CRISPR-Cas9 plasmid movement into the cell following multiple injection treatments, and thereby allowing greater GFP KO. While this idea potentially explains why greater plasmid delivery may be possible, it does assume that diffusion is a major factor in plasmid motion across a cell membrane following LAN, a behavior that is not supported by the diffusion controls (DC) used in this study.

Another explanation for the increased GFP KO with samples injected x3 is related to how quickly the target cells remove the delivered plasmid. Prior to injection, samples are pre-treated with chloroquine, an agent designed to inhibit lysosomal action, to increase the half-life of the plasmid in the cytoplasm of target cells. It is possible that initial dosing of plasmids into target cells during the first injection event is enough to saturate functional lysosomes such that when additional plasmids are delivered in subsequent injection events, higher levels of functional CRISPR-Cas9 plasmids are available to disrupt GFP gene function. Again, this idea has not been defined in prior work and requires further investigation.

Another behavior noted in regards to non-linear KO rates deals with the current control exposure during Phase 1. Noted in Table 6.1 is the fact that 1.5 mA samples experience the greatest increase in GFP KO from x1 injection treatment to x3 injection treatment (mean difference of 59.87%). It has been noted in previous work that lower applied electrical conditions during LAN contribute to higher cell viability rates [208]. It is believed that the because the 1.5 mA, x3

treatment samples received a reduced electrical exposure during injection, that more successfully transfected cells survived to be GFP negative than the 4.5 mA and 6.0 mA treated samples. If that were the case, samples exposed to 1.5 mA would more likely survive the injection process and thereby potentially increase the transfection rate.

Intertwined in the discussion of the non-linear behavior of the GFP KO rates when comparing x1 injections to x3 injections is the fact that mid-range current controlled samples had the best median GFP KO. It is observed in Table 6.2 that the 1.5 mA samples experience the greatest change in GFP KO from x1 to x3 injected samples (a difference of 59.87%), while overall the 4.5 mA samples experience the greatest magnitude in GFP KO, reaching a median value of 93.77% for the x3 injected treatment group. A possible explanation for this behavior is that 4.5 mA protocols offers the best balance between effective electrical attraction/release of the DNA during the LAN process, while being a mild stressor in terms of cell viability. Even though the 1.5 mA protocol is milder in terms of cellular stress, a feature seen in electroporation studies to improve cell viability [212], perhaps the 4.5 mA protocol is better at balancing the cellular stress with effective attraction and release of the DNA, a parameter shown to increase DNA motion when done at higher magnitudes in processes like electrophoresis [50, 139, 140].

Having demonstrated the ability to effectively KO gene function using CRISPR-Cas9 plasmids, future work regarding LAN may aim to either optimize this reported process or explore other genomic mechanisms that CRISPR-Cas9 can perform, such as transcriptional activation/repression or gene insertion [130–135], in terms of other cell types, such as primary cell lines or stem cells. Primary cell line targets are of interest because of the potential therapeutic options it creates in regards to gene medicine and gene therapy applications, such as enhancing chronic wound healing [178, 213–216]. Stem cells are also of interest because of similar gene therapy potentials as well as applications related to transgenic animal generation. Specifically, a common method for creating chimeric transgenic animals involves genetic modification of stem cells prior to introduction to the blastocyst [217–220]. The methods used to genetically modify these stem cells (i.e. electroporation, liposomal reagents) are characteristically threatening to cell survivability and/or have lower transfection rates [28, 221, 222]. As discussed, LAN could provide a viable alternative in this area given the fact that genetic modifications and cell survival can occur at high rates, and therefore requires further investigation.

CHAPTER 7. CHRONIC WOUND HEALING AND GENE MEDICINE

The following chapter was constructed from two journal articles. The first portion of the chapter provides a general overview of chronic wounds. Part of the information for this section comes from an article entitled "Biologic Basis of Nerve Decompression Surgery for Focal Entrapment Diabetic Peripheral Neuropathy", which was published in the *Journal of Diabetes Science and Technology* in 2014 [208], presented at the Association of Extremity Nerve Surgeons (AENS) annual meeting, and winner of the Scott Nickerson Award (Houston, TX, 2013).

The second portion of this chapter is a review of transduction and transfection technologies that have been used in chronic wound healing and highlights emerging concepts that could bridge current challenges. The information for this section comes from an article entitled "A Review of Biotechnologies for Enhanced Chronic Wound Healing", which was submitted to *Experimental Dermatology* and is currently under review.

It is intended that the reader can use the information from this chapter as a context for the work presented in Chapter 8. While some of the material that is presented here is discussed elsewhere in this dissertation, this chapter provides a much more comprehensive context to the subject material of chronic wounds and genetic engineering technologies.

7.1 General Chronic Wounds Overview

Chronic wounds globally affect an estimated 50 million patients causing a huge social and economic impact on patients and communities. The cost of general wound care is estimated to be $25 billion annually in the US alone and rapidly growing, mainly due to aging populations, increasing rates of obesity, and the increased occurrence of diabetes [223, 224]. Just in terms of diabetes, the International Diabetes Federation reports that 415 million adults have diabetes and this will rise to 642 million by 2040 [225]. When these data are married with an anticipated 25%

lifetime risk for ulceration for people with diabetes, the need for effective wound healing takes on a palpable sense of urgency [226–228].

Chronic wounds are complex micro-environments because they can be caused by a variety of mechanisms. Common factors involved with wound creation include: metabolic disfunction, vascular disfunction, peripheral neuropathy, tissue insult (through blunt and/or repetitive micro-trauma), drugs and medications, poor nutrition, etc. [226, 229–232]. The intertwined nature of these factors makes treating each patient uniquely difficult. Yet despite many of these challenges, modern medicine has delivered critically important therapies.

For instance, diabetic patients frequently experience foot ulcerations. These ulcers are regularly a result of metabolic disfunction creating focal entrapment peripheral neuropathy in the distal limbs and the patient unknowingly creating tissue damage through biomechanical over-load, burns, blunt trauma, etc. Moreover, compromised vascular supply to the region due to vascular calcification secondary to diabetes and/or autonomic disfuction in smaller vessels makes healing these ulcers difficult without intervention. Furthermore, wounds can harbor and foster bacterial colonies and/or foreign bodies, which can inflame surrounding tissue and add to delays in healing.

Fortunately, intervention therapies exist. In terms of focal entrapment neuropathy, Dellon is credited for extending carpal tunnel surgical release of constrainted anatomic locals to lower extremity entrapment sites, leading to neuropathic reversals [208]. In terms of vascular re-supply, it is common practice to re-purpose the great saphenous vein for arterial by-pass to the lower limb, thus facilitating better nutrient and immune cell supply to affected limbs. In terms of bacterial management, antibiotics exist that can attack a variety of organisms, although the emergence of antibiotic resistant bacteria is a rising concern.

Despite these critical therapuetic advances, one element that still is difficult in terms of healing an open wound is actually getting resident wound bed cells to quickly close the wound. While there are many techniques that use environmental controls to get the wound to initiate healing, such as debridement (surgical or agent-based) of non-viable tissues that can both surround and be contained in the wound bed, reduction of inflammation and/or infection with anti-inflammatories and antibiotics, moisture correction with wound dressings, and re-epithelialization and granulation of the wound bed by promotional adjuvants [233, 234], there are still wounds that are recalcitrant to these methods and do not close.

7.2 Wound Closure Technologies

In response to this immense chronic wound challenge, researchers have explored and continue to explore novel alternative approaches to enhance healing processes by genetically engineering wound beds. The purpose of this review is to highlight two key aspects of research involving the genetic modification of chronic wound beds for enhanced healing outcomes. First, this review will survey both viral transduction and non-viral transfection technologies that have been employed in wound healing, spotlighting animal experimentation, relative strengths and weaknesses associated with each, and general mechanisms. Second, this review will also consider emerging concepts related to the transfection process specifically, genomic targeting with CRISPR-Cas9 and new delivery methods. Further exploration of wound characterization technologies that help guide decisions regarding molecular targets, including wound diagnostics (i.e. bar coding) and molecular targets for improved healing, will be briefly discussed.

7.2.1 Viral Transduction

Re-purposing viral vectors with the desired therapeutic molecular load is a classical approach to genetic modification of cutaneous target cells. While this has been done with several virus types in other areas of gene medicine, primarily three virus types have been used specifically in wound healing applications, which include: adenovirus, adeno-associated virus, and the retroviridae family (retrovirus and lentivirus).

Adenoviruses

Adenoviruses (ADV) are non-enveloped viruses containing double-stranded DNA and are prominently used in wound healing literature. Mechanistically, ADV enters the host cell via receptor mediated endocytosis, transported and then escaped from an endosome, and then has its capsid bind to the nuclear pore complex of the nucleus and deliver its DNA into the nuclear space where it is not integrated into the host genome (thus not a risk of insertional mutagenesis) [38, 235]. Once in the nucleus, the DNA can be processed to eventually be expressed as a protein (see Figure 7.1 for more information about ADV function).

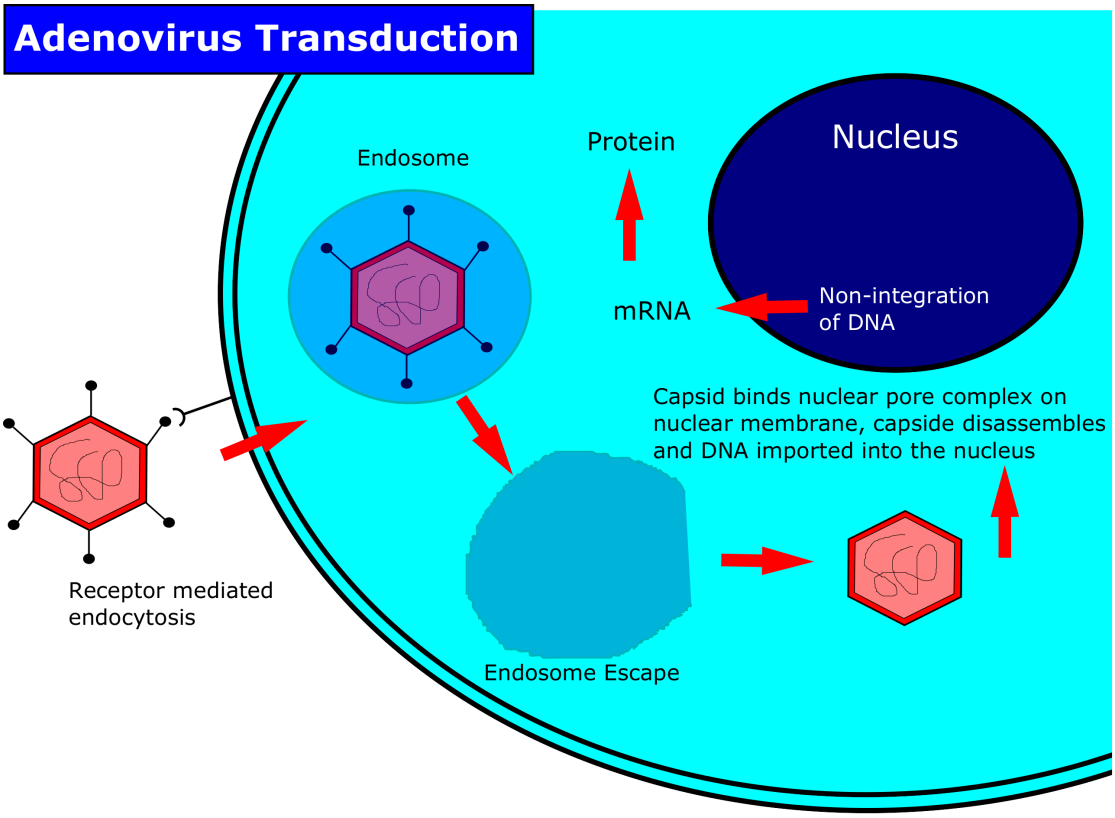

Features

- Does not integrate into host genome, making expression transient and insertational mutagenesis not a concern
- Can achieve infection of target cells, regardless of position in the cell cycle
- Exposure to ADV is common, thus antibodies to the ADV can inactivate engineered ADV before or upon delivery to the cell
- Can reach transduction rates of 70% to 80% in fibroblasts and keratinocytes
- Acute inflammation responses in patients likely occur due to capsid proteins of virus
- Pay-load capacitiy: 8.5 kb

Figure 7.1: Adenovirus transduction occurs as the non-enveloped virus containing double-stranded DNA binds to coxsackievirus and adenovirus receptors (CAR) and are internalized into the host cell. Once inside, the virus is contained in an endosome, from which it can escape and then bind to the nuclear pore complex on the nuclear membrane. The capsid then disassembles and the viral DNA is imported into the nucleus where it can be transcribed and later translated in the cytosol to an effector protein

Advantages of ADV in context of wound healing include: transduction rates of 70-80% in fibroblasts and keratinocytes [236], transient expression [178], no insertional mutagenesis [38], and the ability to infect target cells regardless of cell cycle stage [237]. Unfortunately, ADV also can cause acute inflammatory responses (likely due to capsid proteins) [29], has commonly infected roughly 90% of people (thus patients may have antibodies developed to the virus making it difficult to be effective), and has a modest pay load capacity of 8.5 kb [37].

Experimentally the utility of ADV has been shown by its ability to effect production of several key proteins (such as platelet-derived growth factor-B (PDGF-B), inducible nitric oxide synthase (iNOS), and vascular endothelial growth factor (VEGF)) [238–242] and in one case, a receptor (i.e. ErbB3 receptor) [243] for wound healing. In regards to VEGF, a key angiogenic protein used to increase blood flow to wounds, two investigators have explored using adenoviruses for VEGF delivery. Romano Di Peppe et al. demonstrated with a topical application of the vector in healing impaired diabetic mice, that a 3.7-fold increase in blood vessel density was noted 7 days post-treatment [240]. A companion study was attempted in porcine, using a micro-needling delivery of VEGF-carrying adenovirus in which higher levels of VEGF were noted in the wound environment but unfortunately did not lead to an associated elevation in neovascularization [241]. More recently, Okwueze et al. demonstrated using a recombinant ADV re-programmed with an ErbB3 receptor gene, a receptor that produces a cascade leading to re-epithelialization, that significant improvements in wound healing maturity could be achieved [243]. This work is of particular note because it demonstrated that EGF-like ligand could initiate/control healing by topical application an attractive clinical feature.

As mentioned earlier, ADV have also shown the ability to successfully modify human primary keratinocytes and fibroblasts at rates as high as 79% [236]. While encouraging in terms of efficiency, this study unfortunately also highlights the fact that cytotoxic effects were observed after 10 days post-treatment. These cytotoxic effects, coupled with the fact that adenovirus capsid proteins can produce acute inflammatory reactions which can disrupt healing in itself [29, 239], have influenced exploration of other viral vectors.

Adeno-associated Viruses

Adeno-associated viruses (AAV) are non-enveloped viruses containing single-stranded DNA. Functionally, AAV generally operate similar to ADV with the main exception being that once the DNA of the AAV enters the nucleus, it forms either an episomal structure or in rare cases, can integrate into the host genome (thus carrying a low risk of insertional mutagenesis [244]). Once in the nucleus, the DNA can be expressed to eventually produce a protein (see Figure 7.2 for more information about AAV function).

The advantages of AAV include: being highly stable, particularly resistant to heat inactivation [245], low immunogenicity [237], able to target non-proliferating cells [237], mostly non-pathogenic to humans [178], and have broad tissue tropism [178]. The downside of AAV use is that they can require high MOI (multiplicity of infection) to transduce cells [237] and have a relative low pay load capacity of 4 to 5 kb [37].

In companion studies using AAV to express VEGF-A in mice and rat models, it was shown histologically that more consistent wound healing (in comparison to ADV) has been noted in terms of angiogenesis, re-epithelialization, and extracellular matrix deposition [215, 246]. Additional work involving AAV has shown that AAV2/5 and AAV2/8 exhibit affinity for epidermal and dermal cell targets which can be engineered to be enhanced further by modifying capsid proteins, making it a useful vehicle even if skin tissues are missed when placing the viral-load [247, 248].

Other Viruses

Lesser used wound modifying viruses include members of the retroviridae family. Retroviruses have larger load capacity than AAV AVD (10 kb), albeit it is still fairly modest [37] and can integrate into the host genome [237]. Retroviruses are characteristically more instable, cannot transduce non-dividing cells (with the exception of lentiviruses, a genus in the retroviridae family), and have lower modification rates [245]. In experimentation, it was shown that retroviruses containing a PDGF-AA gene facilitated a 300-fold increase in in vitro levels of PDGF-AA after 7 days, producing thickened connective tissue as well as an increase in regional blood vessels [249]. More recently, lentivirus transfection with stromal cell derived factor 1 alpha (SDF-1alpha) has been shown in diabetic mice models to enhance granulation tissue formation, which is attributed

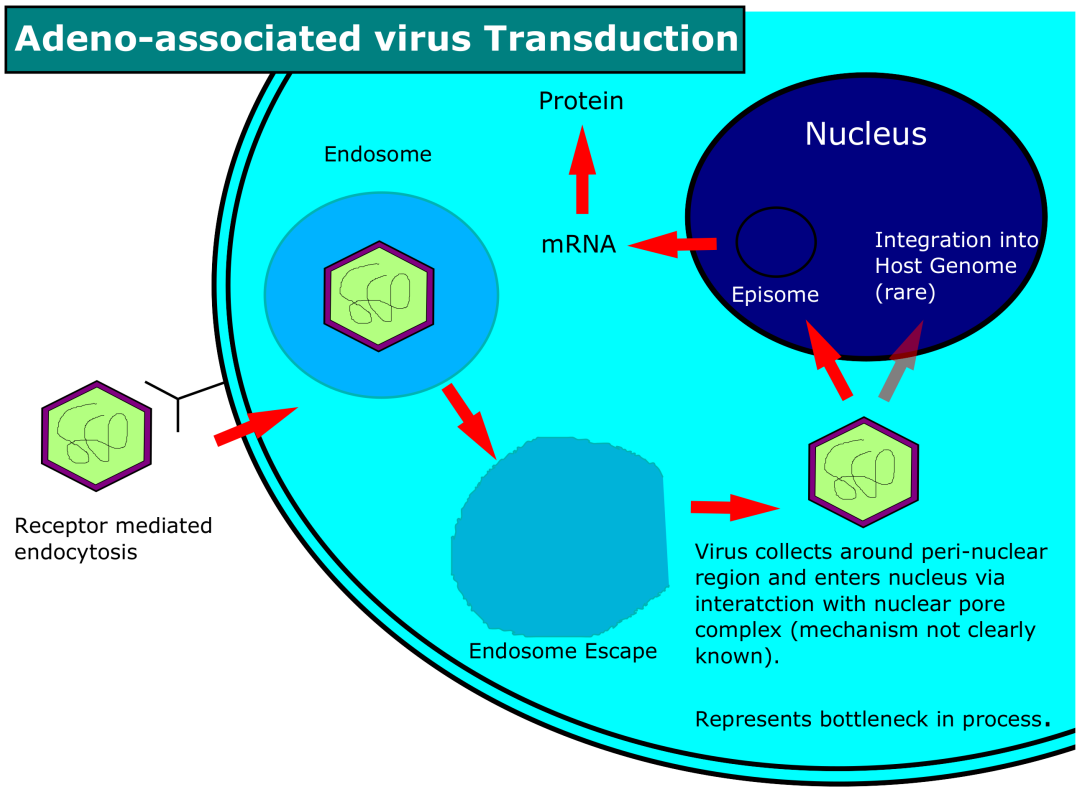

Features

- Highly stable, heat inactivation resistant
- Low risk for insertional mutagenesis, although it can occur
- Broad tissue tropism, making it useful in many applications
- Characteristically lower immunogenicity
- Can target non-proliferating cells, which can be less important in wounds
- Require high multiplicity of infection (MOI) to transduce some cell targets
- Labor intensive to produce
- Mostly non-pathogenic to humans
- Lower transduction efficiency because of hindered trafficking into the nucleus
- Pay-load capacitiy: 4-5 kb

Figure 7.2: Adeno-associated virus transduction occurs as the non-enveloped virus containing single-stranded DNA binds to the host cell and is internalized. Once inside, the virus is contained in an endosome, from which it can escape, collects around the nucleus, and then bind to the nuclear pore complex on the nuclear membrane. The exact mechanism for entry is not clearly understood, but it terms of transduction, nuclear entry represents the rate limiting step for successful transduction. Once the viral DNA is in the nucleus, it can form into an episome or in rare cases integrate into the host genome. DNA is then transcribed, followed by mRNA translation for protein production

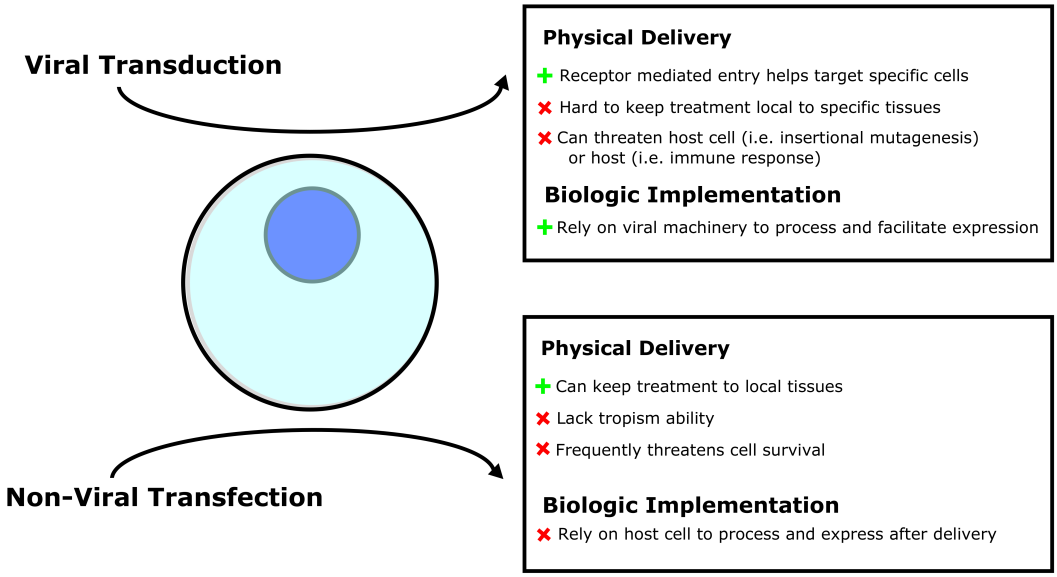

Figure 7.3: General differences between viral transduction and non-viral transfection. Note: Green plus signs are features viewed as positive characteristics while red "x" marks are viewed as negative characteristics

to increased cell mobilization and recruitment [216]. While this group of viral vectors are useful, there is concern that with integration capabilities that insertional mutagenesis is a problem and therefore limits potential clinical use as a solo technology [46, 186].

7.2.2 Non-Viral Transfection

Some clinical challenges exist that make using viral vectors difficult to use (i.e. limits on payload capacity, cytotoxic effects, immune reactions, difficulty containing viral particles to tissue specific locations, etc.) [30–32, 35, 37, 43, 46, 178, 186] and have caused researchers to explore alternative non-viral modalities for gene transfection of wounds. Figure 7.3 presents general differences between viral and non-viral methods in the context of wound healing and provides an idea of the current limitations of each.

Non-viral transfection technologies have undergone an evolutionary development as both the understanding of biologic systems has improved and the ability to use that knowledge has increased. Early works with non-viral transfection in the field of wound healing began with naked DNA injections and micro-seeding, a process of naked DNA introduction via a modified tattoo

machine [214, 250, 251]. While novel in approach, many of these direct insertion approaches had little success in terms of molecular expression or wound healing mainly because of the inability to keep the DNA intact in the extracellular environment as well as the poor delivery of the DNA across the target cells outer membrane.

In an effort to more specifically deliver genetic loads across the cell membrane of target cells, more sophisticated methods began to be used, which include reagent-based methods like liposomal agents and instrumentation-based methods like the gene gun. One of the first studies to report both gene expression and functional improvements using non-viral transfection was a team that used liposomal agents to deliver a plasmid for acidic fibroblast growth factor (aFGF) [252]. Encapsulated in a cationic liposome, the plasmid was topically applied to both incisional and excisional wounds in diabetic mice. Both immunohistologic assays and mechanical testing showed that treated wounds responded significantly better. Follow-up work using a similar premise showed that using liposomes filled with multiple genes was significantly more effective at achieving biologic effects in wound healing than single gene filled liposomes [253], a result that is useful given that robust healing employs multiple factors.

The instrumentation-based method called the gene gun, also known as particle bombardment, is another method for plasmid transfer to target cells that has seen functional success. Typically, gene guns use either gold or tungsten particles with plasmids attached. These particles are propelled towards target cells, penetrate the cell membrane, and are then able to have the plasmid removed for molecular effect. Two studies have demonstrated functional results of using plasmids coding for PDGF and EGF [249, 254]. In the case of the PDGF, it was noted that an increase in tensile strength occurred, whereas the EFG study showed an improvement in epithelialization and granulation tissue.

In addition to the gene gun, various forms of electroporation have also been employed for several cutaneous disorders generally [255] and wound healing specifically [67, 256–259]. Functionally, electroporation generally consists of brief, high pulses of voltage across target cell membranes and causes transient formation of pores in the membrane, allowing passage of molecular loads. Although designed to address slightly different elements of the healing cascade, much of the electroporation work has shown functional results ranging from increased regional angiogenesis to enhanced re-epithelialization. While effective in many cell types, electroporation has disadvan-

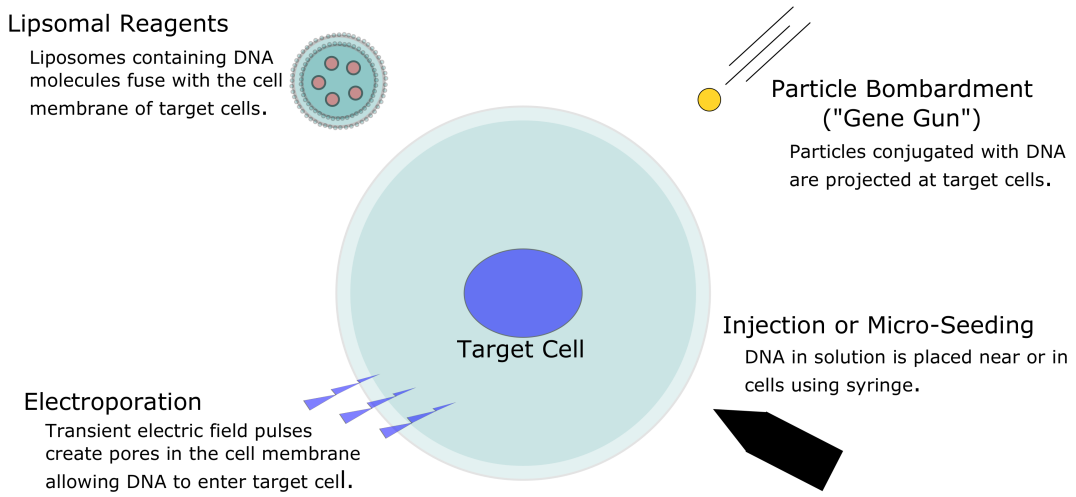

Figure 7.4: General mechanisms for non-viral transfections methods

tages related to the transient indiscriminate movement of molecules across the cell membrane and the permanent membrane damage that can follow the high voltage pulses that can lead to cell death [260, 261] (see Figure 7.4 for more information about non-viral transfection mechanisms).

Shown in Table 7.1 and Table 7.2 is a summary of both viral and non-viral animal-wound studies that show how these methods have been applied to wound healing and the outcomes of those studies. (Note: Direct injection refers to the placement of the viral particles directly into the wound bed via injection with a syringe; indirect injection refers to *in vitro* transduction of cultured cells using viral particles and then placement of these modified cells into the wound bed via injection with a syringe.)

7.2.3 Emerging Concepts

While many of the methods discussed up to this point have shown encouraging improvements in wound healing outcomes, there still is no transduction/transfection method that robustly solves the chronic wound healing problem. Illustrated in Figure 7.5 is a list of criteria that have helped form technologies aimed at wound healing up to this point and now guide emerging concepts in the field.

Table 7.1: Animal Experimentation involving Viral Transduction of Wounds

Method of Transfet	Gene	Animal Model	Effect	Source
Adenovirus by Direct Injection	PDGF-B	Mouse	Diabetic treated mice experienced significant reductions in epithelial gaps (50%) and increases in granulation tissue area (3.2 fold) 7 days post-treatment.	[238]
Adenovirus by Direct Injection	PDGF-B	Rabbit	Treated samples have increased granulation tissue volume in ischemic wounds.	[239]
Adenovirus by Needle Array Direct Injection	VEGF	Porcine	Increased expression of VEGF in wound beds. No associated elevation in neovascularization or re-epithelialization.	[241]
Adenovirus by Gene Gun	ErbB3 Receptor	Porcine	Following treatment, wounds were given topically applied EGF-like ligands to stimulate ErbB3 receptor. Significant wound re-surfacing and granulation tissue thickness were observed 5 days post-treatment.	[243]
Adenovirus by Indirect Injection	eGFP	Rat	Used as a proof-of-concept of adenoviral delivery to burn wounds. Transfection rates were significantly elevated 10% to 40% in human fibroblasts and keratinocytes.	[236]
Adenovirus by Topical Application	iNOS	Mouse	Wounds treated at the time of wounding were able to overcome iNOS deficient states allowing for faster wound closure times.	[242]
Adenovirus by Topical Application	VEGF	Mouse	Treated wounds experienced significant wound closure between 3 and 9 days post-treatment. Length density of arterioles were also significantly increased (2 fold).	[240]
Adeno-Associated Virus by Indirect Injection	N/A	Mouse	Demonstrated that AAV2/5 and AAV2/8 exhibit dermal and epidermal tropism when placed deep to the skin surface and offers a potentially useful mechanism for wound healing.	[247]
Adeno-Associated Virus by Indirect Injection	VEGF	Mouse	Increased angiogenesis, re-epithelialization, and extracellular matrix production resulting in increased wound breaking strength.	[215]
Adeno-Associated Virus by Indirect Injection	VEGF	Rat	Statistically significant histological scores obtained 18 days post-treatments in terms of epidermal and dermal regeneration, granulation tissue thickness, and angiogenesis.	[246]
Retrovirus by Indirect Injection	Beta-galactosidase and hGH	Porcine	Increased hGH protein concentrations observed for 8 days post-treatment, leading to significantly increased healing time.	[262]
Retrovirus by Indirect Injection	PDGF-AA	Mouse	Modified in vitro keratinocytes exhibit 300-fold increase in PDGF-AA levels.	[213]
Lentivirus by Direction Injection	SDF-1alpha	Mouse	Treatments exhibited significantly increased granulation tissue at 7 days, while wound surface area did not decrease differently from controls, they did experience greater epithelialization.	[216]

Table 7.2: Animal Experimentation involving Non-Viral Transfection of Wounds

Method of Transfet	Gene	Animal Model	Effect	Source
Direct Injection	IL-8	Porcine	Used to show neutrophil recruitment post-treatment.	[251]
Electroporation	HIF-1alpha	Mouse	Treated mice express 10-fold increase in circulating angiogenic cells with increased local treatment site levels of VEGF, PLFGF, PDGF-B, and ANGPT2.	[67]
Electroporation	KGF-1	Mouse	Demonstrated that 90% of treated wounds healed in 12 days versus only 40% in controls.	[259]
Electroporation	KGF-1	Rat	Increased re-epithelialization of wound by 60% over control after 12 days.	[258]
Electroporation	TGF-beta1	Mouse	Showed that 5 to 7 days post-treatment that wounds showed increased re-epithelization, collagen synthesis, and angiogenesis. Also demonstrated that diabetic skin is more sensitive to electroporative damage.	[257]
Electroporation	VEGF	Rat	Significantly increased skin flap perfusion 10 and 14 days post-treatment.	[256]
Gene Gun	EGF-R	Porcine	Increased EGF-R 24 to 48 hrs. post-treatment at different levels of skin based on varied pressures used to propel gene carrying particle.	[254]
Gene Gun	PDGF-A and -B	Rat	Transient increases in wound tensile strength over controls as high as 3.5-fold increase at 7 days.	[249]
Injection of Cationic Dendrimer	VEGF	Mouse	Increased VEGF expression and healing of wound 6 days post-treatment.	[263]
Liposomal Formation	FGF	Mouse	Increased FGF expression and wound break strength post-treatment.	[252]
Liposomal Formation	IGF-1/KGF	Rat	Increased skin regeneration of wound 250% over control.	[253]
Micro-Seeding	EGF	Porcine	Increased EGF expression 2 days post-treatment, reaching four to seven fold times greater than single injected skin samples and two to three times higher expression over particle-mediated gene transfer.	[214]

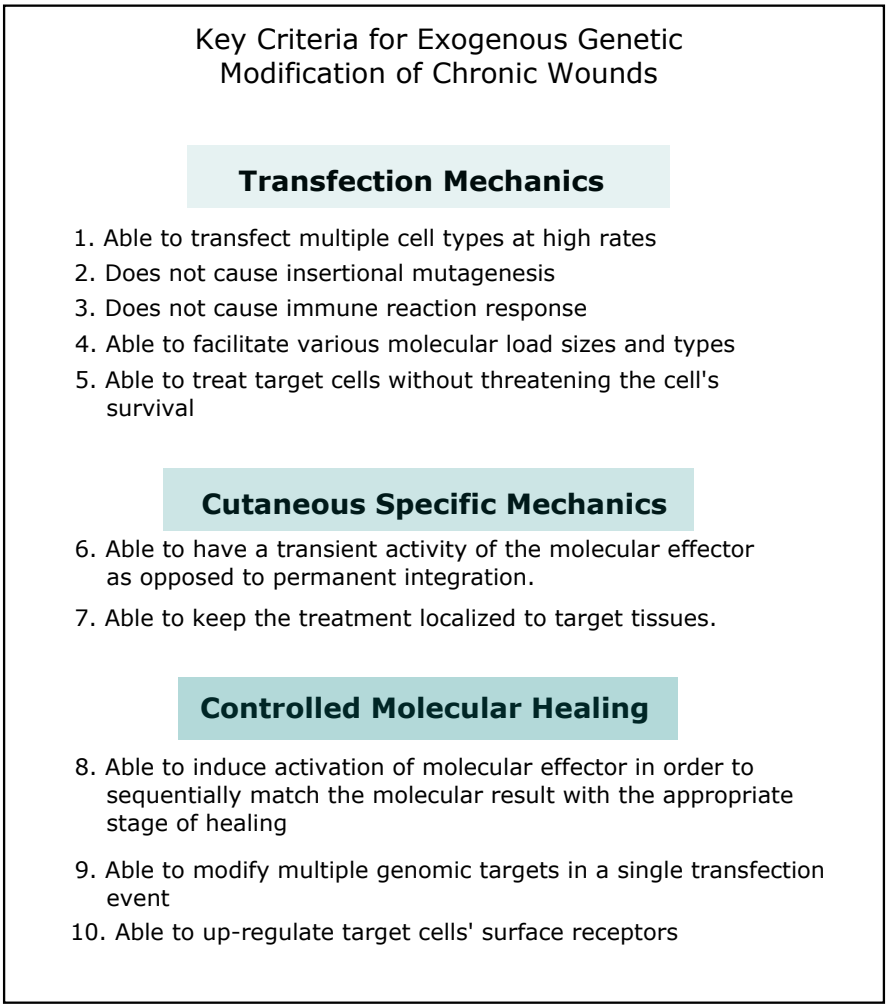

Figure 7.5: Presents key criteria used to develop transduction/transfection technologies for wound healing applications

One of the most important ideas that has and continues to promise enhancements to genetic methods in wounds is the combination of approaching the wound in terms of characterizing the wound system (i.e. wound diagnostics via bar coding and identification of molecular targets that play an important role in healing) and then matching those characterizations with appropriate methods (i.e. site-directed genomic enhancement, new delivery methods). Presented briefly here is a discussion of wound system characterization followed by method improvements (see Figure 7.6).

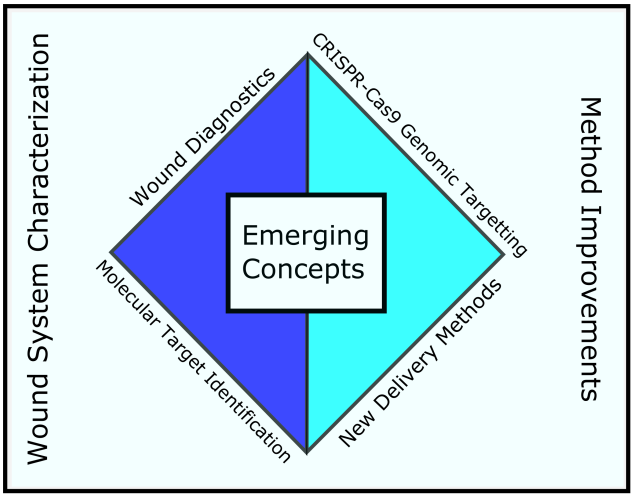

Figure 7.6: Illustrates the interplay between wound system characterization and new method developments that create meaningful emerging technologies

Wound Diagnostics

Bar coding is an advanced wound diagnostic concept that is designed to monitor the molecular dysfunction in wounds. It consists of a taking samples of tissue or fluid from patients wounds to characterize levels of molecular markers present to help determine the state of the wound and identify key missing elements related to healing [264]. Demidova-Rice et al. [233] notes that by using bar coding, providers are able to hone in on specific growth factors and potential receptors that are absent or expressed at diminished levels.

To help illustrate the utility that can come from bar coding, it is critical to understand that in a chronic wound there are a variety of dysfunctional activities that can be occurring and that correctly identifying the problems can greatly increase the potential for healing. For instance, fibroblasts found in chronic wounds have a lower growth factor receptor density and consequently, have a lower mitogenic responses to ligands such as platelet derived growth factor-AB (PDGF-AB), insulin growth factor (IGF), fibroblast growth factor-basic (bFGF), and epidermal growth factor (EGF) [265–267]. The believed underlying cause of lower receptor density is directly related to elevated levels of interstitial proteases, that damage surface receptors on the resident cells. Complicating the situation further, if high levels of bacteria (greater than 10^5) or bacterial tox-

ins are present, excessive inflammatory responses can also occur, further degrading extracellular growth factors and receptors [233].

This marks a salient point in regards to why genetic approaches to wound healing are necessary. Without properly functioning surface receptors on resident wound cells, it is less effective or ineffective to attempt to control molecular behavior via application of exogenous ligands. This behavior is evidenced by disappointing clinical results achieved with becaplermin (rPDGF-BB), the only FDA approved topically applied growth factor ligand commercial available. Genetic modification to resident wound bed cells provide a means whereby cells can both locally produce essential growth factors and up-regulate necessary surface receptors that facilitate intracellular biochemical healing cascades (see Figure 7.7)

The utility of bar coding for pin-pointing molecular dysfunction in regards to chronic wounds cannot be overstated. Unfortunately, the current practice of bar coding is not widely adopted.

Molecular Target Identification

Behm et al. [268] offers a well written compilation of mediators that play a significant role in wound healing. Listed are several traditionally accepted mediators, sources from which these mediators and natively derived, cell types and receptor types upon which these mediators will act, and key functions that the mediators initiate.

In addition to these mediators, the reader may also consider other molecular targets that have more recently been identified in the literature and include: HIF-2α, Toll-like receptor 3 (TLR3) agonist polyriboinosinic-polyribocytidlylic acid (Poly(I:C)), IL-22, adiponectin [269–273].

Additionally, as mentioned earlier, the value of surface receptors initiating local cellular response towards healing continues to be investigated as noted by findings supporting the effects of Toll-like receptor 4 (TLR4), CD9, and the cross talk between insulin growth factor receptor 1 (IGF-1R) and estrogen receptors (ERα) receptors on wound closure [273–275].

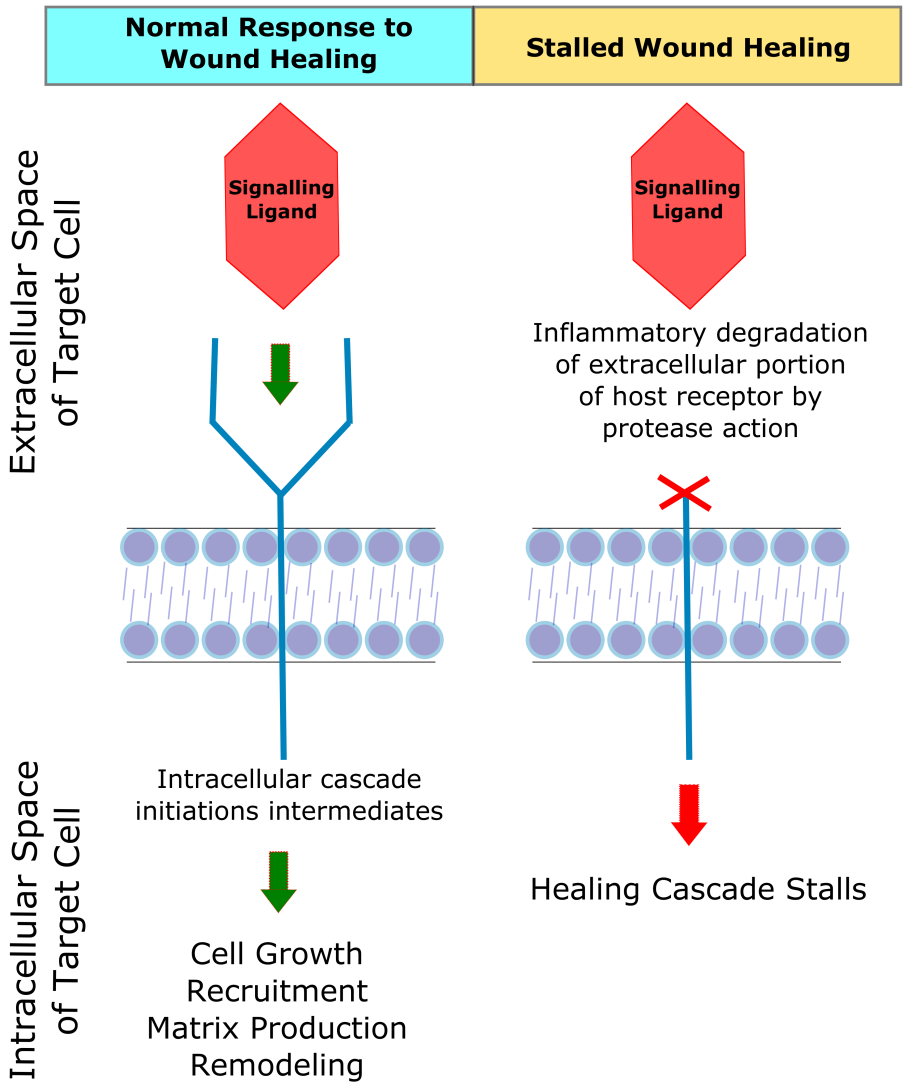

Figure 7.7: Illustration of receptor during normal healing and stalled healing secondary to degradation in chronic wounds

CRISPR-Cas9 Genomic Target Modification

A critical interplay occurs between the logistical delivery of genetic pay loads and the native biologic mechanisms in target cells required to promote exogenous DNA expression. In the case of viral transfection, this interplay is clearly integrated because the virus is involved in the delivery as well as the expression of the desired gene. In the case of non-viral transfection, this interplay is not integrated, and historically been a major source for reduced efficiency in expression rates relative to viral methods [18, 20–22].

Fortunately, a relatively new nuclease editing tool, known as CRISPR-Cas9, has been developed which can facilitate meeting many of the stated wound healing criteria when coupled with an efficient physical delivery modality. CRISPR-Cas9 nuclease editing systems work with essentially two elements, the gRNA and the Cas9 protein. gRNA sequences are short programmable sequences that provide a genomic address for the associated generic Cas9 protein to locate target loci and modify it [96, 183]. Once bound to the target, Cas9 can initiate a variety of effects which include: direct gene insertion (permanent effect) [130, 131], direct gene knock-out (permanent effect) [97], transcriptional activation (transient effect) [132–134], or transcriptional repression (transient effect) [132, 135]. Furthermore, since the gRNA and Cas9 protein operate in two distinct roles, by providing multiple different gRNA sequences, multiple genomic modifications can occur in a single transfection event [136–138, 209].

The multiple functions of CRISPR-Cas9 are potentially very useful for chronic wounds. First, CRISPR-Cas9 constructs are relatively simple to construct and are small. Second, CRISPR-Cas9 can specifically modify nearly any genomic target (making insertional mutagenesis much less of a concern) and can use the gene library already found in the host genome rather than having to consistently rely on inserting exogenous DNA. This is particularly useful for wounds because enhanced performance on a transient basis is useful for matching healing stage to the gene therapy. Third, if using non-viral methods, the risk of an immune response is near absent. Fourth, CRISPR-Cas9 can modify multiple genomic targets in a single event making it possible to leverage and mobilize many of the known molecular effectors for healing as opposed to only one or two as demonstrated by Table 7.1 and Table 7.2.

Further demonstration of CRISPR-Cas9s potential in wound healing is that CRISPR-Cas9 has been used already in many other related applications including: Duchenne Muscular Dystrophy [138], following the progression of disease phenotype expression in diseases such as Friedreichs ataxia [276], development of novel HIV therapies [277], use as in situ functional assays [278], and transgenic plant breeding [279]. Given the promising results of many of the studies, it is only a matter of time before CRISPR-Cas9 plasmids are applied to chronic wound healing.

New Delivery Systems

Tied closely to the promising biologic mechanisms of CRISPR-Cas9 is the idea of combining CRISPR-Cas9 with transfection methods specifically designed to interface with skin conditions. Two existing methods that could be easily employed if dosed in a way to mitigate cell death: 1) topically applied liposomal reagents or 2) optimized electroporation. As discussed earlier, both of these methods have been shown to deliver at relatively efficient rates to cutaneous targets [253, 255].

Other technologies that have not yet been used in animal experimentation but have demonstrated good results in proof-of-concept cell culture conditions include conjugated nanoparticles [280], microfabricated needles [281, 282], microfabricated nanowires [119], and multi-electrode arrays [283]. Additionally, another technology that leverages both physical and electrical actions to modify target cells is an in vitro instrumentation-based method called nanoinjection. First generation nanoinjection consisted of a micro-electromechanical system (MEMS) that used electrostatic attraction of DNA onto a silicon micro-sized solid lance that was then inserted into mouse embryos before electrically releasing exogenous DNA into the host [25–27, 210]. This same technology has been modified in its second generation to consist of a micro-fabricated silicon wafer that has been etched to create a grid of four million 10 micron length lances spaced every 10 microns that allow for effective delivery of genetic loads to hundreds of thousands of cells simultaneously [23, 84]. As an emerging method, nanoinjection shows promise in regards to CRISPR-Cas9 chronic wound applications, given the high efficiency of transfection and high cell survival rates [24].

7.3 Conclusion

Given the present nature of how widespread chronic wounds are and that they are complicated, multi-faceted conditions, it is important that research continue to explore alternatives to traditional approaches. This review provides a context to technologies that view healing chronic wounds from the inside-out. Genetically engineering chronic wounds for enhanced healing outcomes is not yet fully realize; however, it is clear that there are viable approaches and that new combinations of tools can help overcome current shortcomings.

CHAPTER 8. CRISPR-CAS9 TRANSCRIPTIONAL UP-REGULATION OF PDGFR-β IN PRIMARY NEONATAL FIBROBLASTS

The following chapter comes from a journal article under review by *PLoS ONE* and is entitled "CRISPR-Cas9 Transcriptional Up-Regulation of PDGFR-β in Primary Neonatal Fibroblasts following Lance Array Nanoinjection".[1] As a result, there may be some material that is contained elsewhere in this dissertation but is presented here as a representation of this original journal article.

8.1 Introduction

Chronic wounds represent a health crisis that affects an estimated 50 million patients and carries high costs in terms of human suffering, quality of life, and health care [223, 224]. To give perspective to how quickly this global crisis is growing in terms of cases caused by diabetes alone, in 2016 it is reported by the International Diabetes Federation that 415 million adults are diabetic. By 2040, the diabetic population is projected to increase by an additional 227 million people [225]. When juxtaposed with the fact that 25% of these patients will have at least one diabetic ulcer within their lifetime, it is clear that the current chronic wound challenges will become much larger in the near future making it of paramount importance to have effective therapies to combat this surge [226].

The key to preventing an escalation of complications related to chronic wounds is to get wound closure quickly. Many of the traditional treatment approaches (i.e. surgical debridement, moisture correction dressings, tissue-engineered human skin grafts, etc.) attempt to kickstart native healing by trying to control environmental factors in the wound in order to over-come this stalled state. Essentially this approach is seeking wound closure from the outside-in.

[1] This work has also been accepted as part of an oral presentation at the 2016 International Society for Transgenic Technologies (ISTT) annual meeting (Prague, Czech Republic) and as a poster presentation at the Kaiser Permenante Foot and Ankle Summit (Oakland, CA).

Regrettably, traditional wound care methods can take long periods of time before wound closure occurs and in some cases, traditional care fails completely necessitating amputation [231]. In an effort to create a second front for wound treatment, researchers have focused on creating technologies that can genetically modify native wound cells in order to facilitate healing. Essentially this approach is seeking wound closure from the inside-out. Attempted wound healing transfection methods using this model include: recombinant viral vectors [236, 243], liposomal reagents [253], particle bombardment with gold- or tungsten- conjugated to DNA [254], and electroporation [67, 256, 257].

Unfortunately, these efforts have had mixed results for two major reasons. First, current gene modifying technologies experience trade-offs between efficient modification and safety. Viral transduction can be effective at targeting skin cells but can also have inherent safety issues (i.e. viral induced immune responses) [29, 32, 239]. Non-viral transfection can be moderately effective in the skin but frequently causes cell cytotoxicity or survivability concerns (i.e. liposomal reagents, particle bombardment, electroporation) [37]. Second, nearly all animal experimentation with genetic wound healing has focused on increasing production of ligands important to healing but not the surface receptors upon which these ligands must act. Demidova-Rice et al. [284] discusses the incompleteness of this approach by commenting on the disappointing clinical trial results with topically applied becaplermin, a platelet derived growth factor ligand (PDGF-BB) that is critical for healing [285]. The attributed cause to less than desired healing results has to do with the fact that resident cells in chronic wounds have dramatically fewer surface receptors due to excessive extracellular protease action, therefore preventing ligand-initiated healing even in the presence of elevated ligand levels (see Figure 8.1).

The purpose of this work is to present an alternative, non-viral transfection method that uses a micro-electromechanical system (MEMS-based), known as Lance Array Nanoinjection (LAN), in conjunction with a platelet derived growth factor receptor-β (PDGFR-β) CRISPR-Cas9 transcriptional activation plasmid. In contrast to previous works, this work demonstrates a method that can both efficiently and safely modify primary neonatal fibroblasts and demonstrates its utility in terms of increasing the surface receptor PDGFR-β on fibroblasts.

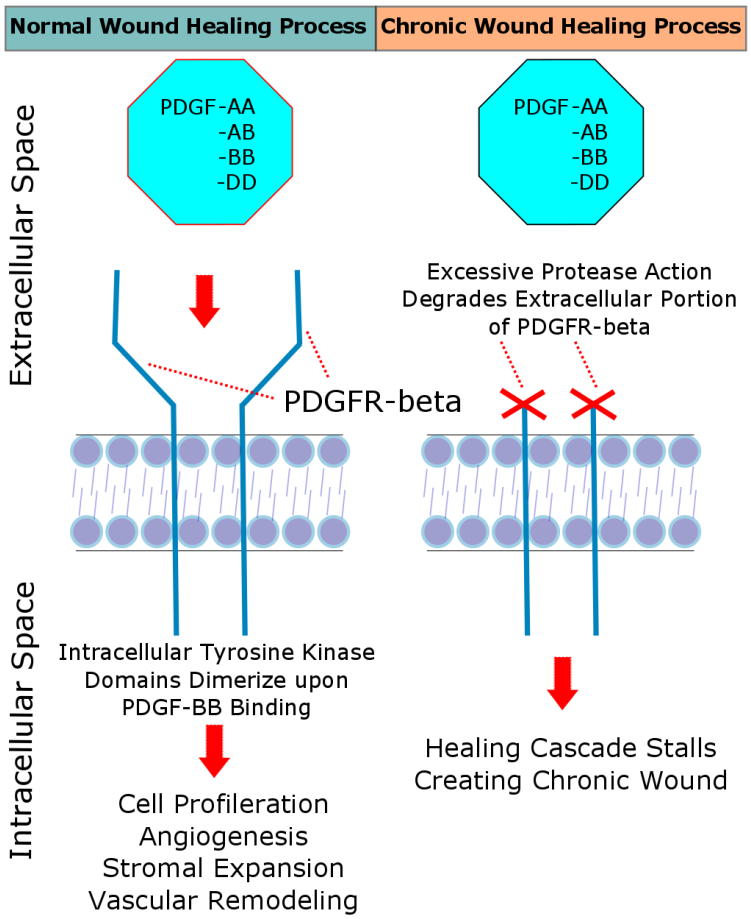

Figure 8.1: Illustrates the interaction between PDGF growth factor isoforms (-AA, -AB, -BB, and -DD) with PDGFR-beta in both normal (left) and chronic (right) wound healing conditions

8.2 Materials and Methods

8.2.1 Lance Array Nanoinjection Device

Figure 8.2 shows a schematic view of the Lance Array Nanoinjection (LAN) device with the inserted silicon lance array. The LAN device has four major components, which include the: stepper motor, orthoplanar spring, silicon lance array, and cell culture platform. At the top end, a stepper motor, which is used to control vertical motion of the silicon lance array, is attached to an orthoplanar spring, which facilitates vertical displacement by preventing unwanted torsion motions [84]. As the stepper motor moves the silicon lance array downward, the lance array is able to interact with the fibroblast cell culture (as detailed in Figure 8.2). To help align this process, the

fibroblasts are seeded on a glass slide, which is locked into place by the cell culture platform. For reference, the silicon lance array is a microfabricated-etched array of 4 million lances, measuring 10 μm in length and spaced in a grid pattern every 10 μm. [23] describes the fabrication process required for the silicon lance array construction.

8.2.2 Lance Array Nanoinjection Process

LAN occurs in a series of three steps shown in Figure 8.2. These steps include:

Step 1: Staging

Step 1 involves staging of the silicon lance array in the solution containing the cell culture. For electrically stimulated samples, cell cultures experience extracellular current control exposure of either 3.0 mA or 4.5 mA for 20 seconds. For treatment samples that have the CRISPR-Cas9 plasmid added, this step facilitates the attachment of the negatively charged DNA onto the silicon lance structures in preparation for physical injection of target cell membranes.

Step 2: Injection

Step 2 consists of the lance arrays being lowered towards the cell culture until the lances have penetrated the cell membranes of the fibroblasts and contacted the glass slide substrate to which the fibroblasts are adhered. There is no electrical exposure at the time the lances penetrate the cell membrane. For samples that have CRISPR-Cas9 plasmid added, this step allows the DNA to cross the cell membrane.

Step 3: Electrical Delivery

Once the lance array is lowered into the cell cultures penetrating the cell membranes, all electrically treated samples were given an application of 10 square-wave pulses with an amplitude of 0 to -7V applied for 20 ms. Following the pulses, a 5 second period of -1.5V DC is applied and then the lance array is removed from the cell culture. For treatment samples that have CRISPR-Cas9 plasmid added, this step helps to release the DNA into the intracellular space of the fibroblasts.

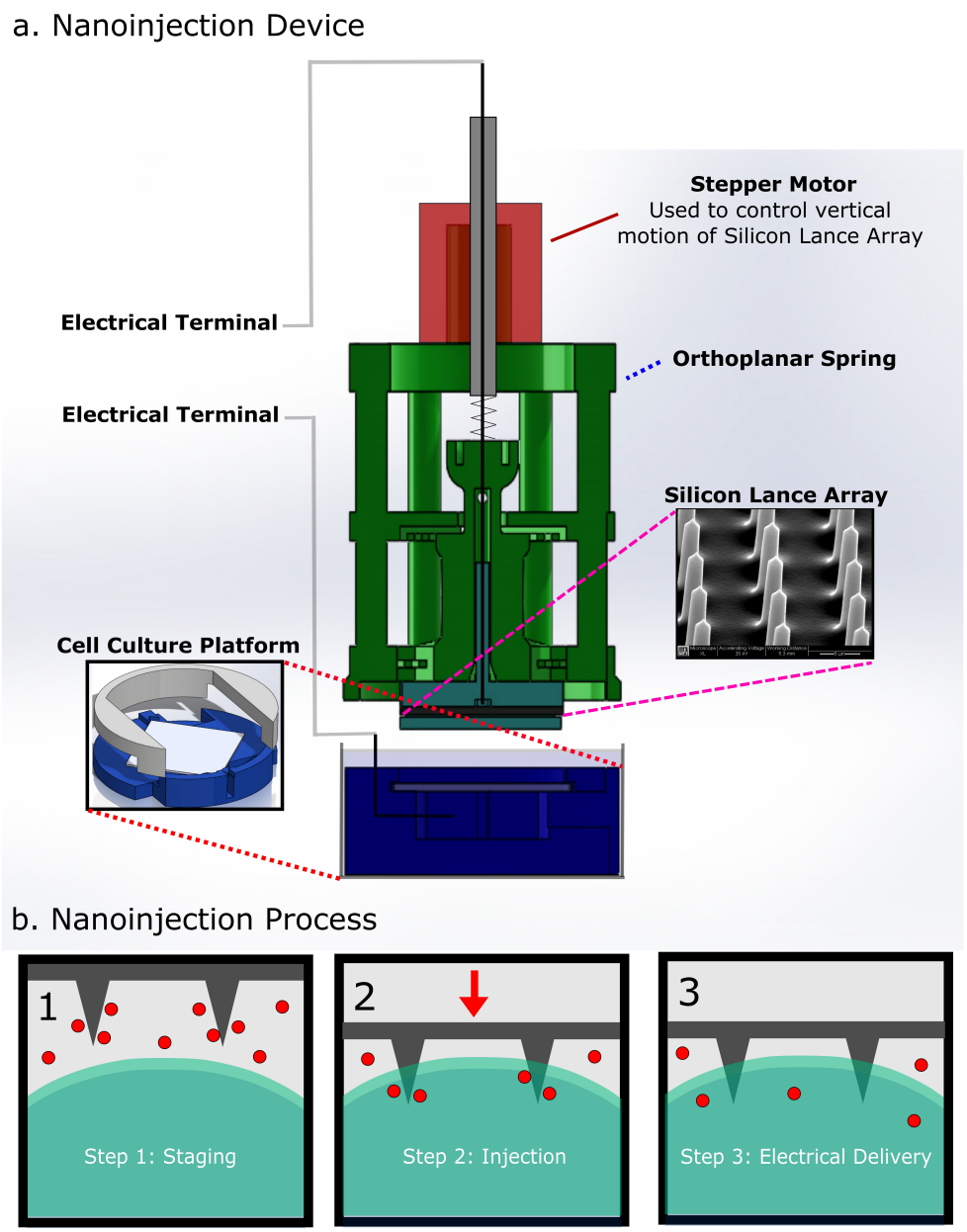

Figure 8.2: Illustrates Lance Array Nanoinjection Device (a) and Process (b). a) LAN device in a cross-sectional view consists of four major parts, which include: (top to bottom) stepper motor, orthoplanar spring, silicon lance array, and cell culture platform. Shown in isometric view on the lower left is a view of the cell culture platform, illustrating how the glass slide containing the fibroblast culture locks into place for injection. Shown in isometric view on the lower right is a SEM image of the lances on the silicon-etched array. Lances are spaced every 10 μm in a grid pattern, measuring 10 μm in length and 1-2.5 μm in diameter. b) Displays the LAN process in three major steps which include: Staging, Injection, and Electrical Delivery (refer to Lance Array Nanoinjection Process for details on activities that occur during each step)

8.2.3 Biologic Testing

Primary neonatal fibroblasts BJ ATTC CRL-2522 were prepared for injection by being plated on glass slides at 37C and 5% carbon dioxide in Dulbeccos Modified Eagles Medium (DMEM, Gibco) containing 10% Fetal Bovine Serum (FBS, Denville Scientific) and penicillin/streptomyocin 24 hrs. prior to injection. Because it was anticipated that the fibroblasts would proliferate following treatment, cells were plated with a cell confluency or cell density of 50% to 60% across a 1 cm diameter area in order to provide space for cell division to occur.

Following the 24 hr. incubation in growth media, the cell culture plates were removed from the incubator. Cell cultures were visualized under a light microscope to ensure consistency in cell confluency and then had growth media removed and replaced with 2 mL of phosphate buffered solution (PBS, Gibco) in each well. Sample wells that were treated with DNA received 2 μg of CRISPR-Cas9 transcriptional activation plasmid mixture (per manufacturer protocol; Santa Cruz Biotechnology Inc., sc-400187). This DNA mixture contained information to encode for a deactivated Cas9 nuclease fused to a VP64 domain (used to activate transcription) and a gRNA sequence for targeting the PDGFR- gene.

The following describe the different controls and treatments used for experimentation:

- **Non-Treated Control (NTC):** Received no injection, no electrical exposure, and no DNA.
- **Lance Only, Injected 1 Time (LO,x1):** Samples were injected one time without electrical exposure and no DNA.
- **Lance Only, Injected 2 Times (LO,x2):** Samples were injected twice, with a one hour rest period between injections. Both injection events were done without electrical exposure and no DNA.
- **Background Control, 3.0 mA, Injected 1 Time (BC3,x1):** Samples were injected one time with electrical exposure and no DNA. Specifically, these samples received 3.0 mA during Step 1 of the injection process (refer to Figure 8.2).
- **Background Control, 3.0 mA, Injected 2 Times (BC3,x2):** Samples were injected twice, with a one hour rest period between injections. Both injection events were done with electri-

cal exposure and no DNA. Specifically, these samples received 3.0 mA during Step 1 of the injection process (refer to Figure 8.2)

- **Background Control, 4.5 mA, Injected 1 Time (BC4.5,x1):** Samples were injected one time with electrical exposure and no DNA. Specifically, these samples received 4.5 mA during Step 1 of the injection process (refer to Figure 8.2).

- **Background Control LAN, 4.5 mA, Injected 2 Times (BC4.5,x2):** Samples were injected twice, with a one hour rest period between injections. Both injection events were done with electrical exposure and no DNA. Specifically, these samples received 4.5 mA during Step 1 of the injection process (refer to Figure 8.2).

- **Diffusion Treatment, Injected 2 Times (DT,x2):** Samples were injected twice with 2 μg of CRISPR-DNA mixture in each sample, with a one hour rest period between injections. Both injection events were done without electrical exposure.

- **LAN Treatment, 3.0 mA, Injected 2 Times (LAN 3.0,x2):** Samples were injected twice with 2 μg of CRISPR-DNA mixture in each sample, with a one hour rest period between injections. Both injection events were done with electrical exposure. Specifically, these samples received 3.0 mA during Step 1 of the injection process (refer to Figure 8.2).

- **LAN Treatment, 4.5 mA, Injected 2 Times (LAN 4.5,x2):** Samples were injected twice with 2 μg of CRISPR-DNA mixture in each sample, with a one hour rest period between injections. Both injection events were done with electrical exposure. Specifically, these samples received 4.5 mA during Step 1 of the injection process (refer to Figure 8.2).

8.2.4 Flow Cytometry Preparation

Prior to running flow cytometry for test samples, calibration of FITC as a marker and the baseline activity of native PDGFR-β was performed. For FITC calibration, a FITC-CD90 conjugated antibody (BioLegend, 328107) was applied to the fibroblasts and flowed, matching expression levels previously recorded for fibroblasts [286, 287]. For PDGFR-β baseline measurement of pre-treated cells, cells were labelled with a FITC-PDGFR-β conjugated antibody (Santa Cruz

Biotechnology Inc., sc-19995). Results showed PDGFR-β levels in living cells to be $<1\%$ prior to testing, which indicated that increases due to treatment could be measured.

All samples were returned to the incubator for 48 hrs. post-injection before preparing the samples for flow cytometry (per CRISPR Activation Plasmid Transfection Protocol, Santa Cruz Biotechnology Inc.). After that time, samples were removed from the incubator and cell cultures were scraped from the glass slides. Each well's contents were then transferred to a FACS tube and centrifuged at 2000 rpm for 10 min. Samples were then decanted and rinsed with 1 mL of PBS and centrifuged again at 2000 rpm for 5 minutes. Samples were decanted again and then given 100 μL of ice cooled PBS and 20 μL of FITC-PDFGR-β conjugated label (Santa Cruz Biotechnology Inc., sc-19995). After incubating on ice for 12-15 minutes, samples were then rinsed in 2 mL of PBS and centrifuged at 2000 rpm for 5 min. Samples were decanted again, re-suspended in 250 μL of ice cooled PBS and 40 μL of propidium iodide (PI, Sigma Aldrich). PI was added to all samples as a cell viability stain because it is impermeable to living cells membranes.

8.2.5 Flow Cytometry and Statistical Analysis

Characterization of the samples was performed using flow cytometry (Attune Acoustic Focusing Flow Cytometer, Life Technologies). For each sample well, 20,000 events were captured. Post-flow analysis was conducted using Attune Cytometric 2.1 software (Applied Biosystems, Life Technologies). Gating of the data occurred to two steps. First, the samples were evaluated for cell viability using gating for PI signals. Second, living cells were then gated for the relative FITC-PDGFR-β signal, thus establishing the relative level of living, PDGFR-β positive cells in each sample.

Once primary level data was generated for each sample, data was statistically analyzed in JMP by first screening for the presence of statistical significance using ANOVA testing followed by further testing using student t-tests to determine relative significance between sample types (α = 0.05).

Table 8.1: P-values for sample comparison of the Number of Living Cells

Comparison	NTC	LO,x1	LO,x2	BC3,x1	BC3,x2	BC4.5,x1
LO,x1	0.2258	–	–	–	–	–
BC3,x1	0.2416	0.0176	–	–	–	–
BC4.5,x1	0.0043	<0.0001	0.0778	–	–	–
LO,x2	0.0011	<0.0001	0.0269	0.6291	–	–
BC3,x2	0.0246	0.0009	0.2236	0.6898	0.4032	–
BC4.5,x2	0.0013	<0.0001	0.0250	0.5199	0.8451	0.3351

8.3 Results

In an effort to compartmentalize the effects of LAN with and without the PDGFR- CRISPR-Cas9 plasmid, the Results and Discussion sections will be divided into two sub-sections. The Electro-Mechanical effects of LAN will examine the controls and treatment samples that had no plasmid added. Treatment samples that had the PDGFR-β CRISPR-Cas9 plasmid added will be examined in a second group, where all samples injected twice (with or without DNA) will be examined to show the difference between those samples given the CRISPR-Cas9 plasmid.

8.3.1 Electro-Mechanical Effects

Figure 8.3 shows box plot results for the number of Living Cells and the Number of Living/PDGFR-β Cells for the seven types that did not receive DNA during injection. Detailed in Table 8.1 and Table 8.2 are the p-values for the student t-test comparisons of the different samples within this group and shown in Table 8.5 is a statistical summary for all samples. Of particular note, samples that were injected twice had a significantly higher number of Living Fibroblasts and Living/PDGFR-β Fibroblasts compared to NTC. Statistical comparison between one and two times injected samples for analogously treated sample types also have significant differences (i.e. LO,x1 vs LO,x2 and BC3,x1 vs BC,x2), except for the BC4.5,x1 vs BC4.5,x2 comparison. This trend is further illustrated in Table 8.5.

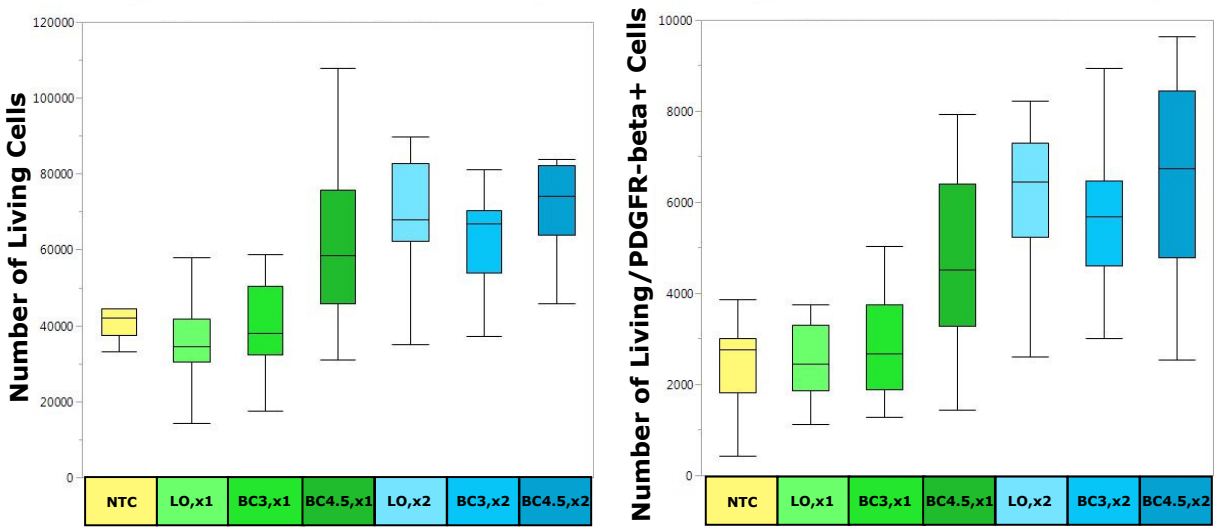

Figure 8.3: Shows box plot results for the Number of Living Cells (left) and the Number of Living/PDGFR-β+ Cells (right), with outliers removed. For convenience, see Table 1 to see statistically significant relationships between the different sample types for Electro-mechanical experimentation

Table 8.2: P-values for sample comparison of the Number of Living/PDGFR-β+ cells

Comparison	NTC	LO,x1	LO,x2	BC3,x1	BC3,x2	BC4.5,x1
LO,x1	0.3927	–	–	–	–	–
BC3,x1	0.1001	0.4518	–	–	–	–
BC4.5,x1	0.0003	0.0560	0.0338	–	–	–
LO,x2	<0.0001	0.0002	0.0014	0.2538	–	–
BC3,x2	0.0002	0.0036	0.0203	0.6956	0.5101	–
BC4.5,x2	<0.0001	<0.0001	0.0006	0.1236	0.6287	0.2861

8.3.2 CRISPR-Cas9 Effects

Figure 8.4 shows box plot results for the number of Living Cells and the Number of Living/PDGFR-β Cells for the comparisons of the NTC relative to the twice injected sample types. Shown in Table 8.3 and Table 8.4 are the p-values for the student t-test comparisons of the different samples within this group. Table 3 provides a statistical summary for these samples types. Seen in these comparisons is that the three DNA injected samples (i.e. DC,x2; LAN3,x2; and LAN4.5,x2) were significantly higher than the NTC for both the number of Living Cells and the number of

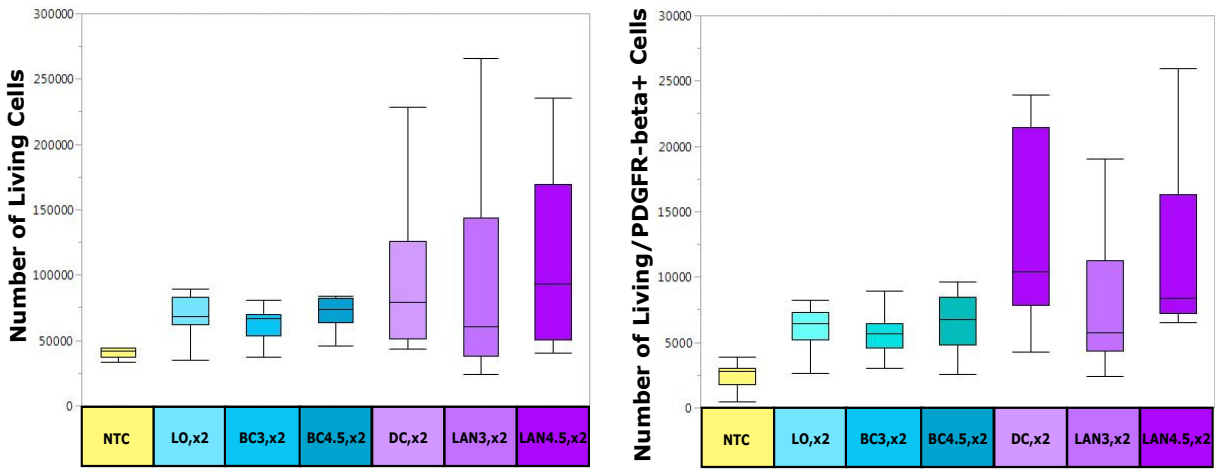

Figure 8.4: Shows box plot results for the Number of Living Cells (left) and the Number of Living/PDGFR-β+ Cells (right), with outliers removed. For convenience, see Table 2 to see statistically significant relationships between the different sample types for CRISPR-Cas9 experimentation

Table 8.3: P-values for comparison of the Number of Living Cells

Comparison	NTC	LO,x2	BC3,x2	BC4.5,x2	DC,x2	LAN3,x2
DC,x2	0.0233	0.1819	0.1383	0.2361	–	–
LAN3,x2	0.0034	0.0434	0.0343	0.0683	0.4971	–
LAN4.5,x2	0.0002	0.0040	0.0035	0.0085	0.1221	0.3827

Living/PDGFR-β Cells, with the exception of the number of Living/PDGFR-β Cells in the NTC vs. DC,x2 comparison.

Comparison of the DNA treated samples to the non-DNA treated samples reveal that there is only a consistently significant difference between LAN4.5,x2 and the non-DNA treated samples (i.e. LO,x2; BC3,x2; and BC4.5,x2) for both the number of Living Cells and the number of Living/PDGFR-β Cells. There is an increase in the mean fold cell counts in both categories for all DNA treated samples compared to non-DNA treated samples.

As a group, LAN4.5,x2 performed the best in both measures but was not significantly different from other DNA treated samples (i.e. DC,x2 or LAN3,x2). Table 8.5 highlights the fold increases among the DNA sample types, indicating large mean fold increases over the NTC in the Number of Living/PDGFR-β with LAN4.5,x2 having an increase of 15.29-fold.

Table 8.4: P-Values for sample comparison of the Number of Living/PDGFR-β+ cells

Comparison	NTC	LO,x2	BC3,x2	BC4.5,x2	DC,x2	LAN3,x2
DC,x2	0.1694	0.2900	0.3035	0.3419	–	–
LAN3,x2	0.0338	0.0686	0.0821	0.0967	0.4515	–
LAN4.5,x2	0.0057	0.0134	0.0189	0.0232	0.1604	0.5124

Table 8.5: Statistical summary for all sample types in PDGFR-β Experimentation

Sample Type	Sample Size (n)	Mean Living Cell Counts	Fold Increase in Living Cell Counts over NTC	Mean Living / PDGFR-β Cell Counts	Fold Increase in Living / PDGFR-β Cell Counts over NTC
NTC	19	44,730	–	2311	–
LO,x1	18	35,580	0.80	3023	1.31
LO,x2	20	69,243	1.55	6213	2.69
BC3,x1	21	53,245	1.19	3635	1.57
BC3,x2	15	62,696	1.40	5643	2.44
BC4.5,x1	21	65,786	1.47	5308	2.30
BC4.5,x2	15	70,772	1.58	6631	2.87
DC,x2	18	102,666	2.30	18,532	8.02
LAN3,x2	18	120,059	2.68	27,514	11.91
LAN4.5,x2	18	142,435	3.18	35,327	15.29

8.4 Discussion

8.4.1 Electro-Mechanical Stimulation

To the authors' knowledge, the effect of electro-mechanical stimulation (EMS) of mammalian cells through direct interaction with the intracellular space of the target cell has not been previously observed, particularly in the context of its effects on PDGFR-β and cell proliferation of fibroblasts. Other researchers have investigated the effects of mixed mechanical conditions that can stimulate cellular gene expression and/or biochemical behavior. For instance, Hu et al. used direct magneto-mechanical actuation of PDGFR-β surface receptors on human mesenchymal stem cells using magnetic nano-particles to demonstrate that higher osteogenic gene marker expression could occur after 7 and 12 days of stimulation [222]. Similar concepts of actuating mechano-sensitive surface receptors on mammalian cells have been reported in other works as well [288–290]. In addition to magneto-mechanical stimulation, researchers have also reported results of indirect or external stimulation using either high or low electric fields to generate biochemical response [291, 292]. Nevertheless, no previous work has shown that with brief intracellular

electro-mechanical stimulation, such as that experienced during LAN, that increases in PDGFR- expression and cell count can be observed.

An explanation of the mechanism(s) generating both the receptor and proliferation response in the fibroblasts following LAN induced EMS are not understood. Bonazzi et al. [293] reviews much of what is currently known about the biophysics of galvanotactic effects on mammalian cells in response to external electric fields. In his work, it is suggested that the general thought is that electric fields cause an intracellular response that involves a complex signal transduction cascade that eventually leads to the reorganization of the cytoskeleton and directed cell growth. Furthermore, Bonazzi et al. hypothesized that by virtue of gradients in the transmembrane potential values in the target cells, imbalances in ion fluxes via voltage gated ion channels may be disrupted during electric field exposure and thereby signal up-regulation of biologic intermediates, citing other researchers who have observed this behavior with electric field exposure on GTPase cdc42p, Rho/Rac pathway, integrin signaling, and phophatidylinositol signaling pathways [294–298].

In terms of LAN, these previous works involving galvanotactic stimulation and its effect on mammalian cells provide only a partial explanation of what is observed in this work. For LO,x1 and LO,x2 samples types, electrical stimulation is not used, meaning the increases in both the PDGFR-β and the cell count are only due to the mechanical response of lancing with the lance array. Noted in Table 8.5 is that the fold increase for the number of Living/PDGFR-β+ cells for the LO,x2 sample group is between the BC3,x2 and BC4.5,x2 groups. Also, in Table 8.1 and Table 8.2 it can be seen that there is no statistical difference between any of the twice injected, non-DNA treated sample types. Examination of Table 8.1 and Table 8.2 in regards to the same comparisons for the single injected samples reveal that BC4.5,x1 is significantly higher than BC3,x1 and nearly significantly higher than LO,x1.

How do these LAN results relate to the galvanotactic hypothesis? It is possible that the physical lancing of the target cell membranes during LAN mimics partially the external electrical field effects observed in works cited by Bonazzi et al. During the transient membrane openings following LAN, it is probable that ion imbalances are created across the membrane. As ions travel across the membrane to re-establish the transmembrane potential, it is possible that these ions could trigger intracellular cascades related to growth and receptor production a mechanism similar to the one Bonazzi et al. discuses for transmembrane ion disturbances observed with external

electric fields exposure. Furthermore, for samples that use electrical application, it is possible that past a certain threshold (i.e. like that used for 4.5 mA samples) in LAN samples, that using electrical stimulation in combination with the physical lancing action can increase this intracellular molecular cascade activity and thereby increase PDGFR- and cell counts. This hypothesis, while suggested by other's findings, requires further investigation.

8.4.2 CRISPR-Cas9 Effects

One of the key elements of this experiment is that it shows that EMS by itself can cause increases in cell growth and the number of living/PDGFR-β+ cells. The CRISPR-Cas9 portion of the experimentation, in addition to these EMS findings, illustrates an improved biologic response mainly for LAN4.5,x2 sample types. The increased efficacy in regards to the higher EMS conditions relative to the LAN4.5,x2 have been discussed above.

As far as the CRISPR-Cas9 effects in regards to skin targets, experimentation of this kind has not yet been conducted and represents a key finding for wound healing applications. Basic science related to CRISPR-Cas9 is rapidly expanding both in terms of functionality of the Cas9 component [97, 133, 299] and the gRNA (guide RNA) sequences that facilitate the action of the Cas9 [209]. Nevertheless, the application of CRISPR-Cas9 in the realm of wound healing is still in its infancy.

The implications of both the EMS effect unique to LAN and the enhanced effect noted with CRISPR-Cas9 in these primary neonatal fibroblasts is significant in terms of wound healing therapy for four reasons. First, the combination of LAN with CRISPR-Cas9 shown in this work has achieved high modification rates, reaching between 8 and 15 fold increases in the number of living/PDGFR-β+ cells. As noted earlier, many non-viral transfection technologies have historically struggled to obtain rates this high [178, 245].

Second, LAN in conjunction with CRISPR-Cas9 modification of a surface receptor is a relatively safe method of cutaneous modification. The use of a transcriptional activating CRISPR-Cas9 plasmid is transient, meaning specifically that there are no structural changes to the host genome. Furthermore, by modifying the receptor, a level of cellular control can occur by regulating the amount of PDGF ligand available to bind to the receptor.

Third, PDGFR-β is an essential element for wound healing and without it significant wound healing delays occur [285]. As noted earlier, chronic wounds have excessive protease action, which degrades the extracellular portion of the PDGFR-β making the receptor inoperable. As a result, lack of PDGFR-β signaling results in dramatic reductions in recruitment of immune and stromal cells to the wound, decreased proliferation of resident wound bed cells, and functional inactivity of fibroblasts and pericytes. Thus by improving PDGFR-β presence, treated wounds can initiate healing sooner.

Lastly, these findings are particularly useful because it demonstrates that molecular effectors (i.e. DNA, RNA, protein, etc.) are not necessarily required in order to alter cellular receptor expression, which could be useful for current wound healing applications. For instance, commonly used artificial skin grafts, which consist of primary neonatal fibroblasts seeded on a matrix, could be pre-treated with LAN induced EMS prior to placement into chronic wounds. Theoretically, these artificial skin grafts could experience marked increases in fibroblast growth and PDGFR-β expression, thereby decreasing healing times – a critical element to preventing wound complications.

CHAPTER 9. SUMMARY OF FINDINGS AND POTENTIAL FUTURE WORK

Several key discoveries have been discussed in this research in regards to Lance Array Nanoinjection (LAN) and its ability to transfect both culture cells and primary human cells. Categorically, these findings have been segregated into three main objectives.

9.1 Key Findings Review

The first objective focussed on several enironomental variables related to the LAN process, highlighting the impact that they make on cell transfection rates and survival post-injection. The following provides a brief summary of key findings related to the investigation of environmental factors impacting LAN outcomes.

- **Chapter 2: Saline Solution Effects on Propidium Iodide Uptake** Experimentation with three different saline solution types revealed that PBS with potassium performs slightly better than HBSS and PBS without potassium in regards to PI uptake but makes no impact on cell survival.

- **Chapter 3: The Effects of Lance Geometry and Carbon Coating of Silicon Lances** Experimentation with three different lance geometries demonstrated that Flat, Narrow shaped lances have a slightly better cell viability rate than Flat, Wide and Pointed, but Pointed lances had the best PI uptake. Carbon coating of lances made little difference on cell viability or PI uptake.

- **Chapter 4: Transient Low Temperature** This work demonstrated that transient low temperatures around 3C were sufficient to increase PI uptake into HeLa cells 8.3 times higher than controls and 173% higher than samples at 23C (given the same injection parameter). Furthermore, between 3 and 6 minutes post-injection, many of the induced pores close – a behavior that was observed at different magnitudes for all samples regardless of temperature.

- **Chapter 5: Injection Speed and Serial Injection** Investigation with five different injection speeds showed that slower injection speeds with HeLa cells (0.08 mm/sec) allow nearly all cells to remain adherent, thus making serial injections (multiple injections into the same cell culture) possible. These results allowed further exploration into slow, serial injection experiments with both HeLa cells and primary neonatal fibroblast using PI as an indicator. Results showed an injection dose response, meaning more PI delivery with more injections.

The second objective focussed on genetic modification of cultured HeLa cells using an indicator marker. For this work, an isogenic GFP+ HeLa cell line was created that constitutively expressed the GFP protein. In order to measure the degree with which LAN could successfully genetically modify these cells, a CRISPR-Cas9 plasmid was created which targeted just up-stream of the promoter for the GFP gene. Using LAN to deliver the plasmid containing information for both the gRNA sequence required to target the GFP promoter region and the Cas9 which could induce a non-homologous end joining (NHEJ) knock-out when guided with the gRNA, it was observed that high levels of GFP negative cells could be generated (median GFP knock-out rates of 93.22% in samples injected three times). Similar to earlier work as well, it was observed in this work that the degree of GFP knock-out correlated to the number of times the samples were injected.

The third objective investigated the ability of LAN to genetically modify primary, neonatal fibroblasts, a historically difficult cell line to modify, using a clinically useful target – PDGFR-β. Similar to the GFP-Knock-Out project, this work also used a CRISPR-Cas9 plasmid system. The main difference with this system and the knock-out system was that this CRISPR-Cas9 construct was designed to activate transient up-regulation of an existing gene instead of knock-out of an engineered gene. Results showed that levels higher than 15-fold could be observed 48 hrs. post-treatment using the combination of both the CRISPR-Cas9 system and LAN.

9.2 Research Impact

The discoveries made during this research have been significant. LAN represents a viable transfection technology that satisfies many of the key criteria required for robust transfection which include: high transfection efficiency, high cell survival rates, effective in clinically useful cell lines,

flexible pay load capacity, and no insertional mutagenesis. Prior to this work, to the authors' knowledge, such an accomplishment by a viral transduction or non-viral transfection system has not yet been achieved.

9.3 Future Work

The success with the latter portions of the research in regards to CRISPR-Cas9 and LAN are particularly exciting. Chronic wounds are discussed and demonstrated to be a viable direction for LAN clinical application – a direction that would require additional investigation for clinical trial. However, because of the broad range of capabilities associated with CRISPR-Cas9, using CRISPR-Cas9 in conjunction with LAN make the list of potential applications compelling and the number of potential future directions for LAN broad.

Within the context of current research areas, there are two logical directions for further research investigation regarding LAN (in addition to what has been discussed with chronic wounds). The first direction would be extending LAN to be able to work with non-adherent induced pluripotent stem cells (iPSCs). iPSCs represent an exciting frontier in being able to re-program host-derived, fully-differentiated cells into stem cells [75, 76, 300, 301]. Once in stem cell state, these cells can be used to remedy a large number of disease states, particularly if coupled with CRISPR-Cas9 [92, 180]. Leveraging the ability of LAN to either initially deliver genes to initiate the transformative process to the stem cell state or facilitating modification of these stem cells in en masse could be tremendously useful.

A second logical direction for future LAN research involves combining the scope of the first generation single nanoinjection system with the advances made in the second generation with LAN. Specifically this means using the Lance Array Nanoinjection system presented in this work, in conjunction with CRISPR-Cas9, to create a high-through-put transgenic organism generation system. Transgenic animals are difficult still to create, particularly with the need to visualize the pro-nuclei during micro-injection. Nanoinjection does not have that requirement [27]. Moreover, being able to generate large numbers of modified cells quickly, can facilitate basic research investigation into critical mechanisms related to the genome for both animals and plants [279, 302–306].

REFERENCES

[1] Shimamura, M., Nakagami, H., Koriyama, H., and Morishita, R., 2013. "Gene therapy and cell-based therapies for therapeutic angiogenesis in peripheral artery disease." *BioMed Research International,* **2013**, pp. 1–8. 1, 57

[2] Griesenbach, U., Pytel, K. M., and Alton, E. W., 2015. "Cystic Fibrosis gene therapy in the UK and elsewhere." *Human Gene Therapy,* **26**(5), May, pp. 266–275. 1, 57

[3] Byrne, B. J., Falk, D. J., Clement, N., and Mah, C. S., 2012. "Gene therapy approaches for lysosomal storage disease: Next-generation treatment." *Human Gene Therapy,* **23**(8), Aug, pp. 808–815. 1, 57

[4] Yla-Herttuala, S., 2012. "Endgame: Glybera finally recommended for approval as the first gene therapy drug in the european union." *Molecular Therapy,* **20**(10), Oct, pp. 1831–1832. 1, 38, 57

[5] Sahel, J.-A., and Roska, B., 2013. "Gene therapy for blindness." *Annual Review of Neuroscience,* **36**(1), Jul, pp. 467–488. 1, 38, 57

[6] Bainbridge, J. W., Smith, A. J., Barker, S. S., Robbie, S., Henderson, R., Balaggan, K., Viswanathan, A., Holder, G. E., Stockman, A., Tyler, N., and et al., 2008. "Effect of gene therapy on visual function in Leber's Congenital Amaurosis." *N Engl J Med,* **358**(21), May, pp. 2231–2239. 1, 38, 57

[7] Hauswirth, W. W., Aleman, T. S., Kaushal, S., Cideciyan, A. V., Schwartz, S. B., Wang, L., Conlon, T. J., Boye, S. L., Flotte, T. R., Byrne, B. J., and et al., 2008. "Treatment of Leber Congenital Amaurosis due to RPE65 mutations by ocular subretinal injection of adeno-associated virus gene vector: Short-term results of a phase I trial." *Human Gene Therapy,* **19**(10), Oct, pp. 979–990. 1, 38, 57

[8] Jacobson, S. G., 2012. "Gene therapy for Leber Congenital Amaurosis caused by RPE65 mutations." *Arch Ophthalmol,* **130**(1), Jan, p. 9. 1, 38, 57

[9] Maguire, A. M., Simonelli, F., Pierce, E. A., Pugh, E. N., Mingozzi, F., Bennicelli, J., Banfi, S., Marshall, K. A., Testa, F., Surace, E. M., and et al., 2008. "Safety and efficacy of gene transfer for Leber's Congenital Amaurosis." *N Engl J Med,* **358**(21), May, pp. 2240–2248. 1, 38, 57

[10] High, K. H., Nathwani, A., Spencer, T., and Lillicrap, D., 2014. "Current status of haemophilia gene therapy." *Haemophilia,* **20**, Apr, pp. 43–49. 1, 38, 57

[11] Patel, N., Reiss, U., Davidoff, A. M., and Nathwani, A. C., 2014. "Progress towards gene therapy for haemophilia B." *Int J Hematol,* **99**(4), Feb, pp. 372–376. 1, 38, 57

[12] Kranias, E. G., and Hajjar, R. J., 2012. "Modulation of cardiac contractility by the Phopholamban/SERCA2a regulatome." *Circulation Research,* **110**(12), Jun, pp. 1646–1660. 1, 38, 57

[13] Sikkel, M. B., Hayward, C., MacLeod, K. T., Harding, S. E., and Lyon, A. R., 2013. "SERCA2a gene therapy in heart failure: an anti-arrhythmic positive inotrope." *Br J Pharmacol,* **171**(1), Dec, pp. 38–54. 1, 38, 57

[14] Jessup, M., Greenberg, B., Mancini, D., Cappola, T., Pauly, D. F., Jaski, B., Yaroshinsky, A., Zsebo, K. M., Dittrich, H., and Hajjar, R. J., 2011. "Calcium upregulation by percutaneous administration of gene therapy in cardiac disease (CUPID): A phase 2 trial of intracoronary gene therapy of sarcoplasmic reticulum Ca2+-ATPase in patients with advanced heart failure." *Circulation,* **124**(3), Jun, pp. 304–313. 1, 38, 57

[15] Zsebo, K., Yaroshinsky, A., Rudy, J. J., Wagner, K., Greenberg, B., Jessup, M., and Hajjar, R. J., 2013. "Long-term effects of AAV1/SERCA2a gene transfer in patients with severe heart failure: Analysis of recurrent cardiovascular events and mortality." *Circulation Research,* **114**(1), Sep, pp. 101–108. 1, 38, 57

[16] Kochenderfer, J. N., and Rosenberg, S. A., 2013. "Treating B-cell cancer with T cells expressing anti-CD19 chimeric antigen receptors." *Nature Reviews Clinical Oncology,* **10**(5), Apr, pp. 267–276. 1, 38, 57

[17] Simonato, M., Bennett, J., Boulis, N. M., Castro, M. G., Fink, D. J., Goins, W. F., Gray, S. J., Lowenstein, P. R., Vandenberghe, L. H., Wilson, T. J., and et al., 2013. "Progress in gene therapy for neurological disorders." *Nature Reviews Neurology,* **9**(5), Apr, pp. 277–291. 1, 38, 57

[18] Mellott, A. J., Forrest, M. L., and Detamore, M. S., 2012. "Physical non-viral gene delivery methods for tissue engineering." *Ann Biomed Eng,* **41**(3), Oct, pp. 446–468. 1, 57, 108

[19] Doherty, G. J., and McMahon, H. T., 2009. "Mechanisms of endocytosis." *Annual Review of Biochemistry,* **78**(1), Jun, pp. 857–902. 1, 57

[20] Khalil, I. A., Kogure, K., Akita, H., and Harashima, H., 2006. "Uptake pathways and subsequent intracellular trafficking in nonviral gene delivery." *Pharmacological Reviews,* **58:1**(1), Mar, pp. 32–45. 1, 57, 108

[21] Lukacs, G. L., Haggie, P., Seksek, O., Lechardeur, D., Freedman, N., and Verkman, A. S., 2000. "Size-dependent DNA mobility in cytoplasm and nucleus." *Journal of Biological Chemistry,* **275**(3), Jan, pp. 1625–1629. 1, 57, 108

[22] Wiethoff, C. M., and Middaugh, C. R., 2003. "Barriers to nonviral gene delivery." *J. Pharm. Sci.,* **92**(2), Jan, pp. 203–217. 1, 2, 57, 58, 78, 108

[23] Teichert, G. H., Burnett, S., and Jensen, B. D., 2013. "A microneedle array able to inject tens of thousands of cells simultaneously." *J. Micromech. Microeng.,* **23**(9), Aug, p. 095003. 2, 22, 24, 26, 42, 58, 60, 78, 81, 90, 110, 114

[24] Lindstrom, Z. K., Brewer, S. J., Ferguson, M. A., Burnett, S. H., and Jensen, B. D., 2014. "Injection of propidium iodide into HeLa cells using a silicon nanoinjection lance array." *J. Nanotechnol. Eng. Med.,* **5**(2), May, p. 021008. 2, 4, 5, 10, 22, 39, 41, 43, 58, 59, 72, 78, 90, 110

[25] Aten, Q. T., Jensen, B. D., Tamowski, S., Wilson, A. M., Howell, L. L., and Burnett, S. H., 2012. "Nanoinjection: pronuclear DNA delivery using a charged lance." *Transgenic Research,* **21**(6), Mar, pp. 1279–1290. 2, 4, 9, 22, 39, 58, 59, 78, 90, 110

[26] Aten, Q. T., Jensen, B. D., Burnett, S. H., and Howell, L. L., 2011. "Electrostatic accumulation and release of DNA using a micromachined lance." *Journal of Microelectromechanical Systems,* **20**(6), Dec, pp. 1449–1461. 2, 4, 9, 22, 39, 58, 78, 90, 110, 171

[27] Wilson, A. M., Aten, Q. T., Toone, N. C., Black, J. L., Jensen, B. D., Tamowski, S., Howell, L. L., and Burnett, S. H., 2013. "Transgene delivery via intracellular electroporetic nanoinjection." *Transgenic Research,* **22**(5), Oct, pp. 993–1002. 2, 4, 22, 58, 78, 90, 110, 128, 164

[28] Mellott, A. J., Forrest, M. L., and Detamore, M. S., 2012. "Physical non-viral gene delivery methods for tissue engineering." *Annals of Biomedical Engineering,* **41**(3), Oct, pp. 446–468. 2, 58, 59, 75, 78, 89, 92

[29] Ritter, T., Lehmann, M., and Volk, H., 2002. "Improvements in gene therapy: averting the immune response to adenoviral vectors." *BioDrugs,* **16:1**, pp. 3–10. 2, 3, 58, 75, 76, 77, 97, 112

[30] Matrai, J., Chuah, M., and VandenDriessche, T., 2010. "Recent advances in lentiviral vector development and applications." *Molecular Therapy,* **18:3**, pp. 477–490. 2, 3, 58, 75, 76, 77, 100

[31] Follenzi, A., Santambrogio, L., and Annoni, A., 2007. "Immune responses to lentiviral vectors." *Current Gene Therapy,* **7:5**, pp. 306–315. 2, 3, 58, 75, 76, 77, 100

[32] VandenDriessche, T., Thorrez, L., Naldini, L., Follenzi, A., Moons, L., Berneman, Z., Collen, D., and Chuah, M., 2002. "Lentiviral vectors containing the human immunodeficiency virus type-1 central polypurine tract can efficiently transduce nondividing hepatocytes and antigen-presenting cells in vivo." *Blood,* **100:3**, pp. 813–822. 2, 3, 58, 75, 76, 77, 100, 112

[33] Barsoum, J., 1995. *Animal Cell Electroporation and Electriofusion Protocols*. Humana Press. 2, 59

[34] Kozarsky, K. F., and Wilson, J. M., 1993. "Gene therapy: adenovirus vectors." *Current Opinion in Genetics & Development,* **3**, pp. 499–503. 3, 75, 76

[35] Deyle, D. R., and Russell, D. W., 2009. "Adeno-associated virus vector integration." *Current Opinion in Molecular Therapeutics,* **11:4**, pp. 442–447. 3, 75, 76, 77, 100

[36] Monahan, P., and Samulski, J., 2000. "Adeno-associated virus vectors for gene therapy: more pros than cons?." *Molecular Medicine Today,* **6**, pp. 433–440. 3, 75, 76

[37] Gardlik, R., Palffy, R., Hodosy, J., Lukacs, J., Turna, J., and P, C., 2005. "Vectors and delivery systems in gene therapy." *Medical Science Monitor,* **11:4**, pp. RA110–RA121. 3, 75, 76, 78, 97, 98, 100, 112

[38] Silman, N., and Fooks, A., 2000. "Biophysical targetting of adenovirus vectors for gene therapy." *Current Opinion in Molecular Therapeutics,* **2:5**, pp. 524–531. 3, 75, 76, 95, 97

[39] Tenenbaum, L., Lehtonen, E., and Monahan, P., 2003. "Evaluation of rrisk related to the use of adeno-associated virus-based vectors." *Current Gene Therapy,* **3:6**, pp. 545–565. 3, 75, 76

[40] Miyoshi, H., Takahashi, M., Gage, F., and Verma, I., 1997. "Stable and efficient gene transfer into the retina using an HIV-based lentiviral vector." *Proc Natl Acad Sci USA,* **94:19**, pp. 10319–10323. 3, 75, 76

[41] Greenberg, K., Lee, E., Schaffer, D., and Flannery, J., 2006. "Gene delivery to the retina using lentiviral vectors." *Adv Exp Med Biol,* **572**, pp. 255–266. 3, 75, 76

[42] Lundberg, C., Bjorklund, T., Carlsson, T., Jakobsson, J., Hantraye, P., Deglon, N., and Kirik, D., 2008. "Applications of lentiviral vectors for biology and gene therapy of neurological disorders." *Current Gene Therapy,* **8:6**, pp. 461–473. 3, 75, 76

[43] Bessis, N., GarciaCozar, F. J., and Boissier, M. C., 2004. "Immune responses to gene therapy vectors: influence on vector function and effector mechanisms." *Gene Therapy,* **11 Suppl 1**, pp. S10–S17. 3, 75, 76, 100

[44] Hacein-Bey-Abina, S., 2003. "LMO2-associated clonal T cell proliferation in two patients after gene therapy for SCID-X1." *Science,* **302**, pp. 415–419. 3, 75, 76

[45] Verma, I. M., and Somia, N., 1997. "Gene therapy – promises, problems and prospects." *Nature,* **389:6648**, pp. 239–242. 3, 75, 76

[46] Hacein-Bey-Abina, S., Garrigue, A., Wang, G. P., Soulier, J., Lim, A., Morillon, E., Clappier, E., Caccavelli, L., Delabesse, E., Beldjord, K., Asnafi, V., MacIntyre, E., Dal Cortivo, L., Radford, I., Brousse, N., Sigaux, F., Moshous, D., Hauer, J., Borkhardt, A., Belohradsky, B. H., Wintergerst, U., Velez, M. C., Leiva, L., Sorensen, R., Wulffraat, N., Blanche, S., Bushman, F. D., Fischer, A., and Cavazzana-Calvo, M., 2008. "Insertional oncogenesis in 4 patients after retrovirus-mediated gene therapy of SCID-X1." *Journal of Clinical Investigation,* **118:9**, pp. 3132–3142. 3, 75, 76, 100

[47] Aten, Q. T., 2011. "Devices and methods for electro-physical transport of DNA across cell membranes." PhD thesis, Brigham Young University. 4

[48] Teichert, G. H., 2012. "Design and testing of a biological microelectromechanical system for the injection of thousands of cells simultaneously." Master's thesis, Brigham Young University. 4

[49] David, R. A., 2011. "Modeling and testing of DNA motion for nanoinjection." PhD thesis, Brigham Young University. 4

[50] David, R. A., Jensen, B. D., Black, J. L., Burnett, S. H., and Howell, L. L., 2012. "Study of design parameters affecting the motion of DNA for nanoinjection." *J. Micromech. Microeng.,* **22**(5), Mar, pp. 1–11. 4, 40, 92

[51] Toone, N. C., 2012. "Mathematical model and experimental exploration of the nanoinjector lance array." Master's thesis, Brigham Young University. 4

[52] Toone, N. C., and Jensen, B., 2012. "Effects of voltage and distance on stand-alon lance electrodes during repulsion." *Proceedings of the ASME 2012 International Design Engineering Technical Conferences & Computers and Information in Engineering Conference,* **DETC2012-70473**, pp. 33–40. 4

[53] Lindstrom, Z. K., 2014. "Design and experimental testing of nanoinjection protocols for delivering molecules into HeLa cells with a bio-MEMS device." Master's thesis, Brigham Young University. 5

[54] Sessions, J., Hanks, B., Lewis, T., Lindstrom, D., Jensen, B., and Burnett, S., 2014. "Saline solution effects on propidium iodide uptake in nanoinjected HeLa cells." *Proceedings of the ASME 2014 International Design Engineering Technical Conferences & Computers and Information in Engineering Conference,* **DETC2014-35431**, pp. 1–9. 8, 22

[55] Evans, C. H., Ghivizzani, S. C., and Robbins, P. D., 2008. "Orthopedic gene therapy in 2008." *Molecular Therapy,* **17**(2), Dec, pp. 231–244. 8

[56] Chang, P.-C., Seol, Y.-J., Cirelli, J. A., Pellegrini, G., Jin, Q., Franco, L. M., Goldstein, S. A., Chandler, L. A., Sosnowski, B., and Giannobile, W. V., 2009. "PDGF-B gene therapy accelerates bone engineering and oral implant osseointegration." *Gene Therapy,* **17**(1), Sep, pp. 95–104. 8, 21

[57] Zhang, L., Jia, T.-H., Chong, A. C. M., Bai, L., Yu, H., Gong, W., Wooley, P. H., and Yang, S.-Y., 2010. "Cell-based osteoprotegerin therapy for debris-induced aseptic prosthetic loosening on a murine model." *Gene Therapy,* **17**(10), Apr, pp. 1262–1269. 8

[58] Kimelman-Bleich, N., Pelled, G., Zilberman, Y., Kallai, I., Mizrahi, O., Tawackoli, W., Gazit, Z., and Gazit, D., 2010. "Targeted gene-and-host progenitor cell therapy for nonunion bone fracture repair." *Molecular Therapy,* **19**(1), Sep, pp. 53–59. 8

[59] Pelled, G., Ben-Arav, A., Hock, C., Reynolds, D. G., Yazici, C., Zilberman, Y., Gazit, Z., Awad, H., Gazit, D., and Schwarz, E. M., 2010. "Direct gene therapy for bone regeneration: Gene delivery, animal models, and outcome measures." *Tissue Engineering Part B: Reviews,* **16**(1), Feb, pp. 13–20. 8, 9

[60] Wulsten, D., Glatt, V., Ellinghaus, A., Schmidt-Bleek, K., Petersen, A., Schell, H., Lienau, J., Sebald, W., Ploger, F., Seemann, P., and Duda, G., 2011. "Time kinetics of bone defect healing in response to BMP-2 and GDF-5 characterised by in vivo biomechanics." *European Cells and Materials,* **21**, pp. 177–192. 8

[61] Ali A. Sovari, S. C. D. J., 2012. "Gene and cell therapies for the failing heart to prevent sudden arrhythmic death." *Minerva Cardioangiologica,* **60:4**, pp. 363–373. 8

[62] de Munick, E. D., 2009. "Gene and cell therapy for heart failure." *Antioxidants & Redox Signaling,* **11:8**, pp. 2025–2042. 8

[63] Jazwa, A., Kucharzewska, P., Leja, J., Zagorska, A., Sierpniowska, A., Stepniewski, J., Kozakowska, M., Taha, H., Ochiya, T., Derlacz, R., and et al., 2010. "Combined vascular endothelial growth factor-a and fibroblast growth factor 4 gene transfer improves wound healing in diabetic mice." *Genetic Vaccines and Therapy,* **8**(1), p. 6. 8

[64] Karolina Hajdukiewicz, Anna Stachurska, R. P. M. M., 2013. "Study of angiogenic gene ointments designed for skin neovascularization." *Developmental Period Medicine,* **18**, pp. 31–36. 8

[65] Ko, J., Jun, H., Chung, H., Yoon, C., Kim, T., Kwon, M., Lee, S., Jung, S., Kim, M., and Park, J. H., 2011. "Comparison of egf with vegf non-viral gene therapy for cutaneous wound healing of streptozotocin diabetic mice." *Diabetes & Metabolism Journal,* **35**(3), p. 226. 8

[66] Saaristo, A., Tammela, T., Farkkila, A., Karkkainen, M., Suominen, E., Yla-Herttuala, S., and Alitalo, K., 2006. "Vascular endothelial growth factor-c accelerates diabetic wound healing." *The American Journal of Pathology,* **169**(3), Sep, pp. 1080–1087. 8

[67] Liu, L., Marti, G. P., Wei, X., Zhang, X., Zhang, H., Liu, Y. V., Nastai, M., Semenza, G. L., and Harmon, J. W., 2008. "Age-dependent impairment of hif-1alpha expression in diabetic mice: Correction with electroporation-facilitated gene therapy increases wound healing, angiogenesis, and circulating angiogenic cells." *Journal of Cellular Physiology,* **217**(2), Nov, pp. 319–327. 8, 101, 104, 112

[68] Gupta, R., Tongers, J., and Losordo, D. W., 2009. "Human studies of angiogenic gene therapy." *Circulation Research,* **105**(8), Oct, pp. 724–736. 8

[69] Hirt-Burri, N., Ramelet, A.-A., Raffoul, W., de Buys Roessingh, A., Scaletta, C., Pioletti, D., and Applegate, L. A., 2011. "Biologicals and fetal cell therapy for wound and scar management." *ISRN Dermatology,* **2011**, pp. 1–16. 8

[70] Stoff, A., Rivera, A. A., Sanjib Banerjee, N., Moore, S. T., Michael Numnum, T., Espinosa-de-los Monteros, A., Richter, D. F., Siegal, G. P., Chow, L. T., Feldman, D., and et al., 2009. "Promotion of incisional wound repair by human mesenchymal stem cell transplantation." *Experimental Dermatology,* **18**(4), Apr, pp. 362–369. 8

[71] Zibert, J. R., Wallbrecht, K., Schon, M., Mir, L. M., Jacobsen, G. K., Trochon-Joseph, V., Bouquet, C., Villadsen, L. S., Cadossi, R., Skov, L., and et al., 2011. "Halting angiogenesis by non-viral somatic gene therapy alleviates psoriasis and murine psoriasiform skin lesions." *J. Clin. Invest.,* **121**(1), Jan, pp. 410–421. 8

[72] Wang, L., Rosenberg, J. B., De, B. P., Ferris, B., Wang, R., Rivella, S., Kaminsky, S. M., and Crystal, R. G., 2012. "In vivo gene transfer strategies to achieve partial correction of von willebrand disease." *Human Gene Therapy,* **23**(6), Jun, pp. 576–588. 8

[73] Mo Li, J. C. I. B., 2012. "No factor left behind: Generation of transgene-free induced pluripotent stem cells." *Am J Stem Cell,* **1:1**, pp. 75–80. 8

[74] Gehl, J., 2003. "Electroporation: Theory and methods, perspectives for drug delivery, gene therapy and research." *Acta Physiol Scand,* **177**, pp. 437–447. 8, 9, 21

[75] Takahashi, K., Tanabe, K., Ohnuki, M., Narita, M., Ichisaka, T., Tomoda, K., and Yamanaka, S., 2007. "Induction of pluripotent stem cells from adult human fibroblasts by defined factors." *Cell,* **131**(5), Nov, pp. 861–872. 8, 128

[76] Takahashi, K., and Yamanaka, S., 2006. "Induction of pluripotent stem cells from mouse embryonic and adult fibroblast cultures by defined factors." *Cell,* **126**(4), Aug, pp. 663–676. 8, 128

[77] Yamano, S., Dai, J., and Moursi, A. M., 2010. "Comparison of transfection efficiency of nonviral gene transfer reagents." *Molecular Biotechnology,* **46**(3), Nov, pp. 287–300. 8, 9, 21

[78] Vry, J. D., Martinez-Martinez, P., Losen, M., Bode, G. H., Temel, Y., Steckler, T., Steinbusch, H. W., Baets, M. D., and Prickaerts, J., 2010. "Low current-driven micro-electroporation allows efficient in vivo delivery of nonviral DNA into the adult mouse brain." *Molecular Therapy,* **18**(6), Apr, pp. 1183–1191. 8, 9

[79] Lufino, M. M., Edser, P. A., and Wade-Martins, R., 2008. "Advances in high-capacity extrachromosomal vector technology: Episomal maintenance, vector delivery, and transgene expression." *Molecular Therapy,* **16**(9), Jul, pp. 1525–1538. 9

[80] del Rosal, B., Sun, C., Loufakis, D. N., Lu, C., and Jaque, D., 2013. "Thermal loading in flow-through electroporation microfluidic devices." *Lab on a Chip,* **13**(15), p. 3119. 9

[81] Teichert, G. H., 2012. "Design and testing of a biological microelectromechanical micro system for the injection of thousands of cells simultaneously." Master's thesis, Brigham Young University. 10

[82] Djuzenova, C., Zimmerman, U., Frank, H., Sukhorukov, V., Richter, E., and Fuhr, G., 1996. "Effect of medium conductivity and composition on the uptake of propidium iodide into electropermeabilized myeloma cells." *Biochem Biophys Acta,* **1284:2**, pp. 143–152. 10

[83] Parise, J.J., H. L., and Magleby, S., 2001. "Ortho-planar linear motion springs." *Mechanism and Machine Theory,* **36**, pp. 1281–1299. 10

[84] Teichert, G., and Jensen, B. D., 2013. "Design and fabrication of a fully-compliant mechanism for control of cellular injection array.." *Production Engineering Research and Development,* **7**, pp. 561–568. 10, 26, 81, 90, 110, 113

[85] Darzynkiewicz, Z., Bruno, S., Bino, G., Gorczyca, W., Hotz, M., Lassota, P., and Traganos, F., 1992. "Features of apoptotic cells measured by flow cytometry." *Cytometry,* **13**, pp. 795–808. 11

[86] Vernes, L., H. C. R. C., 2000. "Flow cytometry of apoptotic cell death." *Journal of Immunological Methods,* **243**, pp. 167–190. 11

[87] Crissman, H., and Hirons, G., 1994. "Staining of dna in live and fixed cells." *Methods in Cell Biology,* **41**, pp. 195–209. 11

[88] Arndt-Jovin, D., and Jovin, T., 1989. "Flourescence labeling and microscopy of dna." *Methods in Cell Biology,* **30**, pp. 417–448. 12

[89] Evans, C., Ghivizzani, S., and Robbins, P., 2008. "Orthopedic gene therapy in 2008." *Molecular Therapy,* **17**(2), Dec, pp. 231–244. 21

[90] Fontes, A., and Lakshmipathy, U., 2013. "Advances in genetic modification of pluripotent stem cells." *Biotechnology Advances,* **31**(7), Nov, pp. 994–1001. 21

[91] Focosi, D., Amabile, G., Di Ruscio, A., Quaranta, P., Tenen, D. G., and Pistello, M., 2014. "Induced pluripotent stem cells in hematology: current and future applications." *Blood Cancer Journal,* **4**(5), May, p. e211. 21

[92] Wobus, A. M., and Loser, P., 2011. "Present state and future perspectives of using pluripotent stem cells in toxicology research." *Arch Toxicol,* **85**(2), Jan, pp. 79–117. 21, 128

[93] Han, J. W., and Yoon, Y.-s., 2011. "Induced pluripotent stem cells: Emerging techniques for nuclear reprogramming." *Antioxidants & Redox Signaling,* **15**(7), Oct, pp. 1799–1820. 21

[94] Robinton, D. A., and Daley, G. Q., 2012. "The promise of induced pluripotent stem cells in research and therapy." *Nature,* **481**(7381), Jan, pp. 295–305. 21

[95] Bikard, D., and Marraffini, L. A., 2013. "Control of gene expression by CRISPR-Cas systems." *F1000Prime Reports,* **5**, Nov, pp. 1–8. 21

[96] Zhang, F., Wen, Y., and Guo, X., 2014. "CRISPR/Cas9 for genome editing: progress, implications and challenges." *Human Molecular Genetics,* **23**(R1), Mar, pp. R40–R46. 21, 109

[97] Shalem, O., Sanjana, N. E., Hartenian, E., Shi, X., Scott, D. A., Mikkelsen, T. S., Heckl, D., Ebert, B. L., Root, D. E., Doench, J. G., and et al., 2013. "Genome-scale CRISPR-Cas9 knockout screening in human cells." *Science,* **343**(6166), Dec, pp. 84–87. 21, 38, 109, 124

[98] Tong, S., Fine, E. J., Lin, Y., Cradick, T. J., and Bao, G., 2013. "Nanomedicine: Tiny particles and machines give huge gains." *Annals of Biomedical Engineering,* **42**(2), Dec, pp. 243–259. 21

[99] Devulapally, R., and Paulmurugan, R., 2013. "Polymer nanoparticles for drug and small silencing RNA delivery to treat cancers of different phenotypes." *WIREs Nanomed Nanobiotechnology,* **6**(1), Aug, pp. 40–60. 21

[100] Nitta, S., and Numata, K., 2013. "Biopolymer-based nanoparticles for drug/gene delivery and tissue engineering." *International Journal of Molecular Sciences,* **14**(1), Jan, pp. 1629–1654. 21

[101] Phang, R.-Z., Tay, F. C., Goh, S.-L., Lau, C.-H., Zhu, H., Tan, W.-K., Liang, Q., Chen, C., Du, S., Li, Z., and et al., 2013. "Zinc finger nuclease-expressing baculoviral vectors mediate targeted genome integration of reprogramming factor genes to facilitate the generation of human induced pluripotent stem cells." *Stem Cells Translational Medicine,* **2**(12), Oct, pp. 935–945. 21

[102] Zhu, H., Lau, C., Goh, S., Liang, Q., Chen, C., Du, S., Phang, R.-Z., Tay, F. C., Tan, W.-K., Li, Z., and et al., 2013. "Baculoviral transduction facilitates TALEN-mediated targeted transgene integration and Cre/LoxP cassette exchange in human-induced pluripotent stem cells." *Nucleic Acids Research,* **41**(19), Aug, pp. 1–12. 21

[103] Goncalves, M. A. F. V., Holkers, M., van Nierop, G. P., Wieringa, R., Pau, M. G., and de Vries, A. A. F., 2008. "Targeted chromosomal insertion of large DNA into the human genome by a fiber-modified high-capacity adenovirus-based vector system." *PLoS ONE,* **3**(8), Aug, pp. 1–14. 21

[104] Prakash, S., Tomaro-Duchesneau, C., Saha, S., Kahouli, and Malhotra, M., 2013. "Development and characterization of chitosan-PEG-TAT nanoparticles for the intracellular delivery of siRNA." *International Journal of Nanomedicine*, May, p. 2041. 21

[105] Lu, H., Dai, Y., Lv, L., and Zhao, H., 2014. "Chitosan-graft-polyethylenimine/DNA nanoparticles as novel non-viral gene delivery vectors targeting osteoarthritis." *PLoS ONE,* **9**(1), Jan, p. e84703. 21

[106] Seo, E. J., Jang, I. H., Do, E. K., Cheon, H. C., Heo, S. C., Kwon, Y. W., Jeong, G. O., Kim, B. R., and Kim, J. H., 2013. "Efficient production of retroviruses using PLGA/bPEI-DNA nanoparticles and application for reprogramming somatic cells." *PLoS ONE,* **8**(9), Sep, pp. 1–12. 21

[107] Gao, X., Kim, K.-S., and Liu, D., 2007. "Nonviral gene delivery: What we know and what is next." *J. American Association of Pharmaceutical Scientists,* **9**(1), Mar, pp. E92–E104. 21

[108] Togtema, M., Pichardo, S., Jackson, R., Lambert, P. F., Curiel, L., and Zehbe, I., 2012. "Sonoporation delivery of monoclonal antibodies against human papillomavirus 16 E6 restores p53 expression in transformed cervical keratinocytes." *PLoS ONE,* **7**(11), Nov, p. e50730. 21

[109] Aiuti, A., Biasco, L., Scaramuzza, S., Ferrua, F., Cicalese, M. P., Baricordi, C., Dionisio, F., Calabria, A., Giannelli, S., Castiello, M. C., and et al., 2013. "Lentiviral hematopoietic stem cell gene therapy in patients with Wiskott-Aldrich Syndrome." *Science,* **341**(6148), Jul, p. 1233151. 21

[110] Kobiler, O., Drayman, N., Butin-Israeli, V., and Oppenheim, A., 2012. "Virus strategies for passing the nuclear envelope barrier." *Nucleus,* **3**(6), Nov, pp. 526–539. 21

[111] Boissel, L., Betancur, M., Lu, W., Wels, W. S., Marino, T., Van Etten, R. A., and Klingemann, H., 2012. "Comparison of mRNA and lentiviral based transfection of natural killer cells with chimeric antigen receptors recognizing lymphoid antigens." *Leuk Lymphoma,* **53**(5), May, pp. 958–965. 21, 39

[112] Yang, T., Zhang, B., Pat, B. K., Wei, M. Q., and Gobe, G. C., 2010. "Lentiviral-mediated RNA interference against TGF-Beta receptor type II in renal epithelial and fibroblast cell populations in vitro demonstrates regulated renal fibrogenesis that is more efficient than a nonlentiviral vector." *Journal of Biomedicine and Biotechnology,* **2010**, pp. 1–12. 21, 39

[113] Ou, W., Marino, M. P., Suzuki, A., Joshi, B., Husain, S. R., Maisner, A., Galanis, E., Puri, R. K., and Reiser, J., 2012. "Specific targeting of human interleukin IL-13 receptor alpha-2-positive cells with lentiviral vectors displaying IL-13." *Human Gene Therapy Methods,* **23**(2), Apr, pp. 137–147. 21, 39

[114] Yang, H., Joo, K.-I., Ziegler, L., and Wang, P., 2009. "Cell type-specific targeting with surface-engineered lentiviral vectors co-displaying OKT3 antibody and fusogenic molecule." *Pharmaceutical Research,* **26**(6), Mar, pp. 1432–1445. 21, 39

[115] Koonin, E. V., and Yutin, N., 2010. "Origin and evolution of eukaryotic large nucleo-cytoplasmic DNA viruses." *Intervirology,* **53**(5), pp. 284–292. 21

[116] Checks, E., 2003. "Harmful potential of viral vectors fuels doubts over gene therapy." *Nature,* **423**, pp. 573–574. 22, 39

[117] Kang, H. C., Samsonova, O., Kang, S.-W., and Bae, Y. H., 2012. "The effect of environmental pH on polymeric transfection efficiency." *Biomaterials,* **33**(5), Feb, pp. 1651–1662. 22, 39

[118] Shalek, A. K., Gaublomme, J. T., Wang, L., Yosef, N., Chevrier, N., Andersen, M. S., Robinson, J. T., Pochet, N., Neuberg, D., Gertner, R. S., and et al., 2012. "Nanowire-mediated delivery enables functional interrogation of primary immune cells: Application to the analysis of chronic lymphocytic leukemia." *Nano Lett.,* **12**(12), Dec, pp. 6498–6504. 22

[119] Shalek, A. K., Robinson, J. T., Karp, E. S., Lee, J. S., Ahn, D.-R., Yoon, M.-H., Sutton, A., Jorgolli, M., Gertner, R. S., Gujral, T. S., and et al., 2010. "Vertical silicon nanowires as a universal platform for delivering biomolecules into living cells." *Proceedings of the National Academy of Sciences,* **107**(5), Jan, pp. 1870–1875. 22, 110

[120] Robinson, J. T., Jorgolli, M., and Park, H., 2013. "Nanowire electrodes for high-density stimulation and measurement of neural circuits." *Front. Neural Circuits,* **7**. 22

[121] Robinson, J. T., Jorgolli, M., Shalek, A. K., Yoon, M.-H., Gertner, R. S., and Park, H., 2012. "Vertical nanowire electrode arrays as a scalable platform for intracellular interfacing to neuronal circuits." *Nature Nanotechnology,* **7**(3), Jan, pp. 180–184. 22

[122] Shi, P., Scott, M. A., Ghosh, B., Wan, D., Wissner-Gross, Z., Mazitschek, R., Haggarty, S. J., and Yanik, M. F., 2011. "Synapse microarray identification of small molecules that enhance synaptogenesis." *Nat Comms,* **2**, Oct, p. 510. 22

[123] Ramsey, F., and Schafer, D., 2013. *The Statistical Sleuth: A Course in Methods of Data Analysis, 3E*. Brooks/Cole. 30

[124] Obataya, I., Nakamura, C., Han, S., Nakamura, N., and Miyake, J., 2005. "Mechanical sensing of the penetration of various nanoneedles into a living cell using atomic force microscopy." *Biosensors and Bioelectronics,* **20**(8), Feb, pp. 1652–1655. 32, 33

[125] Lewis, T., Burnett, S. H., and Jensen, B. D., 2015. "Injection force effects on propidium iodide uptake in nanoinjected HeLa cells." *Proceedings of the ASME 2014 International*

Design Engineering Technical Conferences & Computers and Information in Engineering Conference, **DETC2015-47630**, pp. 1–10. 32

[126] Ousterout, D. G., Kabadi, A. M., Thakore, P. I., Perez-Pinera, P., Brown, M. T., Majoros, W. H., Reddy, T. E., and Gersbach, C. A., 2015. "Correction of dystrophin expression in cells from duchenne muscular dystrophy patients through genomic excision of exon 51 by zinc finger nucleases." *Molecular Therapy,* **23**(3), Dec, pp. 523–532. 38

[127] Petersen, B., and Niemann, H., 2015. "Molecular scissors and their application in genetically modified farm animals." *Transgenic Research,* **24**(3), Jan, pp. 381–396. 38, 77

[128] Nicholson, S. A., 2015. "Progress and prospects of engineered sequence-specific DNA modulating technologies for the management of liver diseases." *World Journal of Hepatology,* **7**(6), pp. 859–873. 38, 77

[129] Seruggia, D., and Montoliu, L., 2014. "The new CRISPR-Cas system: RNA-guided genome engineering to efficiently produce any desired genetic alteration in animals." *Transgenic Research,* **23**(5), Aug, pp. 707–716. 38, 77

[130] Kimura, Y., Oda, M., Nakatani, T., Sekita, Y., Monfort, A., Wutz, A., Mochizuki, H., and Nakano, T., 2015. "CRISPR/Cas9-mediated reporter knock-in in mouse haploid embryonic stem cells." *Sci. Rep.,* **5**, Jun, p. 10710. 38, 92, 109

[131] Kimura, Y., Hisano, Y., Kawahara, A., and Higashijima, S.-i., 2014. "Efficient generation of knock-in transgenic zebrafish carrying reporter/driver genes by CRISPR/Cas9-mediated genome engineering." *Sci. Rep.,* **4**, Oct, p. 6545. 38, 92, 109

[132] Gilbert, L. A., Larson, M. H., Morsut, L., Liu, Z., Brar, G. A., Torres, S. E., Stern-Ginossar, N., Brandman, O., Whitehead, E. H., Doudna, J. A., and et al., 2013. "CRISPR-mediated modular RNA-guided regulation of transcription in eukaryotes." *Cell,* **154**(2), Jul, pp. 442–451. 38, 92, 109

[133] Maeder, M. L., Linder, S. J., Cascio, V. M., Fu, Y., Ho, Q. H., and Joung, J. K., 2013. "CRISPR RNA-guided activation of endogenous human genes." *Nature Methods,* **10**(10), Jul, pp. 977–979. 38, 92, 109, 124

[134] Cheng, A. W., Wang, H., Yang, H., Shi, L., Katz, Y., Theunissen, T. W., Rangarajan, S., Shivalila, C. S., Dadon, D. B., and Jaenisch, R., 2013. "Multiplexed activation of endogenous genes by CRISPR-on, an RNA-guided transcriptional activator system." *Cell Research,* **23**(10), Aug, pp. 1163–1171. 38, 92, 109

[135] Qi, L. S., Larson, M. H., Gilbert, L. A., Doudna, J. A., Weissman, J. S., Arkin, A. P., and Lim, W. A., 2013. "Repurposing CRISPR as an RNA-guided platform for sequence-specific control of gene expression." *Cell,* **152**(5), Feb, pp. 1173–1183. 38, 92, 109

[136] Cong, L., Ran, F. A., Cox, D., Lin, S., Barretto, R., Habib, N., Hsu, P. D., Wu, X., Jiang, W., Marraffini, L. A., and et al., 2013. "Multiplex genome engineering using CRISPR/Cas systems." *Science,* **339**(6121), Jan, pp. 819–823. 38, 109

[137] Wang, H., Yang, H., Shivalila, C. S., Dawlaty, M. M., Cheng, A. W., Zhang, F., and Jaenisch, R., 2013. "One-step generation of mice carrying mutations in multiple genes by CRISPR/Cas-mediated genome engineering." *Cell,* **153**(4), May, pp. 910–918. 38, 77, 109

[138] Ousterout, D. G., Kabadi, A. M., Thakore, P. I., Majoros, W. H., Reddy, T. E., and Gersbach, C. A., 2015. "Multiplex CRISPR/Cas9-based genome editing for correction of dystrophin mutations that cause duchenne muscular dystrophy." *Nature Communications,* **6**, Feb, p. 6244. 38, 77, 109

[139] David, R. A., Jensen, B. D., Black, J. L., Burnett, S. H., and Howell, L. L., 2011. "Effects of dissimilar electrode materials and electrode position on DNA motion during electrophoresis." *J. Nanotechnol. Eng. Med.,* **2**(2), pp. 1–6. 40, 92

[140] David, R. A., Jensen, B. D., Black, J. L., Burnett, S. H., and Howell, L. L., 2010. "Modeling and experimental validation of DNA motion in uniform and nonuniform DC electric fields." *J. Nanotechnol. Eng. Med.,* **1**(4), pp. 1–8. 40, 90, 92

[141] Al-Fageeh, M. B., and Smales, C. M., 2006. "Control and regulation of the cellular responses to cold shock: the responses in yeast and mammalian systems." *Biochemical Journal,* **397**(2), Jul, p. 247. 40

[142] Zhao, W., Tian, Y., Cai, M., Wang, F., Wu, J., Gao, J., Liu, S., Jiang, J., Jiang, S., and Wang, H., 2014. "Studying the nucleated mammalian cell membrane by single molecule approaches." *PLoS ONE,* **9**(5), May, p. e91595. 40

[143] Freeman, S., 2005. *Biological Science*. Pearson Prentice Hall. 40

[144] Hazel, J., 1995. "Thermal adaptation in biological membranes: is homeoviscous adapation the explanation?." *Ann. Rev. Physiol.,* **57**, pp. 19–42. 40

[145] Avery SV, Lloyd D, H. J., 1995. "Temperature-dependent changes in plasma-membrane lipid order and the phagocytotic activity of the amoeba Acanthamoeba castellanii are closely correlated.." *Biochem J.,* **312**, pp. 811–816. 40

[146] Carty SM, Sreekumar KR, R. C., 1999. "Effect of cold shock on lipid A biosynthesis in Escherichia coli: induction at 12C of a an acyltransferase specific for palmitoleoyl-acyl carrier protein.." *J. Biol. Chem.,* **274**, pp. 9677–9685. 40

[147] Cossins, A., and Macdonald, A., 1989. "The adapation of biological membranes to temperature and pressure: fish from the deep and cold.." *J. Bioenerg. Biomembr.,* **21**, pp. 115–135. 40

[148] Dickens, B., and Thompson Jr., G., 1981. "Rapid membrane response during low-temperature acclimation: correlation of early changes in the physical properties and lipid composition of Tetrahymena microsomal membranes.." *Biochimica et Biophysica Acta,* **644**, pp. 211–218. 40

[149] Sunyer, R., Trepat, X., Fredberg, J. J., Farre, R., and Navajas, D., 2009. "The temperature dependence of cell mechanics measured by atomic force microscopy." *Physical Biology,* **6**(2), Jun, p. 025009. 40

[150] Chiou, Y.-W., Lin, H.-K., Tang, M.-J., Lin, H.-H., and Yeh, M.-L., 2013. "The influence of physical and physiological cues on atomic force microscopy-based cell stiffness assessment." *PLoS ONE,* **8**(10), Oct, p. e77384. 40

[151] Neutelings, T., Lambert, C. A., Nusgens, B. V., and Colige, A. C., 2013. "Effects of mild cold shock 25C followed by warming up at 37C on the cellular stress response." *PLoS ONE,* **8**(7), Jul, p. e69687. 40, 46

[152] Abreu-Blanco, M. T., Watts, J. J., Verboon, J. M., and Parkhurst, S. M., 2012. "Cytoskeleton responses in wound repair." *Cell. Mol. Life Sci.,* **69**(15), Feb, pp. 2469–2483. 40, 41

[153] Abreu-Blanco, M. T., Verboon, J. M., and Parkhurst, S. M., 2011. "Single cell wound repair." *BioArchitecture,* **1**(3), May, pp. 114–121. 40, 41, 91

[154] Abreu-Blanco, M. T., Verboon, J. M., and Parkhurst, S. M., 2011. "Cell wound repair in Drosophila occurs through three distinct phases of membrane and cytoskeletal remodeling." *The Journal of Cell Biology,* **193**(3), Apr, pp. 455–464. 40, 41, 91

[155] Fujita, J., 1999. "Cold shock response in mammalian cells." *Journal of Molecular Microbiology and Biotechnology,* **1**, pp. 243–255. 46

[156] Plesofsky, N., and Brambl, R., 1999. "Glucose metabolism in Neurospora is altered by heat shock and by disruption of HSP30." *Biochimica et Biophysica Acta (BBA) - Molecular Cell Research,* **1449**(1), Feb, pp. 73–82. 46

[157] Sonna, L., Fujita, J., Gaffin, S., and Lilly, C., 2002. "Effects of heat and cold stress on mammalian gene expression.." *Journal of Applied Physiology,* **92**, pp. 1725–1742. 46

[158] Fraker, M. E., and Peacor, S. D., 2008. "Statistical tests for biological interactions: A comparison of permutation tests and analysis of variance." *Acta Oecologica,* **33**(1), Jan, pp. 66–72. 50

[159] Negendank, W., and Shaller, C., 1982. "Temperature-dependence of ATP level, organic phosphate production and Na,K-ATPase in human lymphocytes." *Physiol Chem Phys,* **14:6**, pp. 513–518. 55

[160] Davies, D., 2015. Flow cytometric analysis of cell cycle with propidium iodide DNA staining Tech. rep., FACS Laboratory, London Research Institute, Cancer Research UK. 55

[161] Jen, C.-P., Wu, W.-M., Li, M., and Lin, Y.-C., 2004. "Site-specific enhancement of gene transfection utilizing an attracting electric field for DNA plasmids on the electroporation microchip." *J. Microelectromech. Syst.,* **13**(6), Dec, pp. 947–955. 57

[162] Choi, S.-O., Park, J.-H., Choi, Y., Kim, Y., Gill, H., Yoon, Y.-K., Prausnitz, M., and Allen, M., 2005. "An electrically active microneedle array for electroporation of skin for gene delivery." *The 13th International Conference on Solid-State Sensors, Actuators and Microsystems, 2005. Digest of Technical Papers. TRANSDUCERS '05.,* **2**, pp. 1513–1516. 57

[163] Lin, Y.-C., 2005. "Electroporation microchips for gene transfection." *Conference, Emerging Information Technology 2005.*, pp. 1–4. 57

[164] Saito, T. K., Suekane, O., Akagi, T., Taguchi, A., and Ichiki, T., 2009. "Large-scale high-performance cell membrane perforation, with nanoimprinted mass producible perforator." *2009 IEEE/NIH Life Science Systems and Applications Workshop*, Apr, pp. 5–8. 57

[165] Mazda, O., Kishida, T., Matsui, M., Nakano, H., Yoshimoto, K., Shimada, T., Nakai, S., Imanishr, J., and Hisa, Y., 2009. "Nonviral gene administration by means of the epstein-barr virus (ebv)-based episomal vectors and it application to gene therapy and regenerative medicine." *2009 International Symposium on Micro-NanoMechatronics and Human Science*, Nov, pp. 182–187. 57

[166] Caprette, D. R., 2012. Using a counting chamber (Rice University) Online: http://www.ruf.rice.edu / bioslabs/methods /microscopy/cellcounting.html, August. 65

[167] Helenius, J., Heisenberg, C.-P., Gaub, H. E., and Muller, D. J., 2008. "Single-cell force spectroscopy." *Journal of Cell Science,* **121**(11), May, pp. 1785–1791. 67

[168] Benoit, M., Gabriel, D., Gerisch, G., and Gaub, H. E.", 2000.." *Nat. Cell Biol.,* **2**(6), Apr, pp. 313–317. 67

[169] Florin, E., Moy, V., and Gaub, H., 1994. "Adhesion forces between individual ligand-receptor pairs." *Science,* **264**(5157), Apr, pp. 415–417. 67

[170] Zhang, X., Wojcikiewicz, E., and Moy, V. T., 2002. "Force spectroscopy of the leukocyte function-associated antigen-1/intercellular adhesion molecule-1 interaction." *Biophysical Journal,* **83**(4), Oct, pp. 2270–2279. 67

[171] Lehenkari, P., and Horton, M., 1999. "Single integrin molecule adhesion forces in intact cells measured by atomic force microscopy." *Biochemical and Biophysical Research Communications,* **259**(3), Jun, pp. 645–650. 67

[172] Evans, E., and Calderwood, D., 2007. "Forces and bond dynamics in cell adhesion." *Science,* **316**, pp. 1148–1153. 67

[173] Hong, Z., Staiculescu, M. C., Hampel, P., Levitan, I., and Forgacs, G., 2012. "How cholesterol regulates endothelial biomechanics." *Front. Physio.,* **3**. 67

[174] Jens Friedrichs, Carsten Werner, D. J. M., 2013. *Adhesion Protein Protocols, 3E.* Humana Press, ch. Quantifying Cellular Adhesion to Convalently Immobilized Extracellular Matrix Proteins by Single-Cell Force Spectroscopy, pp. 19–37. 67

[175] Avci-Adali, M., Behring, A., Keller, T., Krajewski, S., Schlensak, C., and Wendel, H., 2014. "Optimized conditions for successful transfection of human endothelial cells with in vitro synthesized and modified mRNA for induction of protein expression." *Journal of Biological Engineering,* **8**(1), p. 8. 74

[176] Protocol, 2008. Transfection of human fibroblasts, online: www.protocol-online.org/biology-forums, Apr. 74

[177] Mirus, 2015. Transit-x2 dynamic delivery system, online: www.mirusbio.com/products/transfection/transit-x2-dynamic-delivery-system. 74

[178] Branski, L., Gauglitz, G., Herndon, D., and Jeschke, M., 2009. "A review of gene and stem cell therapy in cutaneous wound healing." *Burns,* **35:2**, pp. 171–180. 76, 92, 97, 98, 100, 124

[179] Horii, T., Tamura, D., Morita, S., Kimura, M., and Hatada, I., 2013. "Generation of an ICf syndrome model by efficient genome editing of human induced pluripotent stem cells using the CRISPR system." *International Journal of Molecular Sciences,* **14**(10), Sep, pp. 19774–19781. 77

[180] Feng, W., Dai, Y., Mou, L., Cooper, D., Shi, D., and Cai, Z., 2015. "The potential of the combination of CRISPR/Cas9 and pluripotent stem cells to provide human organs from chimaeric pigs." *International Journal of Molecular Sciences,* **16**(3), Mar, pp. 6545–6556. 77, 128

[181] Li, H. L., Fujimoto, N., Sasakawa, N., Shirai, S., Ohkame, T., Sakuma, T., Tanaka, M., Amano, N., Watanabe, A., Sakurai, H., and et al., 2015. "Precise correction of the dystrophin gene in Duchenne Muscular Dystrophy patient induced pluripotent stem cells by TALEN and CRISPR-Cas9." *Stem Cell Reports,* **4**(1), Jan, pp. 143–154. 77

[182] Mou, H., Kennedy, Z., Anderson, D. G., Yin, H., and Xue, W., 2015. "Precision cancer mouse models through genome editing with crispr-cas9." *Genome Medicine,* **7**(1), Jun, pp. 1–11. 77

[183] Ran, F. A., Hsu, P. D., Wright, J., Agarwala, V., Scott, D. A., and Zhang, F., 2013. "Genome engineering using the CRISPR-Cas9 system." *Nat Protoc,* **8**(11), Oct, pp. 2281–2308. 77, 80, 86, 109

[184] Ding, Q., Regan, S. N., Xia, Y., Oostrom, L. A., Cowan, C. A., and Musunuru, K., 2013. "Enhanced efficiency of human pluripotent stem cell genome editing through replacing TALENs with CRISPRs." *Cell Stem Cell,* **12**(4), Apr, pp. 393–394. 77

[185] Pennisi, E., 2013. "The CRISPR craze." *Science,* **341**(6148), Aug, pp. 833–836. 77

[186] Hacein-Bey-Abina, S., Von Kalle, C., Schmidt, M., McCormack, M. P., Wulffraat, N., Leboulch, P., Lim, A., Osborne, C. S., Pawliuk, R., Morillon, E., Sorensen, R., Forster, A., Fraser, P., Cohen, J. I., de Saint Basile, G., Alexander, I., Wintergerst, U., Frebourg, T., Aurias, A., Stoppa-Lyonnet, D., Romana, S., Radford-Weiss, I., Gross, F., Valensi, F., Delabesse, E., Macintyre, E., Sigaux, F., Soulier, J., Leiva, L. E., Wissler, M., Prinz, C., Rabbitts, T. H., Le Deist, F., Fischer, A., and Cavazzana-Calvo, M., 2003. "Lmo2-associated clonal t cell proliferation in two patients after gene therapy for scid-x1." *Science,* **302:5644**, pp. 415–419. 77, 100

[187] Zhou, Y., Zhu, S., Cai, C., Yuan, P., Li, C., Huang, Y., and Wei, W., 2014. "High-throughput screening of a CRISPR/Cas9 library for functional genomics in human cells." *Nature,* **509**(7501), Apr, pp. 487–491. 78, 90

[188] Itaka, K., and Kataoka, K., 2009. "Recent development of nonviral gene delivery systems with virus-like structures and mechanisms." *European Journal of Pharmaceutics and Biopharmaceutics,* **71**(3), Mar, pp. 475–483. 78

[189] Park, J. S., Na, K., Woo, D. G., Yang, H. N., Kim, J. M., Kim, J. H., Chung, H.-M., and Park, K.-H., 2010. "Non-viral gene delivery of DNA polyplexed with nanoparticles transfected into human mesenchymal stem cells." *Biomaterials,* **31**(1), Jan, pp. 124–132. 78

[190] van Gaal, E. V., van Eijk, R., Oosting, R. S., Kok, R. J., Hennink, W. E., Crommelin, D. J., and Mastrobattista, E., 2011. "How to screen non-viral gene delivery systems in vitro?." *Journal of Controlled Release,* **154**(3), Sep, pp. 218–232. 78

[191] Pouton, C. W., and Seymour, L. W., 2001. "Key issues in non-viral gene delivery." *Adv Drug Deliv Rev,* **46**, pp. 187–203. 78

[192] Ferrari, S., Geddes, D. M., and Alton, E. W., 2002. "Barriers to and new approaches for gene therapy and gene delivery in cystic fibrosis." *Adv Drug Deliv Rev,* **54**, pp. 1373–1393. 78

[193] Lungwitz, U., Breunig, M., Blunk, T., and Gopferich, A., 2005. "Polyethylenimine-based non-viral gene delivery systems." *European Journal of Pharmaceutics and Biopharmaceutics,* **60**(2), Jul, pp. 247–266. 78

[194] Kodama, K., Katayama, Y., Shoji, Y., and Nakashima, H., 2006. "The features and shortcomings for gene delivery of current non-viral carriers." *Curr Med Chem,* **13**, pp. 2155–2161. 78

[195] Ferrer-Miralles, N., Vazquez, E., and Villaverde, A., 2008. "Membrane-active peptides for non-viral gene therapy: making the safest easier." *Trends in Biotechnology,* **26**(5), May, pp. 267–275. 78

[196] Baoum, A., Dhillon, N., Buch, S., and Berkland, C., 2010. "Cationic surface modification of PLG nanoparticles offers sustained gene delivery to pulmonary epithelial cells." *J. Pharm. Sci.,* **99**, pp. 2413–2422. 78

[197] Baoum, A. A., and Berkland, C., 2011. "Calcium condensation of DNA complexed with cell-penetrating peptides offers efficient, noncytotoxic gene delivery." *Journal of Pharmaceutical Sciences,* **100**(5), May, pp. 1637–1642. 78

[198] Baoum, A., Ovcharenko, D., and Berkland, C., 2012. "Calcium condensed cell penetrating peptide complexes offer highly efficient, low toxicity gene silencing." *International Journal of Pharmaceutics,* **427**(1), May, pp. 134–142. 78

[199] Godbey, W. T., Wu, K. K., and Mikos, A. G., 1999. "Poly(ethylenimine) and its role in gene delivery." *J Control Release,* **60**, pp. 2–3. 78

[200] Godbey, W. T., and Mikos, A. G., 2001. "Recent progress in gene delivery using non-viral transfer complexes." *J Control Release,* **72**, pp. 115–125. 78

[201] Merdan, T., Kopecek, J., and Kissel, T., 2002. "Prospects for cationic polymers in gene and oligonucleotide therapy against cancer." *Adv. Drug Deliv. Rev.,* **54**, pp. 715–758. 78

[202] Park, T., Jeong, J., and Kim, S., 2006. "Current status of polymeric gene delivery systems." *Advanced Drug Delivery Reviews,* **58**(4), Jul, pp. 467–486. 78

[203] Middaugh, C. R., and Ramsey, J. D., 2007. "Analysis of cationic-lipid-plasmid-dna complexes." *Anal. Chem.,* **79**, pp. 7240–7248. 78

[204] Green, J., Langer, R., and Anderson, D., 2008. "A combinatorial polymer library approach yields insight into nonviral gene delivery." *Acc. Chem. Res.,* **106**, pp. 8918–8922. 78

[205] Jo, J.-i., and Tabata, Y., 2008. "Non-viral gene transfection technologies for genetic engineering of stem cells." *European Journal of Pharmaceutics and Biopharmaceutics,* **68**(1), Jan, pp. 90–104. 78

[206] Midoux, P., Pichon, C., Yaouanc, J., and Jaffres, P., 2009. "Chemical vectors for gene delivery: a current review on polymers, peptides and lipids containing histidine or imidazole as nucleic acid carriers." *Br. J. Pharmacol.,* **157**, pp. 166–178. 78

[207] Mehier-Humbert, S., and Guy, R. H., 2005. "Physical methods for gene transfer: Improving the kinetics of gene delivery into cells." *Advanced Drug Delivery Reviews,* **57**(5), Apr, pp. 733–53. 78

[208] Sessions, J., and Nickerson, D. S., 2014. "Biologic basis of nerve decompression surgery for focal entrapments in diabetic peripheral neuropathy." *Journal of Diabetes Science and Technology,* **8**(2), Feb, pp. 412–418. 78, 84, 90, 91, 93, 94

[209] Mali, P., Yang, L., Esvelt, K. M., Aach, J., Guell, M., DiCarlo, J. E., Norville, J. E., and Church, G. M., 2013. "RNA-guided human genome engineering via cas9." *Science,* **339**(6121), Jan, pp. 823–826. 80, 109, 124

[210] Aten, Q. T., Jensen, B. D., and Burnett, S. H., 2008. "Testing of a pumpless MEMS microinjection needle emplyoying electrostatic attraction and repulsion of DNA." *Proceedings of the ASME 2008 International Design Engineering Technical Conferences*, pp. 1–8. 90, 110

[211] Maggio, I., Holkers, M., Liu, J., Janssen, J. M., Chen, X., and Gon??alves, M. A. F. V., 2014. "Adenoviral vector delivery of RNA-guided CRISPR/Cas9 nuclease complexes induces targeted mutagenesis in a diverse array of human cells." *Scientific Reports,* **4**, May, pp. 1–11. 90

[212] Canatella, P., Karr, J., Petros, J., and Prausnitz, M., 2001. "Quantitative study of electroporation-mediated molecular uptake and cell viability." *Biophysical Journal,* **80**, pp. 755–764. 92

[213] Eming, S. A., Lee, J., Snow, R. G., Tompkins, R. G., Yarmush, M. L., and Morgan, J. R., 1995. "Genetically modified human epidermis overexpressing PDGF-A directs the development of a cellular and vascular connective tissue stroma when transplanted to athymic mice–implications for the use of genetically modified keratinocytes to modulate dermal regeneration." *J Invest Dermatol,* **105:6**, pp. 756–763. 92, 103

[214] Eriksson, E., Yao, F., Svensjo, T., Winkler, T., Slama, J., Macklin, M. D., Andree, C., McGregor, M., Hinshaw, V., and Swain, W. F., 1998. "In vivo gene transfer to skin and wound by microseeding." *Journal of Surgical Research,* **78**(2), Aug, pp. 85–91. 92, 101, 104

[215] Galeano, M., Deodato, B., Altavilla, D., Cucinotta, D., Arsic, N., Marini, H., Torre, V., Giacca, M., and Squadrito, F., 2003. "Adeno-associated viral vector vector-mediated human vascular endothelial growth factor gene transfer stimulates angiogenesis and wound healing in the genetically diabetic mouse." *Diabetologia,* **46:4**, pp. 546–555. 92, 98, 103

[216] Badillo, A. T., Chung, S., Zhang, L., Zoltick, P., and Liechty, K. W., 2007. "Lentiviral gene transfer of SDF-1alpha to wounds improves diabetic wound healing." *Journal of Surgical Research,* **143**(1), Nov, pp. 35–42. 92, 100, 103

[217] Ohtsuka, S., Nishikawa-Torikai, S., and Niwa, H., 2012. "E-cadherin promotes incorporation of mouse epiblast stem cells into normal development." *PLoS ONE,* **7**(9), Sep, p. e45220. 92

[218] Polejaeva, I., and Mitalipov, S., 2012. "Stem cell potency and the ability to contribute to chimeric organisms." *Reproduction,* **145**(3), Dec, pp. R81–R88. 92

[219] Guo, J., Wu, B., Li, S., Bao, S., Zhao, L., Hu, S., Sun, W., Su, J., Dai, Y., and Li, X., 2014. "Contribution of mouse embryonic stem cells and induced pluripotent stem cells to chimeras through injection and coculture of embryos." *Stem Cells International,* **2014**, pp. 1–9. 92

[220] Murayama, H., Masaki, H., Sato, H., Hayama, T., Yamaguchi, T., and Nakauchi, H., 2015. "Successful reprogramming of epiblast stem cells by blocking nuclear localization of beta-catenin." *Stem Cell Reports,* **4**(1), Jan, pp. 103–113. 92

[221] Huang, J., Deng, K., Wu, H., Liu, Z., Chen, Z., Cao, S., Zhou, L., Ye, X., Keefe, D. L., and Liu, L., 2008. "Efficient production of mice from embryonic stem cells injected into four- or eight-cell embryos by piezo micromanipulation." *Stem Cells,* **26**(7), Jul, pp. 1883–1890. 92

[222] Hu, B., Haj, A., and Dobson, J., 2013. "Receptor-targeted, magneto-mechanical stimulation of osteogenic differentiation of human bone marrow-derived mesenchymal stem cells." *International Journal of Molecular Sciences,* **14**(9), Sep, pp. 19276–19293. 92, 122

[223] Sen, C. K., Gordillo, G. M., Roy, S., Kirsner, R., Lambert, L., Hunt, T. K., Gottrup, F., Gurtner, G. C., and Longaker, M. T., 2009. "Human skin wounds: A major and snowballing threat to public health and the economy." *Wound Repair and Regeneration,* **17**(6), Nov, pp. 763–771. 93, 111

[224] Raghava, P., 2014. "Global wound care market outlook: Analysis of wound care technologies." *Frost and Sullivan*. 93, 111

[225] International Diabetes Federation, 2016. Diabetes Atlas, 7E Tech. rep., International Diabetes Federation. 93, 111

[226] Alavi, A., Sibbald, R. G., Mayer, D., Goodman, L., Botros, M., Armstrong, D. G., Woo, K., Boeni, T., Ayello, E. A., and Kirsner, R. S., 2014. "Diabetic foot ulcers." *Journal of the American Academy of Dermatology,* **70**(1), Jan, pp. 1.e1–1.e18. 94, 111

[227] Singh, N., 2005. "Preventing foot ulcers in patients with diabetes." *JAMA,* **293:2**(2), Jan, pp. 217–228. 94

[228] Reiber, G., 1996. "The epidemiology of diabetic foot problems." *Diabet Med,* **13 Suppl 1**, pp. S6–S11. 94

[229] Guo, S., and DiPietro, L. A., 2010. "Factors affecting wound healing." *Journal of Dental Research,* **89**(3), Feb, pp. 219–229. 94

[230] Bus, S. A., van Deursen, R. W., Armstrong, D. G., Lewis, J., Caravaggi, C. F., and Cavanagh, P. R., 2015. "Footwear and offloading interventions to prevent and heal foot ulcers and reduce plantar pressure in patients with diabetes: a systematic review." *Diabetes Metab Res Rev*, Sep. 94

[231] Lew, E. J., Mills, J. L., and Armstrong, D. G., 2015. "The deteriorating dfu: prioritising risk factors to avoid amputation." *Journal of Wound Care,* **24**(Sup5b), May, pp. 31–37. 94, 112

[232] Miller, J., and Armstrong, D. G., 2014. "Offloading the diabetic and ischemic foot: solutions for the vascular specialist." *Seminars in Vascular Surgery,* **27**(1), Mar, pp. 68–74. 94

[233] Demidova-Rice, T. N., Hamblin, M. R., and Herman, I. M., 2012. "Acute and impaired wound healing: pathophysiology and current methods for drug delivery, part 1: normal and chronic wounds: biology, causes, and approaches to care." *Advances in Skin & Wound Care,* **25:7**(7), pp. 304–314. 94, 106, 107

[234] Armstrong, D. G., Lavery, L. A., Nixon, B. P., and Boulton, A. J. M., 2004. "It's not what you put on, but what you take off: Techniques for debriding and off-loading the diabetic foot wound." *Clinical Infectious Diseases,* **39**(Supplement 2), Aug, pp. S92–S99. 94

[235] Bett, A., Prevec, L., and Graham, F., 1993. "Packaging capacity and stability of human adenovirus type 5 vectors." *J Virology,* **67:10**, pp. 5911–5921. 95

[236] Hirsch, T., and Peter, S., 2006. "Adenoviral gene delivery to primary human cutaneous cells and burn wounds." *Mol. Med.,* **12**(9-10), pp. 199–207. 97, 103, 112

[237] Mali, S., 2013. "Deliver systsmes for gene therapy." *Indian J Hum Genet,* **19:1**, pp. 3–8. 97, 98

[238] Keswani, S. G., Katz, A. B., Lim, F.-Y., Zoltick, P., Radu, A., Alaee, D., Herlyn, M., and Crombleholme, T. M., 2004. "Adenoviral mediated gene transfer of PDGF-B enhances wound healing in type i and type ii diabetic wounds." *Wound Repair Regen,* **12**(5), Oct, pp. 497–504. 97, 103

[239] Liechty, K. W., Nesbit, M., Herlyn, M., Radu, A., Adzick, N. S., and Crombleholme, T. M., 1999. "Adenoviral-mediated overexpression of platelet-derived growth factor-b corrects ischemic impaired wound healing." *Journal of Investigative Dermatology,* **113**(3), Sep, pp. 375–383. 97, 103, 112

[240] Romano Di Peppe, S., Mangoni, A., Zambruno, G., Spinetti, G., Melillo, G., Napolitano, M., and Capogrossi, M. C., 2002. "Adenovirus-mediated VEGF165 gene transfer enhances wound healing by promoting angiogenesis in CD1 diabetic mice." *Gene Ther,* **9**(19), Oct, pp. 1271–1277. 97, 103

[241] Vranckx, J. J., Yao, F., Petrie, N., Augustinova, H., Hoeller, D., Visovatti, S., Slama, J., and Eriksson, E., 2005. "In vivo gene delivery factorVEGF121 to full-thickness wounds in aged pigs results in high levels of VEGF expression but not in accelerated healing." *Wound Repair and Regeneration,* **13**(1), Jan, pp. 51–60. 97, 103

[242] Yamasaki, K., Edington, H. D., McClosky, C., Tzeng, E., Lizonova, A., Kovesdi, I., Steed, D. L., and Billiar, T. R., 1998. "Reversal of impaired wound repair in iNOS-deficient mice by topical adenoviral-mediated inos gene transfer.." *J. Clin. Invest.,* **101**(5), Mar, pp. 967–971. 97, 103

[243] Okwueze, M. I., Cardwell, N. L., Pollins, A. C., and Nanney, L. B., 2006. "Modulation of porcine wound repair with a transfected ErbB3 gene and relevant EGF-like ligands." *Journal of Investigative Dermatology,* **127**(5), Nov, pp. 1030–1041. 97, 103, 112

[244] Schultz, B. R., and Chamberlain, J. S., 2008. "Recombinant adeno-associated virus transduction and integration." *Molecular Therapy,* **16**(7), May, pp. 1189–1199. 98

[245] Branski, L. K., Pereira, C. T., Herndon, D. N., and Jeschke, M. G., 2006. "Gene therapy in wound healing: present status and future directions." *Gene Ther,* **14**(1), Aug, pp. 1–10. 98, 124

[246] Deodato, B., Arsic, N., Zentilin, L., Galeano, M., Santoro, D., Torre, V., Altavilla, D., Valdembri, D., Bussolino, F., Squadrito, F., and et al., 2002. "Recombinant AAV vector encoding human VEGF165 enhances wound healing." *Gene Ther,* **9**(12), Jun, pp. 777–785. 98, 103

[247] Keswani, S. G., Balaji, S., Le, L., Leung, A., Lim, F.-Y., Habli, M., Jones, H. N., Wilson, J. M., and Crombleholme, T. M., 2012. "Pseudotyped adeno-associated viral vector tropism and transduction efficiencies in murine wound healing." *Wound Repair Regen,* **20:4**, Jun, pp. 592–600. 98, 103

[248] Sallach, J., Di Pasquale, G., Larcher, F., Niehoff, N., Rubsam, M., Huber, A., Chiorini, J., Almarza, D., Eming, S. A., Ulus, H., and et al., 2014. "Tropism-modified aav vectors overcome barriers to successful cutaneous therapy." *Molecular Therapy,* **22:5**, Jan, pp. 929–939. 98

[249] Eming, S. A., Whitsitt, J. S., He, L., Krieg, T., Morgan, J. R., and Davidson, J. M., 1999. "Particle-mediated gene transfer of PDGF isoforms promotes wound repair." *Journal of Investigative Dermatology,* **112**(3), Mar, pp. 297–302. 98, 101, 104

[250] Hengge, U. R., Walker, P. S., and Vogel, J. C., 1996. "Expression of naked DNA in human, pig, and mouse skin.." *J. Clin. Invest.,* **97**(12), Jun, pp. 2911–2916. 101

[251] Hengge, U. R., Chan, E., Foster, R., Walker, P. S., and Vogel, J. C., 1995. "Cytokine gene expression in epidermis with biological effects following injection of naked DNA." *Nature Genetics,* **10**, pp. 1–6. 101, 104

[252] Sun, L., Xu, L., Chang, H., Henry, F. A., Miller, R. M., Harmon, J. M., and Nielsen, T. B., 1997. "Transfection with aFGF cDNA improves wound healing." *J Invest Dermatol,* **108:3**, pp. 313–318. 101, 104

[253] Jeschke, M. G., and Klein, D., 2004. "Liposomal gene transfer of multiple genes is more effective than gene transfer of a single gene." *Gene Ther,* **11:10**(10), Feb, pp. 847–855. 101, 104, 110, 112

[254] Nanney, L. B., Paulsen, S., Davidson, M. K., Cardwell, N. L., Whitsitt, J. S., and Davidson, J. M., 2000. "Boosting epidermal growth factor receptor expression by gene gun transfection stimulates epidermal growth in vivo." *Wound Repair Regen,* **8:2**, pp. 117–127. 101, 104, 112

[255] Gothelf, A., and Gehl, J., 2010. "Gene electrotransfer to skin; review of existing literature and clinical perspectives." *Curr Gene Ther,* **10:4**, pp. 287–299. 101, 110

[256] Ferraro, B., Cruz, Y. L., Coppola, D., and Heller, R., 2009. "Intradermal delivery of plasmid VEGF165 by electroporation promotes wound healing." *Molecular Therapy,* **17**(4), Feb, pp. 651–657. 101, 104, 112

[257] Lee, P.-Y., Chesnoy, S., and Huang, L., 2004. "Electroporatic delivery of TGF-beta1 gene works synergistically with electric therapy to enhance diabetic wound healing in db/db mice." *Journal of Investigative Dermatology,* **123**(4), Oct, pp. 791–798. 101, 104, 112

[258] Lin, M. P., Marti, G. P., Dieb, R., Wang, J., Ferguson, M., Qaiser, R., Bonde, P., Duncan, M. D., and Harmon, J. W., 2006. "Delivery of plasmid DNA expression vector for keratinocyte growth factor-1 using electroporation to improve cutaneous wound healing in a septic rat model." *Wound Repair Regen,* **14**(5), Sep, pp. 618–624. 101, 104

[259] Marti, G., Ferguson, M., Wang, J., Byrnes, C., Dieb, R., Qaiser, R., Bonde, P., Duncan, M. D., and Harmon, J. W., 2004. "Electroporative transfection with kgf-1 DNA improves wound healing in a diabetic mouse model." *Gene Ther,* **11**(24), Oct, pp. 1780–1785. 101, 104

[260] Gauglitz, G. G., and Jeschke, M. G., 2011. "Combined gene and stem cell therapy for cutaneous wound healing." *Molecular Pharmaceutics,* **8**(5), Oct, pp. 1471–1479. 102

[261] Potter, H., and Heller, R., 2010. "Transfection by electroporation." *Current Protocols in Molecular Biology,* **Chapter 9**, May, p. Unit 9:3. 102

[262] Vogt, P., Tompson, S., Andree, C., Liu, P., Breuing, K., Hatzis, D., Brown, H., Mulligan, R., and Eriksson, E., 1994. "Genetically modified keratinocytes transplanted to wounds reconstitute the epidermis." *Proc Natl Acad Sci U S A,* **91**, pp. 9307–9311. 103

[263] Kwon, M. J., An, S., Choi, S., Nam, K., Jung, H. S., Yoon, C. S., Ko, J. H., Jun, H. J., Kim, T. K., Jung, S. J., and et al., 2012. "Effective healing of diabetic skin wounds by using

nonviral gene therapy based on minicircle vascular endothelial growth factor DNA and a cationic dendrimer." *J Gene Med,* **14**(4), Apr, pp. 272–278. 104

[264] Tomic-Canic, M., Ayello, E. A., Stojadinovic, O., Golinko, M. S., and Brem, H., 2008. "Using gene transcription patterns (bar coding scans) to guide wound debridement and healing." *Advances in Skin & Wound Care,* **21**(10), pp. 487–492. 106

[265] Loot, M. A., Kenter, S. B., Au, F. L., van Galen, W. J., Middelkoop, E., Bos, J. D., and Mekkes, J. R., 2002. "Fibroblasts derived from chronic diabetic ulcers differ in their response to stimulation with EGF, IGF-I, bFGF and PDGF-AB compared to controls." *Eur J Cell Biol,* **81:3**, pp. 153–160. 106

[266] Seidman, C., Raffetto, J. D., Marien, B., Kroon, C., Seah, C. C., and Menzoian, J. O., 2003. "bFGF-induced alterations in cellular markers of senescence in growth-rescued fibroblasts from chronic venous ulcer and venous reflux patients." *Annals of Vascular Surgery,* **17**(3), May, pp. 239–244. 106

[267] Vasquez, R., Marien, B. J., Gram, C., Goodwin, D., Menzoain, J., and Raffetto, J. D., 2004. "Proliferative capacity of venous ulcer wound fibroblasts in the presence of platelet-derived growth factor." *Vasc Endovascular Surg,* **38:4**, pp. 355–360. 106

[268] Behm, B., Babilas, P., Landthaler, M., and Schreml, S., 2011. "Cytokines, chemokines and growth factors in wound healing." *Journal of the European Academy of Dermatology and Venereology,* **26**(7), Dec, pp. 812–820. 107

[269] Cowburn, A. S., Alexander, L. E. C., Southwood, M., Nizet, V., Chilvers, E. R., and Johnson, R. S., 2013. "Epidermal deletion of HIF-2alpha stimulates wound closure." *Journal of Investigative Dermatology,* **134**(3), Sep, pp. 801–808. 107

[270] Lin, Q., Wang, L., Lin, Y., Liu, X., Ren, X., Wen, S., Du, X., Lu, T., Su, S. Y., Yang, X., and et al., 2012. "Toll-like receptor 3 ligand polyinosinic:polycytidylic acid promotes wound healing in human and murine skin." *Journal of Investigative Dermatology,* **132**(8), May, pp. 2085–2092. 107

[271] McGee, H. M., Schmidt, B. A., Booth, C. J., Yancopoulos, G. D., Valenzuela, D. M., Murphy, A. J., Stevens, S., Flavell, R. A., and Horsley, V., 2012. "Il-22 promotes fibroblast-mediated wound repair in the skin." *Journal of Investigative Dermatology,* **133**(5), Dec, pp. 1321–1329. 107

[272] Salathia, N. S., Shi, J., Zhang, J., and Glynne, R. J., 2012. "An in vivo screen of secreted proteins identifies adiponectin as a regulator of murine cutaneous wound healing." *Journal of Investigative Dermatology,* **133**(3), Oct, pp. 812–821. 107

[273] Zhang, J., Dong, J., Gu, H., Yu, S., Zhang, X., Gou, Y., Xu, W., Burd, A., Huang, L., Miyado, K., and et al., 2012. "CD9 is critical for cutaneous wound healing through JNK signaling." *Journal of Investigative Dermatology,* **132**(1), Jan, pp. 226–236. 107

[274] Chen, L., Guo, S., Ranzer, M. J., and DiPietro, L. A., 2012. "Toll-like receptor 4 has an essential role in early skin wound healing." *Journal of Investigative Dermatology,* **133**(1), Sep, pp. 258–267. 107

[275] Emmerson, E., Campbell, L., Davies, F. C. J., Ross, N. L., Ashcroft, G. S., Krust, A., Chambon, P., and Hardman, M. J., 2012. "Insulin-like growth factor-1 promotes wound healing in estrogen-deprived mice: New insights into cutaneous IGF-1R/ERalpha cross talk." *Journal of Investigative Dermatology,* **132**(12), Jul, pp. 2838–2848. 107

[276] Vannocci, T., Faggianelli, N., Zaccagnino, S., della Rosa, I., Adinolfi, S., and Pastore, A., 2015. "A new cellular model to follow friedreich's ataxia development in a time-resolved way." *Disease Models & Mechanisms,* **8**(7), Apr, pp. 711–719. 109

[277] Manjunath, N., Yi, G., Dang, Y., and Shankar, P., 2013. "Newer gene editing technologies toward HIV gene therapy." *Viruses,* **5**(11), Nov, pp. 2748–2766. 109

[278] Malina, A., Mills, J. R., Cencic, R., Yan, Y., Fraser, J., Schippers, L. M., Paquet, M., Dostie, J., and Pelletier, J., 2013. "Repurposing CRISPR/Cas9 for in situ functional assays." *Genes & Development,* **27**(23), Dec, pp. 2602–2614. 109

[279] Belhaj, K., Chaparro-Garcia, A., Kamoun, S., and Nekrasov, V., 2013. "Plant genome editing made easy: targeted mutagenesis in model and crop plants using the CRISPR/Cas system." *Plant Methods,* **9**(1), p. 39. 109, 128

[280] Ding, Y., Jiang, Z., Saha, K., Kim, C. S., Kim, S. T., Landis, R. F., and Rotello, V. M., 2014. "Gold nanoparticles for nucleic acid delivery." *Molecular Therapy,* **22**(6), Mar, pp. 1075–1083. 110

[281] Pearton, M., Saller, V., Coulman, S. A., Gateley, C., Anstey, A. V., Zarnitsyn, V., and Birchall, J. C., 2012. "Microneedle delivery of plasmid DNA to living human skin: Formulation coating, skin insertion and gene expression." *Journal of Controlled Release,* **160**(3), Jun, pp. 561–569. 110

[282] Yan, K., Todo, H., and Sugibayashi, K., 2010. "Transdermal drug delivery by in-skin electroporation using a microneedle array." *International Journal of Pharmaceutics,* **397**(1-2), Sep, pp. 77–83. 110

[283] Heller, R., Cruz, Y., Heller, L. C., Gilbert, R. A., and Jaroszeski, M. J., 2010. "Electrically mediated delivery of plasmid DNA to the skin, using a multielectrode array." *Human Gene Therapy,* **21**(3), Mar, pp. 357–362. 110

[284] Demidova-Rice, T. N., Hamblin, M. R., and Herman, I. M., 2012. "Acute and impaired wound healing: pathophysiology and current methods for drug delivery, part 2: role of growth factors in normal and pathological wound healing: therapeutic potential and methods of delivery." *Advances in Skin & Wound Care,* **25:8**(7), pp. 349–370. 112

[285] Rajkumar, V. S., Shiwen, X., Bostrom, M., Leoni, P., Muddle, J., Ivarsson, M., Gerdin, B., Denton, C. P., Bou-Gharios, G., Black, C. M., and et al., 2006. "Platelet-derived growth factor-beta receptor activation is essential for fibroblast and pericyte recruitment during cutaneous wound healing." *The American Journal of Pathology,* **169**(6), Dec, pp. 2254–2265. 112, 125

[286] Halfon, S., Abramov, N., Grinblat, B., and Ginis, I., 2011. "Markers distinguishing mesenchymal stem cells from fibroblasts are downregulated with passaging." *Stem Cells and Development,* **20**(1), Jan, pp. 53–66. 117

[287] Kisselbach, L., Merges, M., Bossie, A., and Boyd, A., 2009. "CD90 expression on human primary cells and elimination of contaminating fibroblasts from cell cultures." *Cytotechnology,* **59**(1), Jan, pp. 31–44. 117

[288] Hu, K., 2014. "All roads lead to induced pluripotent stem cells: The technologies of ipsc generation." *Stem Cells and Development,* **23**(12), Jun, pp. 1285–1300. 122

[289] Kanczler, J. M., Sura, H. S., Magnay, J., Green, D., Oreffo, R. O., Dobson, J. P., and El Haj, A. J., 2010. "Controlled differentiation of human bone marrow stromal cells using magnetic nanoparticle technology." *Tissue Engineering Part A,* **16**(10), Oct, pp. 3241–3250. 122

[290] Santos, L. J., Reis, R. L., and Gomes, M. E., 2015. "Harnessing magnetic-mechano actuation in regenerative medicine and tissue engineering." *Trends in Biotechnology,* **33**(8), Aug, pp. 471–479. 122

[291] Huang, C.-W., Chen, H.-Y., Yen, M.-H., Chen, J. J. W., Young, T.-H., and Cheng, J.-Y., 2011. "Gene expression of human lung cancer cell line cl1-5 in response to a direct current electric field." *PLoS ONE,* **6**(10), Oct, p. e25928. 122

[292] Sheikh, A. Q., Taghian, T., Hemingway, B., Cho, H., Kogan, A. B., and Narmoneva, D. A., 2012. "Regulation of endothelial MAPK/ERK signalling and capillary morphogenesis by low-amplitude electric field." *Journal of The Royal Society Interface,* **10**(78), Sep, pp. 1–13. 122

[293] Bonazzi, D., and Minc, N., 2014. "Dissecting the molecular mechanisms of electrotactic effects." *Advances in Wound Care,* **3**(2), Feb, pp. 139–148. 123

[294] Minc, N., and Chang, F., 2010. "Electrical control of cell polarization in the fission yeast schizosaccharomyces pombe." *Current Biology,* **20**(8), Apr, pp. 710–716. 123

[295] Pullar, C., Baier, B., Kariya, Y., Russell, A., Horst, B., Marinkovich, M., and Isseroff, R., 2006. "Beta4 integrin and epidermal growth factor coordinately regulate electric field-mediated didirection migration via Rac1." *Molecular Biology of the Cell,* **17**, pp. 4925–4935. 123

[296] Rajnicek, A. M., 2006. "Temporally and spatially coordinated roles for Rho, Rac, Cdc42 and their effectors in growth cone guidance by a physiological electric field." *Journal of Cell Science,* **119**(9), May, pp. 1723–1735. 123

[297] Sato, M. J., Kuwayama, H., van Egmond, W. N., Takayama, A. L. K., Takagi, H., van Haastert, P. J. M., Yanagida, T., and Ueda, M., 2009. "Switching direction in electric-signal-induced cell migration by cyclic guanosine monophosphate and phosphatidylinositol signaling." *Proceedings of the National Academy of Sciences,* **106**(16), Apr, pp. 6667–6672. 123

[298] Zhao, M., Song, B., Pu, J., Wada, T., Reid, B., Tai, G., Wang, F., Guo, A., Walczysko, P., Gu, Y., and et al., 2006. "Electrical signals control wound healing through phosphatidylinositol-3-OH kinase-gamma and PTEN." *Nature,* **442**(7101), Jul, pp. 457–460. 123

[299] Konermann, S., Brigham, M. D., Trevino, A. E., Joung, J., Abudayyeh, O. O., Barcena, C., Hsu, P. D., Habib, N., Gootenberg, J. S., Nishimasu, H., and et al., 2014. "Genome-scale transcriptional activation by an engineered CRISPR-Cas9 complex." *Nature,* **517**(7536), Dec, pp. 583–588. 124

[300] Yamanaka, S., 2009. "A fresh look at iPS cells." *Cell,* **137**(1), Apr, pp. 13–17. 128

[301] Rodriguez-Piza, I., Richaud-Patin, Y., Vassena, R., Gonzalez, F., Barrero, M. J., Veiga, A., Raya, A., and Izpisua Belmonte, J. C., 2009. "Reprogramming of human fibroblasts to induced pluripotent stem cells under xeno-free conditions." *Stem Cells*, pp. 36–44. 128

[302] Nakagawa, Y., Sakuma, T., Sakamoto, T., Ohmuraya, M., Nakagata, N., and Yamamoto, T., 2015. "Production of knockout mice by DNA microinjection of various CRISPR/Cas9 vectors into freeze-thawed fertilized oocytes." *BMC Biotechnol,* **15**(1), May, pp. 1–10. 128

[303] Pelletier, S., Gingras, S., and Green, D. R., 2015. "Mouse genome engineering via CRISPR-Cas9 for study of immune function." *Immunity,* **42**(1), Jan, pp. 18–27. 128

[304] Hsu, P. D., Lander, E. S., and Zhang, F., 2014. "Development and applications of CRISPR-Cas9 for genome engineering." *Cell,* **157**(6), Jun, pp. 1262–1278. 128

[305] Xing, H.-L., Dong, L., Wang, Z.-P., Zhang, H.-Y., Han, C.-Y., Liu, B., Wang, X.-C., and Chen, Q.-J., 2014. "A CRISPR/Cas9 toolkit for multiplex genome editing in plants." *BMC Plant Biology,* **14**(1), p. 327. 128

[306] Lowder, L. G., Zhang, D., Baltes, N. J., Paul, J. W., Tang, X., Zheng, X., Voytas, D. F., Hsieh, T.-F., Zhang, Y., and Qi, Y., 2015. "A CRISPR/Cas9 toolbox for multiplexed plant genome editing and transcriptional regulation." *Plant Physiol.,* **169**(2), Aug, pp. 971–985. 128

[307] Lin, S., Staahl, B. T., Alla, R. K., and Doudna, J. A., 2014. "Enhanced homology-directed human genome engineering by controlled timing of crispr/cas9 delivery." *eLife,* **3**, Dec. 171

APPENDIX A. MATERIALS AND PROTOCOLS

The following appendix was constructed to serve as a resource for important material preparations and protocols used in the lab.

A.1 Calcium Phosphate Transfection Protocol

The following protocol was originally obtained from Caleb Cornaby and modified as better techniques were identified through experimentation. It is worth noting, this protocol is designed to transfect several different cell lines. In my experimentation, HeLa cells have been the target cell of choice. While this is not an optimized protocol for HeLa cells, it is very effective in transfecting HeLa cells both in terms of modification rate and cell survival.

As an aside, calcium phosphate transfection operates on the basis of getting a salt to precipitate around DNA molecules. These conjugates then are taken into the cell (through an unknown mechanism but it is believed to be pinocytosis-like) where the salt is dissolved away and the DNA can then be incorporated into the host's genome.

A.1.1 Cell Preparation: Materials List

- 6-Well Plate
- DMEM

A.1.2 Cell Preparation (-1 Day)

- Prepare 6 Well-Plate by placing approximately $30 * 10^6$ cells into each well. Recommended method: Using cells from cell passaging after 4 days growth in flask, 100-120 μL per well.
- Add 1 mL of DMEM media to each well.
- Incubate for 24 hours at 37C, 5% carbon dioxide.

A.1.3 Transfection: Materials List

This protocol makes enough solution for 8 total treatment wells on 6 Well-Plate (Makes it convenient so that you can have non-treated wells next to treated wells.)

- 7.5 mL DMEM (warmed to 37C)
- Chloroquine (25 mM stock)
- 50 mL conical tube
- 1.5 mL Eppendorf Tube
- HBS (Hepes Buffered Solution) (2x, pH 7.0): Note pH is critical.
- Sodium Phosphate (75 μM, 100x)
- Calcium Chloride (2.5 M)
- DNA
- dH20 (de-ionized water)
- 10 mL serological pipet
- 5 mL serological pipet

For material preparation for this section, refer to the end of the Calcium Phosphate Transfection protocol.

A.1.4 Transfection Prep (0 Day)

Prior to transfection, remove the 6 Well Plate from the incubator to examine cells under the microscope to determine the degree of cell confluency (how much space exists between cells). Approximately 40-60% confluency is desired. If there are too many cells, the transfection efficiency will be lower than desired because successful Calcium Phosphate transfection requires cell division for the DNA to enter the intermittently dis-assembled cell nuclear membrane. Cell division requires available space for the cells to grow.

A.1.5 Transfection (0 Day)

Performed under a Hood

1. Put 7.5 mL of DMEM into the 37 C water bath so it is warm by Step 9.
2. Remove 6 Well Plate from the incubator, remove old media from the day before and replace with 1 mL of DMEM in each well (this is not the warmed DMEM).
3. Treat each well in 6 Well Plate with: 2 μL of Chloroquine (that is 2 μL of chloroquine per 1 mL of media). (This is a critical step because the Chloroquine acts to transiently inhibit lysosomes from degrading the DNA introduced through the transfection.)

   Once Chloroquine placed, let it sit for at least 5-10 minutes (up to 3 hrs is fine) while preparing transfection reagents. Swirl gently and put the plates back in the incubator while performing the next steps.

4. Mix the following using 50 mL conical tube and 1.5 mL Eppendorf Tube:

   In the 50 mL Conical Tube: 500 μL HBS (2x, pH 7.0) + 10 μL Sodium Phosphate (100x).

   In the 1.5 mL Eppendorf Tube: 62.5 μL Calcium Chloride (2.5 M) + 12500 ng of DNA + dH20 (enough dH20 to make the total volume of fluid in the Eppendorf Tube to equal 500 μL total)

   Note: To clarify the mass of DNA added, consider the following example:

   Given a DNA concentration of: 2497 ng/μL, in order to have 12500 ng of DNA, it requires 5 μL of DNA [ie (12500 ng)*(2497 ng/μL)] Thus adding 5 mL of DNA to the 1.5 mL Eppendorf Tube is enough for transfecting the 8 total wells.

   Intermediate Transfection Mix

5. Take the 50 mL Conical Tube and place the 5 mL serological pipet tip into the fluid and begin blowing a constant stream of air into the fluid creating bubbles. **THIS IS CRITICAL – IF THERE IS NOT A CONSISTENT STREAM OF BUBBLES THE ENTIRE PROCEDURE WILL FAIL.**

6. In the other hand, pull all of the fluid of the 1.5 Eppendorf Tube into a micro-pipet tip and slowly, drop-wise add to the bubbling fluid in the 50 mL Conical Tube – this is the **Intermediate Transfection Mix**.

7. Following mixture of the solutions, wait for 15 minutes (up to 30 minutes is fine).

8. Remove 6 Well-Plates from the incubator and remove the chloroquine-containing media from each well in the 6 Well Plate.

   Final Transfection Mix

9. Take the 7.5 mL of warmed DMEM and invert the container several times to mix solution.

   Add 1 mL of the **Intermediate Transfection Mix** to the warmed DMEM, creating a total of 8.5 mL of solution creating the **Final Transfection Mix**.

10. Add 1 mL of the **Final Transfection Mix** to each treatment well of the 6 Well-Plate. Use all of the transfection mix if there is extra.

11. Incubate at 37 C, 5% CO2 for 1 day. Check for expression on inverted fluorescent microscope.

A.1.6 Material Preparation Appendix

HBS (HEPES Buffered Solution, 2x)

1. Weigh out the following ingredients: 8.0 g NaCl, 0.37 g KCl, 0.099 g Na2HPO, 1.0 Dextrose (D-glucose), and 5.0 g HEPES.

2. Dissolve the dry ingredients into 450 mL of H20, adjust the pH to 7.04 to 7.06. Note: **This is a critical balancing step for transfection to work.**
3. Fill the container with 50 mL more of H20, bringing the total fluid content to 500 mL. Recheck the pH to make sure it is still 7.04 to 7.06.
4. Autoclave.
5. Store at Room Temperature.

Calcium Chloride (2.5 M, CaCl2)

1. Weigh out the following ingredients: 0.238 g HEPES, 27.75 g CaCl2.
2. Dissolve the dry ingredients in 90 mL of H20, adjust the pH to 7.2.
3. Fill the container with 10 mL more of H20, bringing the total fluid content to 100 mL. Recheck the pH to make sure it is still 7.2.
4. Autoclave.
5. Store at Room Temperature.

Sodium Phosphate (75 μM)

1. Take stock solution and dilute to 75 μM.
2. Autoclave.
3. Store at Room Temperature.

Chloroquine

1. Order 25mM solution.
2. Aliquot if desired.
3. Store in fridge.

A.2 Cell Passaging and Plate Prep for Injections

Several different cell types have been used in the lab recently (i.e. HeLa 229, RPE, HEK, and BJ Fibroblasts). The following protocol is a general process for passaging these cells and pearls fo wisdom for getting good growth results. **It should be noted that for good results with any cell culture, a consistent pattern for passaging in terms of days since the previous passaging, cell confluency at the time of passaging, and the quality of cell growth media are critical.** (Note:

Most failures for good growth of cell cultures is directly related to one of these three items. True cell culture contamination is rare if a researcher uses sterile technique.)

In order to provide these details concisely, a simple list of important materials (Note: Some items will not be listed for convenience sake. It is assumed that the reader is aware of sterile technique in a cell culture hood and basic lab procedures.) and a detailed list of procedural steps are provided below.

A.2.1 Materials

- Sterile Dulbeccos Modified Eagle Medium (DMEM)(with 10% FBS and penicillin/streptomycin). Note: If you are working with RPE (retinal pigmented epithelial) cells, then F12 FBS must be used. Also, for all FBS solutions mixed with DMEM used for cell culturing, the FBS must undergo heat inactivation of the complement, otherwise it can be problematic for proper cell growth. Heat Inactivation will be covered in this appendix.)
- Sterile Phosphate Buffered Solution (PBS)
- Sterile 5x Trypsin ($\approx$ 2.5 mL)
- T75 Flask of cells to be passaged
- Pipette-aid
- Waste beaker
- serological pipettes for fluid transfer
- 6-Well Plate with 18mm x 18mm glass slides placed into each well

A.2.2 Protocol

The following protocol should be performed in a cell culture hood using sterile technique. Prior to every passage event, you must look at the cell cultures under a microscope to access two major items. First, you want to see if how many of the cells are living. If it has been several days since the last passaging event, the cells may begin to die, which means they will shrink and darken. Depending on how many cells are dead, it may not be worth the time and expense to passage the cells. It is absolutely critical, particularly if you are in an experimental stage of research, to be consistently passaging the cells (i.e 3-4 days). Otherwise, the cells can go into a quiescent state – and once there, they are super hard to transfect. Second, you want to see how confluent or densely spaced the cells are. This will provide key incite into how much to dilute cells during the passaging or plating process. I my experience, cell confluency during plate prep is critical – too much and the transfection efficiencies are low because the cells aren't able to grow; and too little, and the cells typically died.

1. Spray hands and all materials use for passaging with ethanol before placing into the hood. Prior to opening sterile containers or handling cell cultures, items in the hood need to be

UV sterilized, so Place all items (except liquids and flask of cells) into the clean hood and turn on the UV for at least 15 minutes. For proper material handling, have a place for sterile solution containers on one side and disposeable items and waste containers on the other.

2. Once items are sterilized, place fluid solutions and cell culture in the hood, having sprayed them with ethanol before placing in the hood.

3. Using a 25mL pipette, remove the old media from the flask and discard into waste beaker

4. Using a new 10mL pipette, add 10 mL PBS solution to the flask to help rinse unbound or loosely bound cells into solution. Depending on the cell type you are working with, different levels of care must be taken at this step. For HeLa, RPE, and BJ Fibroblasts, a gentle rinse is perfectly fine for the cell cultures. For HEK cells, you must be very careful to not rinse the entire culture into solution because there are much more loosely bound. Do not do more than a gentle tilting of the flask with HEK cells.

5. Using the 5 mL pipette, add 2.5 mL Trypsin to the flask. (The trypsin enzymatically cleaves adhesion proteins between cell cultures and the flask surface.)

6. Place the flask in the incubator for 3-5 minutes. For HeLa and RPE cells, a full five minutes is required for cells to be trypsinized. For HEK cells, 3 minutes is plenty. For BJ Fibroblasts, 4 minutes is enough – however, if the cells are overgrown a great deal, it can be difficult to get good cell separation because fibroblasts love to cluster.

   Note: It should be recognized that trypsin is indiscriminate as far as what proteins it cleaves, so depending on what kind of experiment you are running, you may elect for cell scraping rather than trypsin for cell removal from the flask. Also note, over trypsinized some cell types can kill the cell of interest.

7. Remove flask from incubator.

   For HeLa and RPE cells, swirl the solution in the flask until all cells are no longer adhered. HeLa cells in particular are very adherent cells and may require you to hit the flask against the work-surface to break the cells up. After that, use a pipette to and pipette up and down a portion of the fluid to ensure break up of the cell clusters.

   For HEK cells and BJ Fibroblasts, once you remove the flask from the incubator, gently swirl the cells. That should be enough to break the cells loose. Then slowly pipette up and down a portion of the fluid to ensure break up of the cell clusters. **If you hit the flask containing BJ Fibroblasts against the work-surface like you would a HeLa flask, you will kill the cell culture – BE VERY CAREFUL WITH BJ FIBROBLASTS AT THIS STAGE.**

   Note: An excellent trypsinized cell culture has a cloudy, white appearances, with no visable cell clumps.

   IMPORTANT: This step is a vulnerable step for the cell's survival, rapidly finish this step and move to the next step.

8. Using a 10 mL pipette, add 7.5 mL DMEM media to the flask. Note: The DMEM media contains FBS, which serves to de-activate the trypsin. Once the DMEM is placed into the

flask, use the same pipette to thoroughly mix the solution to ensure proper mixture and de-activation of the trypsin.

9. Pull all the cell solution back into the 10 mL pipette. At this point, you can use the 10 mL solution containing your cell culture for plate prep for Nanoinjection or for freezing back cells for later use.

10. Add desired amount of cell solution back to the flask (i.e. for a 1:20 ratio, put 0.5 mL back; for a 1:2 ratio, put 5 mL back)

11. Discard remaining cell solution into waste beaker if not using any cells for injection or freezing cell back.

12. Once the desired amount of cell solution is added back to the flask, use a 25 mL pipette and add enough DMEM to the flask to bring the total amount of solution to $\approx$ 20 mL.

13. Label the flask with the date and amount returned to the flask. Place flask back into incubator, being sure to loosen the lid to allow CO_2 access.

14. Clean up materials and wipe down hood with ethanol

A.2.3 Plate Preparation

For proper plate preparation prior to injection, the following steps should be taken the day before injections are planned.

1. Follow the cell passage protocol up to the point where you have cells in solution. At this point, transfer roughly 1.5 to 2 mL of cell solution (per 6-well plate) to a 10 mL conical tube. Depending on how concentrated the cells are and how confluent you need your cells for injection, you will need to add DMEM to the conical tube to get the proper concentration of cells for proper plate prep. **This step cannot be over-emphasized. Knowing exactly how much to dilute the cells for this step takes experience and serial testing. Simply guess how much to dilute the cells is not a great use of time.**

2. Once proper dilution of the cells in the 10 mL conical tube is achieved, take 120 μl of cell solution from the tube and place in the center of each glass slide in the bottom of the individual 6-Well Plate.

3. Following completion of seeding each well's glass slide, place the 6-Well Plate(s) into the incubator.

4. After 1-2 hours, remove the 6-Well Plates from the incubator and provide 2 mL of DMEM/FBS growth media to the cells. Return the cells to the incubator for the night. The plates are ready for injection the next day.

A.3 Solution Material Preparation

All media preparation must be performed in the sterile hood. Non-fluid supplies should be UV sterilized for 15 minutes prior to the aliquoting of fluids.

A.3.1 Trypsin Preparation

Trypsin is frequently used in the lab in the context of 6-Well-based experimentation. The following is a protocol used to aliquot trypsin for those uses.

Materials

- New 100 mL bottle of 10X Trypsin (thawed)(Sigma brand, Chem Stockroom)
- Phosphate Buffered Solution (PBS, Chem Stockroom)
- (x17) 15 mL conical tubes
- (x1) 10 mL serological pipettes
- (x3) 25 mL serological pipettes

Protocol

1. Using the 10 mL pipette, add 6 mL 10X Trypsin to 16 of the tubes
2. Using the same 10 mL pipette, add remaining 10X Trypsin to the final tube
3. Using a 25 mL pipette, add 6 mL PBS solution to each tube already containing 6 mL Trypsin (use a new 25 mL pipette each time PBS is needed and always fill to the 35 mL line)
4. Add PBS solution to the final tube until the Trypsin is diluted 1:1
5. Label tubes: Date of Preparation, 5x Trypsin, and Initials of Person that Prepared
6. Place tubes in -20C Freezer

A.3.2 Fetal Bovine Serum (FBS) Preparation

FBS can contain complement proteins that can be damaging to cell cultures and requires heat inactivation to prevent that from happening. The followin protocol provides details on how to do that and aliquot the solutions in preparation for DMEM growth media prep.

Materials

- New 500 mL bottle of FBS (thawed, Chem Stockroom)
- (x9) 50 mL conical tubes
- (x8) 15 mL conical tubes

Protocol

1. Heat in-activate the FBS (FBS) by warming FBS is 57C water bath for 1 hour. Be aware that the FBS will come in a frozen bottle. It takes time to just de-frost the bottle and then heat it to 57C. **Do not let the FBS sit at 57C more than 4 hours – it will cause the proteins to become gelatinous – a big problem for testing. Since FBS is expensive, you must watch this carefully.**
2. Allow FBS to cool to room temperature. This can take a couple hours.
3. In the hood, pipette 50 mL FBS to 8 of the 50 mL tubes and 5 mL FBS to the eight 15 mL tubes.
4. Label tubes and place tubes in -20C Freezer.

A.3.3 DMEM Growth Media Preparation

Materials

- Un-opened 500 mL bottle of DMEM (Chem Stockroom)
- 55 mL thawed fetal bovine serum (FBS, Chem Stockroom): (1) 50 mL tube* + (1) 5 mL tube aliquots*
- Penicillin/Streptomyocin (Chem stockroom): (1) 5 mL aliquot of 10,000 U/mL penicillin/streptomyocin
- **L-Glutamine (200 mM, online order): (1) 5 mL aliquot (Sigma G7513, 100 mL)

NOTES:
*Indicate supplies that were pre-prepared following protocols specific to their preparation
**L-Glutamine needs to be added to media solutions if the media is not being used quickly; L-Glutamine is an essential amino acid and degrades over time, by providing extra, the cells are able to have nutrition to continue growth

Protocol

1. Thaw heat inactivated FBS (total 55 mL) to Room Temperature.
2. Thaw Penicillin/Streptomyocin and L-Glutamine aliquots to room temperature.
3. Spray containers with alcohol (70%) and place in hood
4. Under the hood, combine the FBS (55 mL), Penicillin/Streptomyocin, and L-Glutamine to the 500 mL of DMEM.
5. Secure media container cap, slightly agitate the media solution, label, and remove from hood
6. Place media container in refrigerator for storage.

APPENDIX B. ATTEMPTED EXPERIMENTS THAT YIELDED NO CONCLUSIONS

The following details experiments that were attempted but produced no conclusions for various reasons. These details are presented here merely as a cataloging of the attempts and results.

B.1 The Effects of Cell Synchronization on the Efficiency of Lance Array Nanoinjection on HeLa Cells

Introducing exogenous genetic material into target cells and getting a prescribed expression is the core principle of gene therapy. In effort to facilitate delivery of these loads, several mechanisms have been developed and include a technology previously described as Lance Array Nanoinjection (LAN). In brief, LAN utilizes a combination of physical penetration of the cell membrane with micron-sized silicon etched lances and electrical release of the desired molecular load (i.e. DNA) off of these lances.

In prior research, it was demonstrated with a single lance injector that during the electrical release procedural step that localized electroporation occurs at the nuclear membrane, allowing transient access of the molecular load to the nucleus and consequently causing genetic transformation of the target cell [27].

In this work, it is hypothesized that LAN uses a similar localized, nuclear electroporative mechanism as the single lance nanoinjector and that by using a CAG/GFP plasmid, non-dividing HeLa cells can be successfully transfected to become GFP positive. In order to demonstrate this mechanism, target HeLa cells will be stalled in G0/G1 phase as a way to have target cells in a non-dividing state and fully intact nuclear membrane. This aspect of investigating the capabilities of LAN is considered of value because of the intent to demonstrate LAN as a viable technology in the in situ context where cells may not be dividing quickly.

Secondarily, it is hypothesized that HeLa cells synchronized via thymidine to S and G2 phases will have different transfection efficiencies from G0/G1 for two reasons. First, in S-phase, the cell is actively undergoing DNA replication and as such more likely to incorporate exogenous DNA due to inconsistency that arise during replication. The nuclear membrane is still intact during S-phase and therefore, relative transfection efficiencies discovered for S-phase when compared to G0/G1-phase will elucidate potential transfection events required/occurring with LAN. Second, in late G2-phase, nuclear membranes will breakdown right prior to cell division and act as a window of opportunity for exogenous DNA to enter and later be incorporated into the genome. During late G2-phase, DNA replication has stopped such that cell division can occur. As noted with S-

Table B.1: Cell Cycle and Transfection Rate Predictions

Phase	Nuclear Membrane	DNA Replication
G1/GO	Intact	Inactive
S	Intact	Active
Late G2	Dissolved	Inactive

phase, relative transfection efficiency discovered with G2-phase will indicate transfection events required/occurring with LAN.

B.1.1 Design of Experiment

The experiment will be divided into three sections as follows:

- **Stage 1:** Characterizing the Cell Cycle of Sample Population following Synchronization (Calibration Curve Creation)

  The intent is to synchronize HeLa cell samples using proximity growth inhibition (G1/G0) and thymidine (other phases) to determine the time required to get the cells to reach S-phase and Late G2-phase after release from being stalled. To help establish this calibration curve, the cells will be fixed and stained with propidium iodide every 2 hours for tens hours. Based on prior research, ten hours should be long enough to have the cells go through a complete cell division (4).

  Outcome: Stage 1 is anticipated to give us an idea of what stage the cells should be in at a specific time post-release from having their growth stalled. This will serve as a calibration curve for the LAN treatment samples.

- **Stage 2:** Lance Array Nanoinjection at specific Synchronized Cell Cycles The intent in Stage 2 is to test both hypotheses noted above in regards to LAN and the cell cycle using a CAG/GFP plasmid.

  Consideration: A potential direction that could be added to this stage is performing a similar test using a CRISPR to see if cell cycle stage is a factor in transfection rate.

B.1.2 Methods

- Stage 1: Calibration Curve

  As noted previously, it is anticipated that samples taken every 2 hours following release from two different growth stalling techniques will be used.

  Step 1: G1/G0 Stall

  Proximity Growth Inhibition or Density Arrest keeps the cells in G1. Once cells have been stalled, cells will be fixed, treated with RNAse A, stained with Propidium Iodide, and run

Table B.2: Stage 1: Cell Synchronization

Well	Type	Purpose
1	Non-treated Control	Normalized Cell Viability
2-6	Treated Samples	Determine cell cycle stage after x hrs post-release

through flow cytometry. The results will be analyzed in a third-party software call Flowjo to determine relative amounts of cells in respective phases. Once a clear determination of what protocol is required to achieve the desired G1/G0 stall, Stage 2 will be ready to perform on these non-dividing cells.

Protocols: Proximity Growth Inhibition: Contain below, Fixation: Contain below, Staining: Contain below, Flow: Samples will be run on the Attune flow cytometer, Post-Flow Analysis: Requires the FCS files from Flow. Dr. Weber has offered the use of Flowjo for this step.

It is anticipated that we will need approximately 15 samples per cell cycle time.

- Step 2: G1/S Phase Synchronization and Calibration

  Using excess thymidine, cells will be stalled at the beginning of S-phase. Following release from this point, cells will be fixed and prepared for flow cytometry at 2 hour intervals. The intent is to correlate time elapsed from growth cycle stall release to DNA content via PI intensity signal. Once a clear determination of time required to achieve desired cell growth of a sample population is known, Stage 2 will be ready to perform.

  Protocols: Thymidine Growth Inhibition: Contain below, Fixation: Contain below, Staining: Contain below, Flow: Samples will be run on the Attune flow cytometer, Post-Flow Analysis: Requires the FCS files from Flow. Dr. Weber has offered the use of Flowjo for this step.

  It is anticipated that we will need approximately 15 samples per cell cycle time.

Total samples required for Stage 1: 150 samples
The following protocol is an outline of how to prepare a 6-well plate for testing in Stage 1.

B.1.3 Protocols: Thymidine Growth Inhibition from (Yoshizawa2014)

In this protocol, HeLa cells are treated with thymidine twice sequentially with an interval in between the treatments. Highly synchronous cell cycle populations can be obtained with this method. For tips on the release from the first block and optimization of the protocol for other cells lines, see Notes 2 and 3.

(Prep Day 1: 4 PM) Cell Preparation and First Thymidine Block (0 to 16 hrs)

- Culture HeLa cells in a 10-cm dish until 2530% confluency is achieved.
- Add thymidine to a final concentration of 2.5 mM and incubate at 37 C for 16 h.

(Prep Day 2: 8 AM) First Release (16 hrs to 25 hrs)

- Wash cells twice with 3 mL of pre-warmed PBS or serum-free DMEM.
- Add pre-warmed medium with serum and release cells into cell cycle at 37 C for 9 h. Note: For better synchronization, keep cells warm during the wash and handle only a small number of dishes at one time (at most 45 dishes).

(Prep Day 2: 5 PM) Second Thymidine Block (25 hrs to 39/41 hrs)

- Add thymidine to a final concentration of 2.5 mM and incubate at 37 C for 1416 h.

(Prep Day 3: 7 AM) Second Release (39/41 hrs to Desired Time Post-Release starting from Early S-Phase)

- Wash cells twice with 3 mL of pre-warmed PBS or serum-free DMEM.
- Release cells at 37 C as in step 4 and harvest cells at Desired Time Post-Release starting from Early S-Phase.

Cell Preparation (Treatment: Day 1)

- Synchronize cells to the desired stage of growth.
- Seed 10^6 HeLa cell/ml in 2 mL of DMEM of 6-well plate. Incubate for 24 h (For monolayers; no need to incubate for suspension cells).

Fixation (Treatment: Day 2)

- Remove DMEM from each well and rinse wells with 1.5 mL of PBS and discard PBS.
- Harvest the cells by trypsinizing (for monolayers) by adding 0.5 mL trypsin per well and then incubate for 5 minutes.
- After incubation, add 1 mL of DMEM to each well to de-activate the trypsin.
- Place cell solution (1.5 mL) in Eppendorf tube. Centrifuge the cells at 200 x g for 5 minutes at 4 0C. (If Desired, count the cells to find out total number of cells.)
- Following centrifugation, remove supernant.
- Wash cells by centrifugation (200 x g, 5 min, 4C) in 1 mL PBS in each Eppendorf Tube.
- Remove PBS supernant.
- Resuspend at 2 x 106 cells in 1 ml ICE COLD PBS.

- Take 9 mL of 70% Ethanol (in a 15 ml polypropylene centrifuge tube) and Vortex gently while slowly adding dropwise the ICE COLD PBS cell suspension.
- Store at 4C for AT LEAST 2 hours, 12 - 24 hours is best.

(Treatment: Day 2 or Day 3) Staining with Propidium Iodide (PI)

- Centrifuge the tube at 200 x g, 10 min, 4C to pellet the cells.
- Wash cells at least once with COLD PBS. Cells may form a diffuse ring-shaped pellet, so centrifuge longer (e.g. 200 x g, 10 min, 4C)
- Resuspend cells in 400 μl of Staining Solution and transfer to FACS tube.
- Incubate at 37C for 15 minutes, cover in aluminum to limit light exposure.
- Acquire data on flow cytometer

FlowJo (Post-Analysis)

Utilize FlowJo software from Dr. Webber to determine percentage of cells in each phase.

Material Preparation

DNAse free RNAse-A

RNAse A comes in a powder form and may not actually be purified. In the case of the experiments performed with Cell Synchronization, the RNAse A needs to be free of DNAse that would potentially break down chromosomal DNA, and thereby confounding the flow cytometry results.

- Prepare a 10 mg/mL stock solution of RNAse A powder in 10 mM sodium acetate buffer, pH 5.2.
- Heat to 100C (boiling) for 15 minutes, allow to cool to room temperature.
- Adjust pH to 7.4 using 0.1 volume of 1 M Tris-HCl, pH 7.4.
- Aliquot and store at -20C.

Note: If RNase A is boiled at a neutral pH, precipitation will occur. When boiled at the lower pH, some precipitation may occur because of protein impurities that are present. When Sigma tests the activity of RNAse A, a stock solution is prepared in water at 1 mg/ml.
Storage Instructions

- Store at RNase A at 20 C. Stock solutions stored in frozen aliquots remain active for at least 6 months.
- RNase A is a very stable enzyme and solutions have been reported to withstand temperatures up to 100 C.

- At 100 C, an RNase A solution is most stable between pH 2.0 and 4.5.9
- A major application for RNase A is the removal of RNA from preparations of plasmid DNA. For this application, DNase free RNase A is used at a final concentration of 10 (g/ml).10
- Note: RNase A is stable to both heat and detergents. In addition, it adsorbs strongly to glass. Scrupulous precautions are necessary to ensure RNase A residue does not cause artifacts in processes requiring intact RNA.

B.1.4 Materials

- DMEM
- PBS
- Trypsin
- Eppendorf Tubes
- ICE COLD PBS
- Triton X-100
- Staining Solution: To 10 ml of 0. 1% (v/v) Triton X-100 (Sigma) in PBS (meaning 10 μl of Triton X in 10 mL of PBS); Add 2 mg DNAse-free RNAse A (Sigma) and 0.40 ml of 500 μg/ml PI; Store the left over at -20C covering the tube with tin foil.

Stalling and Cell Cycle Characterization
Double Thymidine Block Protocol

1. Tips on the release from the first block: For better synchronization, keep cells warm during the wash and handle only a small number of dishes at one time (at most 45 dishes or wells).
2. Culture cells in a 6-well plate until 25-30% confluency is achieved on 22mm glass slide with 2mL of DMEM included in each well
3. Add thymidine to a final concentration of 2.5 mM and incubate at 37 C for 16 h.
    - Use the following formula to determine the amount of thymidine stock solution to be added where T(mL) is the amount of thymidine stock solution to be added to Y(mL) amount of media in the well.
    - 0.0025((mg/mL))=(0.100((mg/mL)) * T(mL))/(Y(mL)+ T(mL))
    - Solving for T yields: T(mL)= ((0.0025*Y)/0.0975)
4. Wash cells twice with 0.4 mL of pre-warmed PBS or serum-free DMEM.
5. Add pre-warmed medium with serum and release cells into cell cycle at 37 C for 9 h.

Table B.3: Phase Injections

Well	Type	Purpose
1	Negative	No treatment
2	Block	Double Thymidine Block
3	Positive	Blocked, DNA added
4-6	Injected Sample	Blocked, DNA, Injected

6. Add thymidine to a final concentration of 2.5 mM as explained in Step (4c) and incubate at 37C for 1416 h.

7. Wash cells twice with 3 mL of pre-warmed PBS or serum-free DMEM.

8. Release cells at 37C as in Step 4

Cell Cycle Characterization

Use the cell cycle staining protocol above to determine the results of the stalling as well as track the cells as they progress through the cell cycle. Based upon previous research, HeLa cells released following a double thymidine block will progress through the cycles after the hours specified: S phase 0-4 hours, Enter G2 phase 5-6 hours, Mitosis 7-8 hours, Re-enter S Phase 14-16 hours. This data may be verified by performing the cell cycle staining procedure at various time intervals following release from the double thymidine block.

Phase Injection

Variables will be: Voltages 3, 5, 7, 9; Cell Cycle Phase
Plates

- Utilize 4 plates per experiment run
- Repeat each plate with the same sample types as described above, producing approximately 12 samples per experiment run.
- Repeat experiment twice per voltage setting for each cell cycle phase: Phases (4) S, G2, M, G1/G0; Voltages (4) 3, 5, 7, 9; If two trials of each combination, 32 trials are needed.

B.1.5 Reasons for Experiment Abandonment

In conjunction with an undergraduate researcher, we proposed this work and received an ORCA grant to pursue the work. At the time, I had just begun my research into using CRISPR-Cas9 plasmids and it was proposed once we had started this work to implement CRISPR into this project, thereby investigated when in the cell cycle cells are most likely to incorporate exogenous DNA.

The challenge with this project was about a month and a half into it, in conducting a literature search, I discovered that another group was conducting the same research and published

while we were still in the middle of this project [307]. At that point, it was determined that other research questions were of value and this project was abandoned.

B.2 Electrostatic Attraction of DNA

An important element of the Lance Array Nanoinjection (LAN) process is described as electrostatically attracting DNA from solution onto a series of micron-sized lances, most commonly etched from silicon. This step is of particular interest because the relative factors that affect the amount of DNA that can be accumulated onto the lance array is largely unknown. Recently, Nick Gregory (Nick2015) demonstrated that using LAN and radio-tagged DNA strands, that approximately 50,000 DNA strands are delivered to each target cell during LAN (using a linearized plasmid of 5551 bp at 250 ng/mL of injection solution). These findings strongly suggest that LAN is electrically attracting the DNA onto the lances, however, these findings are not definitive. Because this step is critical to the process of introducing exogenous DNA into the cell, it is imperative that this area of LAN is explored more completely.

B.2.1 Previous Work

In previous work done with the Single Lance Nanoinjector (SLN) [26], it was shown that in an attraction period of 5 minutes 46 seconds, that over 32,000 DNA plasmids of 4700 bp was accumulated onto the single lance (DNA concentration: 1-2μL of 306 ng/μL). In order to get this outcome, +1.5 VDC was applied to the solution with the understanding that by keeping the electrical attraction below decomposition voltage that oxidative damage cannot occur to the MEMS device.

Unfortunately, after having a conversation with Quentin Aten about his testing, it was discovered that the results of the testing making up this paper to be suspect. Dr. Aten could not replicate the results of this paper following experimentation at Nanoinjection LLC. The problem with previous experimentation is believed to be a result of a couple factors. First, during voltage application to an ionic solution, the electrode immediately following the application of a voltage collected oppositely charged ions. As these ions collect, the current in the solution diminishes exponentially. Because the current drops off so quickly, the ability to actually pull DNA out of the ion-rich solution is reduced significantly. Second, the use of voltages above the decomposition voltage results in electrolysis or separation of water into hydrogen and oxygen. This becomes problematic because the bubble formation on the electrodes causes disruption to potentially accumulating DNA molecules. Therefore, a way needs to be created to construct a barrier between the electrode and bubble formation events (particularly on the negatively charged electrode) to diminish this effect.

B.2.2 Hypothesis:

It is hypothesized that DNA can be attracted from an aqueous solution using current controlled application to a metal electrode using DAPI as an indicator stain for the DNA (at DNA concentrations appropriate to standard transfection protocols: 250 to 750 ng/mL of injection solution)

- If that is true, it is further hypothesized that the larger the attraction current, the greater the amount of DNA attraction to the associated electrode.
- If that is true, it is further hypothesized that attraction can occur in a variety of solution types (particularly biologically relevant solutions) including: PBS and DMEM.
- If that is true, it is further hypothesized that DNA transfer can occur following a successful attraction event to a new DNA-free solution and quantified.

B.2.3 Methods

Equipment:

- Zeiss Imager A.1 Fluorescence Microscope
- Settings: Exposure time, saturation, linear brightness scaleo
- Light filter: blue
- Image capture: only at imaging times, helps reduce photo-beaching of the DAPI
- DAQ 1: LabView VI measures the current and voltage in time, helps to characterize the behavior of the voltage as the current is maintained.

DAPI Prep (Adapted from Sigma-Aldrich Counterstaining Protocol)

Main DAPI Supply:

- Take 0.25 mL of H20 and add to the 5 mg DAPI powder inside the provided bottle. Heat or sonication may be required and make sure that the solution is fully dissolved. (Conc: 20 mg/mL)
- Solution stored in the dark at room temperature or 4C, should be stable for 2 to 3 weeks.

Store all solutions in foil in the fridge, solution only useful for up to 3 weeks.

DAPI Dilution for Sample Testing

- Intermediate DAPI Supply: Take 50 L of Main DAPI Supply (contains 1 mg of DAPI) and place into a 10 mL conical tube labelled 300 M Intermediate DAPI Supply; Add to the conical tube 9.5 mL of PBS, shake the tube to mix the DAPI.

- Sample Testing: Take 600 μL from the Intermediate DAPI Supply and add to each sample well, which already contains 2 mL of PBS.

Controls

- Negative Control: Test in 2 mL solution (H2O, PBS, and DMEM) with no DAPI or DNA in solution and monitor appearance without voltage application.
- Positive Control: Test in 2 mL solution (H2O, PBS, and DMEM) with DAPI and no DNA in solution and monitor appearance with and without current application; Test in 2 mL solution (H2O, PBS, and DMEM) with no DAPI but with DNA present in solution and monitor appearance with and without current application.

Test Sample Procedure:

1. Place glass slip into well with the electrodes.
2. Add 2 mL of H20 to treatment sample well.
3. Add DNA to well (250 to 750 ng per mL of injection fluid, 500 to 1500 ng in 2 mL solution, roughly 5kbp in size): Note: Nano-drop confirm the concentration of the DNA concentration
4. Add DAPI solution as outlined in the DAPI Dilution for Sample Testing: Sample Testing.
5. Set-up DAQ1 to capture voltage, current, and resistance through time.
6. Apply current control and capture images at specific time intervals.
7. Variables to consider: Current Magnitude, Duration of Current Exposure, DNA to DAPI Concentration by verifying DNA mass added, Fluid Type, Transfer Hypothesis

B.2.4 Reasons for Experiment Abandonment

Many experiment parameters were attempted in regards to electrostatic attraction of DAPI-labelled DNA onto tungsten tipped micro-manipulator electrodes in PBS solution with no success. Occassionally, it would appear for brief moments that DAPI-stained DNA was collecting on the electrodes. However, these events could not be repeated. After visiting with Dr. Quentin Aten, a former graduate student from the lab that did similar work in regards to the single lance nanoinjection, it was noted that he too experienced similar problems and had not been able to resolve them.

In short, what appears to be the problem is that when the electrode is placed in the ionic solution, as soon as a voltage is applied across the electrode, ions are attracted to the electrode and quickly diminish the voltage potential of the electrode. Without the voltage potential, the DNA in the solution is not attracted to the electrode.

In effort to overcome this, I tried reversing the voltage across the electrode to more or less help remove the collection of ions. This did not work to improve DAPI-DNA collection results. Furthermore, I also tried simply increasing the voltage across the electrode. This lead to localized electrophoresis. The resulting bubble formations helped with bulk fluid motion but failed to improve DAPI-DNA collection on the electrode. Ultimately, this project was dropped from the research.

B.3 Increasing Lenti-Viral Titers in Phoenix HEK cells using Lance Array Nanoinjection

Virology research often requires the production of high titers of engineered viruses. Typically, transfection of Phoenix HEK cell lines for lenti-viral production is performed using calcium-phosphate (Ca-Pho) transfection, achieving transfection rates of approximately 30%. From the HEK cells that are successfully transfected, researchers are able to harvest lenti-viruses produced by these modified HEK cells, where the goal is to have as high as possible viral counts.

In effort to achieve greater transfection rates, it is hypothesized that a non-viral transfection method called Lance Array Nanoinjection can facilitate better transfection and expression rates when compared to Ca-Pho in the context of modifying Phoenix HEK cells to producing lenti-virus. Specifically, the following hypotheses are proposed in the context of comparing LAN to Ca-Pho for Phoenix HEK cell transfection:

- LAN can transfect with greater than or equal efficiency as Ca-Pho in terms of GFP expression.
- LAN transfection efficiency will follow an injection-dose response, meaning the more times the target cells are injected, the greater the transfection rate will be.
- LAN will reach a 10% settling time sooner than Ca-Pho because the injection process can insert viral particles immediately into the cell whereas Ca-Pho takes a day before transfection occurs.
- The rate at which GFP expression is measured post-treatment will correlate to the number of infectious units, meaning the greater the transfection rate with GFP, the greater the number of infectious units measured.

B.3.1 Reasons for Experiment Abandonment

After a series of Lance Array Nanoinjection (LAN) experiments, it was shown that the LAN treated cells were dying in massive numbers when transfecting Phoenix HEK cells with these Lenti-viruses. This was not an expected outcome.

It was hypothesized that the reason for the massive cell death was due to the viral particle interaction with the HEK cells. With non-aided lenti-viral entry into the cells, part of the proteins that are required for entry must interact with the host cell membrane. With LAN injections, that interaction gets by-passed. It is hypothesized that because that interaction does not occur during

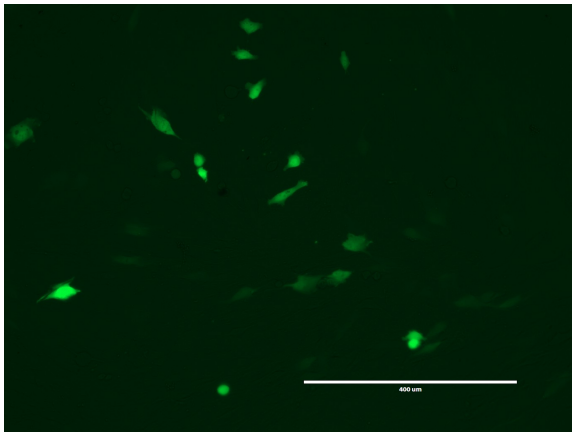

Figure B.1: Fluorescent microscope image of Retinal Pigmented Epithelial cells 1 day post-LAN with CMV/GFP plasmid

LAN treated experiments, that some capsid proteins remain intact on the Lenti-viral particles and threaten the target HEK cells. As a last resort effort, the HEK cells induces cell death to prevent infection.

This hypothesis was not investigated further and remains unknown still. The fact that other projects were doing well at the time of this project and because this project was outside the scope of the immediate NSF project, it was abandoned.

B.4 Retinal Pigmented Epithelial Cell Transfection using CMV/GFP Plasmid

One of the experiment types that was tried several times was using Lance Array Nanoinjection to transfect hard-to-transfect cell lines using plasmids without self-promotional features. This experiment was one of the most difficult in terms of that scope. Retinal Pigmented Epithelial (RPE) cells are difficult to transfect with nearly any transfection method available and we sought to transfect them by inserting a GFP with a CMV promoter.

Initially, our results were promising, showing a fairly high number of transfected cells (roughly 20%), which was significantly higher than the $< 1\%$ results that were reported previously in the lab. However, repeat experiments could not repeat these results and eventually was discontinued. The reason for failed results is not known.

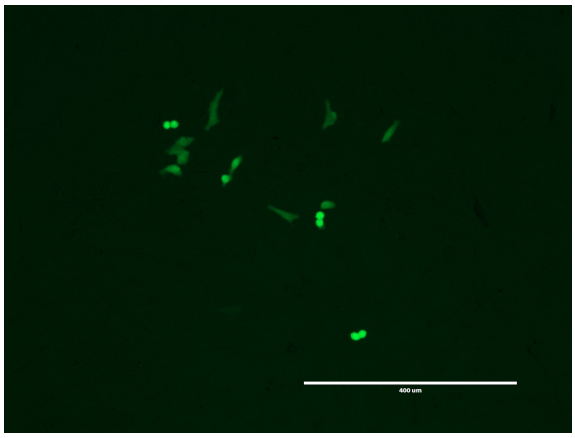

Figure B.2: Fluorescent microscope image of Retinal Pigmented Epithelial cells 3 day post-LAN with CMV/GFP plasmid

APPENDIX C. ARDUINO CODE USED FOR 3D PRINTED CELL PLATFORM LANCE ARRAY NANOINJECTIONS

The following code was originally written by Tyler Lewis for Force Injections using a slower stepper motor (for the entire code see Tyler's thesis). I modified the initial sections of this code to operate for most of the injection experimentation completed since the CRISPR-Cas9 GFP knock-out project (shown below). It operates by causing the stepper motor to vertically travel a total of 4 mm. The three input delays allow for three different electrical parameters to occur during this injection process.

Nanoinjection Program

Created by Tyler Lewis Last updated Mar. 6, 2015 by John Sessions

// Distance travel int distance = 4; // Desired travel distance in mm

// Distance at which input 1 turns off double cutoffdistance = 2; // mm

// Input delay times int input1duration = 20000; // ms of constant DC int input2duration = 20; // ms repel/pulse time int input3duration = 5000; // ms Reverse voltage, withdraw lances

// Pulsed input parameters int pulse = 1; // 0 = no, 1 = yes int periodlength = 2; // period (ms) of pulse duration

// Time delay between each step // This controls the speed of the motor // (1000 microseconds is the minimum possible) int timedelay = 1200; // microseconds

...